

**P2Y Receptor-Mediated Excitation-Contraction Coupling
in Pulmonary Arteries**

**A thesis presented in fulfilment of the requirement for the
degree of Doctor of Philosophy by
Ampuan Haji Mohamad Asrin Ampuan Haji Tengah**

**Strathclyde Institute of Pharmacy & Biomedical Sciences
University of Strathclyde
Glasgow**

2010

The copyright of this thesis belongs to the author under the terms of the United Kingdom Copyright Acts as qualified by University of Strathclyde Regulation 3.49. Due acknowledgement must always be made of the use of any material contained in, or derived from, this thesis.

ACKNOWLEDGMENTS

First of all, I would like to dedicate this PhD to my beloved late parents (Ampuan Hj Tengah Ampuan Daud and Hjh Hajjah Hj Harith) and I wish I could share this achievement with them both.

I would like to thank to my supervisor Dr. Charles Kennedy for all his assistance, guidance, advice and intellectual inputs throughout my PhD journey.

I am also very grateful to the Government of Brunei Darussalam for sponsoring me to pursue the Degree of PhD.

I am thankful to Dr. Robert Drummond for his assistance in my research. I am also thankful to Dr. Callum Mitchell, Dr. Syed Nawazish-i-Hussain and Dr. Suniljit Logantha for their assistance during my PhD project. Thank you to all students and staff in Strathclyde Institute of Pharmacy and Biomedical Sciences for their wonderful company during my time at the university.

Last but not least, I want to thank to my wife, my son and my brothers and sisters for their endless support as it would have not been possible for me to achieve this task without them supporting me.

ABSTRACT

The P2Y receptors present in the rat endothelium-denuded small pulmonary artery were characterised using pharmacological tools. Furthermore, the underlying signalling mechanisms of P2Y receptor-induced contractions were investigated in both intact and membrane-permeabilised arteries.

In intact arteries the endogenous P2Y agonists UTP and UDP evoked concentration-dependent, reproducible contractions, which were inhibited by the Rho kinase inhibitor Y27632, protein kinase C inhibitor GF109203X and the phosphatidylinositol-phospholipase C inhibitor U73122. In membrane-permeabilised preparations UTP and UDP also induced vasoconstriction, which was abolished by Y27632, but unaffected by GF109203X. U73122 modestly inhibited the response to UDP, but had no effect on UTP-evoked contractions. Additionally, the non-selective P2 receptor antagonist suramin reduced these nucleotide-evoked contractions and the reduction was greater for the UDP-evoked response.

Three synthetic P2Y agonists, which show P2Y receptor subtype selectivity INS45973 (P2Y₂ and P2Y₄), INS48823 (P2Y₆) and 3-phenacyl UDP (P2Y₆), evoked concentration-dependent, reproducible contractions of the intact arteries. INS45973 and INS48823 were more potent than UTP and UDP. Preincubation with Y27632 and suramin reduced the contractions evoked by all of the synthetic agonists. In membrane-permeabilised preparations INS45973, INS48823 and 3-phenacyl UDP also evoked vasoconstriction, which was abolished by Y27632, but unaffected by suramin.

The above findings clearly demonstrate the existence of a heterogeneous P2Y receptor population in rat small pulmonary artery smooth muscle cells and at least P2Y₂ and/or P2Y₄, and P2Y₆ receptors were involved in P2Y receptor-mediated vasoconstriction of this vessel. Rho kinase, protein kinase C and phosphatidylinositol-phospholipase C contributed significantly to P2Y receptor-induced contractions, with an exclusive role for Rho kinase in the Ca²⁺ sensitisation-dependent component of this response. In contrast, protein kinase C is not involved in Ca²⁺ sensitisation and how it contributes to UTP- and UDP-induced contractions remains to be determined.

TABLE OF CONTENTS

DECLARATION	I
ACKNOWLEDGMENTS	II
ABSTRACT	III
CONTENTS	IV
ABBREVIATIONS	XI
FIGURES	XIV
TABLES	XIX

CHAPTER 1 – GENERAL INTRODUCTION

1. PULMONARY CIRCULATION	2
1.1. The Pulmonary Vascular Bed	2
1.2. Pulmonary Artery	5
1.2.1. Endothelium	5
1.2.2. Smooth Muscle	6
1.3. Regulation of Tone	8
1.3.1. Autonomic Nervous System	8
1.3.1.1. Adrenergic Control	9
1.3.1.2. Cholinergic Control	9
1.3.1.3. Non-Cholinergic Non-Cholinergic Control	10
1.3.2. Humoral Regulation	11
1.3.3. Respiratory Gases	13
1.3.4. Role of Endothelium	14
1.4. Pulmonary Vascular Disease	14
2. PURINOCEPTORS	15
2.1. P2X Receptors	17
2.2. P2Y Receptors	18
2.2.1. P2Y ₁ Receptor	24
2.2.2. P2Y ₂ Receptor	25
2.2.3. P2Y ₄ Receptor	26

2.2.4.	P2Y ₆ Receptor	28
2.2.5.	P2Y ₁₁ Receptor	29
2.2.6.	P2Y ₁₂ Receptor	30
2.2.7.	P2Y ₁₃ Receptor	31
2.2.8.	P2Y ₁₄ Receptor	32
2.3.	Synthetic P2Y Receptor Agonists	33
2.3.1.	INS45973	34
2.3.2.	INS48823	34
2.3.3.	3-Phenacyl UDP	35
3.	P2Y RECEPTOR AND PULMONARY ARTERIAL SMOOTH MUSCLE	36
3.1.	Distribution and Action of P2Y Receptor	36
3.2.	Possible Physiological and Pathological Functions of Pulmonary P2 Receptors	37
3.3.	Mechanisms of P2Y Receptor-Mediated Contraction	38
3.4.	PLC/IP₃-Mediated Signalling in the Elevation of [Ca²⁺]_i	38
3.5.	Ca²⁺ Sensitisation Pathways	39
3.5.1.	RhoA/Rho Kinase Pathway	40
3.5.2.	PKC Pathway	42
3.5.3.	Possible Role of Ca ²⁺ Sensitisation in Pulmonary Vascular Disease	43
4.	AIMS OF THE STUDY	45

CHAPTER 2 – MATERIALS AND METHODS

1.	CONTRACTILE STUDIES	48
1.1.	Tissue Preparation	48
1.2.	Experimental Protocols	51
1.2.1.	Nucleotides Control Responses	51
1.2.2.	The Role of PI-PLC	51
1.2.3.	The Role of Rho Kinase and PKC	52
1.3.	Permeabilisation Experiment	52

1.3.1.	Effect of Temperature on the Contractile Activity of Intact Rat SPA	52
1.3.2.	Preparation of Permeabilisation with a Range of $[Ca^{2+}]$	53
1.3.3.	General Permeabilisation Protocol for Exploring Optimum Conditions	55
1.3.4.	Effects of Y27632 and GF109203X on Cumulative Ca^{2+} Concentration-Response Curve	55
1.3.5.	Characterisation of Contractions Evoked by pCa 6.5, UTP, UDP and PMA and the Effects of Y27632, GF109203X, U73122 and Suramin on these Contractions	55
1.4.	Contractile Responses of Synthetic P2Y Agonists INS45973, INS48823 and 3-Phenacyl UDP	56
1.4.1.	Potency of Contractions Evoked by INS45973, INS48823 and 3-Phenacyl UDP in Intact Preparation and Effects of Y27632 and Suramin on the Responses of these Agonists	56
1.4.2.	Characterisation of Contractions Evoked by INS45973, INS48823 and 3-Phenacyl UDP in Membrane-Permeabilised Preparations, and the Effects of Y27632 and Suramin on these Contractions	56
1.5.	Drugs and Solutions	56
1.6.	Data Analysis	57

CHAPTER 3 – CHARACTERISATION OF UTP- AND UDP-EVOKED CONTRACTILE RESPONSES

1.	INTRODUCTION	60
2.	RESULTS	62
2.1.	Effect of the Endothelium on Nucleotide-Induced Contractions	62
2.2.	Reproducibility of Nucleotide-Induced Contractions	66
2.3.	Time-Course of Nucleotide-Induced Contractions	66
3.	DISCUSSION	71
3.1.	UTP- and UDP-Evoked Vasoconstriction of SPA, and Contribution of Endothelium in P2Y Receptor-Mediated Contractile Responses	71
3.2.	Reproducibility of Nucleotide-Induced Contractions	72

**CHAPTER 4 – ROLE OF PI-PLC, PKC, AND RHO KINASE-ACTIVATED
Ca²⁺ SENSITISATION IN NUCLEOTIDE-EVOKED
CONTRACTILE RESPONSES IN INTACT PREPARATIONS**

1. INTRODUCTION	75
2. RESULTS	77
2.1. Involvement of PI-PLC in UTP- and UDP-Evoked Contractions	77
2.2. Involvement of PKC and Rho Kinase in UTP- and UDP- Evoked Contractions	87
2.2.1. Effective Concentration of GF109203X and Effect of 10µM Y27632 on PKC	87
2.2.2. Effects of Y27632 and GF109203X on the Peak Contraction Evoked by Nucleotides and KCl	92
2.2.3. Effects of Y27632 and GF109203X on the Nucleotide- Evoked Sustained Contractions	97
3. DISCUSSION	101
3.1. Role of PI-PLC in Contractions Evoked by UTP and UDP	101
3.2. Involvement of PKC and Rho Kinase in UTP- and UDP- Evoked Contractions	102
3.2.1. Effective Concentration of GF109203X and Effect of 10µM Y27632 on PKC	102
3.2.2. Role of Rho Kinase and PKC in P2Y Receptor-Mediated Contractions	102
3.2.3. Role of Rho Kinase and PKC in KCl-Induced Contractions	105

**CHAPTER 5 – ESTABLISHING THE OPTIMUM CONDITIONS FOR THE
PERMEABILISATION PROTOCOL**

1. INTRODUCTION	108
2. RESULTS	110
2.1. Effect of Temperature on the Contractile Activity of Intact Rat SPA	110

2.2.	Effectiveness of Permeabilising Agents	116
2.2.1.	β -Escin	116
2.2.2.	α -Toxin	119
2.3.	The Requirement for ATP in Permeabilisation Buffer	123
2.3.1.	The Response to P2Y Agonists and Free $[Ca^{2+}]$ after Permeabilisation	123
2.3.2.	ATP-Induced Contraction	125
3.	DISCUSSION	127
3.1.	Effect of Temperature on the Contractile Activity of Intact Rat SPA	127
3.2.	EGTA and Free $[Ca^{2+}]$	128
3.3.	Effectiveness of Permeabilising agent - β-Escin and α-Toxin, and Reproducibility of Contractions of the Membrane- Permeabilised Tissue	129
3.4.	The Requirement for ATP in the Permeabilisation Buffer	130
3.5.	Application to the Permeabilisation Protocol	131

**CHAPTER 6 – CHARACTERISATION OF CONTRACTION IN
MEMBRANE-PERMEABILISED PREPARATIONS**

1.	INTRODUCTION	134
2.	RESULTS	135
2.1.	Effects of Preincubation with Y27632 and GF109203X on Cumulative Ca^{2+} Concentration-Response Curves	135
2.2.	Characterisation of Contractions Evoked by pCa 6.5, UTP, UDP and PMA in α-Toxin-Permeabilised Rat SPA	139
2.3.	Effects of Post-Addition of Y27632 and GF109203X on Contractions Evoked by pCa 6.5, UTP, UDP and PMA	146
2.4.	Effects of Post-Addition of U73122 and Suramin on Contractions Evoked by pCa 6.5, UTP and UDP	153
3.	DISCUSSION	156
3.1.	Characterisation of Ca^{2+}-Force Relationship and Agonist	

Responses in α-Toxin-Permeabilised Rat SPA	156
3.2. Involvement of Rho Kinase and PKC in Contractions Evoked by Elevation of $[Ca^{2+}]$, UTP and UDP in α-Toxin-Permeabilised Rat SPA	157
3.3. Effects of U73122 and Suramin on Contractions Evoked by pCa 6.5, UTP and UDP in α-Toxin-Permeabilised Rat SPA	159

CHAPTER 7 – PROFILE OF INS45973-, INS48823- and 3-PHENACYL UDP-EVOKED RESPONSES IN INTACT AND MEMBRANE-PERMEABILISED PREPARATIONS

1. INTRODUCTION	162
2. RESULTS	164
2.1. Intact Rat SPA	164
2.1.1. Contractile Responses of INS45973, INS48823 and 3-Phenacyl UDP	164
2.1.2. Effects of Y27632 and Suramin on Peak Contractions Evoked by INS45973, INS48823 and 3-Phenacyl UDP	167
2.2. Membrane-Permeabilised Rat SPA	171
2.2.1. Characterisation of Contractions Evoked by INS45973, INS48823 and 3-Phenacyl UDP	171
2.2.2. Effects of Y27632 and Suramin on Contractions Evoked by INS45973, INS48823 and 3-Phenacyl UDP	175
3. DISCUSSION	180
3.1. Potency of INS45973, INS48823 and 3-Phenacyl UDP in Evoking Contractions of Intact Rat SPA and Characterisation of the Responses in α-Toxin-Permeabilised Rat SPA	180
3.2. Involvement of Rho Kinase and Effect of Suramin in Contractions Evoked by INS45973, INS48823 and 3-Phenacyl UDP in the Intact and α-toxin-Permeabilised Rat SPA	181

CHAPTER 8 – GENERAL DISCUSSION

1. CHARACTERISATION OF P2Y-INDUCED CONTRACTIONS IN RAT SPA AND P2Y SUBTYPES	185
2. SIGNALLING MECHANISMS UNDERLYING P2Y-INDUCED CONTRACTILE RESPONSES	188
2.1. A Model for P2Y Receptor-Induced Vasoconstriction of Rat SPA	193
3. SIGNALLING MECHANISMS INVOLVED IN KCl-INDUCED CONTRACTILE RESPONSES	195
3.1. A Model for KCl-Induced Vasoconstriction of Rat SPA	195
REFERENCES	197

ABBREVIATIONS

2-MeSADP	2-methylthio adenosine 5'-diphosphate
2-MeSATP	2-methylthio adenosine 5'-triphosphate
3-Phenacyl UDP	3-(2-oxo-2-phenylethyl) uridine 5'-diphosphate
5-HT	Serotonin
α,β -MeATP	α,β -methylene adenosine 5'-triphosphate
Ach	Acetylcholine
ADP	Adenosine 5'-diphosphate
AZD6140	3-{7-[2-3,4-difluoro-phenyl-cyclopropylamino]-5-propylsulfanyl [1,2,3]triazolo[4,5- <i>d</i>]pyrimidine-3-yl}-5-(2-hydroxymethoxy)-cyclopentane-1,2-diol
Ap ₄ A	P ¹ ,P ⁴ -di(adenosine 5'-)tetraphosphate
AR-69931MX	N ⁶ -2-(methylthioethyl)-2-(3,3,3-trifluoropropylthio)- β,γ -dichloromethyl adenosine 5'-triphosphate
AR-C67085MX	2-propylthio-d- β,γ -dichloromethylene-adenosine 5'-triphosphate
ATP	Adenosine 5'-triphosphate
[Ca ²⁺] _i	Intracellular Ca ²⁺ concentration
cAMP	Cyclic adenosine 5'-monophosphate
CICR	Ca ²⁺ -induced Ca ²⁺ release
DAG	Diacylglycerol
DMSO	Dimethyl sulfoxide
EC _{40K}	Concentration of agonist that induced 40% of 40mM KCl response
EC _{80K}	Concentration of agonist that induced 80% of 40mM KCl response
EC _{50max}	Concentration of agonist that induced 50% of the maximum response evoked by 1mM agonist
EGTA	Ethylene glycol-bis(2-aminoethylether)- <i>N,N,N',N'</i> -tetraacetic acid
ET-1	Endothelin-1
GF109203X	2-[1-(3-Dimethylaminopropyl)-1H-indol-3-yl]-3-(1H-indol-3-yl) maleimide
GPCR	G protein-coupled receptor

GTP	Guanosine 5'-triphosphate
GTP γ S	Guanosine 5'-O-(3-thiotriphosphate)
HA1077	1-(5-isoquinolinylsulfonyl) homopiperazine dihydrochloride
HEPES	N-[2-hydroxyethyl]piperazine-N'-[2-ethane-sulphonic acid]
HPV	Hypoxic pulmonary vasoconstriction
INS365	P ¹ ,P ⁴ -di(uridine 5'-)tetraphosphate
INS37217	P ¹ -(uridine 5')-P ⁴ -(2'-deoxycytidine 5')tetraphosphate
INS45973	P ¹ -(uridine 5'-),P ⁴ -(inosine 5'-) tetraphosphate
INS48823	P ¹ -((2-benzyl-1,3-dioxolo-4-yl)uridine 5') P ³ -(uridine 5'-) triphosphate
IP ₃	Inositol trisphosphate
ITP	Inosine 5'-triphosphate
ML-9	1-(5-chloronaphthalene-1-sulfonyl)-1 <i>H</i> -hexahydro-1,4-diazepine
MLC	Regulatory myosin light chain
MLCK	Myosin light chain kinase
MLCP	Myosin light chain phosphatase
MRS2179	2'-deoxy-N ⁶ -methyladenosine-3', 5'-bisphosphate
MRS2279	(<i>N</i>)-methanocarpa-N ⁶ -methyl-2chloro-2'-deoxyadenosine-3',5'bisphosphate
MRS2365	(1'S, 2'R, 3'S, 4'R, 5'S)-4-[(6-amino-2-methylthio-9 <i>H</i> -purin-9-yl-1-diphosphoryl-oxymethyl] bicycle[3.1.0] hexane-2,3-diol
MRS2567	1,2-diphenylethane
MRS2575	1,4-phenylendiisothiocyanate
MRS2578	1,4-di-(phenylthioureido) butane
MYPT-1	MLCP targeting subunit
NA	Noradrenaline
NANC	Non-adrenergic non-cholinergic
NO	Nitric oxide
NTPDase1	Nucleoside triphosphate diphosphohydrolase-1
PaO ₂	O ₂ partial pressure
PDB	Phorbol 12, 13-dibutyrate
PGF _{2α}	Prostaglandin F _{2α}
PIP ₂	Phosphatidylinositol-bisphosphate

PKC	Protein kinase C
PLC	Phospholipase C
PMA	Phorbol 12-myristate 13-acetate
PPADS	Pyridoxal-phosphate-6-azophenyl-2', 4'-disulfonate
RB2	Reactive blue 2
RhoGEF	Rho guanine nucleotide exchange factors
Ro 31-8220	3-[1-[3-(amidinothio)propyl-1H-indol-3-yl]-3-(1-methyl-H-indol-3-yl) maleimide
SPA	Small intrapulmonary artery
SPC	Sphingosylphosphorylcholine
SERCA	Sarcoplasmic/endoplasmic reticulum ATPase
SR	Sarcoplasmic reticulum
TM	Transmembrane domains
U73122	1-[6-[[(17β) -3-methoxyestra-1,3,5(10)-trien-17-yl]amino]hexyl]-1H-pyrrole-2, 5-dione
U73343	1-[6-[[(17β) -3-methoxyestra-1,3,5(10)-trien-17-yl]amino] hexyl]-2,5-pyrrolidinedione
UDP	Uridine 5'-diphosphate
UTP	Uridine 5'-triphosphate
Y27632	(R)-(+)- <i>trans</i> -N-(4-pyridyl)-4-(1-aminoethyl)-cyclohexanecarboxamide dihydrochloride monohydrate

FIGURES

	Page
Figure 1.1. Map of the human pulmonary arterial tree, relating vascular volumes, cross-sectional areas, diameters and wall structure to branch order number	4
Figure 1.2. Chemical structure of the primary endogenous agonists of P2Y receptors	16
Figure 1.3. Topology of human P2Y ₁ receptor showing amino acid sequence, seven TM-spanning helical domains and intracellular C- and extracellular N-terminals	20
Figure 1.4. A phylogenetic tree (dendrogram) showing the relationship among the current members of the P2Y receptor family	22
Figure 2.1. Diagram of rat lungs and heart showing the sections of pulmonary artery that were studied	49
Figure 2.2. The organ bath set up for recording the isolated rat SPA preparations	50
Figure 3.1. Ach-induced vasodilation in rat SPA	63
Figure 3.2. Vasoconstriction evoked by nucleotides in endothelium-intact and -denuded rat SPA	64
Figure 3.3. KCl-evoked vasoconstriction in rat SPA	65
Figure 3.4. Contractions of rat SPA evoked by UTP and UDP	67
Figure 3.5. Contractions of rat SPA evoked by UTP and UDP	68
Figure 3.6. Vasoconstriction of endothelium-denuded rat SPA evoked by nucleotides	69
Figure 3.7. Time-course of UTP and UDP contractile responses in endothelium-denuded rat SPA	70
Figure 4.1. UTP-evoked contractile response in endothelium-denuded SPA before and after preincubation with U73122	79
Figure 4.2. Contractile responses evoked by UDP in endothelium-denuded SPA before and after preincubation with U73122	80
Figure 4.3. Vasoconstriction of endothelium-denuded SPA evoked by PGF _{2α} before and after preincubation with U73122	81
Figure 4.4. KCl-evoked contraction in endothelium-denuded SPA before and after preincubation with U73122	82

Figure 4.5.	Effect of U73122 on peak contractions induced by UTP, UDP, PGF _{2α} and KCl in endothelium-denuded SPA	83
Figure 4.6.	Contractile responses evoked by UTP, UDP, PGF _{2α} and KCl in endothelium-denuded SPA before and after preincubation with U73343	84
Figure 4.7.	Vasoconstriction evoked by UTP, UDP, PGF _{2α} and KCl in endothelium-denuded SPA before and after preincubation with U73343	85
Figure 4.8.	Effect of U73343 on peak contractions induced by UTP, UDP, PGF _{2α} and KCl in endothelium-denuded SPA	86
Figure 4.9.	PMA-evoked vasoconstriction of endothelium-denuded rat SPA	88
Figure 4.10.	The effect of GF109203X on PMA-evoked vasoconstriction of endothelium-denuded rat SPA	89
Figure 4.11.	The effect of Y27632 on PMA-evoked vasoconstriction of endothelium-denuded rat SPA	90
Figure 4.12.	The effect of Y27632 on contractile responses induced by PMA in endothelium-denuded rat SPA	91
Figure 4.13.	Effects of Y27632 and GF109203X on peak contractions evoked by UDP in endothelium-denuded rat SPA	93
Figure 4.14.	Effects of Y27632 and GF109203X on peak contractions evoked by UTP and UDP in endothelium-denuded rat SPA	94
Figure 4.15.	Effects of Y27632 and GF109203X on peak contractions evoked by UTP and UDP in endothelium-denuded rat SPA	95
Figure 4.16.	Effects of Y27632 and GF109203X on KCl-evoked contractions of endothelium-denuded rat SPA	96
Figure 4.17.	Effects of Y27632 and GF109203X on sustained contractions evoked by UTP in endothelium-denuded rat SPA	98
Figure 4.18.	Effects of Y27632 and GF109203X on sustained contractions evoked by UTP and UDP in endothelium-denuded rat SPA	99
Figure 4.19.	Effects of Y27632 and GF109203X on sustained contractions evoked by UTP and UDP in endothelium-denuded rat SPA	100
Figure 5.1.	Vasoconstriction of endothelium-denuded rat SPA to UTP	112
Figure 5.2.	Contractile responses of endothelium-denuded rat SPA to nucleotides	113

Figure 5.3.	Vasoconstriction of endothelium-denuded rat SPA evoked by UTP, UDP and KCl	115
Figure 5.4.	Effect of varying [β -escin] on the contractions evoked by cumulative free [Ca^{2+}] additions and nucleotides in endothelium-denuded rat SPA following permeabilisation	118
Figure 5.5.	Effect of varying [α -toxin] on the contractile responses evoked by cumulative free [Ca^{2+}] additions and UDP in endothelium-denuded rat SPA following permeabilisation	121
Figure 5.6.	Vasoconstriction of α -toxin-permeabilised endothelium-denuded rat SPA in response to increasing free [Ca^{2+}] at pCa 6.5	122
Figure 5.7.	Effect of ATP on the responses to UTP and cumulative free [Ca^{2+}] additions in intact and α -toxin-permeabilised endothelium-denuded rat SPA	124
Figure 5.8.	Effects of nifedipine and thapsigargin on the elevation of basal tension induced by application of the permeabilising buffer's active contractile components ATP and pCa 4.5	126
Figure 6.1.	Contractile responses induced by cumulative free [Ca^{2+}] addition in endothelium-denuded rat SPA treated with α -toxin	136
Figure 6.2.	Effects of Y27632 and GF109203X on cumulative addition of free [Ca^{2+}] in α -toxin-permeabilised endothelium-denuded rat SPA	137
Figure 6.3.	Effects of Y27632 and GF109203X on contractile responses to free [Ca^{2+}] additions in α -toxin-permeabilised endothelium-denuded rat SPA	138
Figure 6.4.	Contractile response of α -toxin-permeabilised endothelium-denuded rat SPA induced by pCa 6.5	141
Figure 6.5.	Addition of UTP and UDP at pCa 9.0 [Ca^{2+}] in endothelium-denuded rat SPA permeabilised with α -toxin	142
Figure 6.6.	Vasoconstriction evoked by UTP in endothelium-denuded rat SPA treated with α -toxin	143
Figure 6.7.	Contractile response of UDP in α -toxin-permeabilised endothelium-denuded rat SPA	144
Figure 6.8.	Effect of PMA addition in α -toxin-permeabilised endothelium-denuded rat SPA	145

Figure 6.9.	Effect of Y27632 on contractions evoked by pCa 6.5, UTP and UDP in α -toxin-permeabilised endothelium-denuded rat SPA	148
Figure 6.10.	Comparison of the amplitude of the Ca ²⁺ sensitisation components of contractions evoked by UTP and UDP in intact and permeabilised endothelium-denuded rat SPA	150
Figure 6.11.	Effect of GF109203X on contractions evoked by pCa 6.5, UTP and UDP in α -toxin-permeabilised endothelium-denuded rat SPA	151
Figure 6.12.	Effect of GF109203X on contractions evoked by PMA in α -toxin-permeabilised endothelium-denuded rat SPA	152
Figure 6.13.	Effect of U73122 on contractions evoked by UTP and UDP in α -toxin-permeabilised endothelium-denuded rat SPA	154
Figure 6.14.	Effect of suramin on contractions evoked by pCa 6.5, UTP and UDP in α -toxin-permeabilised endothelium-denuded rat SPA	155
Figure 7.1.	Vasoconstriction of intact, endothelium-denuded rat SPA to INS45973, INS48823 and 3-phenacyl UDP	165
Figure 7.2.	Contractile responses of intact, endothelium-denuded rat SPA to P2Y agonists	166
Figure 7.3.	Vasoconstriction of intact, endothelium-denuded rat SPA evoked by INS45973, INS48823 and 3-phenacyl UDP	168
Figure 7.4.	Effect of Y27632 on peak contractions evoked by INS45973, INS48823 and 3-phenacyl UDP in intact, endothelium-denuded rat SPA	169
Figure 7.5.	Effect of suramin on peak contractions evoked by INS45973, INS48823 and 3-phenacyl UDP in intact, endothelium-denuded rat SPA	170
Figure 7.6.	Vasoconstriction evoked by INS45973 in endothelium-denuded rat SPA treated with α -toxin	172
Figure 7.7.	Contractile response of INS48823 in α -toxin-permeabilised endothelium-denuded rat SPA	173
Figure 7.8.	Contractions to 3-phenacyl UDP in α -toxin-permeabilised endothelium-denuded rat SPA	174
Figure 7.9.	Effect of Y27632 on contractions evoked by INS45973, INS48823 and 3-phenacyl UDP in α -toxin-permeabilised endothelium-denuded rat SPA	177

Figure 7.10. Comparison of the amplitude of the Ca ²⁺ sensitisation components of contractions evoked by INS45973, INS48823 and 3-phenacyl UDP in intact and permeabilised endothelium-denuded rat SPA	178
Figure 7.11. Effect of suramin on contractions evoked by INS45973, INS48823 and 3-phenacyl UDP in α -toxin-permeabilised endothelium-denuded rat SPA	179
Figure 8.1. A model of signalling mechanisms underlying activation of P2Y receptor	194
Figure 8.2. Overview of possible signalling mechanisms involved in KCl-induced contractions in rat SPA	196

TABLES

		Page
Table 1.1.	The classification of the vessel according to the characteristics of its wall structure and the corresponding branching system	3
Table 1.2.	The effect of circulating mediators and hormones on the pulmonary artery	12
Table 1.3.	The cloned P2Y receptors from various species and its transduction mechanisms	19
Table 1.4.	The distribution and function of P2Y receptors at seven main locations	23
Table 2.1.	The ratios of high Ca ²⁺ -containing (pCa 4.5) and Ca ²⁺ -free solutions used to produce the final mixture with the desired free [Ca ²⁺]	54
Table 5.1.	The potency of nucleotides in inducing contractions of endothelium-denuded rat SPA	114
Table 7.1.	The potency of P2Y agonists in evoking contractions of intact, endothelium-denuded rat SPA	166

Chapter 1:

Introduction

1. THE PULMONARY CIRCULATION

1.1. The Pulmonary Vascular Bed

The pulmonary circulation carries deoxygenated blood from the right side of the heart into the lungs for gas exchange and subsequently the resultant oxygenated blood is transported back to the left side of the heart before being distributed to the rest of the body (Ganong, 1995; Pocock & Richards, 2004). The deoxygenated blood is pumped from the right ventricle of the heart into the pulmonary trunk, which bifurcates into left and right pulmonary arteries that enter the left and right lungs, respectively. Inside the lungs, the deoxygenated blood passes further through a dense network of capillaries within the alveoli where the gas exchange takes place, i.e. CO₂ from the blood diffuses into the alveoli for exhalation, while the inhaled O₂ from alveoli diffuses into the blood. The oxygenated blood is drained into the pulmonary venules, and then to the small and large pulmonary veins. These large veins emerge from each side of the lungs and empty into the left atrium of the heart for systemic circulation.

In humans, pulmonary arteries and veins run together in a single connective tissue sheath in the centre of pulmonary segments and lobules (Hughes & Morrell, 2001; Pocock & Richards, 2004). Airways and the arteries generally branch symmetrically, while a different course of the vein branching pattern runs along the edges of lobules and segment. The branching system of both arteries and veins can be categorised according to the convergent approach, represented by order number (Hughes & Morrell, 2001). Order 1 correlates with the most peripheral branch, while order 15 and 17 denote the main branches of the vein and artery, respectively. The convergent approach is also applicable to the vascular classification that is based on the wall structure, as indicated in the Table 1.1 (Hughes & Morrell, 2001; Pocock & Richards, 2004). Figure 1.1 shows the outline of the human pulmonary arterial architecture that relates vascular volumes, cross-sectional areas, diameter and wall structure to the branch order number.

Table 1.1. The classification of the vessel according to the characteristics of its wall structure and the corresponding branching system.

Types of vessel	Description	Branching system/Order
Elastic	Contain adventitial, muscular and intimal layers, with medial thickness of 1 – 2% that of external diameter	17 to 13
Muscular	Thicker muscle layer compared to external diameter (2 – 5%), with internal and external laminae only. Internal elastic lamina disappears in the smallest arteries	13 to 3
Partially muscular	Spiral arrangement of smooth muscle fibres is exposed once the surrounding muscle coat becomes incomplete. Occurs mostly at diameter 50 to 100µm	5 to 3
Non-muscular	No elastic laminae. Smooth muscle is replaced by “pericyte”. Pericytes may differentiate to smooth muscle cells, their functions include production/organisation of the extravascular matrix and basement membranes	5 to 1
Supernumerary	Wall is relatively thin, branching immediately from parent vessel, and the diameter is 30 to 50% of that of parent. Have sphincters at the origin, presumably to provide a pressure ‘stepdown’ from larger and thicker-wall parent	11 to 12

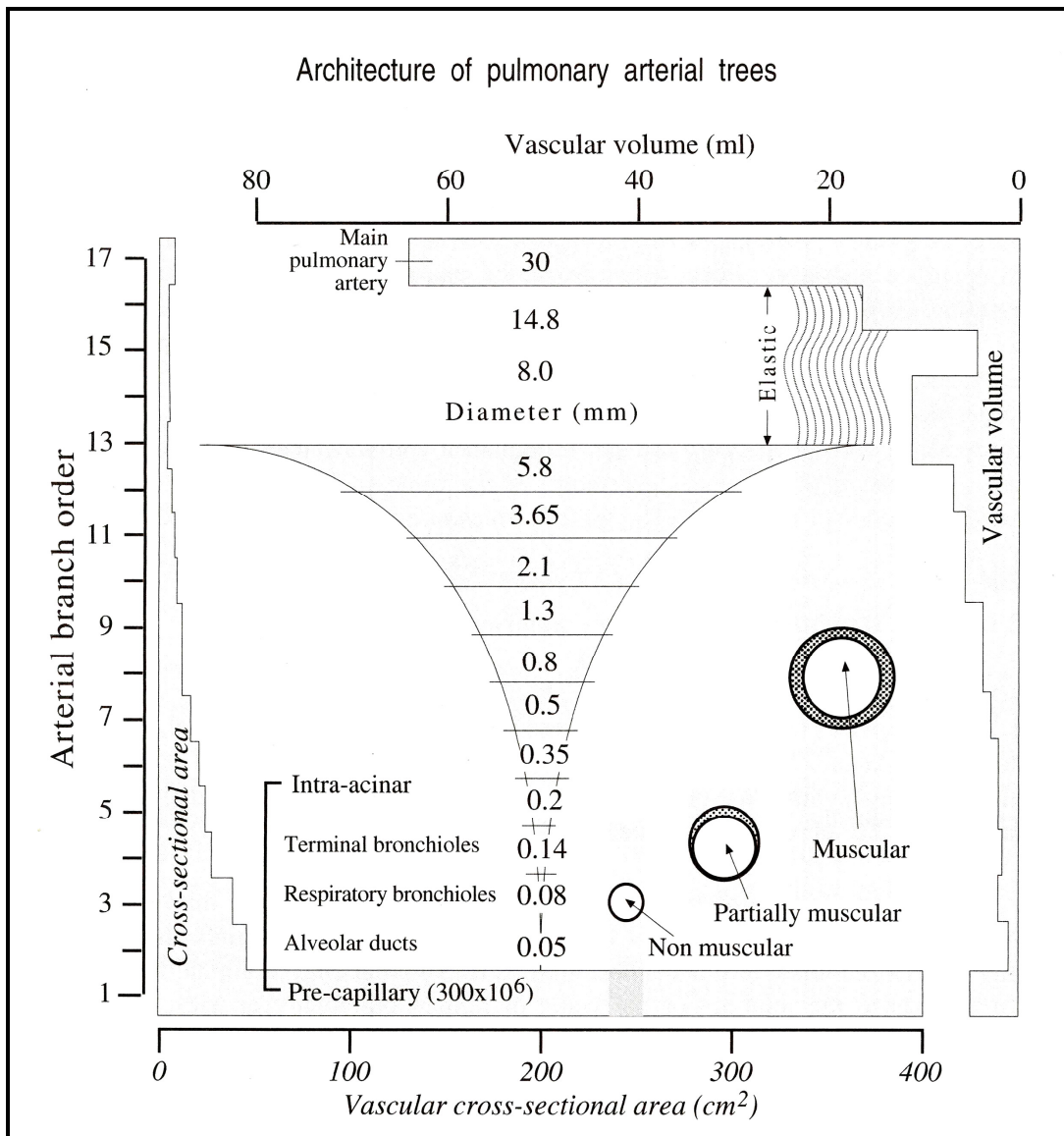


Figure 1.1. Map of the human pulmonary arterial tree, relating vascular volumes, cross-sectional areas, diameters and wall structure to branch order number. [Adapted from Hughes & Morell, 2001]

The arteries and veins in general share many structural similarities, however, the veins do not have an internal elastic lamina and also contain less smooth muscle, but more elastic tissue than their arterial counterparts. This may indicate distinct regulatory mechanisms of their functions. Moreover, both vessels exert different effects on the pulmonary circulation. Constriction of the veins can elevate the pulmonary capillary pressure and consequently may cause pulmonary oedema. In contrast, elevation of the right side of the heart pressure may occur following an increase of pulmonary arterial pressure due to the constriction of pulmonary arteries (Hughes & Morrell, 2001; Pocock & Richards, 2004).

The pulmonary arterial vessels are less thick and have relatively less smooth muscle and elastic tissue as compared to other arterial beds of the systemic circulation (Barnes & Liu, 1995). These crucial aspects of the arterial bed greatly assist to maintain low-pressure and low-vascular resistance of the pulmonary circulation, as is apparent from the considerable difference of mean blood pressures between the pulmonary artery and systemic circulation (15 and 120 mm Hg, respectively), while an equivalent blood flow is recorded at the root of the pulmonary artery and the aorta (Ganong, 1995; Pocock & Richards, 2004). The low-pressure and low-vascular resistance features of pulmonary circulation, coupled with the vast surface area at gas exchanging sites generated by the unique alveolar structure, in turn provide a favorable condition for an efficient CO₂ and O₂ exchange between the blood and the air inside the alveoli.

1.2. Pulmonary Artery

The profound influence of the pulmonary arteries on the pulmonary circulation primarily relies upon its two main cell types; endothelium and smooth muscle.

1.2.1. Endothelium

The endothelium lines the lumen of the vessels and consists of approximately 1×10^{13} cells (Sumpio *et al.*, 2002). It has a wide range of functions, including regulation of fluid and solute exchange, haemostasis and coagulation, immunological responses, vasculogenesis and angiogenesis, and not least, vascular tone and blood flow (Barnes & Liu, 1995; Sumpio *et al.*, 2002). Such functions are executed through the release

of diverse chemicals, such as growth factors, lipid metabolising proteins, antithrombotic factors and vasoactive mediators by the endothelial cells, which have paracrine and endocrine actions, onto the target tissues, including the circulating blood elements and the underlying vascular smooth muscle. The release of active chemicals is triggered by various stimuli, such as neurotransmitters from autonomic nerve terminals innervating the pulmonary vessel and hemodynamic forces (change in blood pressure or flow) (Barnes & Liu, 1995).

Disruption of the normal structure and function of endothelium has been implicated in many pathological processes, including atherosclerosis, primary hypertension and inflammatory syndromes (Veyssier-Belot & Cacoub, 1999). Additionally, it has been shown that endothelial injury can promote the development of hypoxic pulmonary vasoconstriction (HPV) by limiting the ability of endothelial cells to metabolise and clear circulating vasoconstrictors, and more importantly the impairment of these cells to release potent vasodilators, such as nitric oxide (NO) and prostaglandin I₂ (Sumpio *et al.*, 2002).

1.2.2. Smooth Muscle

In contrast to the endothelium, smooth muscle cells lie within the media of the vascular bed usually bounded by internal and external elastic laminae (Hughes & Morrell, 2001). The muscular media of proximal or large pulmonary arteries have abundant elastic laminae, nevertheless as the diameter of the arterial lumen decreases, the elastic lamina are substituted by smooth muscle. As an ultimate 'effector', smooth muscle cells directly modulate the vascular tone and hence the blood flow of the pulmonary circulation, although the crucial contribution of passive factors, such as cardiac output and gravitational force, which can change pulmonary vascular resistance and blood flow independently of the changes in vascular tone should also be noted (Barnes & Liu, 1995; Pocock & Richards, 2004).

The vascular tone of the pulmonary artery is regulated by the activity of the underlying smooth muscle. The contraction or relaxation of this smooth muscle is mainly dependent on the intracellular Ca²⁺ concentration ([Ca²⁺]_i), which can be increased by; a) influx of extracellular Ca²⁺ via membrane proteins, such as receptor-, store- or voltage-operated Ca²⁺ channels; and b) Ca²⁺ release from intracellular

stores (Barnes & Liu, 1995; Sylvester, 2004). Various vasoactive mediators can have a considerable effect on these pathways, for instance they may cause; membrane depolarisation of the smooth muscle, which then triggers the Ca^{2+} influx through the opening of voltage-gated Ca^{2+} channel; or intracellular Ca^{2+} release in response to inositol trisphosphate (IP_3) generation. Either of these processes subsequently leads to $[\text{Ca}^{2+}]_i$ increase and contraction (Barnes & Liu, 1995). Conversely, the mediators may also potentiate membrane hyperpolarisation through the opening of Ca^{2+} -activated K^+ channels, which decreases the opening of voltage-gated Ca^{2+} channel to prevent $[\text{Ca}^{2+}]_i$ increase and eventually induces smooth muscle relaxation. A rise in $[\text{Ca}^{2+}]_i$ can activate the calcium-binding protein, calmodulin, which then activates its main target, myosin light chain kinase (MLCK). Two subunits of myosin light chain with a molecular weight of 17 and 20kDa accompany every myosin heavy chain subunit (Murphy & Rembold, 2005; Eddinger & Meer, 2007). The 17kDa subunit, also called the essential myosin light chain, contributes to stabilising the myosin heavy chain's lever arm (neck domain) during contraction. On the other hand, the 20kDa subunit, also known as the regulatory myosin light chain (MLC), is the target for the phosphorylation by MLCK. Thus, upon its phosphorylation by activated MLCK, MLC activates the head or motor domain of myosin heavy chain, which subsequently permits the myosin head groups to interact with the actin filament for cross-bridging and so contraction is initiated. Phosphorylation of MLC is also regulated by other proteins, including myosin light chain phosphatase (MLCP), which dephosphorylates MLC to cause relaxation (Sylvester, 2004; Somlyo & Somlyo, 2000).

The rise of $[\text{Ca}^{2+}]_i$ can be terminated by two main mechanisms, uptake into the sarcoplasmic reticulum (SR) lumen via sarcoplasmic/endoplasmic reticulum Ca^{2+} -ATPase (SERCA) and extrusion out of the cell by the plasma membrane Ca^{2+} pump and $\text{Na}^+/\text{Ca}^{2+}$ exchanger (Jiang & Stephens, 1994; Shmygol & Wray, 2004; Berridge, 2008). Both SERCA and the plasma membrane Ca^{2+} pump utilise intracellular ATP to pump the Ca^{2+} against its concentration gradient, while the $\text{Na}^+/\text{Ca}^{2+}$ exchanger exploits the high extracellular $[\text{Na}^+]$ to countertransport intracellular Ca^{2+} out of the cell. The role of the SR in maintaining a low level of $[\text{Ca}^{2+}]_i$ is rather complex and appears to facilitate Ca^{2+} extrusion by accumulating Ca^{2+} in its lumen and then

releasing it into the superficial buffer barrier close to the plasma membrane, where it can be readily extruded into the extracellular space (Shmygol & Wray, 2004).

1.3. Regulation of Tone

The pulmonary circulation is affected by both active and passive factors (Daly & Hebb, 1966). Passive factors such as changes in cardiac output, airway pressure and gravitational force, alter the pulmonary resistance and blood flow in the manner that is independent of the vascular tone. However, it is the active factors that have a considerable influence in the pulmonary circulation by regulating the vascular tone, i.e. causing contraction or relaxation of pulmonary arterial smooth muscle, and these factors may be relevant in a particular condition (Suggett *et al.*, 1980). The four main active factors are; autonomic nervous system, gas levels, humoral mechanisms and endothelium (Barnes & Liu, 1995; Pocock & Richards, 2004).

1.3.1. Autonomic Nervous System

The autonomic innervation of the lung originates from the vagus nerve and sympathetic fibers, which together form the pulmonary plexuses. The plexuses lie on the anterior and posterior aspects of the bronchial and vascular structures at the hila of the lungs. The efferent parasympathetic fibres are derived from the dorsal root nucleus of the vagus nerve in the brainstem, while the sympathetic fibres arise from the cervical sympathetic chain and the upper 4 – 5 thoracic sympathetic ganglia. As the plexuses enter the lung, they further branch into the periarterial and peribronchial plexuses, which innervate the pulmonary vasculature and bronchial tree, respectively (Hughes & Morrell, 2001). The autonomic nerves actively modulate the contractile activity of pulmonary smooth muscle and their role appears to be very complex, as it interacts with and responds to the activities of circulating vasoactive mediators and alterations in pulmonary venous pressure imposed by the systemic circulation (Barnes & Liu, 1995; Hughes & Morrell, 2001). With increased understanding of autonomic control mechanisms in recent years, the two traditional pathways; adrenergic and cholinergic, have been expanded with the discovery of non-adrenergic, non-cholinergic (NANC) nerves (Barnes & Liu, 1995).

1.3.1.1. Adrenergic Control

There is a wide variation of distribution and extent of adrenergic innervations in the pulmonary arteries between species. Whereas absent in, for example rat and mouse (El-Bermani *et al.*, 1970; McLean *et al.*, 1985; Barnes & Liu, 1995), the adrenergic nerves are densely distributed in others, such as guinea pig, rabbit, cat and dog (Knight *et al.*, 1981; Barnes & Liu, 1995; Huges & Morrell, 2001). It has been shown that the application of electrical stimulation to the pulmonary arteries of cat (Hyman *et al.*, 1990), dog (Segarra *et al.*, 1999) and rabbit (Jackson *et al.*, 2002) induces vasoconstriction, which is sensitive to both the specific voltage-gated Na⁺ channel blocker tetrodotoxin and the α_1 adrenoceptor antagonist prazosin. These results clearly indicate that the response was neuronal in origin and evoked by noradrenaline (NA) via activation of the α_1 adrenoceptor. Consistent with this finding, exogenous application of NA to the vessels also evoked the contractions that were modestly inhibited by α_2 adrenoceptor antagonist yohimbine, but substantially inhibited after coapplication with prazosin (Hyman *et al.*, 1990). Interestingly, the involvement of α_1 and α_2 adrenoceptors in the NA-evoked contractions of pig pulmonary arteries was age-dependent, whereby α_1 and α_2 adrenoceptors were more prominent in young and adult, respectively, in mediating the contractile response to NA (Schindler *et al.*, 2004). In contrast, the application of either electrical stimulation (Hyman *et al.*, 1990) or exogenous NA (Schindler *et al.*, 2004) induced a relaxation of the precontracted pulmonary arteries of cat and pig, respectively, which was inhibited by β_2 antagonist propranolol, thus, showing the vasodilatory effect of NA was mediated via β_2 adrenoceptor.

1.3.1.2. Cholinergic Control

The pulmonary arteries are also innervated by cholinergic fibers, but these are not as extensive as seen in the respiratory airways. The distribution of cholinergic nerves varies between species, whereby it is absent in, for example rat, guinea pig, and mouse intrapulmonary artery (El-Bermani *et al.*, 1970; Barnes & Liu, 1995), but present in the corresponding vessels of dog, cat, pig, sheep and rabbit (Knight *et al.*, 1981; El-Bermani *et al.*, 1982; Barnes & Liu, 1995). The functional significance of cholinergic input is less clear compared with the adrenergic nerves. In the intact

conscious dog, intravenous administration of a non-selective muscarinic antagonist atropine resulted in a modest increase and decrease of pulmonary arterial pressure at low and high cardiac output, respectively (Murray *et al.*, 1986). Moreover, an intravenous application of acetylcholine (ACh) to the intact-chest cat (Hyman & Kadowitz, 1988) and rabbit (Hyman & Kadowitz, 1989) induced an increase and decrease of pulmonary lobar arterial pressure at low and high tonic state of the pulmonary arteries, respectively. While both responses were blocked by atropine, only the former component was substantially inhibited by a selective M₁ antagonist pirenzepine, indicating that contractions of the pulmonary vascular bed at low tone was mediated via M₁ muscarinic receptors.

1.3.1.3. Non-Adrenergic Non-Cholinergic Control

The NANC mechanism of neural control was shown to be insensitive to adrenergic or cholinergic blockade (Barnes *et al.*, 1991). NANC nerves may not exist as a separate neural pathway, as its transmitters may rather be released from adrenergic, cholinergic and sensory nerves (Barnes & Liu, 1995). Depending on the neurotransmitters released, this neural pathway can be either excitatory (e-NANC) or inhibitory (i-NANC), to cause contraction or relaxation, respectively. Perivascular nerve stimulation of the rat intrapulmonary artery evoked an excitatory junction potential that was unaffected by either adrenergic or cholinergic blockade, but sensitive to a P2X receptor desensitising agent α,β -methylene adenosine 5'-triphosphate (α,β -MeATP), thus indicating that adenosine 5'-triphosphate (ATP) had been released and mediated the response (Inoue & Kannan, 1988). In contrast, nerve stimulation in the precontracted guinea pig branch pulmonary artery induced a relaxation, which was both dependent on and independent of the endothelium (Liu *et al.*, 1992b; Tasatargil *et al.*, 2003). The endothelium-dependent relaxation was mediated, at least in part, by ATP that induces NO release from endothelial cells, whereas the endothelium-independent response was mediated by NO released from the nerves. Interestingly, relaxation of the precontracted main pulmonary artery of guinea pig was independent of endothelium and mediated by calcitonin gene-related peptide, released from the sensory nerve endings (Maggi *et al.*, 1990; Liu *et al.*, 1992a).

1.3.2. Humoral Regulation

Humoral mechanisms can also regulate the smooth muscles tone of pulmonary arteries. Numerous circulating mediators and hormones act at multiple receptors to mediate the tone-dependent effects (Barnes & Liu, 1995). Table 1.2 summarises several of these chemicals, together with the pre-existing tone of and the general effects on the pulmonary artery.

Table 1.2. The effect of circulating mediators and hormones on the pulmonary artery.

Mediators/ hormones	Species	Vascular tone	Response	References
Angiotensin II	rabbit	resting & precontracted	contraction	Tan & Sim, 2000
Atrial natriuretic peptide	pig	precontracted	relaxation	Matsushita <i>et al.</i> , 1999
Bradykinin	cow	precontracted	relaxation	Tracey <i>et al.</i> , 2002
Endothelin-1 (ET-1)	mouse	resting	contraction	Xu <i>et al.</i> , 2008
Histamine	rabbit rat	resting precontracted	contraction relaxation	Kapilevich <i>et al.</i> , 2001 Lau <i>et al.</i> , 2003
Prostacyclin	sheep	precontracted	relaxation	Lakshminrusimha <i>et al.</i> , 2009
Prostaglandin E ₂	sheep	precontracted	relaxation	Gao <i>et al.</i> , 1998
Prostaglandin F _{2α} (PGF _{2α})	rat	resting	contraction	Snetkov <i>et al.</i> , 2008
Serotonin (5-HT)	human pig	resting precontracted	contraction relaxation	Rodat-Despoix <i>et al.</i> , 2009 Jähnichen <i>et al.</i> , 2005
Substance P	rabbit	resting precontracted	contraction relaxation	Miike <i>et al.</i> , 2009
Vasoactive intestinal peptide	rat	precontracted	relaxation	Shahbazian <i>et al.</i> , 2007

1.3.3. Respiratory Gases

Respiratory gases, i.e. O₂ and CO₂, are able to actively affect the contractile activity of pulmonary smooth muscle. In an area of the lung where high CO₂ partial pressure (hypercapnia) or low O₂ partial pressure (PaO₂) (hypoxia) is present, constriction of vascular smooth muscle will occur to divert the blood flow to better oxygenated areas (Fishman, 1961; Pocock & Richards, 2004). HPV - a physiological response to redirect the blood flow away from hypoxic alveoli is triggered by a reduction of PaO₂ (Barnes & Liu, 1995; Hughes & Morrell, 2001). The mechanism underlying this response remains unclear and several hypotheses have been put forward.

A mediator hypothesis proposed that hypoxia causes induction or suppression of endogenous vasoconstrictors or vasodilators release, respectively. Several chemicals, including catecholamines, histamine, angiotensin II, 5-HT and ATP had been investigated, but they do not appear to be involved in mediating HPV (Barnes & Liu, 1995). Interestingly, ET-1 has been shown to mediate chronic hypoxic pulmonary hypertension in rat (DiCarlo *et al.*, 1995). Moreover, Jernigan *et al.*, (2008) found that chronic hypoxia induced the production of reactive oxygen species in the rat pulmonary artery, which potentiated the Ca²⁺ sensitisation-dependent ET-1 response. This Ca²⁺ sensitisation mechanism was associated with the activation of Rho kinase pathway (Broughton *et al.*, 2008; Jernigan *et al.*, 2008).

Another hypothesis of the hypoxic mechanism involves a direct effect of hypoxia on the pulmonary arterial smooth muscle, where it has been speculated that low PaO₂ may close K⁺ channels, inducing membrane depolarisation and hence contraction (Barnes & Liu, 1995; Hughes & Morrell, 2001). In line with this view, hypoxia has been shown to trigger contraction of fetal bovine pulmonary vascular smooth cells (Murray *et al.*, 1990). Additionally, both the expression and activity of K⁺ channel of rat pulmonary myocytes were inhibited following a subacute hypoxic exposure (Hong *et al.*, 2004).

1.3.4. Role of Endothelium

As mention above, the endothelium plays an important role in the regulation of vascular tone. The excitation of parasympathetic nerve terminals localised in the adventitia and outer media of the pulmonary artery, for example, may trigger the release of ACh (Hughes and Morrell, 2001). ACh then activates the muscarinic receptor in the endothelial cells, which subsequently induces the release of endothelial-derived relaxing factor or NO to cause relaxation of vascular smooth muscle (Tseng & Mitzner, 1992; Altieri *et al.*, 1994; Norel *et al.*, 1996). Relaxation of this smooth muscle via NO release can also be triggered by other substances including NA (Liu *et al.*, 1991), ATP (Liu *et al.*, 1992a), histamine (Szarek *et al.*, 1992) and bradykinin (Tracey *et al.*, 2002).

1.4. Pulmonary Vascular Disease

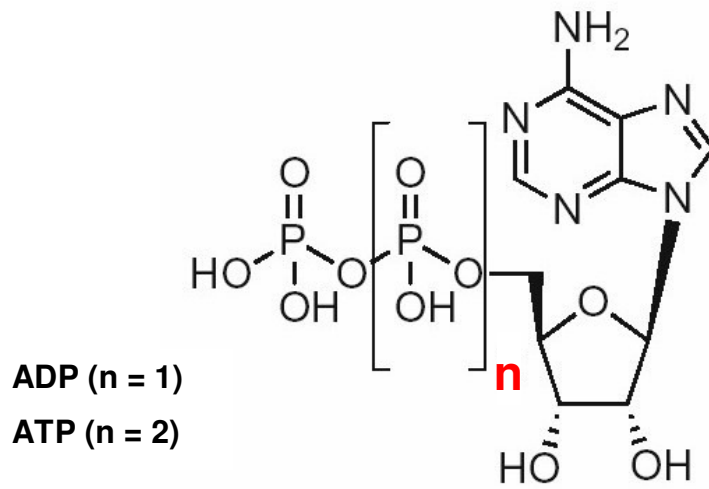
Pulmonary hypertension is a condition associated with a progressively high pulmonary arterial pressure. Although, vascular remodelling is often associated with this condition, abnormal regulation of tone of the vascular bed in lungs also contributes to its development (Reeves & Rubin, 1998; MacLean *et al.*, 2000; Morrell *et al.*, 2009). Additionally, pulmonary hypertension also commonly occurs secondary to other conditions, such as chronic obstructive lung diseases, human immunodeficiency virus infection and congenital systemic to pulmonary shunt (MacLean *et al.*, 2000). Other diseases are also linked to altered tone of pulmonary bed, such as pulmonary thromboembolic disease and pulmonary vasculitis (Reeves & Rubin, 1998). Thus, a clear understanding of mechanisms of regulation of vascular tone is certainly invaluable to assist our knowledge of various pathological pulmonary-associated conditions and hence, developing their novel therapeutic interventions.

2. PURINOCEPTORS

The earliest demonstration of the extracellular purine nucleotides actions and nucleosides as a signalling molecule was made by Drury & Szent-Györgyi in 1929, who showed that a filtrate of heart muscle had the potent effects on activity of the heart and blood vessels. Between the 1950s and 1970s further studies supported the involvement of ATP as a signalling molecule in a wide range of tissues, including the central nervous system, gut, uterus and skeletal muscle (see Burnstock, 1972 for references). An important milestone came in 1972 when Burnstock proposed the original hypothesis of purinergic transmission, describing a tentative model of storage, release, receptor activation by and inactivation of ATP. Despite facing fierce opposition, purinergic signalling has survived and is now generally accepted. Meanwhile, the identification of purinergic receptors began in 1978 when two major subdivisions, P1 and P2 receptors, was proposed with adenosine being the main natural for P1 receptors and ATP and adenosine 5'-diphosphate (ADP) being the main natural ligands for P2 receptors (Burnstock, 1978). Based on cloning studies P1 receptors have since been further divided into the A₁, A_{2A}, A_{2B} and A₃ subtypes, and all of these receptors are G protein-coupled receptors (GPCRs).

Kennedy *et al.*, (1985) demonstrated that activation of P2 receptors mediated both vasoconstriction and endothelium-dependent vasodilation in rat femoral artery. In the same year, Kennedy and Burnstock further showed that α,β -MeATP evoked contraction, while ATP and 2-methylthioATP (2-MeSATP) induced relaxation of rabbit portal vein. Thus, these studies provide clear evidence of the existence of two different populations of P2 receptors in these tissues. On the basis of these and other data Burnstock & Kennedy, (1986) proposed that the contractile effects were mediated by P2X receptors and the relaxant effects by P2Y receptors. Following the cloning of multiple subtypes of each Abbracchio & Burnstock, (1994) proposed that all of the ATP-sensitive ligand gated cation channels be named P2X receptors, while all nucleotide-sensitive GPCRs be called P2Y receptors. Both P2X and P2Y receptors have been shown to comprise of multiple subtypes and some of these are sensitive to purines and pyrimidines (Figure 1.2) (Ralevic & Burnstock, 1998; Kennedy, 2000; Abbracchio *et al.*, 2006; Burnstock, 2006).

a)



b)

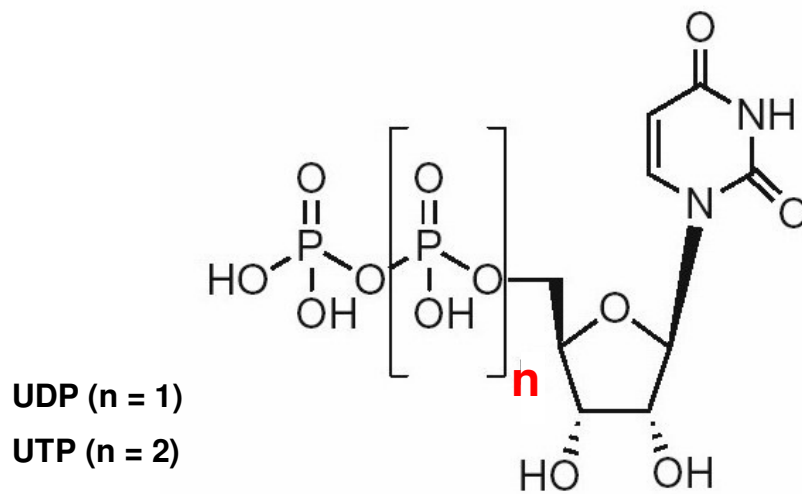


Figure 1.2. Chemical structure of the primary endogenous agonists of P2Y receptors. a) purines – ADP and ATP, and b) pyrimidines – uridine 5'-diphosphate (UDP) and uridine 5'-triphosphate (UTP).

2.1. P2X Receptors

P2X receptors are ligand-gated ion channels, which have selective and almost equal permeability to the cations Na^+ and K^+ , and also significant permeability to Ca^{2+} (Kennedy, 2000; Khakh *et al.*, 2001). At least seven subtypes of mammalian P2X receptors (P2X₁-P2X₇) have been identified in mammals, and these are distributed throughout the body. However, in rat pulmonary artery, only the expression of P2X₁, P2X₂ and P2X₄ receptors at immunohistochemical and mRNA levels have been reported (Nori *et al.*, 1998; Lewis & Evans, 2001). Pharmacological characterisation showed that P2X₁ and P2X₃ receptors desensitise much more rapidly than the other P2X subtypes and are also sensitive to the agonist α,β -MeATP (Khakh *et al.*, 2001). P2X₁ and P2X₃ receptors are inhibited by the antagonists suramin and pyridoxal-phosphate-6-azophenyl-2', 4'-disulfonate (PPADS) (Jarvis & Khakh, 2009). In contrast, P2X₄, P2X₆ and P2X₇ receptors are weakly sensitive to these antagonists.

All P2X subtypes consist of two transmembrane domains, a large cysteine extracellular loop and intracellular C- and N- terminal tails, with the former having a variable length (Kennedy, 2000; Khakh *et al.*, 2001). A functional P2X receptor, which can be a combination of identical or different types of subunit (Khakh *et al.*, 2001), consists of a trimer (Gonzales *et al.*, 2009; Kawate *et al.*, 2009). Activation of P2X receptors leads to a rapid influx of cations, which induces membrane depolarisation, which can trigger the opening of voltage-gated Ca^{2+} channel to cause Ca^{2+} influx (Egan *et al.*, 2006). This leads to various cellular effects, including vasoconstriction of pulmonary artery smooth muscle (via P2X₁ activation).

2.2. P2Y Receptors

P2Y receptors are a family of GPCRs, of which eight mammalian subtypes have been cloned (P2Y_{1, 2, 4, 6, 11, 12, 13} and 14) (Abbracchio *et al.*, 2006) (Table 1.3). The missing numbers represent nonmammalian orthologs or GPCRs that have some sequence homology to P2Y receptors, but lack functional responsiveness to nucleotides. These subtypes consist of 326 (P2Y₆) to 377 (P2Y₄) amino acids and have an intracellular C-terminal and an extracellular N-terminal and seven hydrophobic, transmembrane domains (TM) connected by 3 extracellular loops and 3 intracellular loops (Figure 1.3) (von Kügelgen, 2006). Positively-charged residues in TM3, 6 and 7 are considered to be essential for receptor activation (Erb *et al.*, 1995; Jiang *et al.*, 1997), through interaction with the negative charge of nucleotides.

The signalling mechanisms of P2Y receptors that trigger various cellular responses are complex and are further complicated by several factors, including the agonists, receptor subtypes and multiple-interactions within the signalling molecules/proteins (Abbracchio *et al.*, 2006). However, several broad models of signalling mechanisms have been proposed, which primarily depend on the types of G protein that couple to the P2Y receptors. P2Y_{1, 2, 4, 6, 11} receptors, via G α_q coupling, can induce phospholipase C (PLC) activation that subsequently catalyses the hydrolysis of phosphatidylinositol-bisphosphate (PIP₂) to IP₃ and diacylglycerol (DAG). IP₃ triggers Ca²⁺ release from IP₃-sensitive intracellular calcium stores (Keys *et al.*, 2002), while DAG activates protein kinase C (PKC) to phosphorylate intracellular proteins, ultimately leading to a variety of cellular responses (Harden *et al.*, 1995). The P2Y₁₁ subtype acts via G α_s to increase adenylyl cyclase, whereas P2Y_{12, 13, 14} subtypes act via G α_i to inhibit adenylyl cyclase activity. These actions then increase or decrease the cyclic adenosine 5'-monophosphate (cAMP) level, respectively (Freeman *et al.*, 2001; Hollopeter *et al.*, 2001; Qi *et al.*, 2001; Fumagalli *et al.*, 2004). In addition, P2Y receptors, via a distinct G protein coupling may also; regulate ion channels, e.g. Ca²⁺ channels, to cause membrane depolarisation (Dolphin, 2003), or activate other intracellular proteins, such as RhoA (Jankowski *et al.*, 2003), to stimulate the appropriate responses (Nishida, *et al.*, 2008).

Table 1.3. The cloned P2Y receptors from various species and its transduction mechanisms.

Receptor subtype	Transduction mechanism	Species in which receptor cloned	References
P2Y ₁	$G\alpha_{q/11} \rightarrow \uparrow [Ca^{2+}]_i$	Human Rat Mouse Cow <i>Xenopus</i>	Schachter <i>et al.</i> , 1996 Tokuyama <i>et al.</i> , 1995 Tokuyama <i>et al.</i> , 1995 Henderson <i>et al.</i> , 1995 Cheng <i>et al.</i> , 2003
P2Y ₂	$G\alpha_{q/11} \rightarrow \uparrow [Ca^{2+}]_i$	Human Rat Mouse Pig	Janssens <i>et al.</i> , 1999 Chen <i>et al.</i> , 1996 Lustig <i>et al.</i> , 1993 Shen <i>et al.</i> , 2004
P2Y ₄	$G\alpha_{q/11} \rightarrow \uparrow [Ca^{2+}]_i$	Human Rat Mouse	Communi <i>et al.</i> , 1996a Bogdanov <i>et al.</i> , 1998 Suarez-Huerta <i>et al.</i> , 2001
P2Y ₆	$G\alpha_{q/11} \rightarrow \uparrow [Ca^{2+}]_i$	Human Rat Mouse	Communi <i>et al.</i> , 1996b Chang <i>et al.</i> , 1995 Lazarowski <i>et al.</i> , 2001
P2Y ₁₁	$G\alpha_s \rightarrow \uparrow \text{cAMP}$ $G\alpha_{q/11} \rightarrow \uparrow [Ca^{2+}]_i$	Human Dog Human Dog	van der Weyden <i>et al.</i> , 2000 Qi <i>et al.</i> , 2001 Communi <i>et al.</i> , 1997 Qi <i>et al.</i> , 2001
P2Y ₁₂	$G\alpha_i \rightarrow \downarrow \text{cAMP}$	Human Rat Mouse	Hollopeter <i>et al.</i> , 2001 Hollopeter <i>et al.</i> , 2001 Foster <i>et al.</i> , 2001
P2Y ₁₃	$G\alpha_i \rightarrow \downarrow \text{cAMP}$	Human Rat Mouse	Communi <i>et al.</i> , 2001 Fumagalli <i>et al.</i> , 2004 Zhang <i>et al.</i> , 2002
P2Y ₁₄	$G\alpha_i \rightarrow \downarrow \text{cAMP}$	Human Rat Mouse	Chambers <i>et al.</i> , 2000 Freeman <i>et al.</i> , 2001 Freeman <i>et al.</i> , 2001

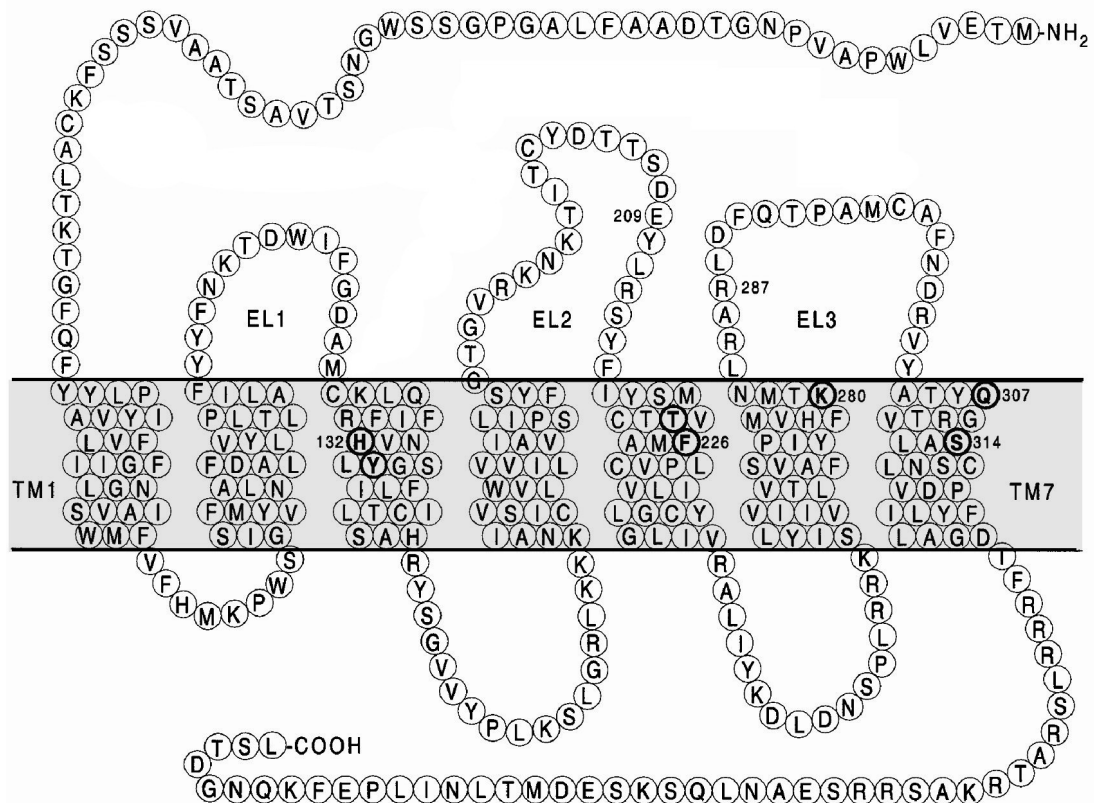


Figure 1.3. Topology of human P2Y₁ receptor showing amino acid sequence, seven TM-spanning helical domains and intracellular C- and extracellular N-terminals. Bold circles and letters indicate amino acids that most likely involve to the nucleotide binding site within the TM regions. [Adapted from von Kügelgen & Wetter, 2000]

TM = Transmembrane region
 EL = Extracellular loop

The P2Y receptor subtypes can be grouped together according to their similarities in various features (Abbracchio *et al.*, 2006). Pharmacologically, the receptors are subdivided broadly into four groups; a) adenine nucleotide-preferring receptors, i.e. P2Y₁, P2Y₁₁, P2Y₁₂ and P2Y₁₃ receptors that respond to ATP and ADP; b) the uracil nucleotide-preferring P2Y₄ and P2Y₆ receptors, which respond to either UTP or UDP; c) receptors that are activated by both adenine and uridine nucleotides, which are P2Y₂, P2Y₄ and P2Y₁₁ receptors; and d) receptors responding solely to the sugar nucleotides UDP-glucose and UDP-galactose, i.e. the P2Y₁₄ receptor. In contrast, another grouping is mainly based on structural and phylogenetic criteria, where three important features are used; 1) amino acid sequence similarity, 2) specific amino acid motifs present in crucial TM (TM7) and 3) the primary G protein coupling (Abbracchio *et al.*, 2006). On the basis of amino acid similarity, the P2Y receptors can be divided into two distinct subgroups; Group 1 comprises P2Y_{1, 2, 4, 6, 11} receptors and Group 2 consists of P2Y_{12, 13, 14} receptors. Within each group all subtypes share a high amino acid sequence identity between the members with the latter group reaching as high as 48% identical (Cattaneo *et al.*, 2003). Figure 1.4 illustrates the phylogenetic tree (dendrogram) representing the relationships of the current P2Y receptor family. The TM7-specific motifs for Group 1 is Q/K-X-X-R, while K-E-X-X-L is present in all members of the second group (Cattaneo *et al.*, 2003). Finally, the Group 1 members are primarily coupled with G $\alpha_{q/11}$ protein and the members of Group 2 are coupled almost exclusively to G $\alpha_{i/o}$ (Abbracchio *et al.*, 2006).

The distribution of P2Y receptors in mammalian organs and systems is very extensive, and they trigger a wide range of effects in all tissues and organs in the body. A brief summary of this information is shown in Table 1.4.

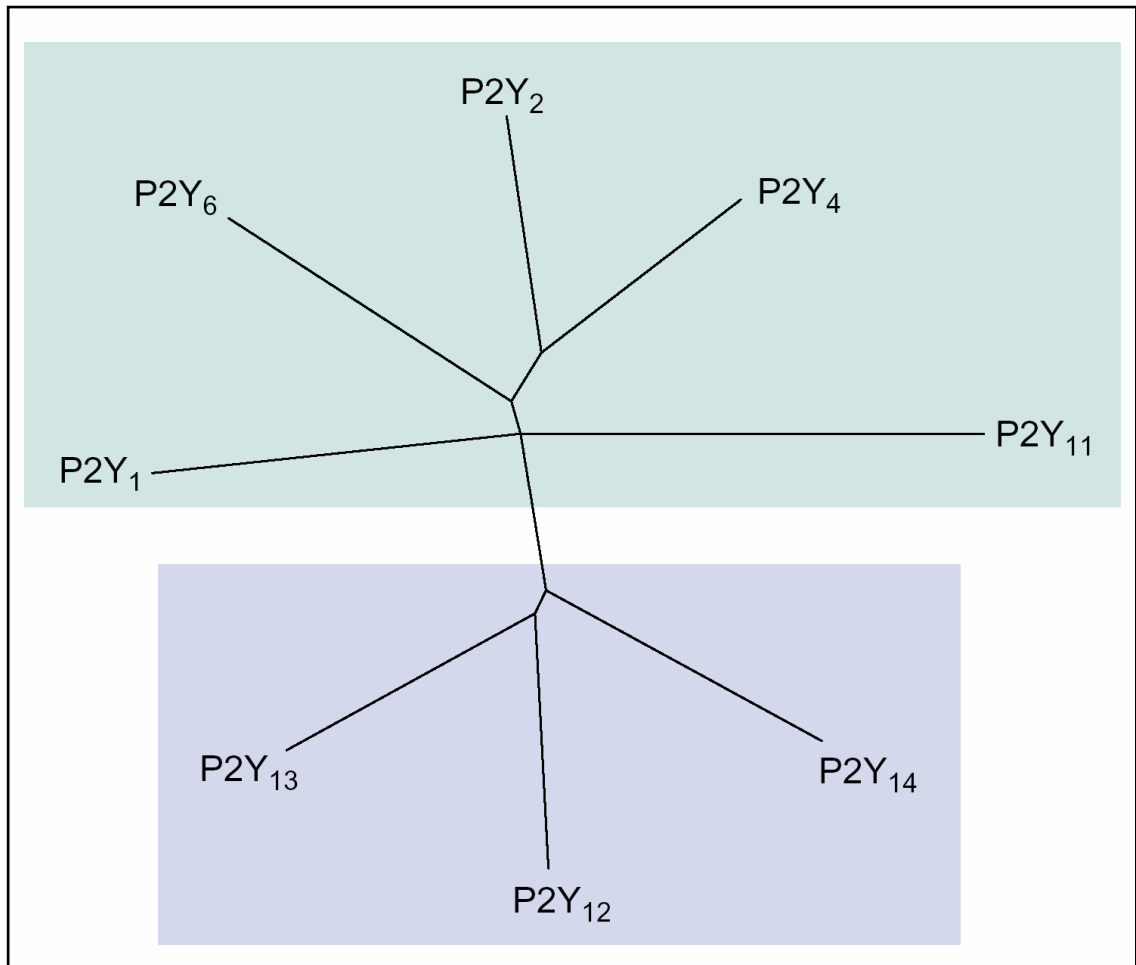


Figure 1.4. A phylogenetic tree (dendrogram) showing the relationships among the current members of the P2Y receptor family. The P2Y receptors can be divided into two subgroups, shown with green and blue backgrounds. The tree was built using TREEVIEW software, and the lines represent the relationship of the amino acid sequences between the P2Y subtypes which were aligned using CLUSTALX. [Adapted from Abbracchio *et al.*, 2003]

Table 1.4. The of distribution and function of P2Y receptors at seven main locations.

Tissues/organs/ systems	Receptors	Functions	References
Central nervous system (e.g. hippocampus, cortex, cerebellum, spinal cord, peripheral nerves, cerebral artery)	P2Y _{1, 2, 4, 6, 12, 14}	Tissue remodelling following injury/damage, release of inflammatory cytokines, modulation of pain transmission, contraction of vessel, prevents tumor necrosis factor- α -induced apoptosis	Chen & Chen, 1998; Neary <i>et al.</i> , 1994, 2003; Okada <i>et al.</i> , 2002; Fumagalli <i>et al.</i> , 2003; Kim <i>et al.</i> , 2003; Malmjö <i>et al.</i> , 2003; Rodrigues <i>et al.</i> , 2005; Heinrich <i>et al.</i> , 2008; Amadio <i>et al.</i> , 2009
Immune cells (e.g. dendritic cell, macrophages, lymphocytes, mast cells)	P2Y _{1, 2, 4, 6, 11, 12}	Prostaglandin production, adhesion of neutrophils to endothelial cells, induction of semimaturation process, release of histamine	Berchtold <i>et al.</i> , 1999; Warny <i>et al.</i> , 2001; Wilkin <i>et al.</i> , 2001; Feng <i>et al.</i> , 2004; Marcet <i>et al.</i> , 2007; Elliott <i>et al.</i> , 2009
Gastrointestinal system (e.g. Gut, liver, biliary system, pancreas, colonic epithelium, myenteric & submucosal plexus)	P2Y _{1, 2, 4, 6, 11, 13, 14}	Stomach contractility, ion secretion, regulation of gluconeogenesis and glycolysis, regulation of NaCl secretion and bile release, activates Cl channel, regulation of high density lipoproteins endocytosis	Roman <i>et al.</i> , 1999; Nguyen <i>et al.</i> , 2001; Köttgen <i>et al.</i> , 2003; Ghanem <i>et al.</i> , 2005; Jacquet <i>et al.</i> , 2005; King & Townsend-Nicholson, 2008; Bassil <i>et al.</i> , 2009; Koltsova <i>et al.</i> , 2009; Balusubramanian <i>et al.</i> , 2010
Kidney and bladder (e.g. kidney tubule & glomerulus, collecting duct, urinary bladder)	P2Y _{1, 2, 4, 6, 11, 12}	Excretion of waste products; release of mediators, proliferation during injury	Insel <i>et al.</i> , 2001; Rost <i>et al.</i> , 2002; Bailey <i>et al.</i> , 2004; Chopra <i>et al.</i> , 2008; Graciano <i>et al.</i> , 2008; Pochynyuk <i>et al.</i> , 2008
Lungs (e.g. smooth muscle, epithelial cells)	P2Y _{1, 2, 6, 14}	Smooth muscle contraction and relaxation, mucin secretion & mucociliary clearance, regulation of epithelial proliferation	Schäfer <i>et al.</i> , 2003; Konduri <i>et al.</i> , 2004; Govindaraju <i>et al.</i> , 2005; Hayashi <i>et al.</i> , 2005; Müller <i>et al.</i> , 2005; Ehre <i>et al.</i> , 2007
Bone and cartilage (e.g. oestoblasts, chondrocytes)	P2Y _{1, 2}	Bone growth, healing and mineralisation	Orriss <i>et al.</i> , 2007; Guzmán-Aránguez <i>et al.</i> , 2008; Alvarenga <i>et al.</i> , 2010
Skin	P2Y _{1, 2, 11}	Wound healing, regulation of mediator release, proliferation in basal cells	Dixon <i>et al.</i> , 1999; Greig <i>et al.</i> , 2003; Inoue <i>et al.</i> , 2007; Pastore <i>et al.</i> , 2007

2.2.1. P2Y₁ Receptor

After the first cloning of the P2Y₁ receptor from the late-embryonic chick brain (Webb *et al.*, 1993), steady progress was made in cloning and characterising the receptor from other species, including cow (Henderson *et al.*, 1995), mouse (Tokuyama *et al.*, 1995), human (Schachter *et al.*, 1996) and *Xenopus* (Cheng *et al.*, 2003). The distribution and functions of the P2Y₁ receptor is very extensive as indicated in Table 1.4. Several of its key functions include involvement in endothelium-dependent relaxation of blood vessels (Guns *et al.*, 2005), induction of arachidonic acid release from astrocytes (Chen & Chen, 1998), insulin secretion (Balusubramanian *et al.*, 2010) and platelet aggregation (Pfefferkorn *et al.*, 2008).

TM3, 6 and 7 are crucial for agonist binding and activation of P2Y₁ receptors. Five amino acid residues from these regions [TM3 – arginine (128); TM6 – lysine (280); TM7 – arginine (310), glutamine (307), serine (314)], together with one residue from TM7 (threonine 222), interact with at least one of the three functional groups of ATP, i.e. α and β phosphate groups, and adenine ring (Jiang *et al.*, 1997; Moro *et al.*, 1998). Additionally, four cysteine residues in the N-terminal (42), near the exofacial (extracellular side) end of TM3 (124) and in extracellular loop 2 (202) and 3 (296) have been reported to be necessary for proper cellular trafficking of P2Y₁ receptors to the surface membrane (Hoffmann *et al.*, 1999).

The first cloning study of chicken P2Y₁ receptor found that ATP was more potent as an agonist than ADP, and the agonist order of potency was 2-MeSATP \geq ATP >ADP \gg α,β -MeATP, β,γ -Methylene ATP, UTP. However, Léon *et al.*, (1997) showed that nucleoside diphosphates, such as ADP and 2-methylthioADP (2-MeSADP), acted as a full agonist whereas ATP was a partial agonist at the cloned human P2Y₁ receptor. Additionally, when they purified the agonists, ATP appeared to demonstrate a competitive antagonistic effect. The difficulty of obtaining a general consensus of ATP activity at this receptor was further complicated when the maximum response to ATP was found to be comparable with the corresponding ADP at the cloned human P2Y₁ receptor (Palmer *et al.*, 1998). This study suggested that the response to ATP might be determined by the level of P2Y₁ receptor expression as the full agonist property of ATP being shown was obtained from the cell lines expressing a high level of the receptor. A subsequent study (Waldo & Harden, 2004)

that utilised the radioligand binding assay and the technique of purification/reconstitution of human P2Y₁ receptor with associated G protein, showed that ATP exhibited partial agonist activity at this receptor. Thus, it can be concluded that ADP, rather than ATP is likely to be the natural ligand of P2Y₁ receptor. Chemical modification of the structure of ADP led to the synthesis of a 2-MeSADP analogue, (1'S, 2'R, 3'S, 4'R, 5'S)-4-[(6-amino-2-methylthio-9H-purin-9-yl-1-diphosphoryl-oxymethyl] bicycle[3.1.0] hexane-2,3-diol (MRS2365), which is the most potent P2Y₁ agonist discovered to date (Chhatriwala *et al.*, 2004).

The P2Y₁ receptor is sensitive to the non-selective antagonists suramin and PPADS (Webb *et al.*, 1993; Léon *et al.*, 1997) and the much more selective and potent antagonists, 2'-deoxy-N⁶-methyladenosine-3', 5'-bisphosphate (MRS2179) (Boyer *et al.*, 1998) and (N)-methanocarpa-N⁶-methyl-2chloro-2'-deoxyadenosine-3',5'-bisphosphate (MRS2279) (Boyer *et al.*, 2002). The latter has been used for binding studies, in which [³H]MRS2279 bound specifically to human P2Y₁ receptor with a K_d of 3.8nM (Waldo & Harden, 2004). The binding displacement order against [³H]MRS2279 was 2-MeSADP > ADP = 2-MeSATP > ATP, and MRS2279 = MRS2179 > adenosine 3', 5'- biphosphate (Waldo *et al.*, 2002; Waldo & Harden, 2004).

2.2.2. P2Y₂ Receptor

The P2Y₂ receptor was first cloned in mouse (Lustig *et al.*, 1993) and subsequently in other species, such as rat (Chen *et al.*, 1996), human (Janssens *et al.*, 1999), and pig (Shen *et al.*, 2004). Again, the distribution and functions of P2Y₂ receptor are extensive, as indicated in Table 1.4. Among the main functions are; modulation of epithelial cell Cl⁻ secretion (Cressman *et al.*, 1999), mediation of endothelium-dependent NO release to induce vasodilatation (Konduri *et al.*, 2004), vasoconstriction in some blood vessels (Govindaraju *et al.*, 2005; Buvinic *et al.*, 2006) and bone growth (Guzmán-Aránguez *et al.*, 2008).

The interaction of agonists with P2Y₂ receptor relies on its positively charged residues in TM6 and 7 (Erb *et al.*, 1995). Additionally, the arginine-glycine-aspartic acid residues in the first extracellular loop form the consensus integrin-binding motif, which facilitates the colocalisation of receptor with integrins and in turn essential for

the receptor's proper function (Erb *et al.*, 2001). The P2Y₂ receptor undergoes agonist-induced desensitisation and this has been associated with putative phosphorylation sites for GPCR kinase at the intracellular C-terminal tail (Garrad *et al.*, 1998).

ATP and UTP have equal potency in activating the receptor, while ADP and UDP are inactive (Lustig *et al.*, 1993; Nicholas *et al.*, 1996), indicating that at least three phosphate residues are essential for receptor activation. Supporting this view, compounds such as P¹,P⁴-di(adenosine 5'-)tetraphosphate (Ap₄A) (Patel *et al.*, 2001), P¹,P⁴-di(uridine 5'-)tetraphosphate (INS365) (Pendergast *et al.*, 2001) and P¹-(uridine 5')-P⁴-(2'-deoxycytidine 5')tetraphosphate (INS37217) (Yerxa *et al.*, 2002) are agonists at the P2Y₂ receptor. Moreover, uridine-5'-O-(3-thiotriphosphate) is also a potent agonist, which is resistant to hydrolysis (Lazarowski *et al.*, 1996). The P2Y₂ receptor can be antagonised by both suramin and reactive blue 2 (RB2), while PPADS is inactive (Janssens *et al.*, 1999).

The involvement of the P2Y₂ receptor in modulating ion transport in epithelial cells (Cressman *et al.*, 1999) led to the utilisation of its potential therapeutic role in treating diseases associated with defective ion transports. Two P2Y₂ agonists, INS365 (Mundasad *et al.*, 2001; Tauber *et al.*, 2004) and INS37217 (Kellerman *et al.*, 2002, 2008) are currently in clinical trials for treatment of dry eye disease and cystic fibrosis, respectively.

2.2.3. P2Y₄ Receptor

The cloning and characterisation of P2Y₄ receptors was initially carried out using human tissue (Communi *et al.*, 1995; Nguyen *et al.*, 1995), and was followed by other species such as rat (Bogdanov *et al.*, 1998) and mouse (Suarez-Huerta *et al.*, 2001). The mRNA receptor is distributed widely in various tissues (see Table 1.4), such as intestine (most abundant), liver, umbilical vein endothelial cells, peripheral blood leukocytes, foetal cardiomyocytes, lung cell lines, heart and brain. Among the functions of the P2Y₄ receptor are mediation of NO release from endothelial cells to induce vasodilation (Konduri *et al.*, 2004), regulation of epithelial Cl⁻ secretion in jejunum (Ghanem *et al.*, 2005) and modulation of presynaptic glutamate release in hippocampus (Rodrigues *et al.*, 2005).

Mixed agonist responses have been observed between the recombinant P2Y₄ receptors from different species. At the human P2Y₄ receptor, guanosine 5'-triphosphate (GTP) (Communi *et al.*, 1996a; Kennedy *et al.*, 2000), inosine 5'-triphosphate (ITP) (Communi *et al.*, 1996a; Kennedy *et al.*, 2000), INS365 (Pendergast *et al.*, 2001) and INS37217 (Yerxa *et al.*, 2002) are all agonists, while UTP represents the most potent agonist (Communi *et al.*, 1996a; Kennedy *et al.*, 2000). Conversely, ATP acts as a competitive antagonist, while Ap₄A is inactive (Kennedy *et al.*, 2000). In contrast, ATP and UTP activate the recombinant rat (Bogdanov *et al.*, 1998; Kennedy *et al.*, 2000) and mouse P2Y₄ (Lazarowski *et al.*, 2001; Suarez-Huerta *et al.*, 2001) receptors with equal potency, and ITP, GTP and cytidine 5'-triphosphate have low potency. With regard to the conflicting effects of ATP at the P2Y₄ receptor, a study of chimeric human/rat P2Y₄ receptors highlighted the possible role of the N-terminal tail and three residues (asparagine-177, isoleucine-183 and leucine-190) of the second extracellular loop in determining the action of ATP (Herold *et al.*, 2004).

The activity of antagonists at the recombinant P2Y₄ receptor is also variable between species. A maximal response to UTP at human P2Y₄ receptor was reduced by PPADS at 100μM by about 50% (Communi *et al.*, 1996a), however, the actions of UTP at the rat P2Y₄ receptor were not affected by a similar concentration of PPADS (Bogdanov *et al.*, 1998). In addition, RB2 modestly inhibited the UTP-evoked response at the human P2Y₄ receptor (Communi *et al.*, 1996a), but virtually abolished the response to UTP at the rat P2Y₄ receptor (Bogdanov *et al.*, 1998). The only reported consistent effect of an antagonist at this receptor for both species is that of suramin, where at 100μM, it was either ineffective (human) or very weak (rat) at inhibiting the UTP-evoked response (Communi *et al.*, 1996a; Bogdanov *et al.*, 1998).

Interestingly, two receptors from *Xenopus* (p2y8) (Bogdanov *et al.*, 1997) and turkey (p2y) (Boyer *et al.*, 2000) have been identified, which resemble the mammalian P2Y₄ receptor. Upon stimulation, the p2y receptor can activate and inhibit PLC and adenylyl cyclase, respectively, and this indicates a dual coupling of receptor to Gα_{q/11} and Gα_i. Interestingly, a partial inhibition by the Gα_i inhibitor pertussis toxin of the IP₃ rise in response to UTP at the human P2Y₄ receptor has also

been reported (Communi *et al.*, 1996a). Together with the previous view of p2y receptor dual G protein coupling, it could suggest the possible association of P2Y₄ receptor with both G $\alpha_{q/11}$ and G $\alpha_{i/o}$.

2.2.4. P2Y₆ Receptor

The P2Y₆ receptor has been cloned and characterised in rats (Chang *et al.*, 1995), humans (Communi *et al.*, 1996b) and mice (Lazarowski *et al.*, 2001). It is distributed extensively in various tissues, including aorta (most abundant), stomach, mesentery, intestine, spleen and lungs (Chang *et al.*, 1995; see also Table 1.4), which explains the diverse cellular responses. Among such responses are regulation of chemokine production and release in monocytes (Marcet *et al.*, 2007), NaCl secretion in colonic epithelial cells (Köttgen *et al.*, 2003), proliferation of lung epithelial tumor cells (Schäfer *et al.*, 2003), contraction of airway smooth muscles (Govindaraju *et al.*, 2005), prevention of apoptotic cell death by interacting with the tumor necrosis factor- α -related signals (Kim *et al.*, 2003) and mediation of human cerebral artery vasoconstriction (Malmsjö *et al.*, 2003).

The P2Y₆ receptor is the smallest member amongst the P2Y receptors family, with 328 amino acid residues (Communi *et al.*, 1996b). It also displays slow desensitisation and internalisation (Robaye *et al.*, 1997; Brinson & Harden, 2001). This feature could be explained by its short intracellular C-terminal sequence, which effectively lacks the key regulator residues (serine-333 and serine-334) that are essential for agonist-induced phosphorylation, and hence, desensitisation and internalisation (Brinson & Harden, 2001).

UDP is a potent agonist, while the other endogenous nucleotides are rather less active at this receptor, as indicated by the more than 100-fold greater potency of UDP compared to UTP (Communi *et al.*, 1996b; Nicholas *et al.*, 1996). Diuridine 5'-triphosphate acts as a selective agonist at P2Y₆ receptor (Pendergast *et al.*, 2001). The rank order of potency of various agonists at the human P2Y₆ receptor is as follows; UDP > UTP > ADP > 2-MeSATP >> ATP (Communi *et al.*, 1996b). With respect to the antagonist response, a selective and competitive compound for the receptor is yet to be produced. However, the traditional antagonists have provided some useful findings whereby RB2 displays antagonist activity at this receptor,

especially from the human origin, while the antagonist activity of PPADS is slightly less potent at this site (Robaye *et al.*, 1997). The rank order of potency of the antagonists is as follows; RB2 > PPADS > suramin. Recently, Mamedova *et al.*, (2004) showed that three diisothiocyanate derivatives; 1,2-diphenylethane (MRS2567), 1,4-di-(phenylthioureido) butane (MRS2578) and 1,4-phenylendiisothiocyanate (MRS2575) displayed potent antagonist activity at the recombinant P2Y₆ receptor, without affecting the response mediated by other P2Y receptors at concentrations as high as 10µM.

2.2.5. P2Y₁₁ Receptor

To date, humans (Communi *et al.*, 1997; van der Weyden *et al.*, 2000) and dogs (Qi *et al.*, 2001) are the only sources for the cloning and characterisation of the P2Y₁₁ receptor. No gene for this receptor has been detected in rodent genomes, thus explaining the lack of detection of functional P2Y₁₁ receptor in both rat and mouse. mRNA of the receptor can be found in several tissues (see Table 1.4), such as spleen, intestine, skin, and kidney. Effects mediated by this receptor include maturation and migration of dendritic cells (Wilkin *et al.*, 2001) and a secretory role in pancreatic duct epithelial cells (Nguyen *et al.*, 2001).

Variation of pharmacological activities between canine and human P2Y₁₁ receptors has been noted, in agreement with only 70% of the amino acid residues being shared between them (Zambon *et al.*, 2001). This differential selectivity might be explained by the substitution of arginine in the human recombinant receptor for glutamine in the canine counterpart, at position 265, which is located at the junction between TM6 and the third extracellular loop (Qi *et al.*, 2001). Thus, the human recombinant receptor demonstrated a positive tendency towards adenine triphosphate-analogues with an agonist rank order of potency as follows; 2-propylthio-d-β,γ-dichloromethylene-ATP (AR-C67085MX) ≥ adenosine 5'-O-(3-thiotriphosphate) ≈ 2'-3'-O-(4-benzoylbenzoyl)ATP > 2'-deoxyATP > ATP > ADP (Communi *et al.*, 1997, 1999; Qi *et al.*, 2001). UTP, GTP, cytidine 5'-triphosphate, thymidine 5'-triphosphate, ITP and dinucleotides are inactive at this receptor (White *et al.*, 2003). In contrast, a greater potency of diphosphates compared with triphosphates was noted at the canine P2Y₁₁ receptor, i.e. 2-MeSADP > adenosine 5'-

O-(2-thiodiphosphate) > ADP > ATP (Qi *et al.*, 2001). In both species, suramin and RB2 antagonised the receptor, although PPADS is inactive (Communi *et al.*, 1999; Qi *et al.*, 2001).

There are several aspects of human P2Y₁₁ receptors that are unique from other P2Y receptors. These distinct aspects include; its gene contains an intron in the coding sequence, relatively low potency of the natural agonist (ATP), and it stimulates both PLC and adenylyl cyclase, indicating dual coupling to G $\alpha_{q/11}$ and G α_s , respectively (Communi *et al.*, 1997, 1999; Qi *et al.*, 2001).

2.2.6. P2Y₁₂ Receptor

In 2001 the P2Y₁₂ receptor, formerly known as orphan GPCR SP199 or P2T_{AC}, was successfully cloned and characterised in humans (Hollopeter *et al.*, 2001), rats (Hollopeter *et al.*, 2001) and mice (Foster *et al.*, 2001). Distributed in the brain (particularly glial cells), spinal cord and kidney (see Table 1.4), this receptor has many functions, including a role in demyelination and axonal injury in multiple sclerosis (Amadio *et al.*, 2009), and fibrinogen-receptor activation, thrombus formation and recruitment of platelets to injury sites (Gachet *et al.*, 2006).

The photolabelling technique, which utilised radiolabelled GTP, has shown that the receptor is coupled to G α_{i2} (Ohlmann *et al.*, 1995). Although ADP acts as an endogenous agonist at the P2Y₁₂ receptor, it is much less potent compared to 2-MeSADP (Zhang *et al.*, 2001; Hollopeter *et al.*, 2001). The rank order of agonist potency is 2-MeSADP >> ADP \geq adenosine 5'-*O*-(2-thiodiphosphate) (Zhang *et al.*, 2001; Kauffenstein *et al.*, 2004). There have been conflicting reports of the action of ATP at the P2Y₁₂ receptor. Established by its ability to antagonise the ADP-induced adenylyl cyclase inhibition, ATP, after being purified from the ADP contamination, has been confirmed to display an antagonistic effect at both human and mouse P2Y₁₂ receptors in platelets (Kauffenstein *et al.*, 2004). Conversely, in P2Y₁₂-expressing cell preparations, including neurons, ATP and its analogues were shown to behave as agonists (Zhang *et al.*, 2001; Unterberger *et al.*, 2002; Ennion *et al.*, 2004). With respect to antagonists, both RB2 and suramin are active, while PPADS is inactive (Takasaki *et al.*, 2001; Zhang *et al.*, 2001). Several potent antagonists have been developed, including N⁶-2-(methylthioethyl)-2-(3,3,3-trifluoropropylthio)- β , γ -

dichloromethyl ATP (AR-69931MX or cangrelor) (Ingall *et al.*, 1999) and 3-{7-[2-3,4-difluoro-phenyl-cyclopropylamino]-5-propylsulfanyl [1,2,3]triazolo[4,5-*d*]pyrimidine-3-yl}-5-(2-hydroxymethoxy)-cyclopentane-1,2-diol (AZD6140), an orally active anti-platelet aggregation compound, which has been shown, from the outcomes of its phase III clinical trial (PLATO trial), to reduce the rate of death from various cardiovascular conditions, such as myocardial infarction, without a significant increase in the rate of bleeding in patients with acute coronary syndromes (Wallentin *et al.*, 2009).

2.2.7. P2Y₁₃ Receptor

The P2Y₁₃ receptor has been cloned and characterised in humans (Communi *et al.*, 2001), mice (Zhang *et al.*, 2002) and rats (Fumagalli *et al.*, 2004). The function of the receptor is not entirely clear, although its mRNA is abundant in the spleen and brain (Communi *et al.*, 2001; Fumagalli *et al.*, 2004). Additionally, it has been detected in other tissues or organs, such as the placenta, liver, bone marrow, lung and heart (Zhang *et al.*, 2002; see also Table 1.4). ADP-mediated effects at P2Y₁₃ receptor, including increased binding of radiolabelled guanosine 5'-O-(3-thiotriphosphate) (GTPγ[³⁵S]), inhibition of cAMP formation and phosphorylation of ERK1/2, can be inhibited by pertussis toxin, indicating coupling of the receptor with Gα_{i/o} (Communi *et al.*, 2001; Marteau *et al.*, 2003).

ADP and diadenosine 5'-triphosphate act as naturally occurring agonists (Zhang *et al.*, 2002; Marteau *et al.*, 2003), while ATP, after purification, either behaves as a weak partial agonist (Marteau *et al.*, 2003) or is virtually inactive (Communi *et al.*, 2001). The relative agonist potency of ADP and 2-MeSADP at the P2Y₁₃ receptor varies between species and cell preparations. Human P2Y₁₃ receptors expressed in CHO-K1 cells were activated by ADP and 2-MeSADP with equal potency in decreasing the cAMP formation (Marteau *et al.*, 2003). However, the same study showed that by using 1321N1 cells, 2-MeSADP was more potent than ADP in displacing [³³P]2-MeSADP from the receptor, and inducing binding of GTPγ[³⁵S] to G proteins. Additionally, 2MeSADP was also more potent than ADP in inducing glycogen synthase kinase-3 phosphorylation in the rat granule neurons (Ortega *et al.*, 2008). A contrasting finding, however, was observed in rat P2Y₁₃ receptor-

expressing 1321N1 cells whereby the potency of ADP was greater than 2MeSADP in inducing binding of GTP γ [³⁵S] to G proteins (Fumagalli *et al.*, 2004). Multiple conformations, kinetics, and preference for G proteins could possibly account for such variable relative potency of ADP and 2-MeSADP. Suramin, PPADS, Ap₄A and 2-methylthio-adenosine 5'-monophosphate as well as the previously recognised as P2Y₁₂ selective antagonist, cangrelor, are all antagonists at this receptor, with a rank order of potency of; cangrelor > suramin > PPADS (Marteau *et al.*, 2003).

2.2.8. P2Y₁₄ Receptor

Previously known as GPR105, KIAA0001 and UDP-glucose receptor, this receptor is 18 - 45% identical to other human P2Y receptors, and has the highest sequence homology with the P2Y₁₂ and P2Y₁₃ receptors (Abbracchio *et al.*, 2003). The amino acid sequence of the human P2Y₁₄ receptor has 80% and 89% similarity to that of rat and mouse counterparts, respectively (Freeman *et al.*, 2001). The distribution of P2Y₁₄ mRNA in human body includes the placenta, adipose tissue, brain, stomach, intestine, lungs, heart bone marrow and thymus (Charlton *et al.*, 1997; Chambers *et al.*, 2000; Freeman *et al.*, 2001; see also Table 1.4). Additionally, the mRNA is also abundantly found in rat brain (Charlton *et al.*, 1997). The role of this receptor is not completely understood. It couples to the G $\alpha_{i/o}$ protein to mediate its action (Chambers *et al.*, 2000; Moore *et al.*, 2003).

There is relatively little knowledge about the pharmacological properties of this receptor, although it is so far exclusively activated by sugar nucleotides (UDP) with a rank order as follows; UDP-glucose > UDP-galactose > UDP-glucuronic acid > UDP-*N*-acetylglucosamine (Chambers *et al.*, 2000). The antagonist activity remains to be defined as study is yet to be conducted to explore the effect of currently available P2 receptor antagonists. However, Fricks *et al.*, (2008) demonstrated that UDP can act as a competitive antagonist and agonist at the recombinant human and rat P2Y₁₄ receptors, respectively, which were transiently coexpressed with the recombinant G $\alpha_{q/i}$ in cell lines. Interestingly, their subsequent study that utilised a native G protein signalling system found that UDP acted as a full agonist with similar potency and efficacy to UDP-glucose at the recombinant human P2Y₁₄ receptor stably expressed in cell lines (Carter *et al.*, 2009). They suggested that these

differential findings could be due to the level of signalling proteins and the types of G protein associated with the signalling system that might influence the receptor activation by a ligand and the subsequent responses.

2.3. Synthetic P2Y Receptor Agonists

Determination of the functions of P2Y receptors has been hindered by a lack of subtype-selective agonists and antagonists. In recent years analogues of dinucleotides have been found to display a degree of selectivity. In addition, dinucleotides are relatively more resistant against the enzymatic degradation compared to mononucleotides (Yerxa *et al.*, 2002; Shaver *et al.*, 2005). For example, INS365 showed a higher potency at the recombinant human P2Y₂ and P2Y₄ receptors than P2Y₆ receptors, with EC₅₀ values of 0.1 – 0.27, 0.4 – 1.22µM, and 16 – 20µM, respectively (Pendergast *et al.*, 2001; Yerxa *et al.*, 2002; Shaver *et al.*, 2005). In contrast, diuridine 5'-triphosphate demonstrated more potent agonist activity at the P2Y₆ receptor than at P2Y₂ and P2Y₄ receptors, by at least 10-fold (EC₅₀ = 22, >100 and 0.2µM, at P2Y₂, P2Y₄ and P2Y₆ receptors, respectively), and was inactive at P2Y₁ receptor (Pendergast *et al.*, 2001). In addition, its potency at P2Y₆ receptor is comparable with UDP (EC₅₀ = 0.042 – 0.1µM) (Pendergast *et al.*, 2001; El-Tayeb *et al.*, 2006).

The drug company Inspire Pharmaceuticals (Durham, USA) have studied and developed several compounds that display a degree of P2Y receptor-subtype selectivity. Of particular relevance to this thesis are two dinucleotides derivatives, P¹-(uridine 5'-),P⁴-(inosine 5'-) tetraphosphate (INS45973) and P¹-((2-benzyl-1,3-dioxolo-4-yl)uridine 5') P³-(uridine 5'-)triphosphate (INS48823). These two compounds are particularly useful for characterising the P2Y receptor-mediated contraction in the pulmonary artery since they have high selectivity at the P2Y subtypes of which the mRNA is expressed in this vessel (Gui *et al.*, 2008). Additionally, a mononucleotide, 3-(2-oxo-2-phenylethyl) UDP (3-phenacyl UDP), which is an agonist with selectivity at the P2Y₆ receptor, is also a valuable tool for this investigation.

2.3.1. INS45973

INS45973 is an analogue of the naturally occurring dinucleotide P2Y agonist Up₄A (Jacobson *et al.*, 2009; Jankowski *et al.*, 2009). While inactive at the human P2Y₁ receptors, this agonist is highly potent at the recombinant human P2Y₂ and P2Y₄ receptors, but not P2Y₆ receptors in elevating [Ca²⁺]_i (EC₅₀ of 0.52, 0.28 and >10μM for P2Y₂, P2Y₄ and P2Y₆ receptors, respectively) (Shaver *et al.*, 2005). When compared with UTP, it is less potent at the P2Y₂ receptor, but has a similar potency at the P2Y₄ receptor (EC₅₀ of UTP = 0.03 and 0.1μM, at P2Y₂ and P2Y₄ receptors, respectively) (Pendergast *et al.*, 2001). To date, limited data are available on the effects of INS45973 in tissues or animals, although it was found to be effective in stimulating vaginal moisture in the ovariectomised rabbit via P2Y₂ receptor activation (Min *et al.*, 2003), and has been shown to activate presynaptic inhibition of glutamate release from the nerve terminal in rat hippocampus via P2Y₂ and/or P2Y₄ receptors (Rodrigues *et al.*, 2005).

2.3.2. INS48823

Another dinucleotide P2Y agonist INS4882 has a high potency at the recombinant human P2Y₆ receptor (EC₅₀ of 0.125μM), with no appreciable activity at P2Y₁, P2Y₂ or P2Y₄ receptors, in inducing the elevation of [Ca²⁺]_i (Korcok *et al.*, 2005). Its potency at P2Y₆ receptor is comparable with UDP (EC₅₀ = 0.042 – 0.1μM) (Pendergast *et al.*, 2001; El-Tayeb *et al.*, 2006). The biological profile of activity of this agonist has been studied in several intact tissues and native cell preparations. In human dendritic cells, INS48823 induced the release of the chemokine CCL20 with an EC₅₀ of 12.7 ± 4.4μM and at 100μM, INS48823 was more effective than UDP in stimulating CCL20 release in the human airway epithelial cells (Marcet *et al.*, 2007). Likewise, INS48823 induced higher rabbit oestoclast survival than UDP at 10μM for both agonists (Korcok *et al.*, 2005). However, INS48823 and UDP were equi-effective in inducing Cl⁻ secretion in the mouse trachea (Schreiber & Kunzelmann, 2005).

2.3.3. 3-Phenacyl UDP

3-phenacyl UDP is a P2Y₆ selective agonist, which is synthesised by adding a large phenacyl residue at N3 position of UDP. In cell lines expressing recombinant human P2Y receptors it induced an increase in [³H]inositol phosphates with EC₅₀ values of 40, >100 and 0.07μM at P2Y₂, P2Y₄ and P2Y₆ receptors, respectively (El-Tayeb *et al.*, 2006). In contrast, it failed to induce a rise of intracellular Ca²⁺ at concentrations of up to 10μM in rat basophilic leukemia-2H3 cells, which express an abundant level of native P2Y₁₄ receptor compared to P2Y₂, P2Y₄ and P2Y₆ receptors (Gao *et al.*, 2010). Information on the biological profile of activity of 3-phenacyl UDP is very limited, although Kauffenstein *et al.*, (2010) have recently shown that 3-phenacyl UDP evoked vasoconstriction of thoracic aorta from the transgenic mice lacking nucleoside triphosphate diphosphohydrolase-1 (NTPDase1), with a potency of about 20-fold lower than UTP and UDP (EC₅₀ = 22.8 ± 12.4μM, 1.06 ± 0.64μM, 1.76 ± 0.94μM for 3-phenacyl UDP, UTP and UDP, respectively).

3. P2Y RECEPTOR AND PULMONARY ARTERIAL SMOOTH MUSCLE

3.1. Distribution and Action of P2Y Receptor

Initially, on the basis of pharmacological responses, it was suggested that in pulmonary arteries P2Y receptors were restricted to the endothelium while P2X receptors, and more specifically the P2X₁ subtype, were primarily expressed in smooth muscle (Liu *et al.*, 1989). However, contraction of the pulmonary artery smooth muscle can also be evoked after P2X receptor blockade, thus clearly indicating the presence of P2Y receptors in the smooth muscle (Rubino & Burnstock, 1996). At present, it is not exactly clear which P2Y subtypes are expressed in pulmonary artery smooth muscle, although Hartley *et al.*, (1998) have identified P2Y₆ receptor mRNA in this tissue. Additionally, the mRNA of four P2Y receptors (P2Y_{1, 2, 4, 6}) has been detected in the pulmonary artery (Konduri *et al.*, 2004; Gui *et al.*, 2008). In other vascular smooth muscle, such as aorta, P2Y₂ and P2Y₆ transcripts were found to be the most abundant, while P2Y₁ is the least or barely detected, and P2Y₄ was only moderately expressed (Erlinge *et al.*, 1998). Wihlborg *et al.*, (2004) have recently reported seven P2Y (P2Y_{1, 2, 4, 6, 11, 12, 13}) receptors in the human mammary vascular smooth muscle through pharmacological profile and mRNA/protein detection. They also found that P2Y₂ receptor mRNA appeared the most abundant. In human mammary vascular tissue, P2Y₁₁ mRNA expression was again detected, although the Western blotting was unable to confirm the protein expression in this tissue (Wang *et al.*, 2002).

Consistent with the previous view on the distribution of P2 receptors, the purine-evoked contraction of vascular smooth muscle was also originally believed to be mediated primarily by P2X receptors, with no contribution from P2Y receptors (Burnstock & Kennedy, 1986). Nevertheless, the involvement of P2Y receptors was apparent when desensitisation and hence inhibition of P2X₁ receptors by α,β -MeATP did not abolish ATP- and UTP-evoked vasoconstriction. In the rat tail artery, α,β -MeATP desensitisation reduced the peak responses evoked by ATP and UTP to about 20% and 70%, respectively of control (McLaren *et al.*, 1998). In rat pulmonary artery, suramin reduced the maximal contractile response of UTP and UDP to about 57% and 76%, respectively (Hartley *et al.*, 1998). Thus, it might indicate the presence of two receptors; one is UTP-activated and suramin-sensitive,

while the other receptor is activated by UDP, and relatively resistant to suramin. Additionally, another study in rat pulmonary artery further supported the view of the possible existence of two distinct P2Y receptors to evoke UTP/UDP-mediated contraction. At one site, the agonist response is insensitive to suramin, PPADS and RB2, while the other site is resistant to PPADS and RB2, but sensitive to suramin (Chootip *et al.*, 2002).

3.2. Possible Physiological and Pathological Functions of Pulmonary P2 Receptors

As mentioned above, a complex balance of factors maintain the pulmonary arteries in a dilated, low-resistance state that maximises the delivery of deoxygenated blood to the alveoli (Barnes & Liu, 1995). Nucleotides appear to contribute to this state as ATP, which is present in red blood cells at mM levels (Erlinge & Burnstock, 2008), is released from these cells as they pass through the pulmonary arterial bed and acts at endothelial P2Y receptors to induce release of NO from the endothelial cells, which in turn acts on the arterial smooth muscle to decrease vascular resistance (Sprague *et al.*, 1996, 2003).

Vasoconstriction mediated by the smooth muscle P2X and P2Y receptors is likely to be prominent when endothelial-relaxant function is compromised, particularly in the pathological conditions, such as hypoxia- or monocrotaline-induced pulmonary hypertension (Adnot *et al.*, 1991; Mam *et al.*, 2010) and chronic obstructive pulmonary disease (Dinh-Xuan *et al.*, 1991). Indeed, extracellular ATP is elevated in the latter disease, which would increase the contribution of P2 receptors to artery regulation. The smooth muscle P2X and P2Y receptors also appear to play a role in hypoxic pulmonary vasoconstriction, as the P2 receptor antagonist suramin inhibited this response in perfused rabbit lungs (Baek *et al.*, 2008). Thus, given the potential roles of nucleotides in both physiological and pathophysiological states, it is important to understand the mechanisms that couple P2 receptors to the constrictor response.

3.3. Mechanisms of P2Y Receptor-Mediated Contraction

As previously noted in section 1.2.1, elevation of $[Ca^{2+}]_i$ via both influx of extracellular Ca^{2+} and release of intracellular Ca^{2+} stores is fundamental for triggering smooth muscle contraction. However, the contribution of extracellular Ca^{2+} influx in P2Y receptor-mediated contractions of the pulmonary arterial smooth muscle has yet to be studied. Nonetheless, the slower, tonic phase of UTP-evoked contractions in the rat tail artery was partially inhibited by Ca^{2+} free external solution (McLaren *et al.*, 1998), indicating that Ca^{2+} influx was induced following P2Y receptor activation. Additionally, various vessels, including rat femoral artery (Saïag *et al.*, 1990), rat aorta (López *et al.*, 2000), rat coronary artery (Welsh & Brayden, 2001) and bovine cerebral artery (Miyagi *et al.*, 1996), also show a degree of dependency on the Ca^{2+} influx for the contractile responses induced by P2Y receptor stimulation.

The complete view on the mechanism of P2Y receptor-mediated contraction in pulmonary smooth muscle remains unclear, and is complicated by the multiple interactions between the signalling pathways within the cellular system. Therefore, further investigation is indeed necessary to clarify this issue. Two main areas were of particular interest in this study; 1) the contribution of PLC/IP₃-mediated signalling pathway, particularly on the elevation of $[Ca^{2+}]_i$, and 2) the sensitisation of contractile proteins to Ca^{2+} .

3.4. PLC/IP₃-Mediated Signalling in the Elevation of $[Ca^{2+}]_i$

To date, several line of evidence have indicated that stimulation of P2Y receptors in vascular smooth muscle leads to the activation of PLC (Murthy & Makhlof, 1998), increased IP₃ production (Flitz *et al.*, 1994; Harper *et al.*, 1998), and release of intracellular Ca^{2+} stores (Saino *et al.*, 2002; Meng *et al.*, 2007). With respect to the rat pulmonary artery smooth muscle, Zheng *et al.*, (2005) recently reported that ATP stimulated an intracellular Ca^{2+} release, which was rather resistant to a ryanodine receptor antagonist. A transient $[Ca^{2+}]_i$ oscillation preceded by a small maintained $[Ca^{2+}]_i$ rise was also induced by ATP in rat isolated pulmonary artery smooth muscle cells (Guibert *et al.*, 1996; Pauvert *et al.*, 2000). The transient $[Ca^{2+}]_i$ oscillation was not affected by either zero Ca^{2+} solution or the Ca^{2+} -induced Ca^{2+} release (CICR)

blocker, tetracaine (Guibert *et al.*, 1996). However, thapsigargin, the sarcoplasmic reticulum Ca^{2+} pump inhibitor, abolished this $[\text{Ca}^{2+}]_i$ oscillation, thus indicating a considerable contribution of the IP_3 -dependent, but not CICR-dependent Ca^{2+} release from the intracellular stores in evoking this transient $[\text{Ca}^{2+}]_i$ rise. In addition, inhibition of IP_3 formation by the cAMP-elevating agent, forskolin (Berman *et al.*, 1994), which acts via the protein kinase A-mediated phosphorylation of G proteins and/or PLC (Kim *et al.*, 1989), reduced the frequency of the transient $[\text{Ca}^{2+}]_i$ oscillation (Guibert *et al.*, 1996). The PKC activator, phorbol 12, 13-dibutyrate (PDB), which also inhibits IP_3 formation (McMillan *et al.*, 1989), reduced the frequency and amplitude of the ATP-evoked transient $[\text{Ca}^{2+}]_i$ oscillation, together with delaying the first $[\text{Ca}^{2+}]_i$ transient response (Guibert *et al.*, 1996). This PDB-induced inhibitory effect was reversed by calphostin C, the PKC inhibitor (Guibert *et al.*, 1996) and hence, these results further support the involvement of IP_3 in mediating P2Y receptor-evoked $[\text{Ca}^{2+}]_i$ rise.

3.5. Ca^{2+} Sensitisation Pathways

Contraction of smooth muscle is governed by phosphorylation of the MLC at serine-19, which is mainly mediated by Ca^{2+} -dependent mechanism, i.e. Ca^{2+} -calmodulin-dependent MLCK. Simultaneously, the phosphorylation of MLC can also be reversed by the endogenous enzyme, MLCP to bring about smooth muscle relaxation (Somlyo & Somlyo, 2003). This dephosphorylating enzyme can be modulated by $[\text{Ca}^{2+}]_i$ -independent mechanisms, termed Ca^{2+} sensitisation. These mechanisms have one feature in common; their ability to regulate Ca^{2+} sensitivity of MLC phosphorylation and contraction by influencing MLCP activity (Somlyo & Somlyo, 2000). Three main mechanisms or signalling pathways have been implicated, RhoA/Rho kinase pathway, PKC pathway and an arachidonic acid-mediated mechanism. The third of these mechanisms is generally associated with inhibition of the MLCP activity by dissociating its regulatory and catalytic subunits, and may also indirectly influence the MLCP activity by the RhoA-independent activation of Rho kinase (Somlyo & Somlyo, 2003). Only the first two mechanisms will be discussed here in detail.

3.5.1. RhoA/Rho Kinase Pathway

The substantial involvement of the RhoA/Rho kinase pathway in modulating Ca^{2+} sensitisation has been emphasised in several recent reviews (Somlyo & Somlyo, 2000, 2003; Loirand *et al.*, 2006). RhoA, a monomeric GTPase, belongs to a Rho-like subfamily of Rho proteins, and acts as a molecular switch for this pathway. The trimeric G proteins, mainly $\text{G}\alpha_{12}$ and $\text{G}\alpha_{13}$, and to a lesser extent $\text{G}\alpha_q$ and $\text{G}\alpha_{i-2}$, play a role in inducing RhoA and GTP interaction via a family of guanine nucleotide exchange factors (RhoGEF), such as p115RhoGEF. Subsequently, the translocation of the activated RhoA/GTP complex to the plasma membrane stimulates several target proteins, including the serine/threonine kinase, Rho kinase. Rho kinase has two isoforms; Rho kinase-1 and Rho kinase-2, of 1354 and 1388 amino acids, respectively and both amino acid sequences are highly conserved, with an overall of 65% homology. The mechanism of Rho kinase activation by this complex has not yet been fully characterised, however, it appears that the translocation of this complex to the plasma membrane is essential in inducing Rho kinase activation. Once activated, Rho kinase phosphorylates the MLCP targeting subunit (MYPT-1), the regulatory subunit of MLCP, at several sites, including threonine-697 and threonine-855 in rat (Tsai & Jiang, 2006; Knock *et al.*, 2008), and threonine-853 in rabbit (Dimopoulos *et al.*, 2007), and essentially inhibits this phosphatase activity, leading to increased contraction without a rise in $[\text{Ca}^{2+}]_i$. Numerous studies investigating the involvement of Rho kinase-mediated Ca^{2+} sensitisation in smooth muscle contractions have commonly used Rho kinase inhibitors, such as (R)-(+)-*trans*-N-(4-pyridyl)-4-(1-aminoethyl)-cyclohexanecarboxamide dihydrochloride monohydrate (Y27632) (Swärd *et al.*, 2000) and 1-(5-isoquinolinylsulfonyl) homopiperazine dihydrochloride (HA1077) (Nagumo *et al.*, 2000).

A contribution of Ca^{2+} sensitisation via Rho kinase in P2Y receptor-mediated contraction in pulmonary smooth muscle has been reported by Jernigan *et al.*, (2004) when UTP-evoked vasoconstriction was virtually abolished by Y27632 in membrane permeabilised rat pulmonary artery. Additionally, the association of the RhoA/Rho kinase pathway and P2Y receptor stimulation in rat aortic smooth muscle has also been investigated (Sauzeau *et al.*, 2000). Stimulation of P2Y receptors increased the amount of membrane-bound RhoA and induced actin stress fiber formation that was

sensitive to RhoA and Rho kinase inhibitors, such as C3 exoenzyme and Y27632, respectively. When an inactive form of RhoA was expressed in the myocytes, the nucleotide-induced actin cytoskeleton formation in these cells was eliminated. Additionally, Jankowski *et al.*, (2003) also demonstrated that the P2Y receptor-evoked contractions of renal glomerulus smooth muscle induced by ATP, ADP and UTP were abolished in the presence of Y27632. However, the contraction stimulated by a potent P2Y₁ receptor agonist, 2-MeSATP, was not affected by this Rho kinase inhibitor. This might suggest a lack of involvement of Rho kinase in P2Y₁ receptor signalling mechanism.

Rho kinase-mediated Ca²⁺ sensitisation was also reported in contractions induced by several agonists in various tissues including; rat pulmonary artery evoked by PGF_{2α} (Knock *et al.*, 2008), rat tail artery evoked by thromboxane A₂ analogue U-46619 (Wilson *et al.*, 2005), and guinea pig ileum evoked by G protein activator, GTPγS (Swärd *et al.*, 2000). Interestingly, Ca²⁺ sensitisation also appears to play a role in KCl-induced smooth muscle contraction and this was initially demonstrated when depolarisation by high K⁺ increased the Ca²⁺ sensitivity in the canine coronary artery (Yanagisawa & Okada, 1994). In addition, recent reviews (Ward *et al.*, 2004; Ratz *et al.*, 2005) further highlighted the association of KCl contractions and Ca²⁺ sensitisation. In several tissues Y27632 substantially inhibited contractions induced by KCl, but without altering the rise in cytoplasmic [Ca²⁺] (Mita *et al.*, 2002; Urban *et al.*, 2003). Urban *et al.*, (2003) further revealed that the KCl-induced response was associated with the induction of Rho kinase translocation from the cytosol to the cell periphery, i.e. caveolae, and was dependent on Ca²⁺. Ca²⁺-dependent activation of Rho kinase was also implicated in KCl-induced contraction of rabbit thoracic aorta, with the upstream mechanism involving the activation of calmodulin and Ca²⁺/calmodulin-dependent protein kinase-II to induce the formation of the Rho/GTP complex (Sakurada *et al.*, 2003). Furthermore, Ca²⁺-independent phospholipase A₂ can also mediate Rho kinase activation and contribute to KCl-induced contractions of rabbit femoral and renal arteries (Ratz *et al.*, 2009).

3.5.2. PKC Pathway

PKC is a serine/threonine kinase and consists of at least 12 isoforms, which are divided into three main groups; conventional (α , β_I , β_{II} , γ), novel (δ , ϵ , η , θ , μ) and atypical (ζ , ι , λ). Five of the PKC isoforms (α , β_I , β_{II} , δ , ϵ and ζ) are expressed in vascular smooth muscles (Cogolludo *et al.*, 2003; Dallas & Khalil, 2003; Andrassy *et al.*, 2005). Inactive PKC, which is located mainly in the cytosolic compartment, translocates to the plasma membrane upon activation (Cogolludo *et al.*, 2003; Dallas & Khalil, 2003). There are several pathways through which PKC mediates the smooth muscle contractile response. One possible pathway involves Ca^{2+} sensitisation mediated by CPI-17, a 17-kDa peptide which was first extracted from porcine aorta (Somlyo & Somlyo, 2003; Ward *et al.*, 2004). This 17-kDa peptide is activated by phosphorylation of its threonine-38 residue by several kinases, including PKC. Li *et al.*, (1998) have shown that phosphorylation and activation of CPI-17 was mainly dependent on PKC and at a constantly low $[Ca^{2+}]_i$, phosphorylated, but not non-phosphorylated CPI-17, was able to induce contractions of membrane-permeabilised rabbit artery smooth muscle by more than 70%. Furthermore, the rate of MLC dephosphorylation by MLCP, measured after the tissue was sub-maximally contracted and treated with 1-(5-chloronaphthalene-1-sulfonyl)-1*H*-hexahydro-1,4-diazepine (ML-9) to abolish the effect of MLCK, was significantly reduced in the presence of phosphorylated CPI-17 compared to control, indicating the profound inhibitory effect of CPI-17 on MLCP function to dephosphorylate MLC. Another mechanism by which PKC mediates contractions is via the regulation of voltage-dependent $Ca_v1.2$ channel activity, which effectively alters the intracellular concentration of Ca^{2+} . Cobine *et al.*, (2007) showed that PKC directly potentiated the activity of $Ca_v1.2$ channels during active tone development of endothelium-denuded rabbit coronary artery. In contrast, PKC also activated this ion channel indirectly by depolarising the membrane through inhibition of voltage-gated K^+ channels (Cogolludo *et al.*, 2003).

Although direct evidence to link the P2Y receptors to PKC/CPI-17-associated Ca^{2+} sensitisation in the pulmonary artery smooth muscle remains to be established, other GPCRs have been shown to activate this signalling pathway. In rabbit femoral artery, Kitazawa *et al.*, (2000) has shown that phenylephrine (α_1 -agonist) and

histamine triggered smooth muscle contraction comparable to that induced by high K^+ , however Western blotting only detected phosphorylated CPI-17 after agonist stimulation and not after high K^+ stimulation. Phosphorylated CPI-17 was also detected when the tissue was treated with $GTP\gamma S$, whereas there was no increase after high $[Ca^{2+}]$ concentration, although both interventions initiated contractile response of this tissue. Equally, the contraction and phosphorylation of CPI-17 induced by histamine was significantly reduced after exposure to guanosine 5'-*O*-(2-thiodiphosphate), a G protein inhibitor, thus suggesting that CPI-17 activation is associated with G protein activity, but independent of Ca^{2+} . Reduction of the histamine-induced contraction and CPI-17 phosphorylation were also seen following treatment with PKC inhibitor 2-[1-(3-Dimethylaminopropyl)-1H-indol-3-yl]-3-(1H-indol-3-yl) maleimide (GF109203X), while only partial reduction was noted with Y27632. These results underline the ability of PKC, and Rho kinase to some extent, to regulate CPI-17 activity. Interestingly, CPI-17 expression level in blood vessels also varies; highest in tonic and lowest in phasic smooth muscles (Somlyo & Somlyo, 2003).

In addition to the involvement in the contractions evoked by various agonists, PKC may also play a role in KCl-induced contractile responses. Although Ratz *et al.*, (2005) had emphasised that the contribution of PKC is minimal, if not absent, in the responses induced by KCl, their more recent papers did show a role for an atypical PKC isoform, PKC ζ , in the KCl-induced vasoconstriction of rabbit femoral and renal arteries (Ratz & Miner, 2009; Ratz *et al.*, 2009). The contractions of aorta and mesenteric arteries induced by KCl were also inhibited by the PKC inhibitor 3-[1-[3-(amidinothio)propyl-1H-indol-3-yl]-3-(1-methyl-H-indol-3-yl) maleimide (Ro 31-8220) (Budzyn *et al.*, 2006). Thus, these data suggest that PKC does appear to play a role in vasoconstriction to KCl stimulation.

3.5.3. Possible Role of Ca^{2+} sensitisation in Pulmonary Vascular Disease

The association of Ca^{2+} sensitisation via the Rho kinase-dependent pathway with the pathophysiology of pulmonary vascular disease, particularly pulmonary hypertension, has been widely studied. Although structural remodelling of pulmonary arteries leading to a fixed elevation of pulmonary resistance is associated

with pulmonary hypertension, sustained vasoconstriction also plays an important role in this pathological condition (Loirand *et al.*, 2006). An increase in both basal tone of the isolated pulmonary artery and pulmonary arterial pressure of the isolated lungs is seen in chronically hypoxic rats (Adnot *et al.*, 1991; Nagaoka *et al.*, 2004; Broughton *et al.*, 2008) and in both cases the increase was depressed by Rho kinase inhibitors. Additionally, the contractile responses of pulmonary artery from hypoxic animal models to GPCR agonists are enhanced compared to the normoxic counterpart. For example, Robertson *et al.*, (2000) showed that the response of rat pulmonary artery to PGF_{2α} was greater in vessels that had been exposed to sustained hypoxia, and the increase was virtually abolished by Y27632. The contribution of Ca²⁺ sensitisation to ET-1-induced contractions is greatly increased in pulmonary artery from chronically hypoxic rats, compared to normoxic controls (Weigand *et al.*, 2006). Interestingly, Jernigan *et al.*, (2004) demonstrated larger UTP-evoked vasoconstriction of permeabilised pulmonary artery from chronically hypoxic than control rats, and this contractile response was inhibited by Y27632. Finally, in rats in which pulmonary thromboembolic-associated pulmonary hypertension was induced by injecting microspheres into the right ventricles, a rise in the plasma ET-1 level and lung Rho kinase expression was seen (Toba *et al.*, 2010). Infusion of the Rho kinase inhibitors HA1077 or Y27632 caused an improvement of right ventricular systolic pressure, arterial oxygen tension and alveolar-arterial difference in PaO₂.

The above studies clearly show an important role for Ca²⁺ sensitisation via Rho kinase in the development of pulmonary hypertension. However, only one study so far actually examined the contribution of P2Y receptors in this pathological condition, therefore, a better understanding of the signalling mechanisms, especially Rho kinase-mediated Ca²⁺ sensitisation pathway, of pulmonary artery contractions evoked by P2Y receptors activation is essential.

4. AIMS OF THE STUDY

The main aim of my project is to study the intracellular pathways through which P2Y receptor agonists induce pulmonary vasoconstriction, in particular PLC, PKC and Ca^{2+} sensitisation of contractile proteins via Rho kinase. Initially, it was necessary to establish a protocol for studying P2Y receptor-mediated vasoconstriction by adding UTP and UDP to rat isolated small intrapulmonary artery (SPA) to characterise the basic profile of the tissue's contractile responses, the influence of the endothelium and the reproducibility of the P2Y receptor-mediated contraction. In order to investigate the involvement of several potential signalling mechanisms that might underlie this vasoconstriction, a number of compounds were used; 1-[6-[[[(17 β)-3-methoxyestra-1,3,5(10)-trien-17-yl]amino]hexyl]-1*H*-pyrrole-2,5-dione (U73122) and 1-[6-[[[(17 β)-3-methoxyestra-1,3,5(10)-trien-17-yl]amino]hexyl]-2,5-pyrrolidinedione (U73343), the selective phosphatidylinositol (PI)-PLC inhibitor and its inactive analogue, respectively, Y27632 and GF109203X, the inhibitors of Rho kinase and PKC, respectively, and suramin, the non-selective P2 receptor antagonist. The selectivity of Y27632 and potency of GF109203X were first assessed against the contractile response of pulmonary artery evoked by the PKC activator, phorbol 12-myristate 13-acetate (PMA). The effects of the above compounds on the nucleotide-evoked vasoconstriction were then investigated in the intact rat SPA preparation.

The next step was to establish the optimum conditions for the permeabilisation of rat SPA by focusing on several key issues; 1) effect of temperature on the contractile activity of the intact rat SPA, 2) preparation of permeabilising solution at various free $[\text{Ca}^{2+}]$, 3) effectiveness of the permeabilising agents, β -escin and α -toxin, and reproducibility of contractions of the permeabilised tissue and 4) the requirement for ATP in the permeabilisation solution. After successfully optimising the membrane-permeabilised technique, the study was continued, using this technique, to investigate directly the role of Ca^{2+} sensitisation in P2Y receptor-mediated contractions of rat SPA, in particular to establish whether Rho kinase and PKC were involved in mediating the UTP- and UDP-evoked contractions via Ca^{2+} sensitisation. Finally, the study further characterised the P2Y receptor-mediated vasoconstriction of rat SPA by using three selective P2Y agonists; INS45973, selective at P2Y₂ and P2Y₄ receptors,

and INS48823 and 3-phenacyl UDP, selective at P2Y₆ receptors. It was carried out both in the intact and membrane-permeabilised preparations.

Chapter 2:

Materials and Methods

1. CONTRACTILE STUDIES

1.1. Tissue Preparation

Animals used in this study were obtained from licensed breeders and housed in the Biological Procedures Unit within the University of Strathclyde. Male Sprague-Dawley rats (150 – 250g) were killed according to Schedule 1 of U.K. Home Office Regulations by cervical dislocation. Thoracotomy was performed immediately to remove the heart and lung *en bloc*, which were placed in a salt solution composed of (mM): NaCl 122; KCl 5, N-[2-hydroxyethyl]piperazine-N'-[2-ethane-sulphonic acid] (HEPES) 10; KH₂PO₄ 0.5; NaH₂PO₄ 0.5; MgCl₂ 1; glucose 11; CaCl₂ 1.8, titrated to pH 7.3 with NaOH and bubbled with medical air (21% O₂, 5% CO₂, 70% N₂). All the lung lobes except for the anterior right lobe (Figure 2.1a) were isolated and used in this study. Each lobe was pinned onto a dissecting dish and bathed in buffer. Under a dissecting microscope, an incision was made from the proximal airway along the bronchial tree to distal bronchus (Figure 2.1b, insert) to facilitate visualisation of the main intrapulmonary artery located inferior to the airway. The bronchial tissue was then carefully removed to expose this artery and after removing the surrounding tissue, a section of this artery with an internal diameter 300µm - 500µm (SPA) was dissected (Figure 2.1, 2.2).

The endothelium of the artery was removed as appropriate by rubbing the vessel lumen gently with a thread. The vessels were cleaned of extra connective tissues, cut into rings about 5mm long and mounted horizontally in 1ml baths on a pair of platinum intraluminal wires (diameter = 125µm) (Figure 2.2). The lower wire was hooked inside the bath while the upper wire was attached to a Grass FTO3 isometric force transducer connected to a MacLab/4e system, using Chart 3.3 software (AD Instruments). Tissues were stretched with care and equilibrated under a resting tension of 0.5g for 60 min at 37°C in fresh buffer. During this period the tissues were washed every 15 min.

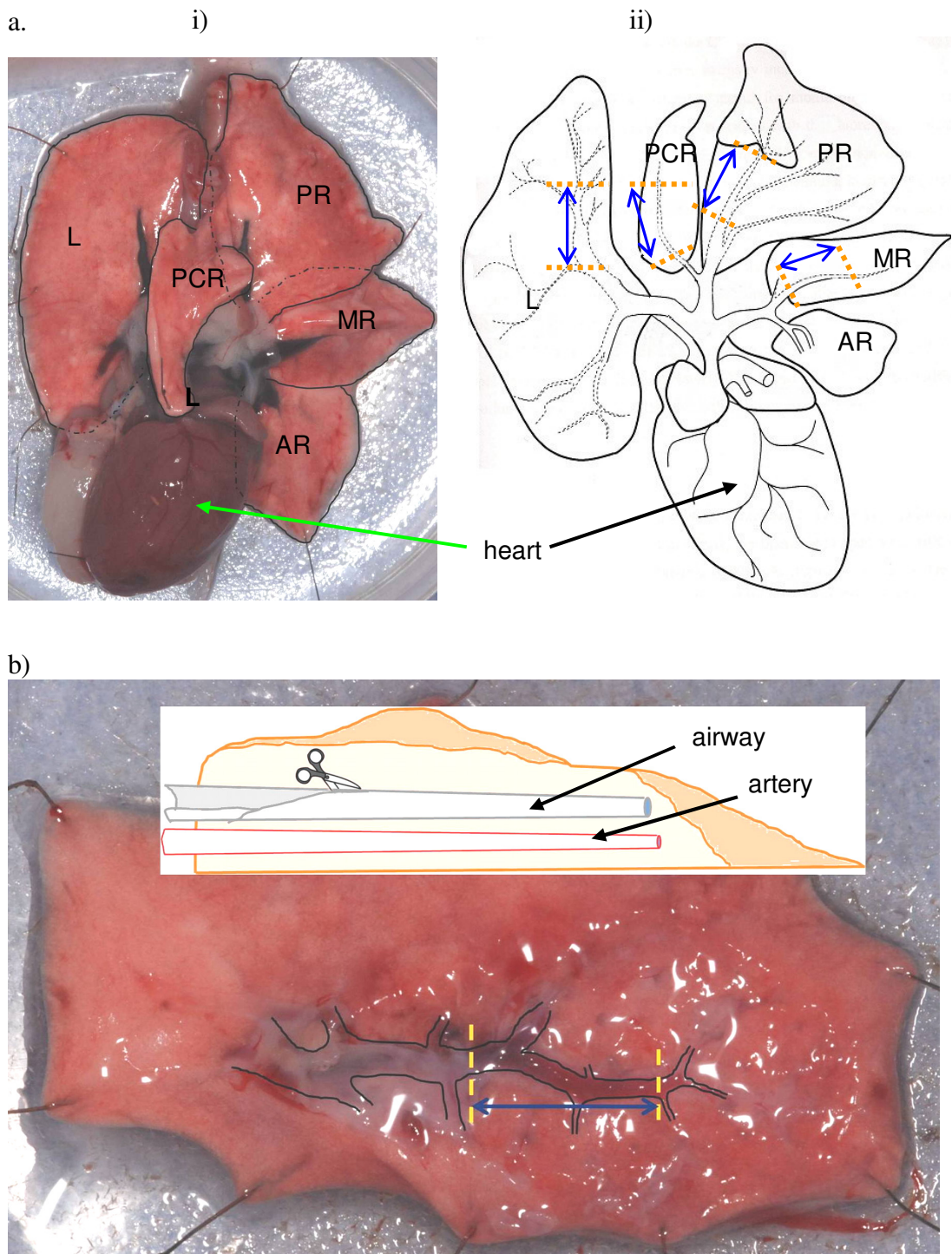


Figure 2.1. Diagram of rat lungs and heart showing the sections of pulmonary artery that were studied. a) represents (i) an actual picture and (ii) a schematic drawing of the lungs and heart, and the lung lobes are indicated as follows: L, left; PCR, postcaval right; PR, posterior right; AR, anterior right. b) The left lung lobe is being dissected and part of the main intrapulmonary artery is exposed. The insert shows the profile of a lung lobe, indicating the dissection procedure where the airway is initially cut to ensure the main intrapulmonary artery located inferior to it is readily visible. The blue arrows in a.ii) and b) show the sections of SPA routinely used in this study. [Figure 2.1a.ii was adapted from Logantha, 2009]

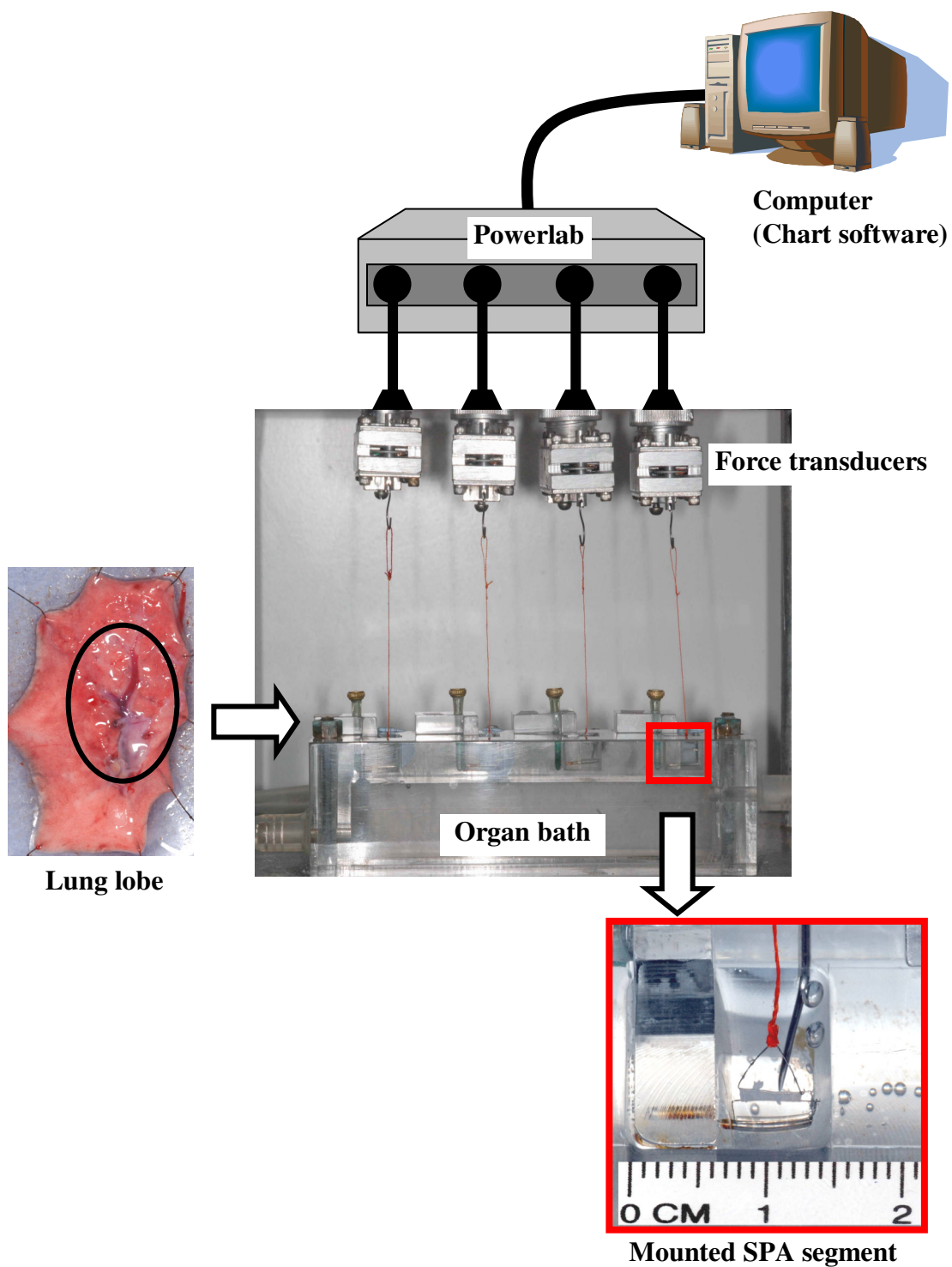


Figure 2.2 The organ bath set up for recording the isolated rat SPA preparations. A section of SPA (circled in black in left hand panel) within a lung lobe and subsequently mounted under isometric conditions in 1ml baths (middle and lower panels).

1.2. Experimental Protocols

1.2.1. Nucleotides Control Responses

A previous study found that the contractile concentration-response curves for UTP and UDP did not reach a maximum in rat SPA (Chootip *et al.*, 2002). Therefore, throughout these experiments, UTP and UDP were applied to the tissues at 300 μ M, which has been shown to produce equi-effective, sub-maximal contractions of this tissue (Chootip *et al.*, 2002). Removal of the endothelium was confirmed by inhibition of the relaxation to 10 μ M ACh, applied for 2 min in vessels precontracted for 5 min with UTP or UDP. It is very difficult to remove the endothelium altogether (De May & Vanhaoutte, 1982; Savineau *et al.*, 1991; Ralevic & Burnstock, 1996), therefore, the tissues in which ACh induced a relaxation of less than 20% of the peak contraction amplitude were considered to be endothelium-denuded. The contraction amplitudes from the control response were also measured at 5 and 7 min after agonist application to validate the effect of ACh. The reproducibility of contractile responses to UTP and UDP was investigated by adding them 6 times for 7 min at 30 min intervals with several washes in between, followed by a single addition of 40mM KCl to the endothelium-intact and –denuded preparations. In each artery, the peak contraction amplitude and the responses amplitude 5 min after addition were measured in response to the nucleotides and KCl, respectively. However, thereafter the KCl response was measured at 7 min. In subsequent experiments three responses to 300 μ M UTP or 300 μ M UDP were obtained before adding potential inhibitors and the mean of the second and third responses was used as the control.

1.2.2. The Role of PI-PLC

The contribution of PI-PLC to the nucleotide-evoked contractions was investigated using the selective PI-PLC inhibitor U73122 (Bleasdale *et al.*, 1990), which has been shown to inhibit contractions mediated by various GPCR in vascular preparations (Kawanabe *et al.*, 2006; Snetkov *et al.*, 2006; Clarke *et al.*, 2008). The inactive analogue of U73122, U73343 (10 or 30 μ M) was used as a control and 10 μ M PGF_{2 α} , which commonly triggers the PI-PLC/IP₃ pathway via activation of FP receptors (Abramovitz *et al.*, 1994), was also utilised as an indicator of the

effectiveness of the U73122 concentration being used. In addition, 40mM KCl was used as a reference agonist to provide a general indication of the selectivity of inhibitors being used. U73122 and U73343 were preincubated for 30 min to allow sufficient time for them to act before addition of the agonist (Kawanabe *et al.*, 2006). A slight variation of protocol for the observation with U73343 was employed. As reported in the results, preincubation of 10 μ M U73343 did not alter the peak contraction of agonists (UTP, UDP and PGF_{2 α}), therefore, 30 μ M U73343 was subsequently added to the same tissues prior to further agonist application.

1.2.3. The Role of Rho Kinase and PKC

The involvement of Rho kinase and PKC in P2Y receptor-evoked contraction was investigated by first assessing the selectivity of 10 μ M Y27632, an inhibitor of Rho kinase (Uehata *et al.*, 1997) and potency of GF109203X, an inhibitor of PKC (Toullec *et al.*, 1991) against the contractile response of SPA evoked by the PKC activator, PMA (10 μ M). 10 μ M Y27632 was used as it has been shown to produce substantial inhibition of Rho kinase in previous studies (Uehata *et al.*, 1997; Jernigan *et al.*, 2004). 3 μ M GF109203X was used initially. However, as reported in the results, it was found to be sub-maximal and so 10 μ M was then tested. 10 μ M Y27632 or 10 μ M GF109203X were either preincubated for 15 min before adding PMA, or added after precontracting the tissue with PMA for 60 min. The effects of 10 μ M Y27632 and 10 μ M GF109203X, either alone or together were then explored against the contractions evoked by the nucleotides, either preincubated for 15 min prior to, or 20 min after the subsequent addition of nucleotides. Inhibitors were also tested against KCl response in a similar manner.

1.3. Permeabilisation Experiment

1.3.1. Effect of Temperature on the Contractile Activity of Intact Rat SPA

Muscle permeabilisation has been studied at several temperatures: 37°C (Jernigan *et al.*, 2004), 30°C (Li *et al.*, 1998) and 26°C (Thomas *et al.*, 2005) and so in initial experiments, the contractile responses to UTP and UDP in intact, unpermeabilised tissues, were characterised at different temperatures. For each nucleotide, three consecutive responses at 300 μ M were evoked, followed by three cumulative

concentration-response curves (0.1 – 1.0mM) at 30 min intervals. Finally, the tissue was challenged with 40mM KCl.

1.3.2. Preparation of Permeabilisation Buffer with a Range of $[Ca^{2+}]$

Unless otherwise stated, the permeabilisation buffer was composed of (mM): KCl 125; $MgCl_2$ 4; HEPES 10; creatine phosphate 10, glucose 11; ethylene glycol-bis(2-aminoethylether)-*N,N,N',N'*-tetraacetic acid (EGTA) 4, titrated to pH 7.1 with KOH. Free $[Ca^{2+}]$ was set by varying the amount of $CaCl_2$ added and was calculated using WinMAXC³², version 2.50 (<http://www.stanford.edu/~cpatton/maxc.html>), which calculates free $[Ca^{2+}]$. The interactions between multiple metals (Ca^{2+} , Mg^{2+}) and multiple binding agents (EGTA, ATP) at the same time is very complex and so this programme reiteratively solves nine equations, as explained in Fabiato & Fabiato, (1979) to calculate free $[Ca^{2+}]$. The ionic strength of the solutions (I) was calculated from the equation $I = 1/2\sum CZ^2$, where C = concentration of ion and Z = charge of ion, at a given temperature and total concentrations of EGTA, ATP, Ca^{2+} and Mg^{2+} .

Adding $CaCl_2$ to the permeabilisation buffer causes a marked decrease in pH, due to dissociation of H^+ from EGTA (Tsien & Pozzan, 1989). To avoid this acidification the method of Tsien & Pozzan, (1989) was adopted. Two EGTA-containing permeabilising solutions A and B (the compositions as described in the Methods) were initially prepared. Solution A contained 4mM $CaCl_2$ (free $[Ca^{2+}] = 3.16\mu M$ or pCa 4.5), while solution B had zero $[Ca^{2+}]$ (Ca^{2+} -free solution). These two solutions were then mixed together in the following volume/volume (v/v) ratios to produce the desired free $[Ca^{2+}]$, calculated by the formula; $[CaEGTA]/[EGTA_{free}]$ or $(high\ Ca^{2+}\text{-containing\ solution})_{volume}/(Ca^{2+}\text{-free\ solution})_{volume} = [Ca^{2+}_{free}]/K_D(Ca^{2+})$, where $K_D(Ca^{2+}) = 2.29 \times 10^{-2}M$ (WinMAXC³²). The ratios of two solutions and the final free $[Ca^{2+}]$ of the mixtures were tabulated in Table 2.1. pH was re-checked and re-adjusted appropriately each time, although the final mixture was routinely observed to be reduced by only ~0.05 pH units at most.

Table 2.1. The ratios of high Ca²⁺-containing (pCa 4.5) and Ca²⁺-free solutions used to produce the final mixture with the desired free [Ca²⁺].

Mixture of (v/v ratios):		Free [Ca ²⁺] of the final mixture	
Solution A (Free [Ca ²⁺] = 3.16μM)	Solution B (Free [Ca ²⁺] = 0μM)	(μM)	(pCa)
10	0	31.6	4.5
10	0.229	10	5.0
10	0.725	3.16	5.5
10	2.290	1	6.0
10	7.247	0.316	6.5
4.367	10	0.1	7.0
1.380	10	0.0316	7.5
0.437	10	0.01	8.0
0.044	10	0.001	9.0

1.3.3. General Permeabilisation Protocol for Exploring Optimum Conditions

First, in the intact rat SPA two KCl-induced responses at a 30 min interval were obtained, followed by a 3 point cumulative concentration-response curve (0.1 – 1.0mM) to the nucleotides in the standard bathing solution. Subsequently, the tissue was incubated with Ca²⁺-free PSS for 10 min, which was then replaced by the permeabilising buffer (pCa 4.5), followed by addition of the permeabilising agent. The permeabilising agent was then left in contact with the tissue until the resulting contraction reached a peak, which was taken as an indication that permeabilisation was complete. The permeabilised tissue was then washed several times with the permeabilising buffer at pCa 9.0, until a stable basal tension was reached. Various experimental protocols were then carried out.

1.3.4. Effects of Y27632 and GF109203X on Cumulative Ca²⁺ Concentration-Response Curve

After a stable basal tension was reached following permeabilisation, cumulative Ca²⁺ concentration-response curve was generated by exposing the tissue to a series of cumulative additions of a range of free [Ca²⁺], i.e. pCa 9.0, 8.0, 7.5, 7.0, 6.5, 6.0, 5.5, 5.0 and 4.5. For studying the effects of both 10µM Y27632 and 10µM GF109203X, either of these inhibitors was first preincubated for 15 min before cumulative additions of [Ca²⁺] was carried out.

1.3.5. Characterisation of Contractions Evoked by pCa 6.5, UTP, UDP and PMA and the Effects of Y27632, GF109203X, U73122 and Suramin on these Contractions

In order to characterise the contractions evoked by pCa 6.5, 300µM UTP, 300µM UDP and 10µM PMA, a time-course study for these contractions was performed. The tissue was exposed to pCa 6.5 and the response was monitored for at least 40 min after reaching the peak. In the agonist response, each of the agonists was added in the presence of [Ca²⁺] at pCa 6.5, i.e. once the response to pCa 6.5 reached its peak. The agonist response was similarly monitored for at least 40 min following its peak. The effects of 10µM Y27632, 10µM GF109203X, 10µM U73122 and 100µM suramin against the above contractions, except for PMA, was investigated by applying this

inhibitor after the contractions reached their peak. For PMA response, only GF109203X was tested against it and was applied after 60 min following the addition of PMA.

1.4. Contractile Responses of Synthetic P2Y Agonists INS45973, INS48823 and 3-Phenacyl UDP

1.4.1. Potency of Contractions Evoked by INS45973, INS48823 and 3-Phenacyl UDP in Intact Preparation and the Effects of Y27632 and Suramin on the Responses of these Agonists

To examine the potency of the P2Y agonists INS45973, INS48823 and 3-phenacyl UDP, two responses to 40mM KCl were initially evoked, followed by a cumulative concentration-response curve (1 μ M – 300 μ M) to one of the agonists. To investigate the effects of Y27632 and suramin, either 10 μ M Y27632 or 100 μ M suramin was preincubated for 15 min prior to the subsequent addition of the agonist.

1.4.2. Characterisation of Contractions Evoked by INS45973, INS48823 and 3-Phenacyl UDP in Membrane-Permeabilised Preparations, and the Effects of Y27632 and Suramin on these Contractions

Consistent with Section 1.3.6, a time-course study for the contractions evoked by 30 μ M INS45973, 50 μ M INS48823 and 50 μ M 3-phenacyl UDP was performed. Each agonist was added in the presence of [Ca²⁺] at pCa 6.5, once the response to pCa 6.5 reached its peak. The agonist response was monitored for at least 40 min following its peak. The effects of 10 μ M Y27632 and 100 μ M suramin against these contractions were investigated by applying the inhibitor after the contractions reached their peak.

1.5. Drugs and Solutions

ACh(Cl), ATP (Na₂ salt), α -toxin, β -escin, creatine phosphate, EGTA, nifedipine, PGF_{2 α} , U73343, UDP (Na salt), UTP (Na₃ salt) were obtained from Sigma, UK. GF109203X, 3-phenacyl UDP (Na₂ salt), suramin, thapsigargin, U73122 and Y27632 were obtained from Tocris, UK and PMA was obtained from Boehringer, Mannheim, Germany. INS45973 (Na₄ salt) and INS48823 ((NH₄)₃ salt) were supplied to Dr. Charles Kennedy personally by Dr. J. L. Boyer, Inspire

Pharmaceuticals, Durham, USA. ACh, ATP, INS45973, INS48823, 3-phenacyl UDP, suramin hexasodium, UDP and UTP were dissolved in double deionised distilled water (ddH₂O) and stored frozen as 10mM stock solutions. α -toxin and KCl were dissolved in ddH₂O as 0.5mg/mL and 1M stock solutions, respectively, and stored at 4°C. GF109203X, nifedipine, PMA, thapsigargin, U73122, U73343 and Y27632 were initially dissolved in dimethyl sulfoxide (DMSO), stored frozen as 10mM stock solutions and diluted in ddH₂O as appropriate. β -escin and PGF_{2 α} were dissolved in methanol and ethanol, respectively, and stored frozen as 10mM stock solutions. EGTA was dissolved in 1N NaCl as a 0.5M stock solution.

1.6. Data Analysis

Calculation and statistical analysis were performed using Graphpad Prism (version 4.03) software. Contractile responses are expressed in mg of tension, as a percentage of; 5 and 7 min tension produced by 40mM KCl, a control response (peak response) produced by a given agonist, the maximum tension produced by 1mM of a given agonist or the maximum tension produced by pCa 4.5 as appropriate. The results are shown as mean \pm S.E.M and n represents the number of arteries used in each experiment from a minimum of four separate animals. Student's paired and unpaired t tests and one-way (with Tukey's comparison) or two-way analysis of variance (ANOVA) were used to compare between groups, as applicable. P values of <0.05 were considered to be statistically significant. Log concentration-agonist/Ca²⁺ response curves were fitted to the Hill equation, the best fits giving values for the EC₅₀ and the Hill slope.

Hill Equation:

$$R = \frac{R_{\max}}{[1 + D/K_D]^n}$$

where

R = Response

R_{\max} = maximal response

D = drug concentrations

K_D = apparent dissociation constant or concentration producing 50% of the maximal response

n = Hill coefficient

Chapter 3:

Characterisation of UTP- and UDP-evoked contractile responses

1. INTRODUCTION

The low tonic state of the pulmonary vasculature is maintained by regulatory factors that influence the underlying activity of arterial smooth muscle (Barnes & Liu, 1995). Purine and pyrimidine nucleotides, such as ATP, UTP and UDP, have been shown to produce significant effects on the activity of this tissue. While ATP acts via both P2X and P2Y receptors, UTP and UDP bind to P2Y receptors only, to induce their effects. Activation of P2Y receptors in the endothelium-denuded pulmonary artery can trigger vasoconstriction (Chootip *et al.*, 2002). In contrast, stimulation of the endothelial P2Y receptors induced relaxation of the precontracted pulmonary artery (Konduri *et al.*, 2004; Gui *et al.*, 2008). At present, evidence of P2Y subtypes expression in this vessel is relatively limited, however, Hartley *et al.*, (1998) identified P2Y₆ mRNA in rat pulmonary artery smooth muscle. Additionally, P2Y₁, P2Y₂ and P2Y₄ mRNA were also detected in juvenile rabbit pulmonary artery (Konduri *et al.*, 2004). Contractile studies by Chootip *et al.*, (2002) indicated that UTP and UDP acted at two distinct P2Y receptors in rat SPA to evoke vasoconstriction.

The vascular endothelium also plays a profound role in the regulation of pulmonary vascular tone (Barnes & Liu, 1995; Sumpio *et al.*, 2002) through the release of vasoactive mediators. For, example, ACh has been demonstrated to trigger the release of endothelium-derived relaxing factor or NO, via activation of muscarinic receptors on the endothelial cells, to induce relaxation of precontracted pulmonary artery smooth muscle (Tseng & Mitzner, 1992; Altieri *et al.*, 1994; Norel *et al.*, 1996). Likewise, both ATP (De Mey & Vanhoutte, 1982) and UTP (Gui *et al.*, 2008) act via endothelial P2Y receptors to induce relaxation of the pulmonary artery. Thus, this effect can provide a useful experimental tool to assess the functional integrity of endothelium and warrants consideration when attempting to explore the effect of a compound on the pulmonary vascular tone.

The aim of this project was to study the intracellular pathways through which P2Y receptor agonists induce pulmonary vasoconstriction. It was, therefore, necessary to establish a protocol for studying P2Y receptor-mediated vasoconstriction. This chapter describes how the initial control experiments were performed by adding nucleotides to rat isolated SPA to characterise the basic profile

of the tissue's contractile responses, the influence of the endothelium and the reproducibility of the P2Y receptor-mediated contraction.

2. RESULTS

2.1. Effect of the Endothelium on Nucleotide-Induced Contractions

Both UTP and UDP (300 μ M), when applied to endothelium-intact rat SPA initiated a slow contraction that reached its maximum amplitude within 5 min and then decayed slowly (Figure 3.1a). The mean peak amplitudes of contractions to UTP and UDP were 175 ± 22 mg (n=6) and 149 ± 23 mg (n=5), respectively. Removal of endothelium, by inserting a thread through the vessel lumen, was confirmed by contracting the tissue with an agonist and subsequently applying ACh for 2 min after 5 min agonist addition. In the endothelium-intact vessels, ACh induced about 50% relaxation of the contractions evoked by either UTP or UDP, which was significantly ($P<0.001$) and substantially greater than in the endothelium-denuded vessels (Figure 3.1). To ensure the ACh-induced relaxation was not influenced by the tendency of the nucleotide-evoked contractions to decay slowly, the control response of both nucleotides in endothelium-intact and denuded vessels measured at peak and 7 min after agonist administration were also compared. It showed that the mean peak contraction amplitude of the nucleotides was not significantly different from the mean response at 7 min in both endothelium-intact and -denuded vessels (Figure 3.2), thus any relaxation if obtained, was clearly due to an actual effect of ACh following its addition. In contrast, the response to 40mM KCl was unaffected by removal of endothelium (Figure 3.3), indicating the tissue's contractile capability had not been compromised by the endothelium-removal protocol.

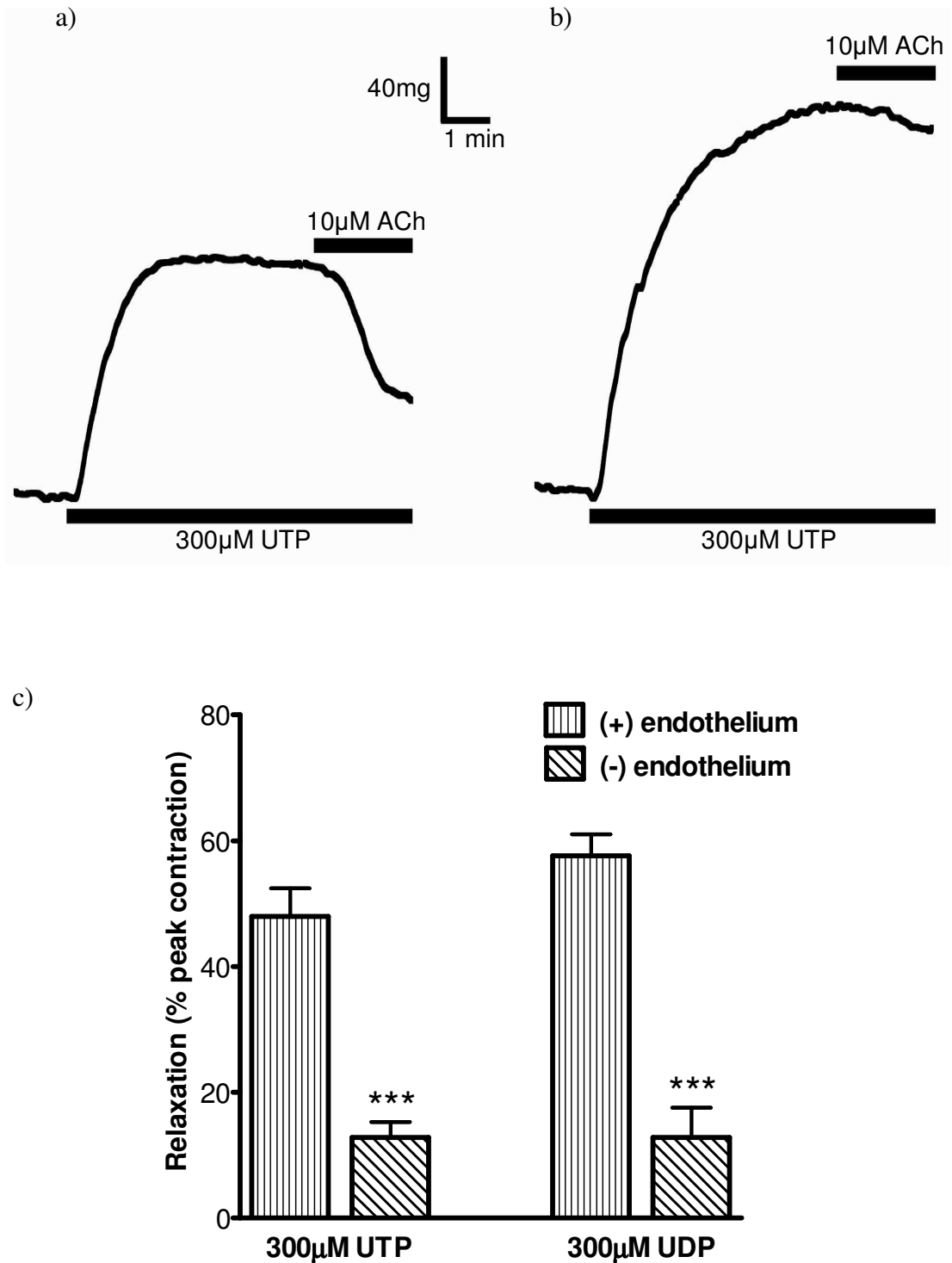


Figure 3.1. ACh-induced vasodilation in rat SPA. The traces show the typical effect of 10µM ACh in a) endothelium-intact and b) endothelium-denuded tissues, precontracted with 300µM UTP. The agonists were added as indicated by the solid bars. c) The mean relaxation amplitudes induced by ACh in endothelium-intact and -denuded vessels following UTP (n=6) and UDP (n=5) additions are shown. The relaxations are expressed as a % of peak contraction before adding ACh, and are shown as mean \pm S.E.M. ***P<0.001 for % relaxation of endothelium-intact versus -denuded vessels for both nucleotides.

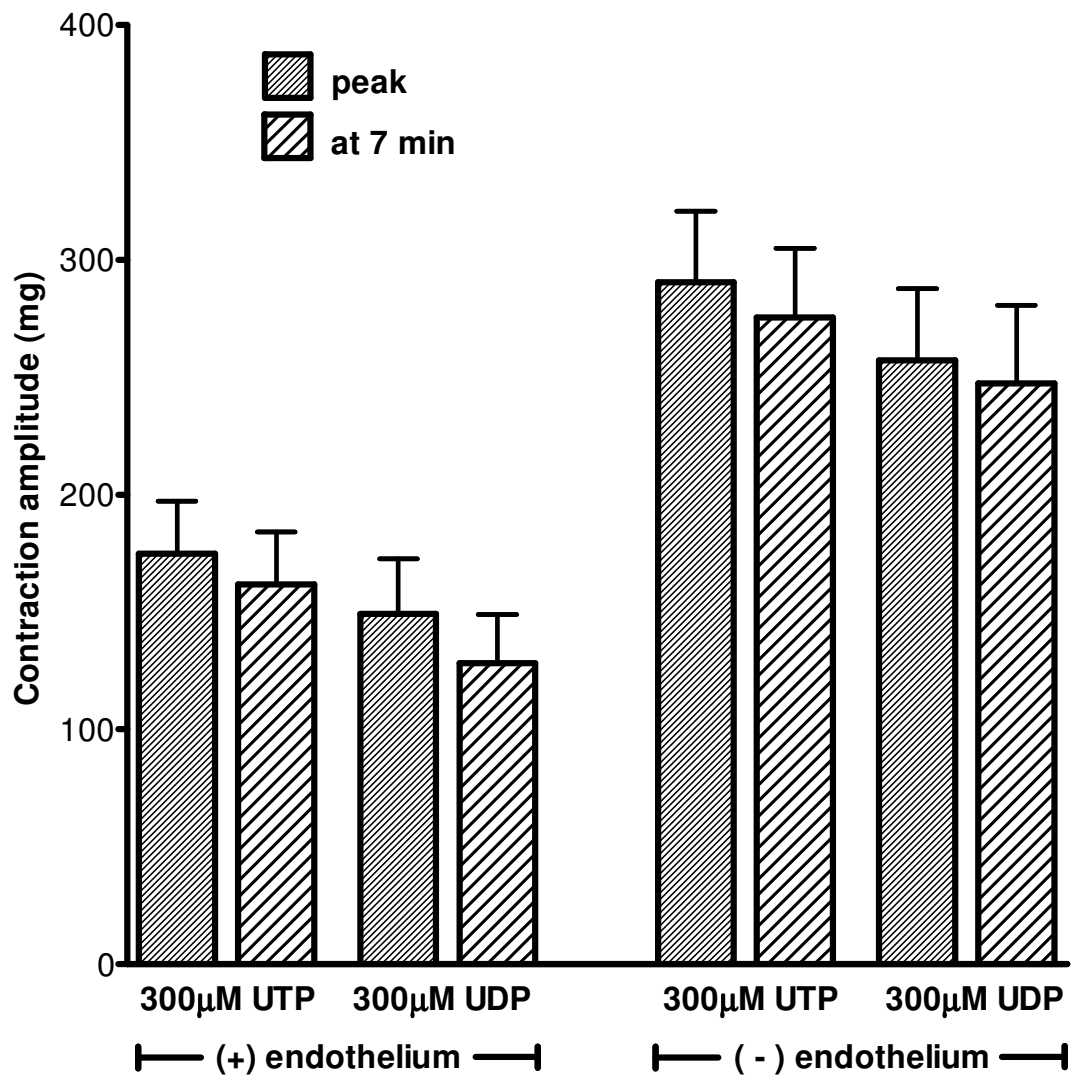


Figure 3.2. Vasoconstriction evoked by nucleotides in endothelium-intact and -denuded rat SPA. The mean contraction amplitudes measured at peak and 7 min following 300µM UTP and 300µM UDP additions in endothelium-intact and -denuded vessels. In both tissues preparations, n values for UTP and UDP, are 6 and 5, respectively. Data are expressed as mean ± S.E.M.

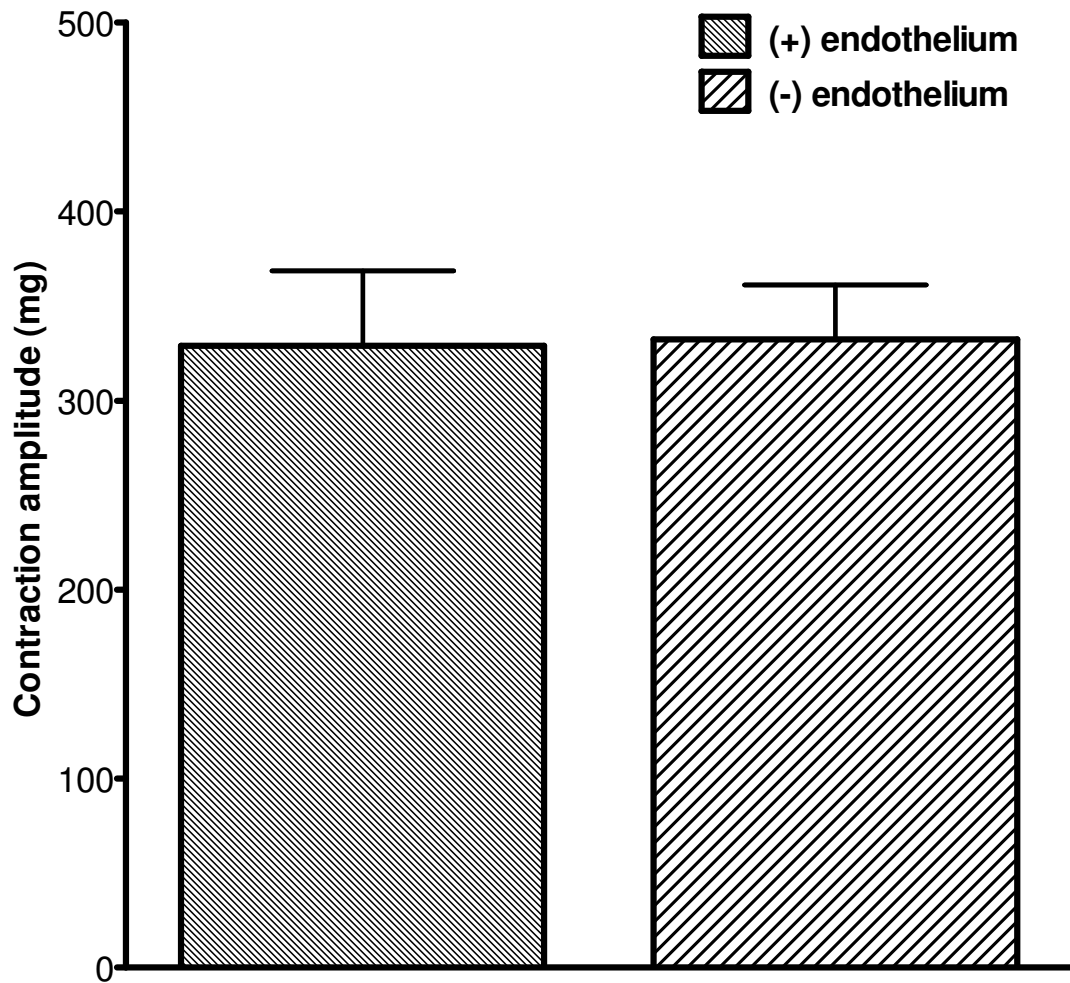


Figure 3.3. KCl-evoked vasoconstriction in rat SPA. The mean contractile response to 40mM KCl in tissues with endothelium intact (n=11) or removed (n=11) are shown. Data are expressed as mean \pm S.E.M.

2.2. Reproducibility of Nucleotide-Induced Contractions

In order to explore the effects of agents that interfere with signalling pathways that may be involved in P2Y receptor-mediated contraction, it is necessary to first determine if repeated administration of the agonist induces reproducible contractions. When UTP and UDP (both 300 μ M) were added 6 times for 5 min at 30 min intervals to endothelium-intact arteries (Figure 3.4), the contraction amplitude tended to increase slightly over the first three additions, but there was no significant difference in the mean amplitude of each of the six responses. Likewise, contractions evoked in endothelium-denuded tissues show no significant change in peak amplitude over 6 separate additions. However, these responses were significantly larger than the responses induced in the presence of an intact endothelium with $P < 0.05$ for both nucleotides (2-way ANOVA to compare overall responses) (Figure 3.4), or $P < 0.01$ and < 0.05 for UTP and UDP, respectively, (first response comparison) (Figure 3.5). Overall, it is clear that 6 repeated additions of either UTP or UDP to endothelium-intact and -denuded vessels produced a reproducible contractile response. Since the responses in the absence of endothelium were significantly larger, all subsequent experiments were carried out in endothelium-denuded preparations. Furthermore, three control responses to 300 μ M UTP or 300 μ M UDP were obtained before adding potential inhibitors. Under these conditions the mean peak contraction amplitudes obtained in this thesis were 369 ± 16 mg ($n=71$) for UTP and 312 ± 15 mg ($n=65$) for UDP.

2.3. Time-Course of Nucleotide-Induced Contractions

The time-course of the contractions was further studied in endothelium-denuded vessels where both maximum responses decayed gradually. There was about 25% reduction of peak contraction after 20 min addition of either agonist (Figure 3.6, 3.7) until a plateau phase was reached at about 20 min after agonist administration, which was maintained for at least another 15 min.

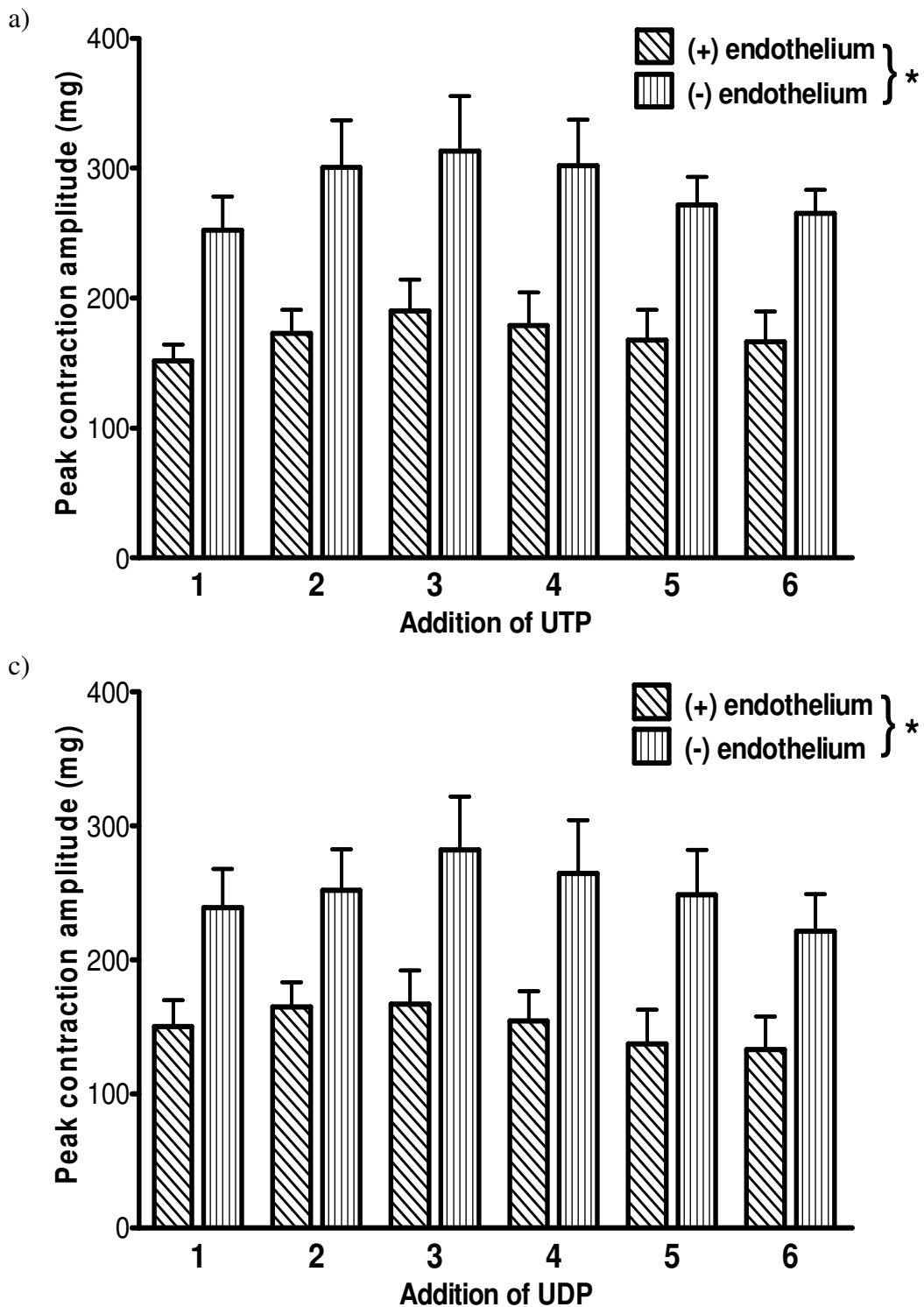


Figure 3.4. Contractions of rat SPA evoked by UTP and UDP. Mean peak contraction amplitudes evoked by adding a) UTP or b) UDP (both 300 μ M) for 6 times at 30 min intervals to the endothelium-intact and -denuded tissues. In both tissues preparations, n values for UTP and UDP, are 6 and 5, respectively. Data are expressed as mean \pm S.E.M. *P<0.05 for both UTP and UDP, in the absence versus presence of intact endothelium (reproducibility and effect of endothelium data sets by 1-way and 2-way ANOVA, respectively).

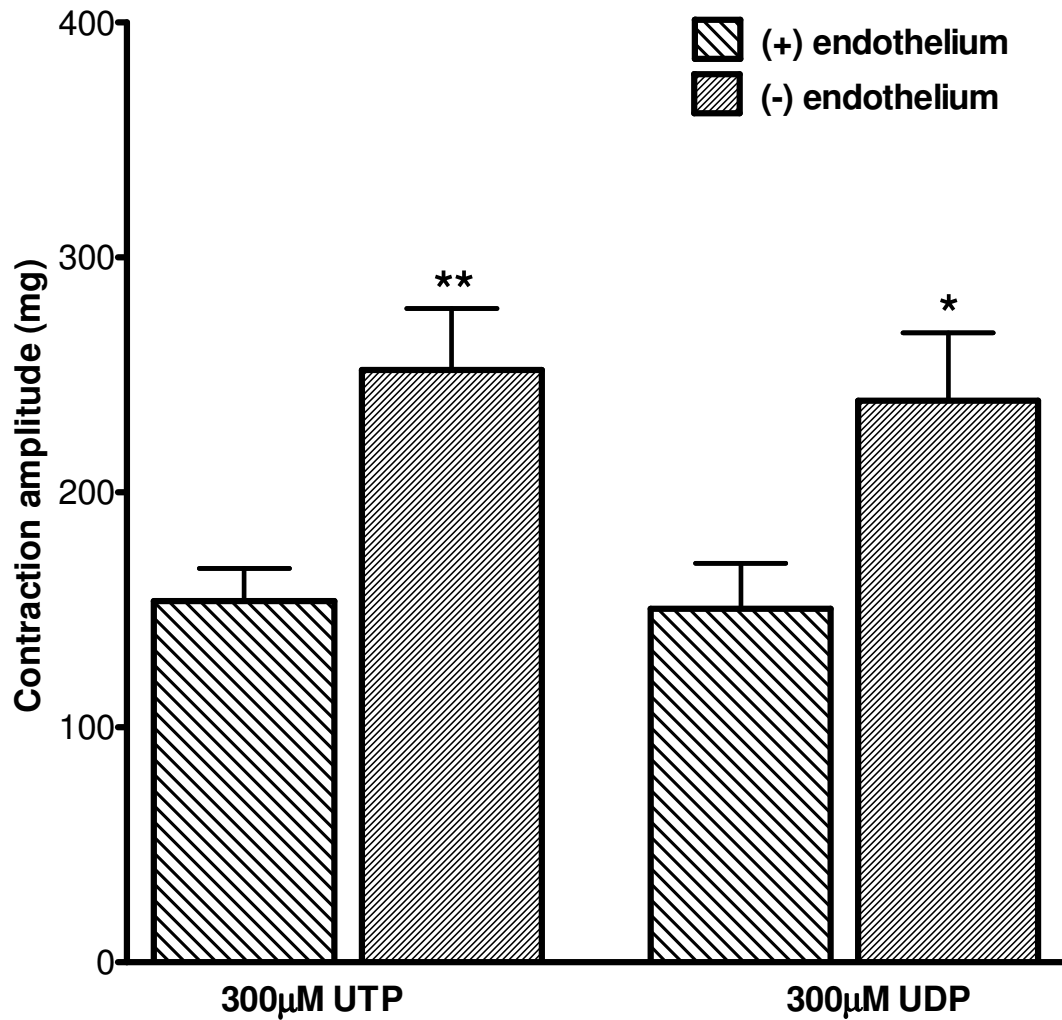


Figure 3.5. Contractions of rat SPA evoked by UTP and UDP. Mean first peak contraction amplitudes obtained from a series of six-repeated additions of UTP or UDP (both 300µM) at 30 min intervals to the endothelium-intact and -denuded tissues. In both tissues preparations, n values for UTP and UDP, are 6 and 5, respectively. Data are expressed as mean \pm S.E.M. **P<0.01 and *P<0.05 for UTP and UDP, respectively, in the presence versus absence of intact endothelium.

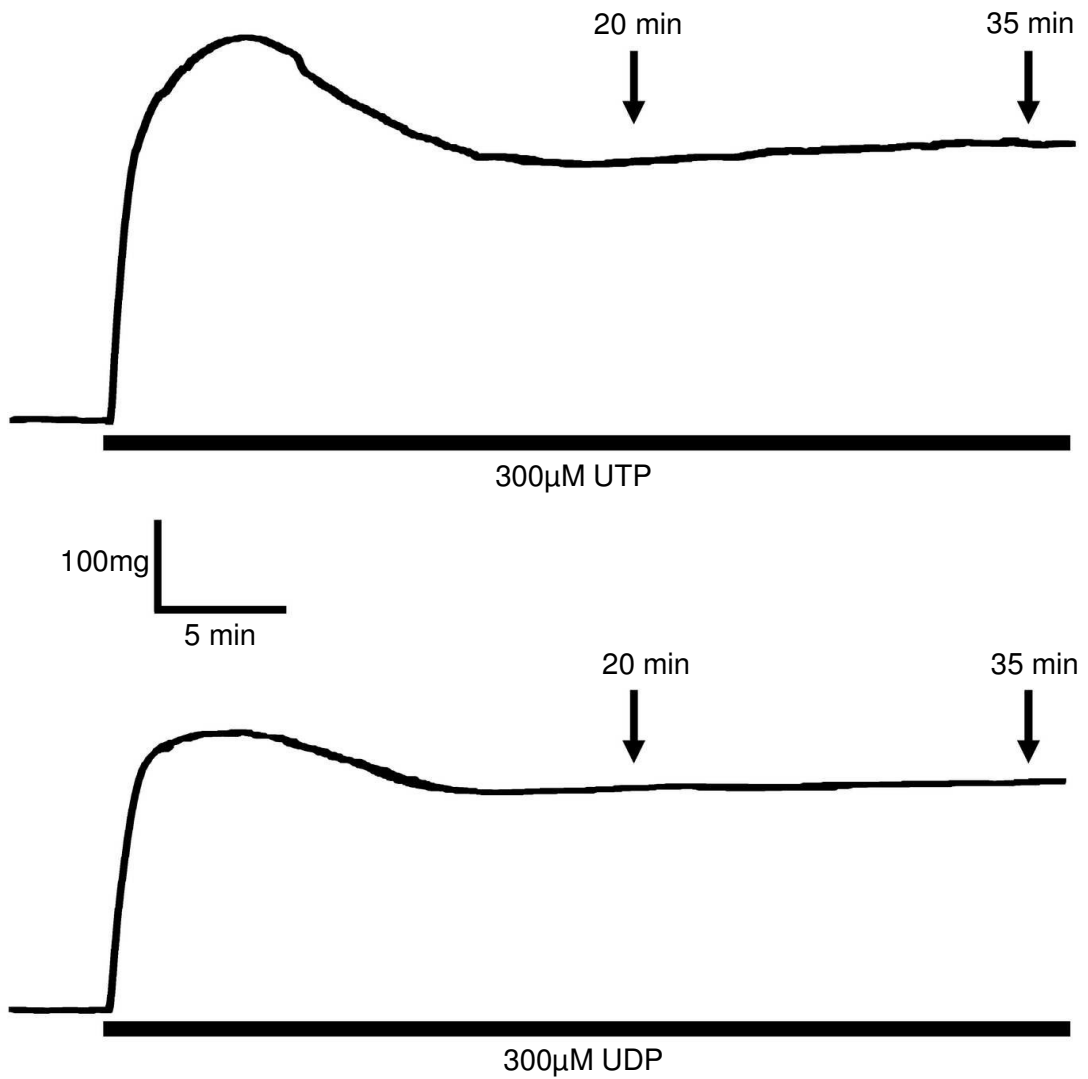


Figure 3.6. Vasoconstriction of endothelium-denuded rat SPA evoked by nucleotides. The traces show typical contractile responses induced by 300µM UTP (upper tracing) and 300µM UDP (lower tracing). Solid bars and arrows indicate application of the agonists and its time interval, respectively.

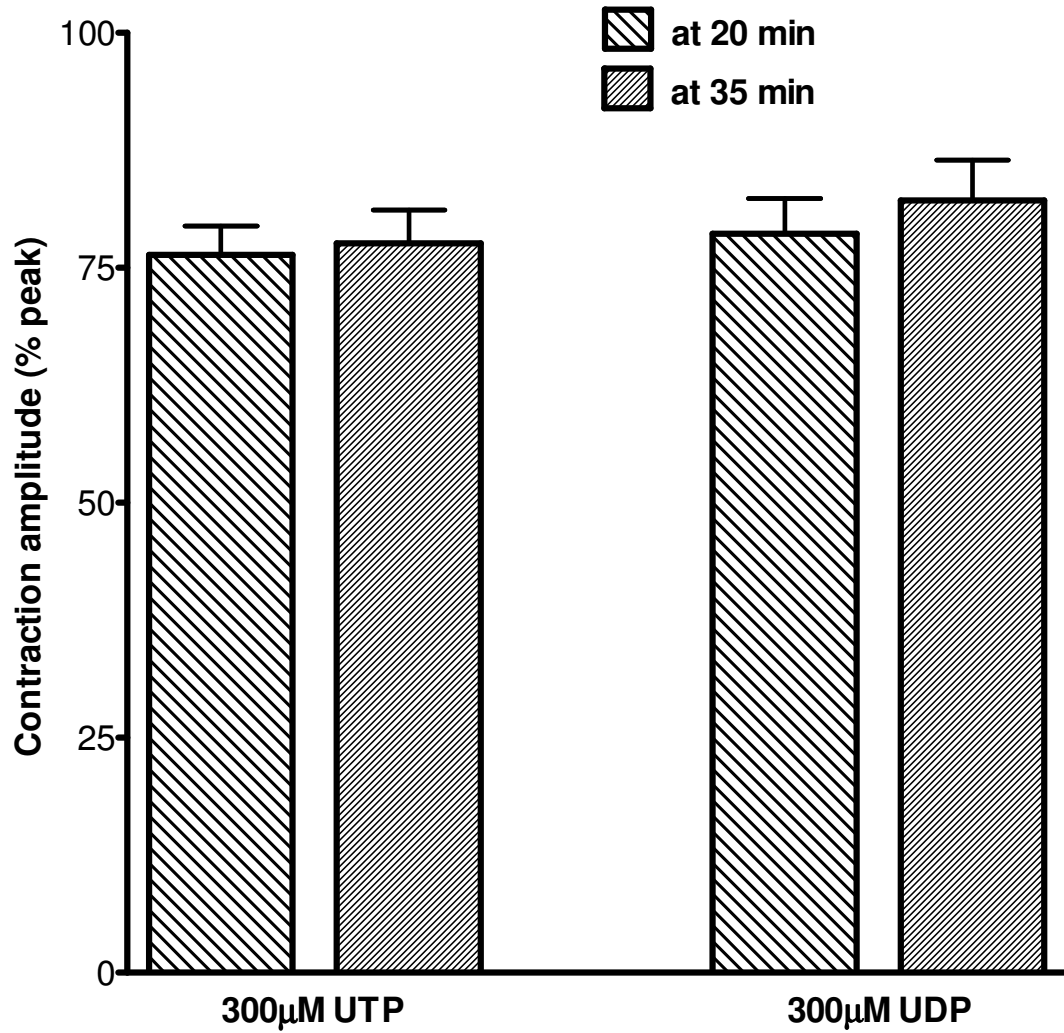


Figure 3.7. Time-course of UTP and UDP contractile responses in endothelium-denuded rat SPA. The mean amplitude of contractions evoked by UTP (n=21) and UDP (n=17) 20 and 35 min following their additions, expressed as % of peak contraction. Data are shown as mean \pm S.E.M.

3. DISCUSSION

The results of these control experiments clearly showed that both UTP and UDP evoked slow contractions, which peaked within 5 min and subsequently decayed slightly before a maintained phase was reached. By disrupting the endothelium of the vessels, the peak contractions of both nucleotides were significantly augmented, however the response to KCl was unaffected. Finally, both UTP and UDP evoked highly reproducible contractile responses after 6 separate applications. Thus, these experiments show that the protocols used are appropriate for the further studies on P2Y receptor-mediated signalling pathways reported in the remainder of this thesis.

3.1. UTP- and UDP-Evoked Vasoconstriction of SPA, and Contribution of Endothelium in P2Y Receptor-Mediated Contractile Responses

In this study, both nucleotides evoked a typical pattern of slowly developing contractions that reached their peak within 5 min and was largely comparable to previous studies (Hartley *et al.*, 1998; Chootip *et al.*, 2002). A slight difference however, in the UTP-evoked contractions was noted. In the present study, the peak responses of the vessels evoked by UTP were significantly larger in the absence compared to presence of endothelium, while previous experiments in this laboratory had observed no difference between both tissue preparations (Chootip *et al.*, 2002). The reason of such contrasting findings is unclear, although the previous study investigated the effect of the endothelium by comparing the potency of UTP by constructing cumulative concentration-response curves in endothelium-intact and -denuded vessels. Thus, an increase in amplitude, with no change in agonist potency after endothelium removal in the previous study might explain the difference from the present findings.

This study also examined the influence of endothelium in vasoconstriction of the rat SPA induced by P2Y receptor activation. Disruption of the endothelium led to the augmentation of vessel's peak contractions evoked by both UTP and UDP. Evidently, such effect indicates the presence of an endothelium-dependent opposing vasodilator action generated following activation of endothelial P2Y receptors by both nucleotides. In line with this view, Konduri *et al.*, (2004) showed that the precontracted endothelium-intact conduit and resistance vessels of juvenile rabbit

pulmonary artery were relaxed upon treatment with UTP and UDP, and the vasodilator response induced by UTP was subsequently abolished following denudation of the endothelium. Although Rubino *et al.*, (1999) were unable to demonstrate UTP- and UDP-evoked relaxation in the precontracted endothelium-intact rat intrapulmonary artery, a recent study (Gui *et al.*, 2008) showed that both nucleotides induced a vasodilator response to the precontracted endothelium-intact left and right rat pulmonary arteries. In addition, the contraction amplitudes evoked by the nucleotides in this tissue were augmented after disruption of endothelium, similarly observed in the current results and the previous study (Chootip *et al.*, 2002).

The involvement of endothelium to mediate vasodilation in response to P2Y receptor agonists has also been reported in many other vessels. For example, the precontracted endothelium-intact canine epicardial coronary artery (Matsumoto *et al.*, 1997), hamster (Ralevic & Burnstock, 1996) and rat (Buvinic *et al.*, 2002) mesenteric artery, and mouse aorta (Guns *et al.*, 2005; Bar *et al.*, 2008) were dilated upon treatment with UTP and this vasodilator response was abolished following denudation of the endothelium in the majority of cases. Equally, UDP also evoked a relaxant effect on precontracted canine epicardial coronary artery (Matsumoto *et al.*, 1997), rat mesenteric artery (Buvinic *et al.*, 2002) and mouse aorta (Guns *et al.*, 2005; Bar *et al.*, 2008). Removal of the endothelium obliterated the relaxant effect induced by UDP in rat mesenteric artery and mouse aorta.

3.2. Reproducibility of Nucleotide-Induced Contractions

The results of this study also demonstrated the reproducibility of UTP- and UDP-evoked contractile responses upon six repeated additions in both endothelium-intact and -denuded vessels. A slight increasing trend was observed for the contraction amplitudes, particularly from the first to third additions for both nucleotides, but there was no significant difference between any of the responses. These findings are, therefore, valuable for establishing a protocol to investigate the agents that interfere with the signalling pathways of the nucleotide-evoked responses. Consequently, three agonist responses were first obtained before performing any interventions. Additionally, as the endothelium plays a substantial role in modulating

the P2Y receptor-mediated contractile responses, the experiments were also carried out using endothelium-denuded preparations to ensure the opposing P2Y receptors vasodilator effect were eliminated.

Chapter 4:

Role of PI-PLC, PKC, and Rho kinase-activated Ca^{2+} sensitisation in nucleotide- evoked contractile responses in intact preparations

1. INTRODUCTION

It is widely recognised that elevation of free $[Ca^{2+}]_i$ via both influx of extracellular Ca^{2+} and release of intracellular Ca^{2+} stores plays a central role in triggering smooth muscle contractile responses (Jiang & Stephens, 1994; Sylvester, 2004; Ratz *et al.*, 2005; Berridge, 2008). In single, dissociated smooth muscle cells of the rat pulmonary artery, ATP induced a transient $[Ca^{2+}]_i$ oscillation followed by a small, maintained $[Ca^{2+}]_i$ (Guibert *et al.*, 1996; Pauvert *et al.*, 2000). The transient $[Ca^{2+}]_i$ oscillation was not affected by either zero extracellular Ca^{2+} solution or the CICR blocker, tetracaine. Similarly, in a subsequent study in rat pulmonary artery, the release of intracellular Ca^{2+} stores, induced by ATP was resistant to ryanodine receptor antagonists (Zheng *et al.*, 2005).

Another mechanism, involving Ca^{2+} sensitisation via Rho kinase, might also contribute to P2Y receptor-evoked pulmonary artery smooth muscle contraction. In membrane-permeabilised rat pulmonary artery, Jernigan *et al.*, (2004) found that UTP-evoked vasoconstriction was independent of a change in $[Ca^{2+}]_i$, but was inhibited by the Rho kinase inhibitor Y27632. Likewise, the contraction of rat renal glomeruli evoked by the P2Y agonists ADP and UTP, was abolished by Y27632 (Jankowski *et al.*, 2003). Additionally, coupling of P2Y receptors to Rho kinase in mediating other cellular responses has also been reported. In rat aortic smooth muscle stimulation of P2Y receptors increased the amount of membrane-bound RhoA and induced actin stress fiber formation that was sensitive to RhoA and Rho kinase inhibitors, such as C3 exoenzyme and Y27632, respectively (Sauzeau *et al.*, 2000).

PKC might also be involved in the P2Y receptor-mediated pulmonary artery smooth muscle contractions, although direct evidence to link such an association remains to be established. However, other GPCR agonists have been reported to act, at least in part, through PKC-induced Ca^{2+} sensitisation to evoke vasoconstriction. One possible pathway involves CPI-17-associated Ca^{2+} sensitisation. Kitazawa *et al.*, (2000) showed that phenylephrine and histamine triggered contractions of rabbit femoral arterial smooth muscle comparable to that induced by high extracellular $[K^+]$, but Western blotting only detected phosphorylated CPI-17 after agonist stimulation and not after high $[K^+]$ stimulation. Reduction of the histamine-induced

contraction and CPI-17 phosphorylation were seen following treatment with GF109203X. Additionally, Li *et al.*, (1998) have shown that at a constantly low $[Ca^{2+}]_i$, phosphorylated, but not non-phosphorylated CPI-17, was able to induce contraction of the β -escin-permeabilised rabbit femoral artery by more than 70%. Another mechanism by which PKC alters $[Ca^{2+}]_i$ to induce contraction is by the regulation of $Ca_v1.2$ channel activity. Cobine *et al.*, (2007) showed that PKC directly potentiated the activity of $Ca_v1.2$ channels during active tone development of endothelium-denuded rabbit coronary artery. In contrast, PKC also activated this ion channel indirectly by depolarising the membrane through inhibition of voltage-gated K^+ channels (Cogolludo *et al.*, 2003).

As a protocol for studying P2Y receptor-mediated vasoconstriction was established in the previous chapter, the studies were proceeded in this chapter to investigate several potential signalling mechanisms that might underlie this vasoconstriction, in particular PI-PLC, PKC and Ca^{2+} sensitisation of contractile proteins via Rho kinase. The involvement of PI-PLC was studied by using the selective PI-PLC inhibitor U73122 and its inactive analogue U73343. Y27632 and GF109203X, the inhibitors of Rho kinase and PKC, respectively, were employed to examine the contribution of these protein kinases. Initially, the selectivity of Y27632 and potency of GF109203X were assessed against the contractile response of pulmonary artery evoked by the PKC activator, PMA. The effects of these inhibitors were then explored against the contractions evoked by the nucleotides. Y27632 and GF109203X, either alone or together were added before UTP and UDP or once the contractions had reached a steady-state.

2. RESULTS

2.1. Involvement of PI-PLC in UTP- and UDP-evoked Contractions

Having shown that UTP and UDP both evoke reproducible contractions of the pulmonary artery, the next set of experiments investigated the involvement of PI-PLC in the contractions induced by these nucleotides. In the initial experiments, preincubation for 15 min with 1 μ M U73122 had no effect on contractions evoked by UTP (n=5) or UDP (n=6). This was a surprise as, at this concentration, U73122 has been shown to inhibit contractions evoked by ET-1 in rabbit isolated basilar artery (Kawanabe *et al.*, 2006). Therefore, the concentration of U73122 was increased 10-fold and 10 μ M PGF_{2 α} was also introduced as an agonist, since it is known to activate PI-PLC via FP receptors expressed in *Xenopus* oocytes and monkey kidney COS-M6 cell lines (Abramovitz *et al.*, 1994). Preincubation with 10 μ M U73122 for 30 min significantly reduced the peak amplitude of contractions evoked by UTP (Figure 4.1), UDP (Figure 4.2) and PGF_{2 α} (Figure 4.3) by more than 50% (P<0.01 for UTP and P<0.05 for UDP and PGF_{2 α}). In contrast, the response to KCl was unchanged (Figure 4.4). Increasing the concentration of U73122 to 30 μ M further enhanced its inhibitory effect, whereby it almost abolished the peak contractions to UTP and UDP (P<0.01 for both), and significantly reduced the PGF_{2 α} -evoked contraction by about 75% (P<0.01). However, this concentration of U73122 also diminished the KCl response by about 50% (P<0.01) (Figure 4.4). The vehicle for U73122 at 30 μ M (DMSO – 0.6% of v/v) had no effect on KCl-induced contractions (Figure 4.4). Comparison of the effects of U73122 showed that it inhibited the responses to UTP, UDP and PGF_{2 α} to a similar extent, but was significantly less effective against KCl (Figure 4.5).

In contrast, 10 μ M U73343 did not significantly alter the peak contractions induced by UTP, UDP and PGF_{2 α} , but did inhibit that to KCl (P<0.001) (Figure 4.6, 4.8). Increasing the concentration of U73343 to 30 μ M virtually abolished the response to KCl (P<0.001), inhibited the PGF_{2 α} -evoked contraction by over 50% (P<0.01) and modestly reduced the responses to UTP and UDP (P<0.01 and P<0.05, respectively) (Figure 4.7, 4.8). Neither U73122 nor U73343 at any of the concentrations applied, induced any change of basal tone of the arteries. Thus, at

10 μ M, U73122 appears to act selectively. Furthermore, the contractions evoked by UTP, UDP and PGF_{2 α} are, at least in part, dependent upon activation of PI-PLC.

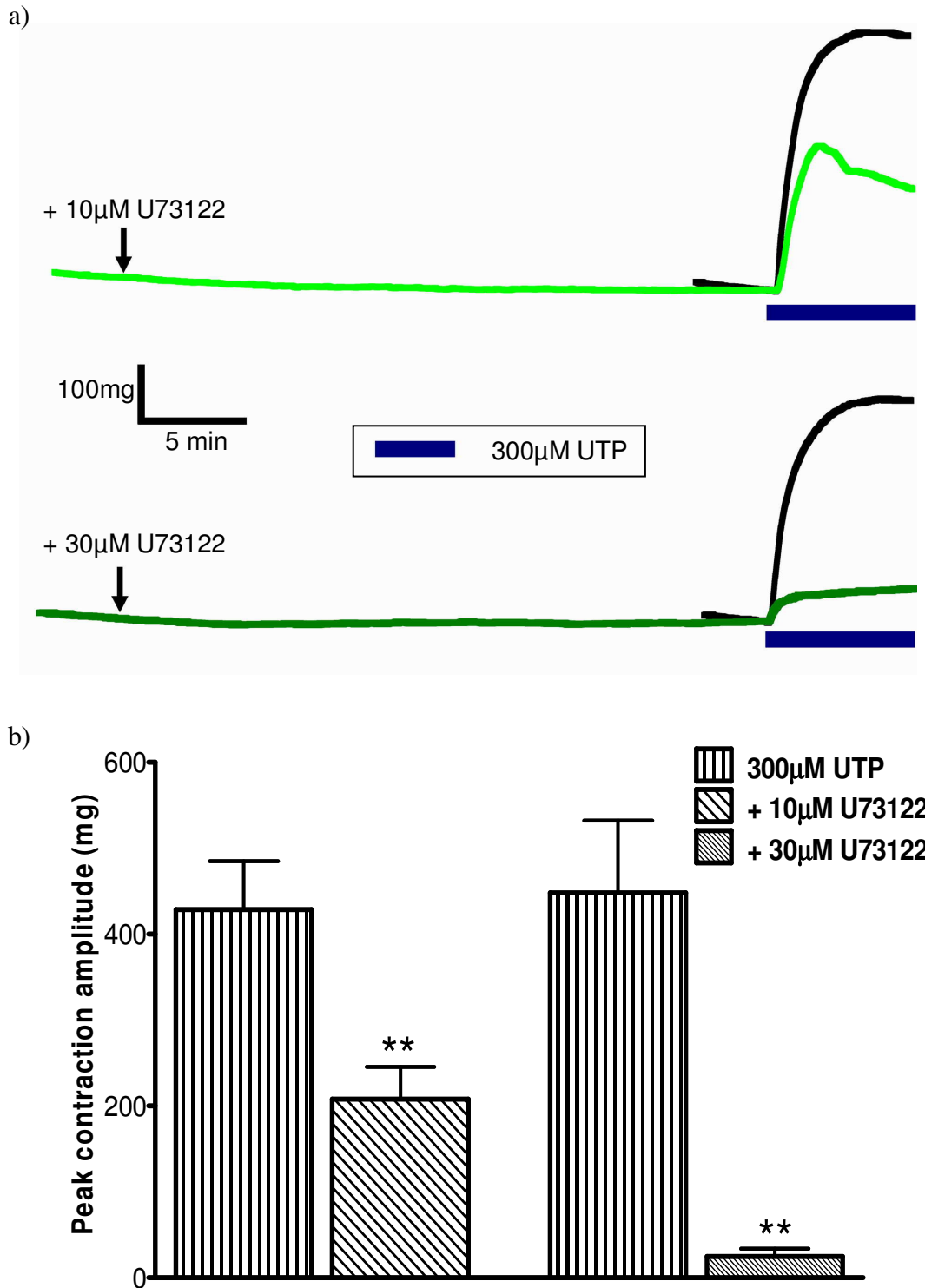


Figure 4.1. UTP-evoked contractile response in endothelium-denuded SPA before and after preincubation with U73122. a) The original traces from two different preparations show superimposed contractions in response to 300µM UTP before (black traces) and after (coloured traces) preincubation with 10 or 30µM U73122 for 30 min. UTP was added as indicated by the solid bar. b) shows the mean peak contraction amplitudes in response to 300µM UTP alone and with either 10 or 30µM U73122. n=5 for both groups. Data are shown as mean ± S.E.M. **P<0.01 for responses in the presence of U73122 compared with the control.

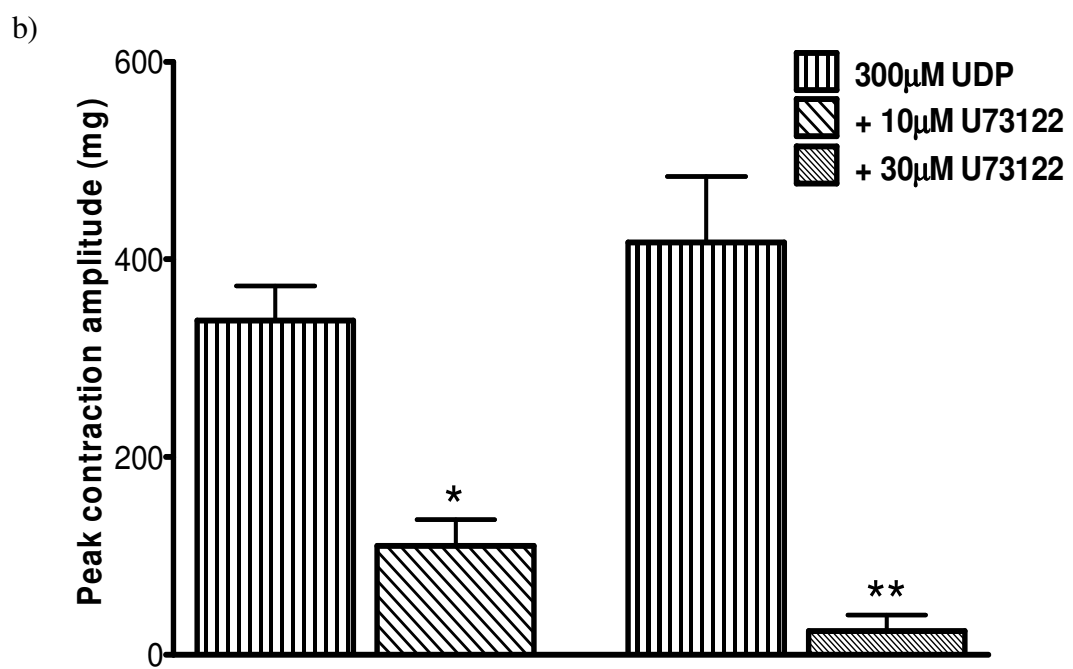
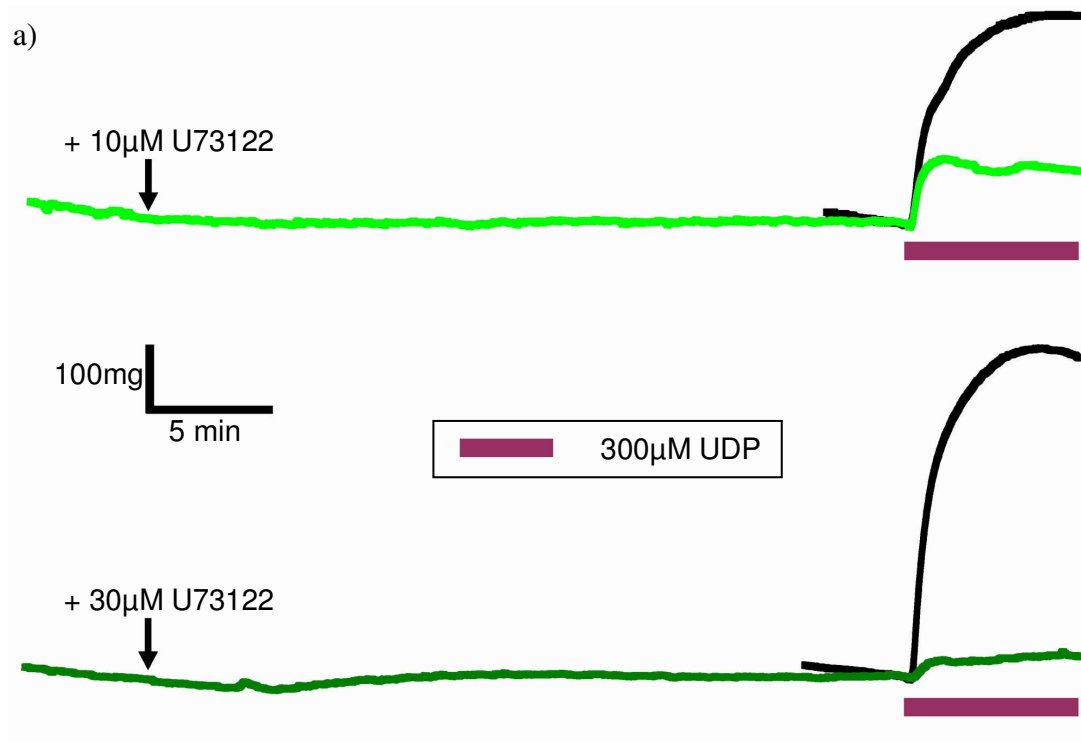


Figure 4.2. Contractile responses evoked by UDP in endothelium-denuded SPA before and after preincubation with U73122. a) The typical traces from two different preparations show superimposed contractions in response to 300µM UDP before (black traces) and after (coloured traces) preincubation with 10 or 30µM U73122. UDP was added as indicated by the solid bar. b) shows the mean peak amplitudes in response to 300µM UDP alone and with either 10 or 30µM U73122. n=5 for both groups. Data are shown as mean ± S.E.M. *P<0.05 and **P<0.01 for responses in the presence of 10 and 30µM U73122, respectively, compared with the control.

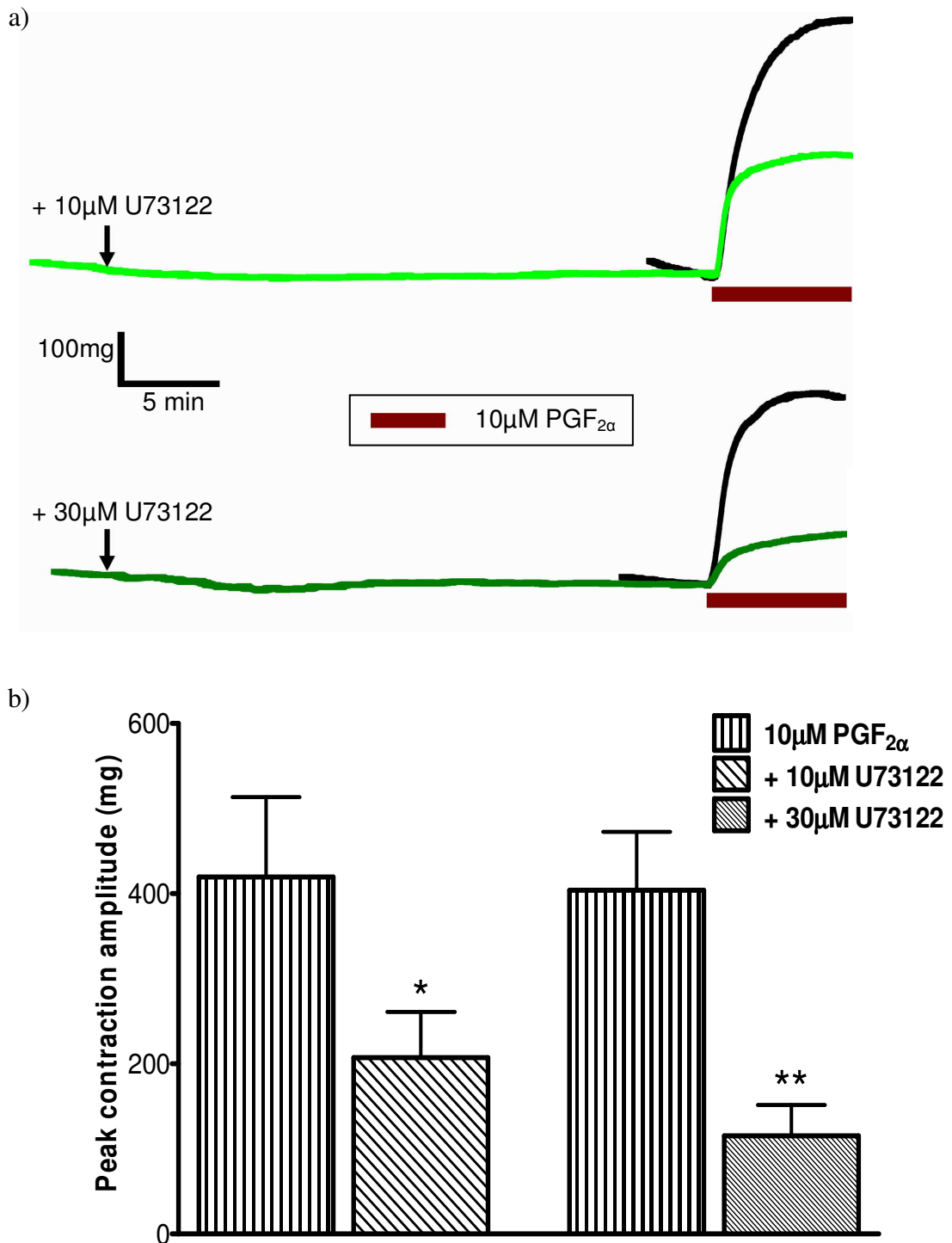


Figure 4.3. Vasoconstriction of endothelium-denuded SPA evoked by PGF_{2α} before and after preincubation with U73122. a) The original traces from two different preparations show superimposed contractions in response to 10µM PGF_{2α} before (black traces) and after (coloured traces) preincubation with 10 or 30µM U73122. PGF_{2α} was added as indicated by the solid bar. b) shows the mean peak amplitudes in response to 10µM PGF_{2α} alone and with either 10 or 30µM U73122. n=5 for both groups. Data are shown as mean ± S.E.M. *P<0.05 and **P<0.01 for responses in the presence of 10 and 30µM U73122, respectively, compared with the control.

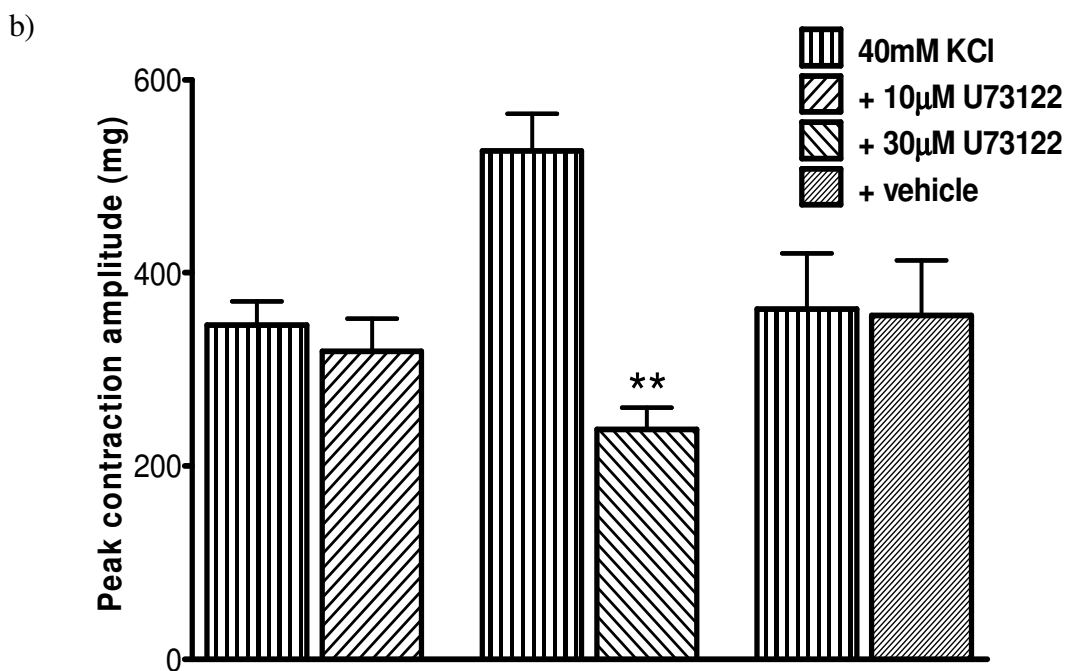
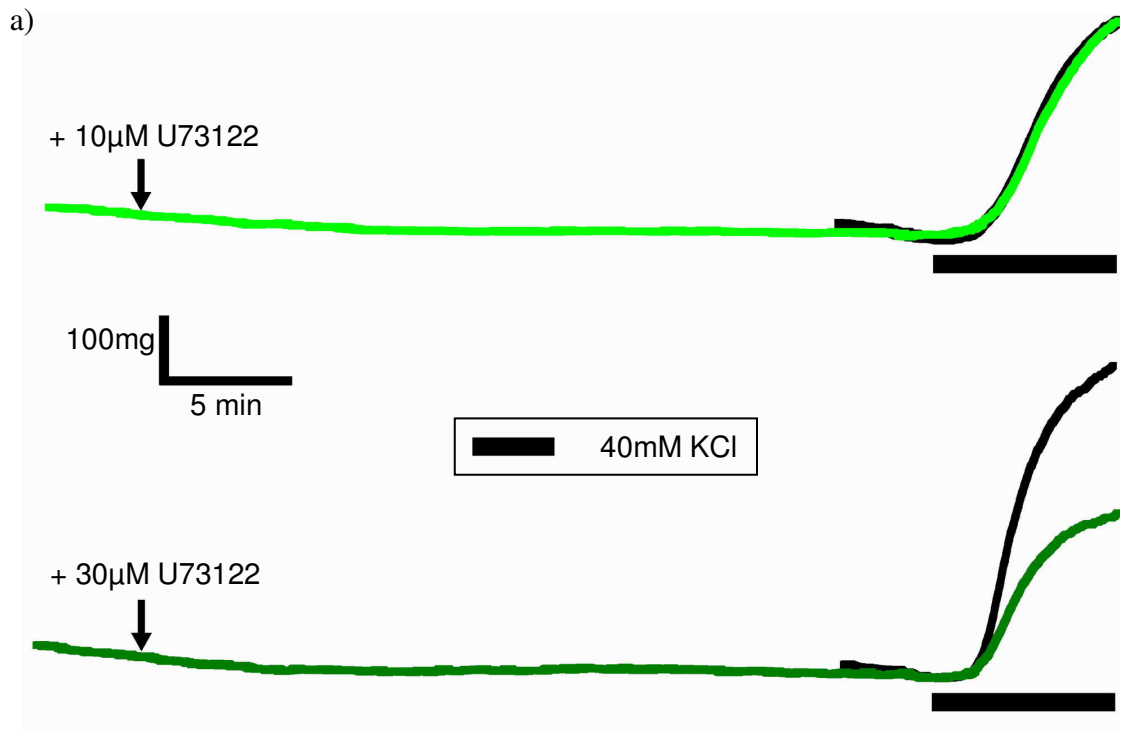


Figure 4.4. KCl-evoked contraction in endothelium-denuded SPA before and after preincubation with U73122. a) The typical traces from two different preparations show superimposed contractions in response to 40mM KCl before (black traces) and after (coloured traces) preincubation with 10 or 30µM U73122. b) shows the mean peak amplitudes in response to 40mM KCl alone and with either U73122 (10 or 30µM) or vehicle (DMSO – 0.6% of v/v). n=5 and 4 for U73122 and vehicle interventions, respectively. Data are shown as mean ± S.E.M. **P<0.01 for response in the presence of 30µM U73122 versus control.

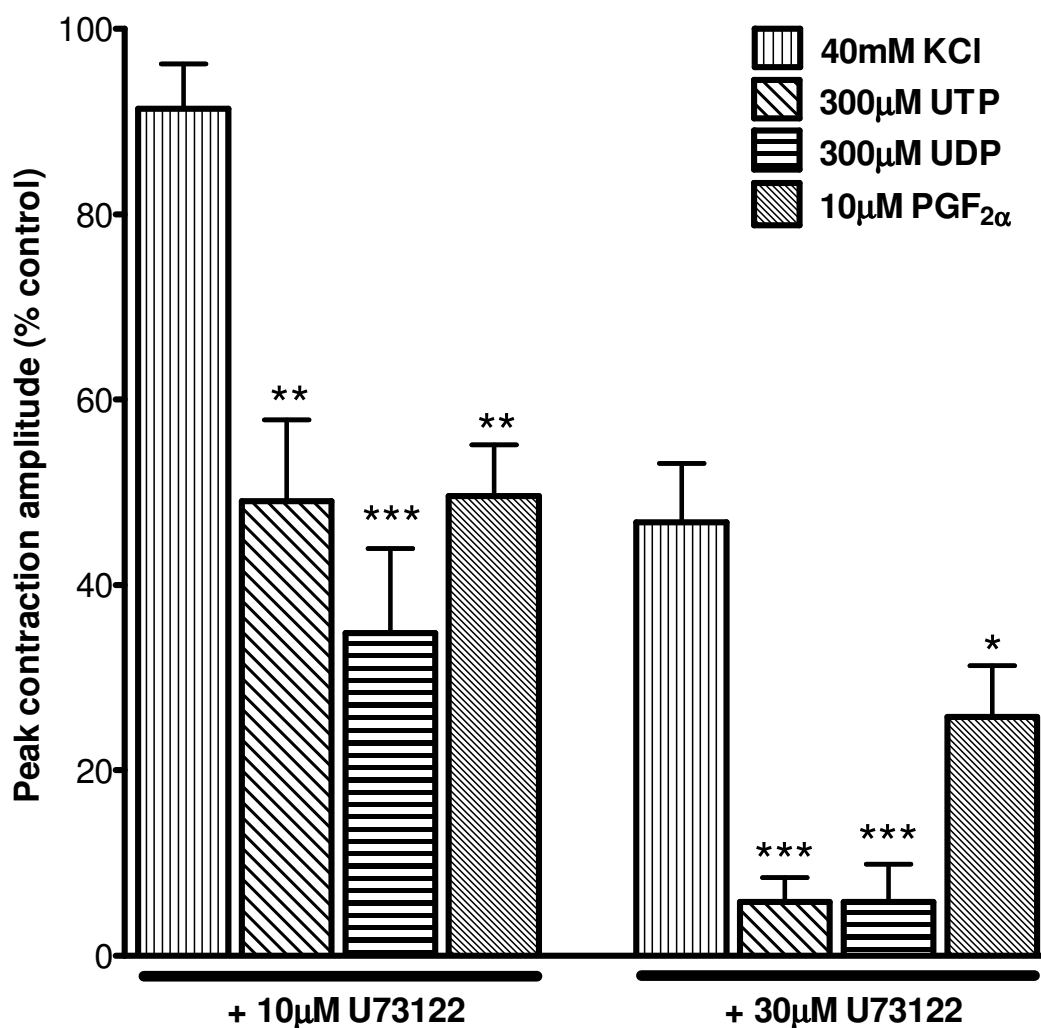


Figure 4.5. Effect of U73122 on peak contractions induced by UTP, UDP, PGF_{2α} and KCl in endothelium-denuded SPA. The mean peak amplitudes of contraction for UTP and UDP (both 300μM), 10μM PGF_{2α} and 40mM KCl in the presence of 10 and 30μM U73122 are shown. n=5 for all data groups. Contractions are expressed as a % of the control contraction obtained before the inhibitor was added. Data are shown as mean ± S.E.M. *P<0.05, **P<0.01 and ***P<0.001 for the effects of U73122 against UTP, UDP and PGF_{2α} compared with against KCl.

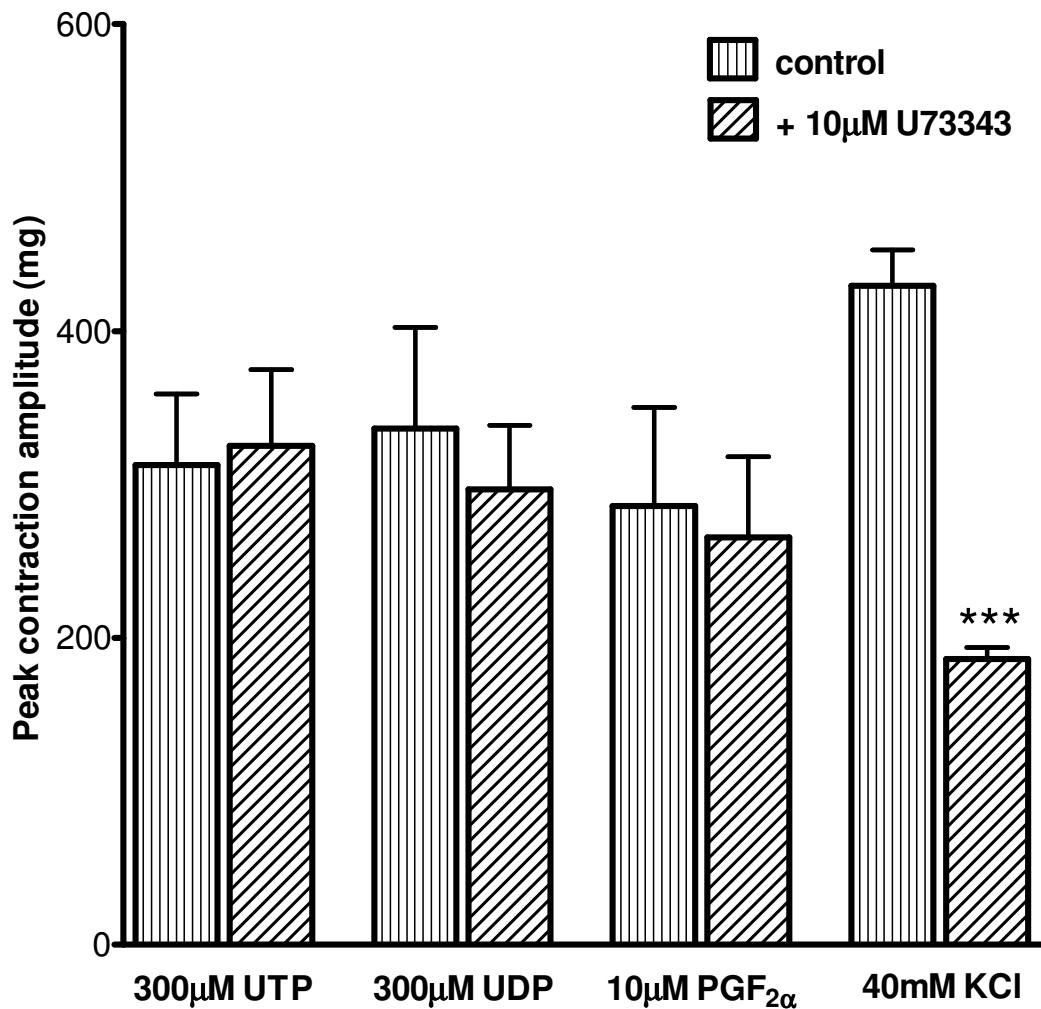


Figure 4.6. Contractile responses evoked by UTP, UDP, PGF_{2α} and KCl in endothelium-denuded SPA before and after preincubation with U73343. The mean peak amplitudes of contraction evoked by UTP and UDP (both 300µM), 10µM PGF_{2α} and 40mM KCl alone and in the presence of 10µM U73343 are shown. n=4 for all data groups. Data are expressed as mean ± S.E.M. ***P<0.001 for KCl response in the presence of U73343 compared with the control.

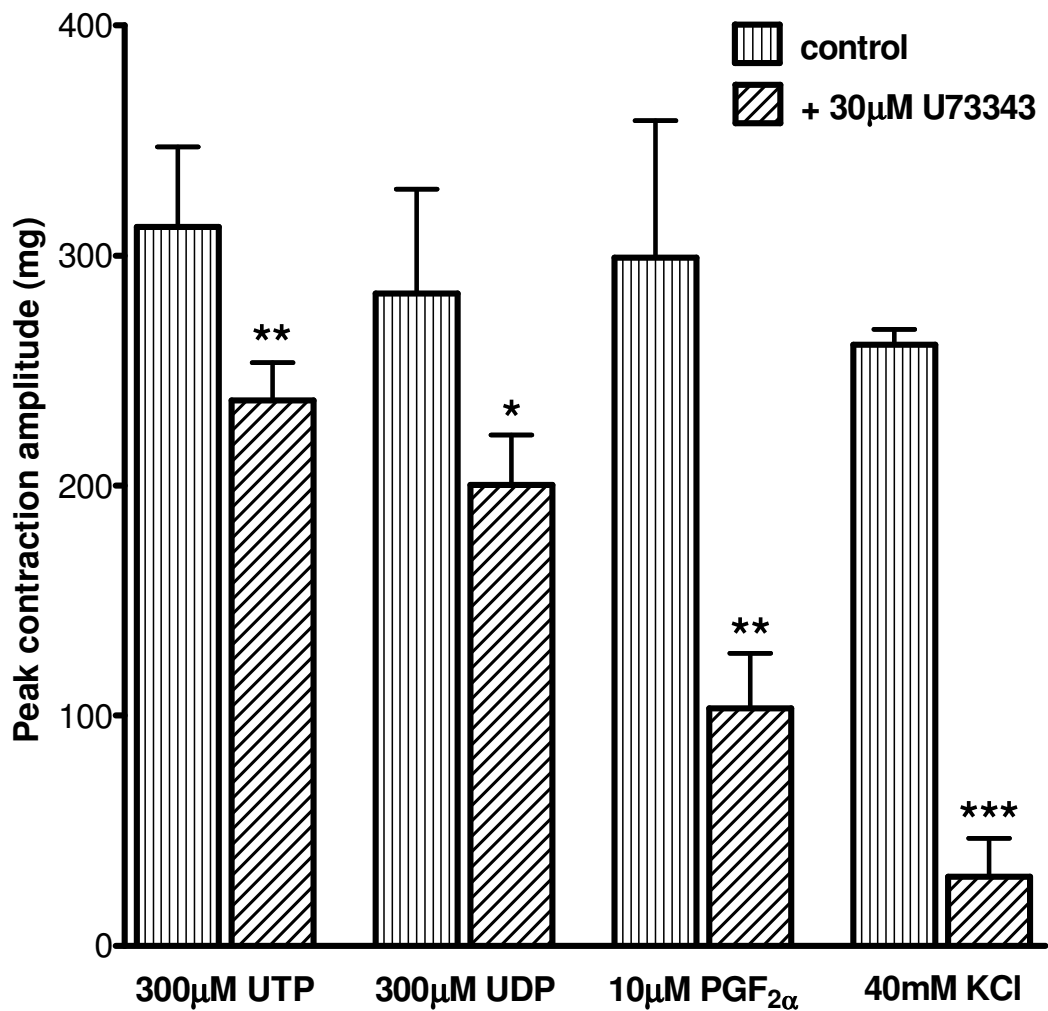


Figure 4.7. Vasoconstriction evoked by UTP, UDP, PGF_{2α} and KCl in endothelium-denuded SPA before and after preincubation with U73343. The mean peak amplitudes of contraction for UTP and UDP (both 300µM), 10µM PGF_{2α} and 40mM KCl alone and in the presence of 30µM U73343 are shown. n=4 for all data groups. Data are expressed as mean ± S.E.M. *P<0.05, **P<0.01 and ***P<0.001 for responses of UTP, UDP, PGF_{2α} and KCl in the presence of U73343 compared with the control.

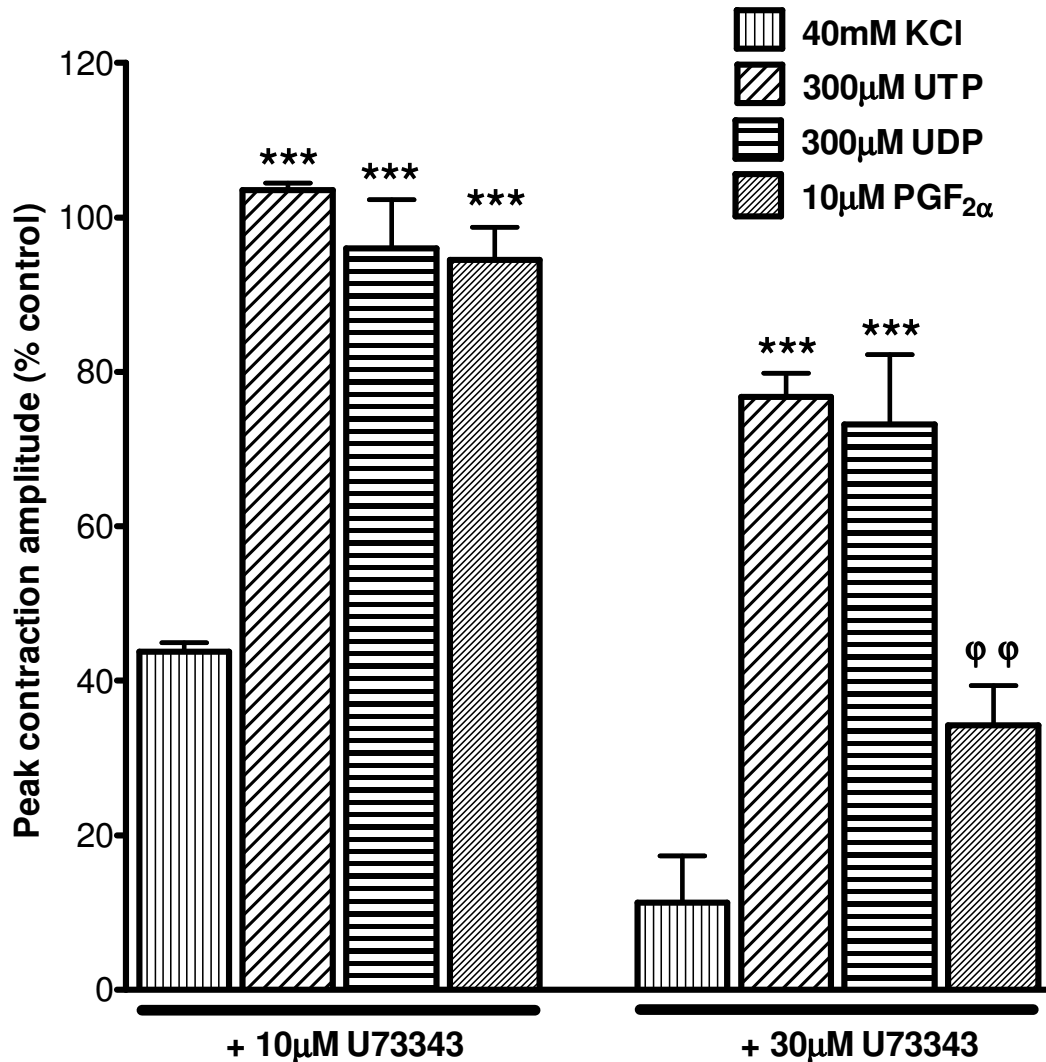


Figure 4.8. Effect of U73343 on peak contractions induced by UTP, UDP, PGF_{2α} and KCl in endothelium-denuded SPA. The mean peak amplitudes of contraction for UTP and UDP (both 300µM), 10µM PGF_{2α} and 40mM KCl in the presence of 10 and 30µM U73343 are shown. n= 4 for all data groups. Contractions are expressed as a % of the control contraction obtained before the inhibitor was added. Data are shown as mean ± S.E.M. ***P<0.001 for the effects of U73343 against UTP, UDP and PGF_{2α} compared with against KCl, and φφP<0.01 for the pair-wise comparisons between either UTP or UDP and PGF_{2α}.

2.2. Involvement of PKC and Rho Kinase in UTP- and UDP-Evoked Contractions

2.2.1. Effective Concentration of GF10923X and Effect of 10 μ M Y27632 on PKC

The initial experiments were designed to establish an effective concentration of the PKC inhibitor GF109203X and to determine if 10 μ M of the Rho kinase inhibitor Y27632 inhibits PKC, as has been suggested previously (Eto *et al.*, 2001; Budzyn *et al.*, 2006). To do so, the PKC activator PMA was used, which at 10 μ M induced a very slow contraction of variable peak amplitude (range = 58 – 390mg) that in most cases reached a peak (168 ± 20 mg, n=18) within 60 min (Figure 4.9a). In six of these tissues, the time-course was further studied and the mean contraction at 90 min was $91.5 \pm 10.4\%$ of that at 60 min ($\%_{90/60}$) (Figure 4.9b). This change was not significant.

3 μ M GF109203X has previously been used to inhibit PKC (Toullec *et al.*, 1991), but in rat isolated pulmonary artery 10 μ M PMA still evoked contractions when added 15 min after 3 μ M GF109203X (n=2) (Figure 4.10a). Furthermore, when 3 μ M GF109203X was added once the PMA-induced contraction had reached a peak, it rapidly caused the contraction to decline (n=3). Therefore, the concentration of GF109203X was increased to 10 μ M, which abolished the contractions, whether applied 15 min before (n=6) or 60 min after (n=6) PMA addition (Figure 4.10b). Thus, 10 μ M GF109203X was used in the remainder of the study.

When 10 μ M Y27632 was added 15 min beforehand, 10 μ M PMA evoked contractions which were 187 ± 45 mg (n=5) at 60 min and maintained over 90 min (Figures 4.11, 4.12). This was not significantly different from the response to PMA described above in the absence of Y27632. Furthermore, when 10 μ M Y27632 was added 60 min after 10 μ M PMA application, no significant change in response amplitude was seen over the next 30 min (Figure 4.11, 4.12). Thus, at 10 μ M Y27632 does not appear to inhibit PKC.

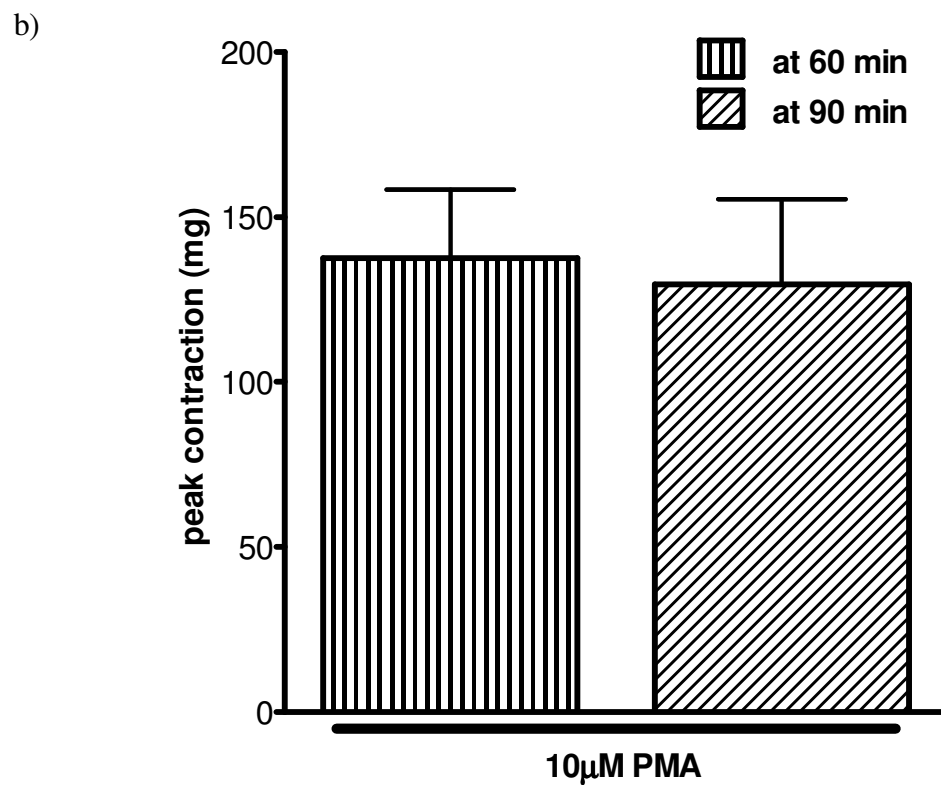
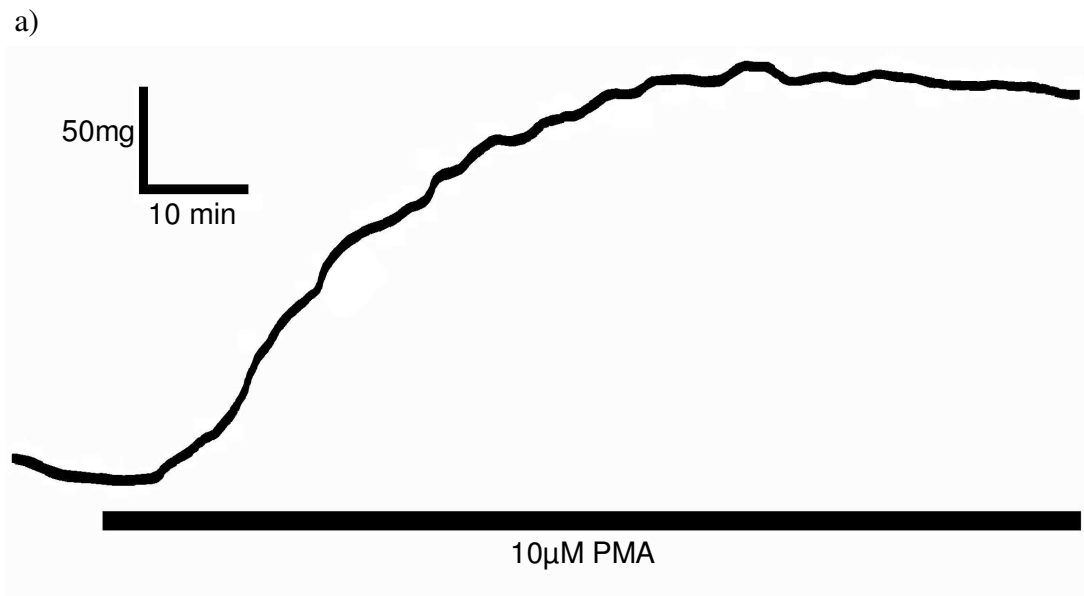


Figure 4.9. PMA-evoked vasoconstriction of endothelium-denuded rat SPA. a) The trace shows a typical contractile response induced by 10µM PMA added for 90 min, as indicated by the solid bar. b) The mean amplitude of contractions measured at 60 min and 90 min following 10µM PMA addition (n=6). Data are expressed as mean ± S.E.M.

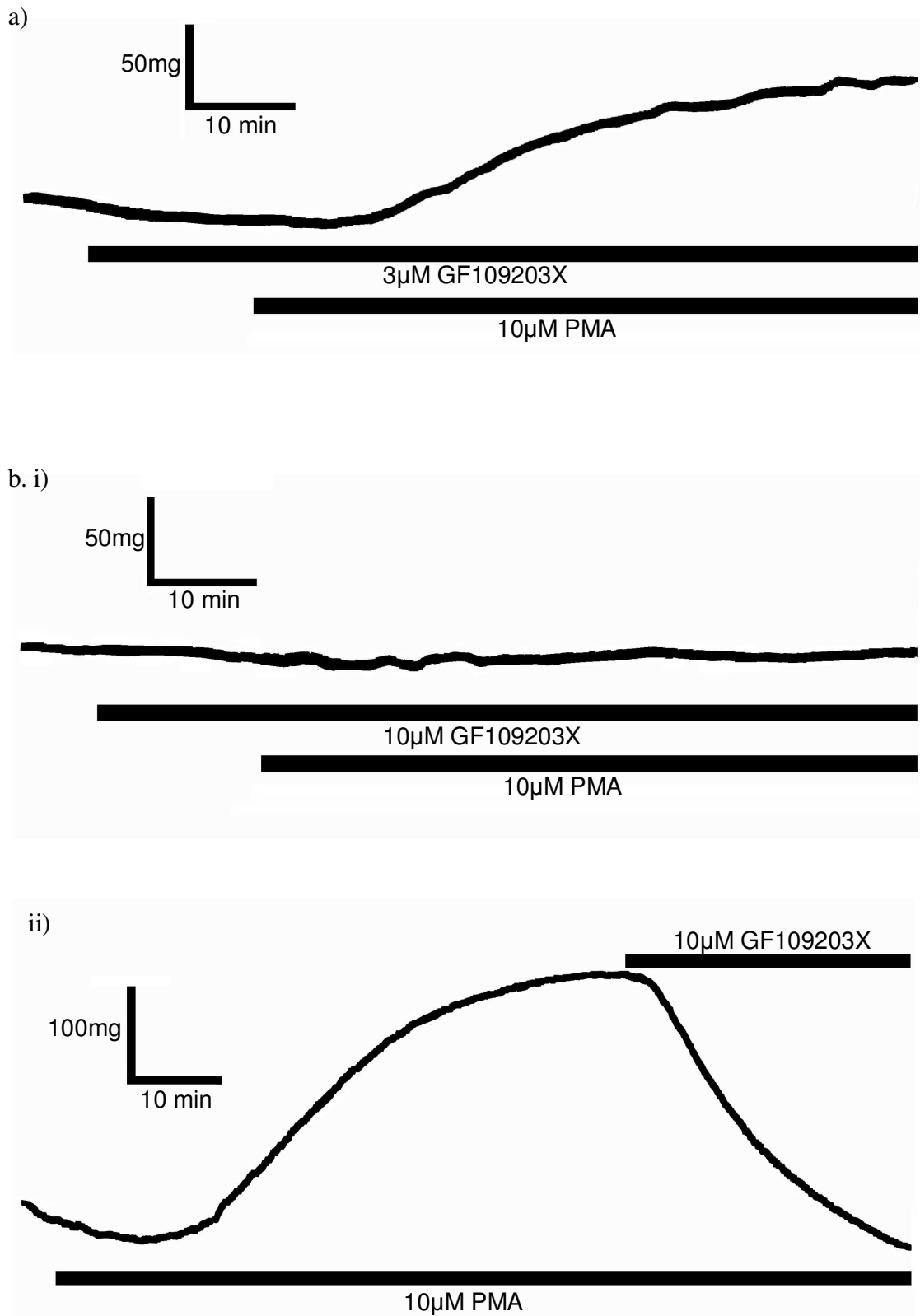


Figure 4.10. The effect of GF109203X on PMA-evoked vasoconstriction of endothelium-denuded rat SPA. The traces show contractions evoked by 10µM PMA after treatment with GF109203X at a) 3µM applied for 15 min before PMA, and b) 10µM applied for i) 15 min before or ii) 60 min after PMA. Both agonist and inhibitor were added as indicated by the solid bars.

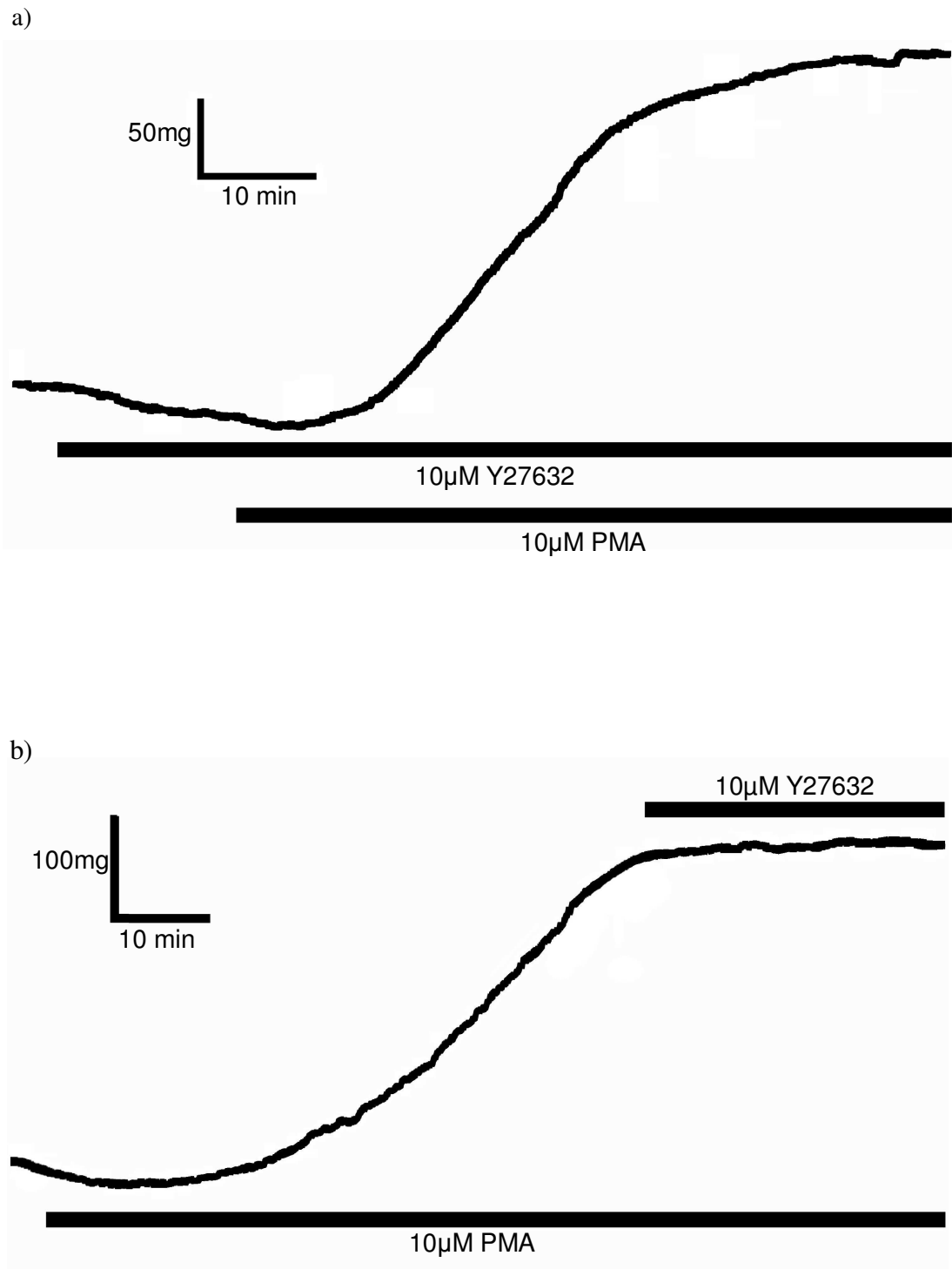


Figure 4.11. The effect of Y27632 on PMA-evoked vasoconstriction of endothelium-denuded rat SPA. The traces show contractions evoked by 10µM PMA in the presence of 10µM Y27632 applied a) for 15 min before PMA and b) 60 min after PMA for 30 min, is shown. Both agonist and inhibitor were added as indicated by the solid bars.

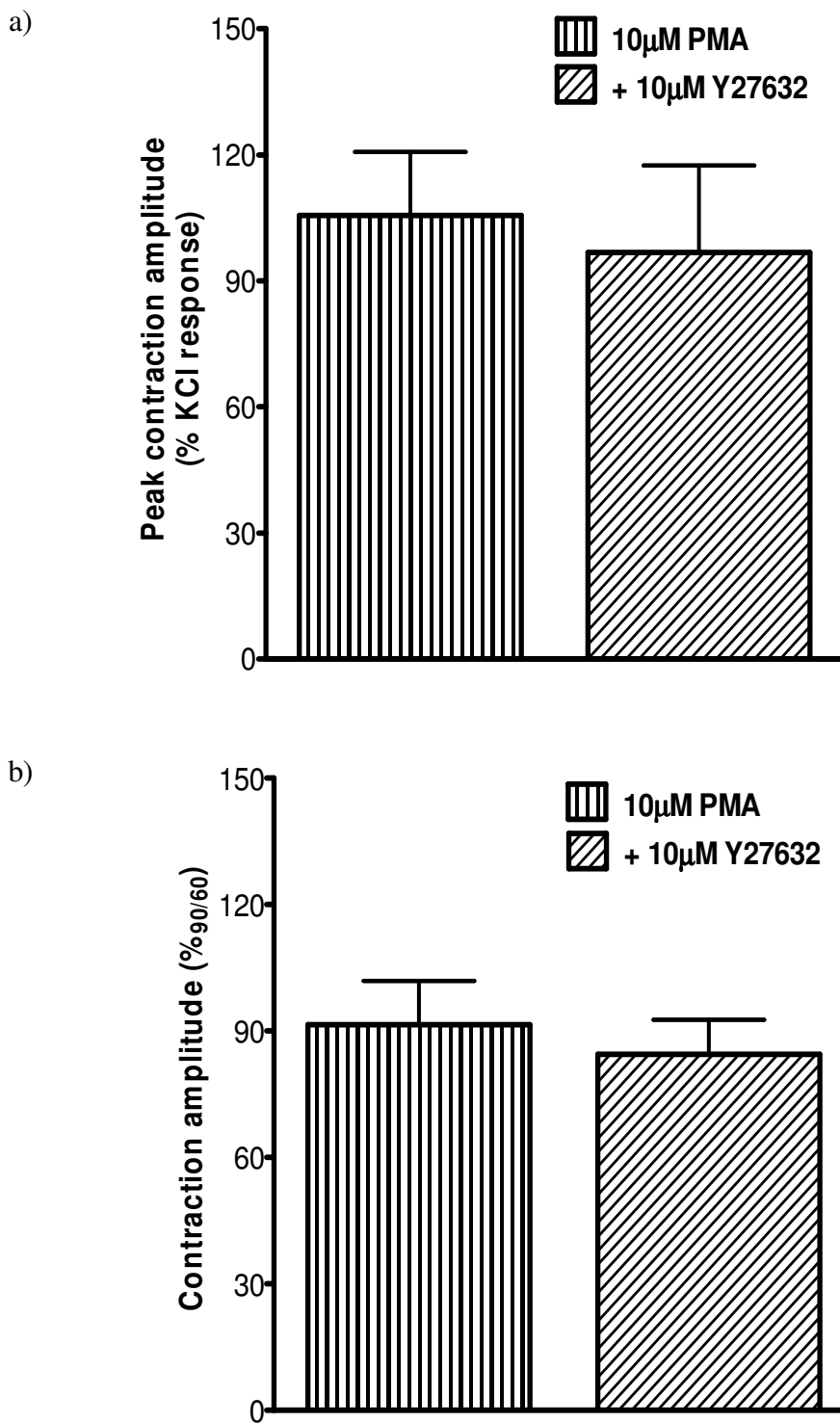


Figure 4.12. The effect of Y27632 on contractile responses induced by PMA in endothelium-denuded rat SPA. (a) shows the mean peak amplitudes of contraction, expressed as a % of 40mM KCl response, evoked by 10µM PMA, without and with 15 min preincubation of 10µM Y27632. b) The mean contractile amplitude of 10µM PMA alone and in the presence of 10µM Y27632 for 30 min applied 60 min after PMA, expressed as a % of contractile response at 60 min are shown. n=6 for all data groups. Data are shown as mean \pm S.E.M.

2.2.2. Effects of Y27632 and GF109203X on the Peak Contraction Evoked by Nucleotides and KCl

To determine the effect of Y27632 and GF109203X on the peak amplitude of contractions induced by UTP and UDP, the inhibitors were preincubated individually or in combination for 15 min prior to the addition of nucleotides. Under these conditions, 10 μ M Y27632 and 10 μ M GF109203X both significantly reduced the peak amplitude of contractions evoked by UTP by $18.8 \pm 2.5\%$ (n=5) and $22.9 \pm 5.5\%$ (n=7) (P<0.01 for both), respectively and to UDP by $31.0 \pm 4.9\%$ (n=6, P<0.05) and $49.0 \pm 5.0\%$ (n=6, P<0.01), respectively (Figure 4.13, 4.14). There was no significant difference in the inhibitory effects of Y27632 and GF109203X against UTP, but GF109203X was significantly more effective than Y27632 against UDP (Figure 4.15). In both cases, the inhibitory effects were significantly larger (UTP inhibited by $49.8 \pm 7.4\%$ (n=6, P<0.05) and UDP inhibited by $75.3 \pm 5.0\%$ (n=6, P<0.01)), and approximately additive when the inhibitors were coapplied (Figure 4.14). Comparison of the effects of the inhibitors against UTP and UDP showed that the inhibition induced by Y27632, GF109203X or Y27632 and GF109203X, was in each case significantly greater against contractions induced by UDP compared with UTP (Figure 4.15) (P<0.05 for all). Thus, Rho kinase and PKC both appear to be involved in the peak of UTP- and UDP-evoked contractions and they act in an additive manner.

The effects of Y27632 and GF109203X (10 μ M for both) were further explored against the contractions induced by 40mM KCl. When preincubated for 15 min, Y27632 significantly reduced the KCl-evoked contraction by $18.6 \pm 2.1\%$ (n=8, P<0.001) (Figure 4.16). GF109203X also significantly reduced the contractions by $65.8 \pm 8.2\%$ (n=5, P<0.001) and this was a significantly greater effect than Y27632 (P<0.001). Coapplication of Y27632 and GF109203X inhibited the response to KCl by $78.1 \pm 6.1\%$ (n=5, P<0.001) and whilst this was significantly greater than the response to Y27632 alone (P<0.001), it was not significantly different from the inhibition induced by GF109203X alone. Thus, both Rho kinase and PKC appear to play a role in the peak of KCl-induced contractions, but in a non-additive manner.

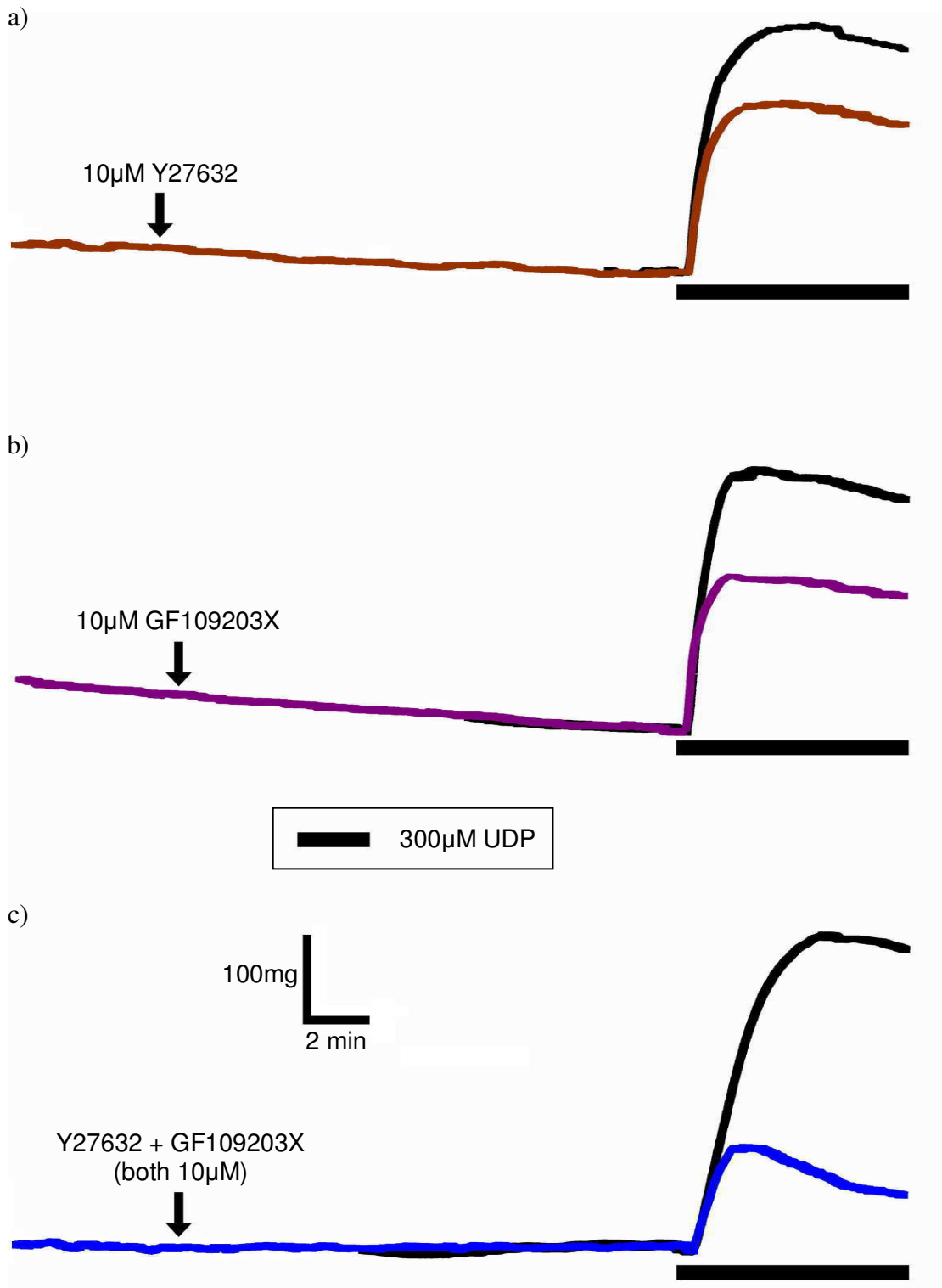


Figure 4.13. Effects of Y27632 and GF109203X on peak contractions evoked by UDP in endothelium-denuded rat SPA. Superimposed traces of contractions evoked by 300µM UDP produced before (black) and after (coloured) 15 min preincubation of a) 10µM Y27632, b) 10µM GF109203X and c) Y27632 + GF109203X (both 10µM). UDP and the inhibitors were added as indicated by the respective black solid bars and arrows.

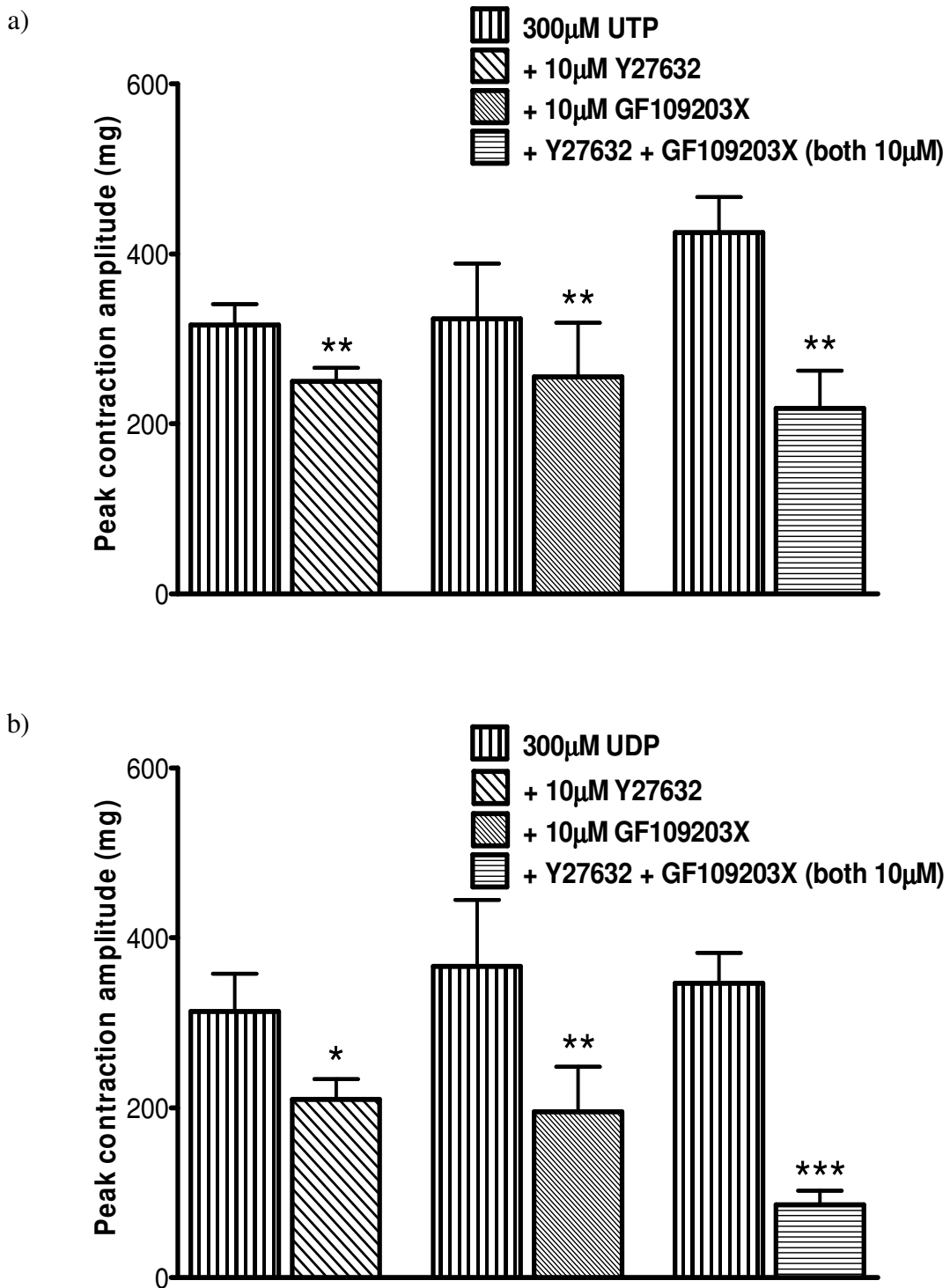


Figure 4.14. Effects of Y27632 and GF109203X on peak contractions evoked by UTP and UDP in endothelium-denuded rat SPA. The mean peak contraction amplitude of a) UTP and b) UDP (300µM for both) before and after 15 min preincubation with Y27632 and GF109203X (both 10µM), individually or in combination. n=5, 7 and 6 for Y27632, GF109203X and Y27632 + GF109203X, respectively, against UTP, and n=6 for all UDP data groups. Data are expressed as mean \pm S.E.M. *P<0.05, **P<0.01 and ***P<0.001 for the treated groups versus control.

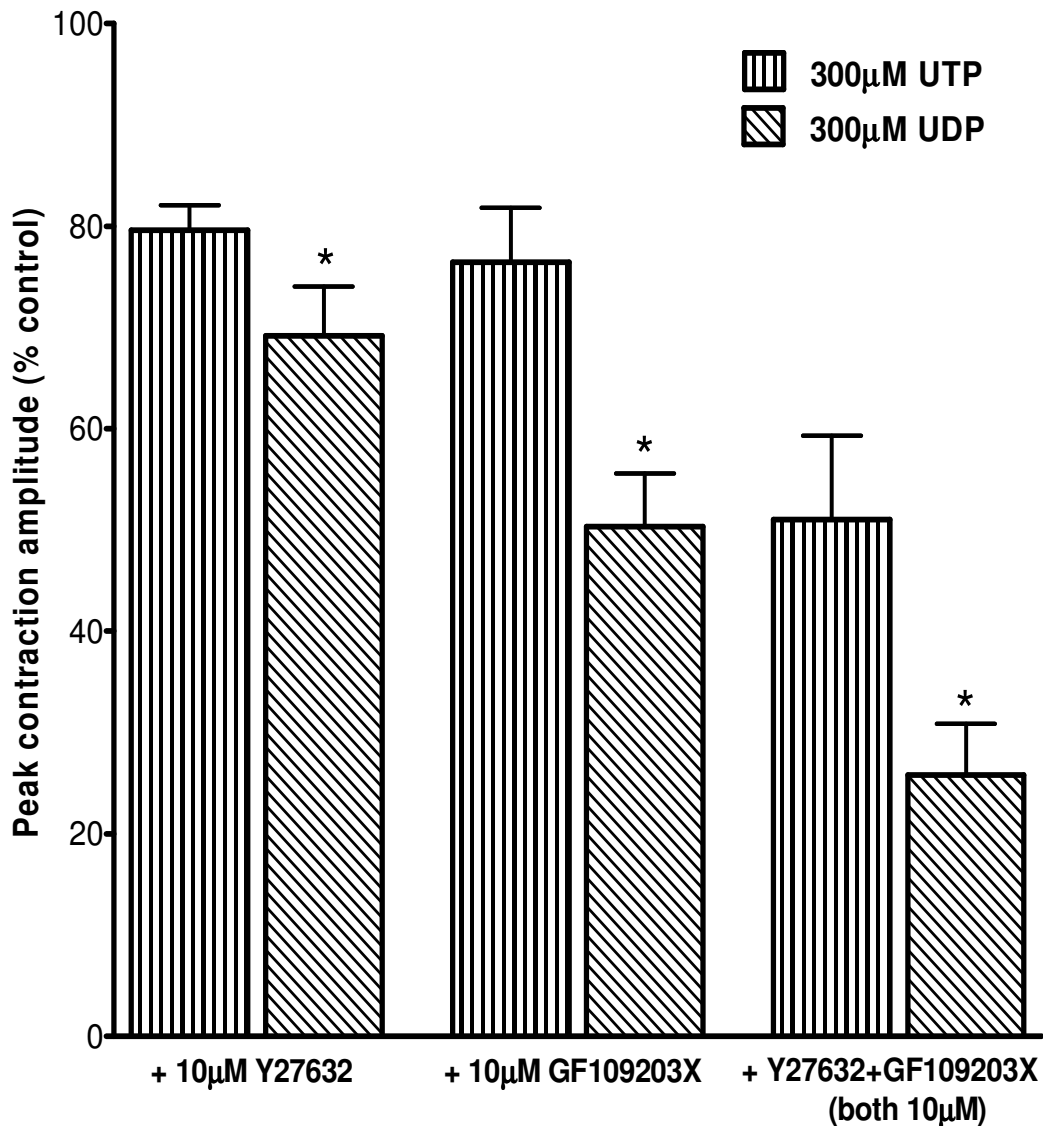


Figure 4.15. Effects of Y27632 and GF109203X on peak contractions evoked by UTP and UDP in endothelium-denuded rat SPA. The mean peak contraction amplitude to UTP and UDP (both 300µM) following 15 min preincubation of Y27632 and GF109203X (both 10µM), individually or in combination. n=5, 7 and 6 for Y27632, GF109203X and Y27632 + GF109203X, respectively, against UTP and n=6 for all UDP treated groups. Contractions are expressed as a % of the control contraction obtained before the inhibitors were added. Data are shown as mean ± S.E.M. *P<0.05 for treatment with either inhibitor alone or in combination against UTP compared with against UDP.

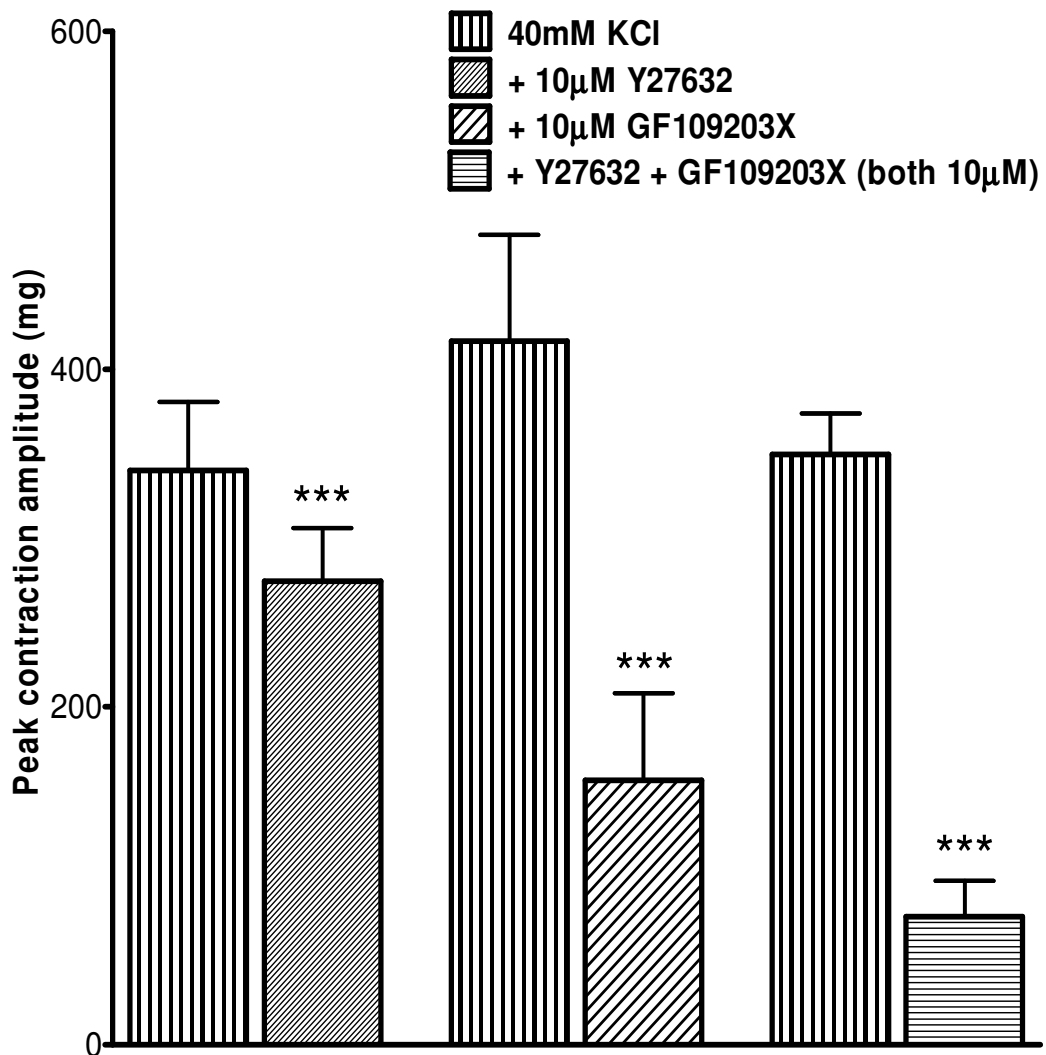


Figure 4.16. Effects of Y27632 and GF109203X on KCl-evoked contractions of endothelium-denuded rat SPA. The mean peak contraction amplitude of 40mM KCl before and after 15 min preincubation with Y27632 and GF109203X (both 10µM), individually or in combination. n=9 and 5 for Y27632 and GF109203X and Y27632 + GF109203X, respectively, against KCl. Data are shown as mean ± S.E.M. ***P<0.001 for treated groups versus control.

2.2.3. Effects of Y27632 and GF109203X on the Nucleotide-Evoked Sustained Contractions

The previous experiments showed that Rho kinase and PKC both contribute to the peak of the contractions induced by UTP and UDP. The aim of the next experiments was to determine if they also play a role in the subsequent plateau phase of the nucleotide-evoked contractions. To do so, the inhibitors were applied for 15 min once the nucleotide-evoked contractions had reached the plateau phase, i.e. at 20 min after adding the nucleotides (Figure 4.17). This plateau phase was maintained in the continued presence of agonist alone for at least another 15 min (Figure 3.6, 3.7 in chapter 3). Both 10 μ M Y27632 and 10 μ M GF109203X significantly diminished the plateau responses evoked by UTP by $18.2 \pm 3.4\%$ (n=6, P<0.01) and $35.0 \pm 4.6\%$ (n=8, P<0.001), respectively, and by UDP by $16.1 \pm 1.4\%$ (n=6, P<0.001) and $29.8 \pm 5.5\%$ (n=5, P<0.05), respectively (Figure 4.18). Additionally, coapplication of the inhibitors depressed the response to UTP by $38.3 \pm 8.1\%$ (n=7), which was not significantly different from the effect of either inhibitor applied on its own (Figure 4.17, 4.18). In contrast, the effect of coadministration against the contractions evoked by UDP ($48.7 \pm 9.0\%$ inhibition, (n=6)) was significantly greater than that of Y27632 (P<0.05), though not GF109203X alone (Figure 4.17, 4.18). Interestingly, there was no significant difference in the effects of the inhibitors against UTP compared with against UDP, either when the inhibitors were applied on their own or together. Thus Rho kinase and PKC both appear to contribute to the plateau phase of UTP- and UDP-evoked contractions, but an additive effect was only seen for the UDP-evoked response.

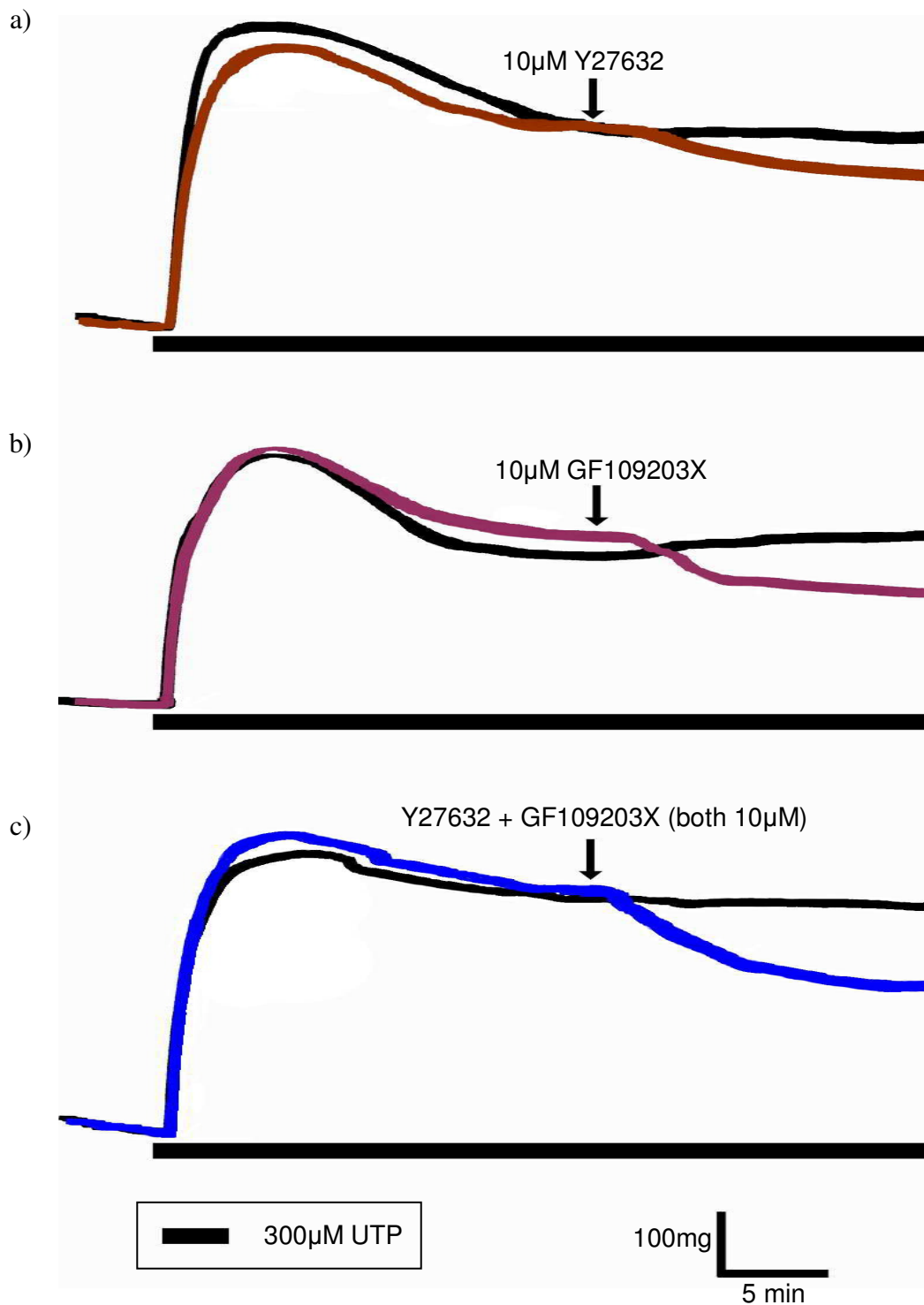


Figure 4.17. Effects of Y27632 and GF109203X on sustained contractions evoked by UTP in endothelium-denuded rat SPA. Superimposed traces obtained from the same tissues before (black) and after (coloured) adding a) 10 μM Y27632, b) 10 μM GF109203X or c) both together, once the contractions evoked by 300 μM UTP had reached the plateau phase, i.e. 20 min after adding agonist. UTP and the inhibitors were added as indicated by the black solid bars and the black arrows, respectively.

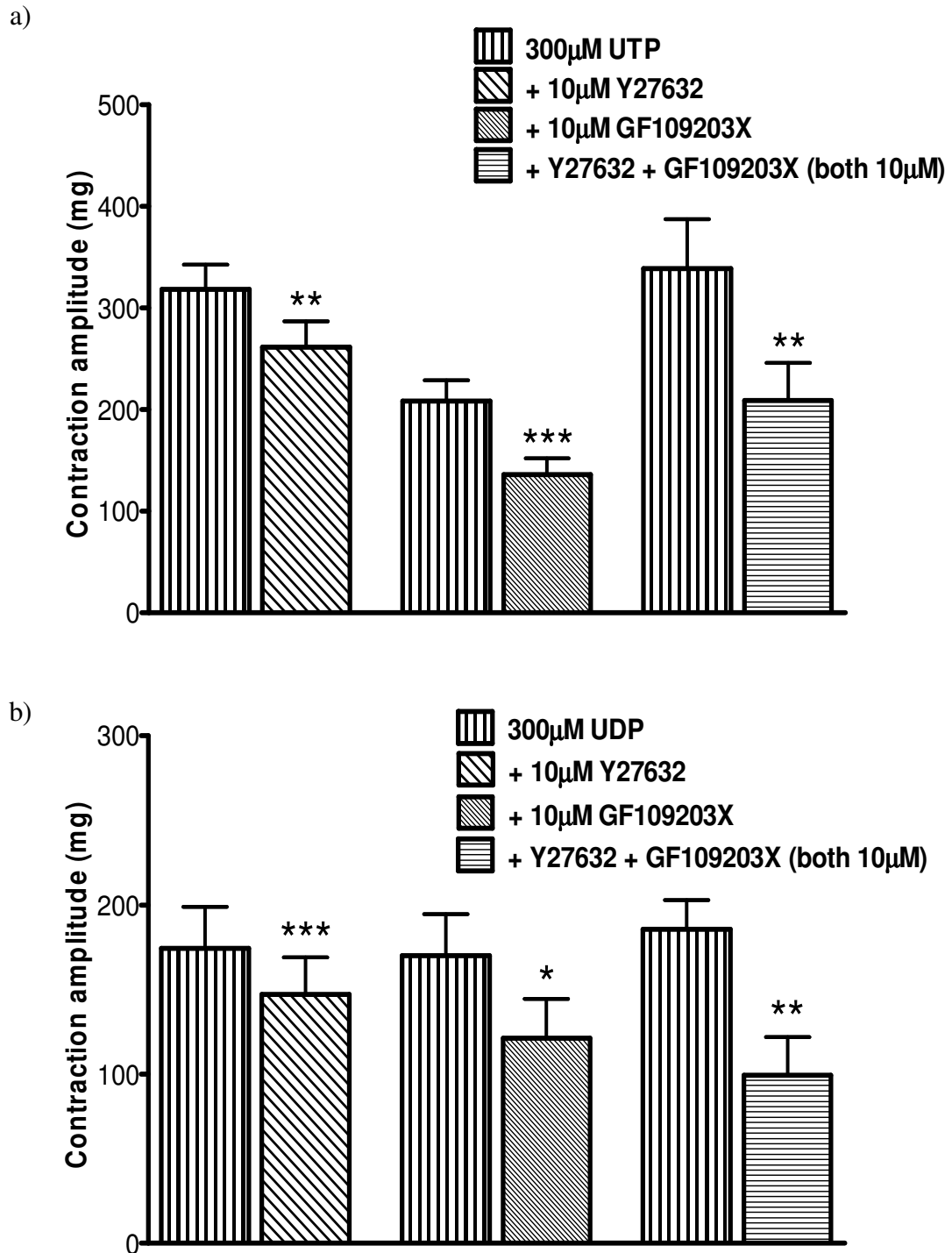


Figure 4.18. Effects of Y27632 and GF109203X on sustained contractions evoked by UTP and UDP in endothelium-denuded rat SPA. The mean sustained contractions after adding both inhibitors (10µM), alone or together once the contractions evoked by a) UTP or b) UDP (both 300µM) had reached the plateau phase. n=6, 8 and 7 for Y27632, GF109203X and Y27632 + GF109203X, respectively, against UTP, and n=5 and 6 for GF109203X and Y27632 and Y27632 + GF109203X, respectively, against UDP. Data are shown as mean ± S.E.M. *P<0.05, **P<0.01 and ***P<0.001 for treated groups versus control.

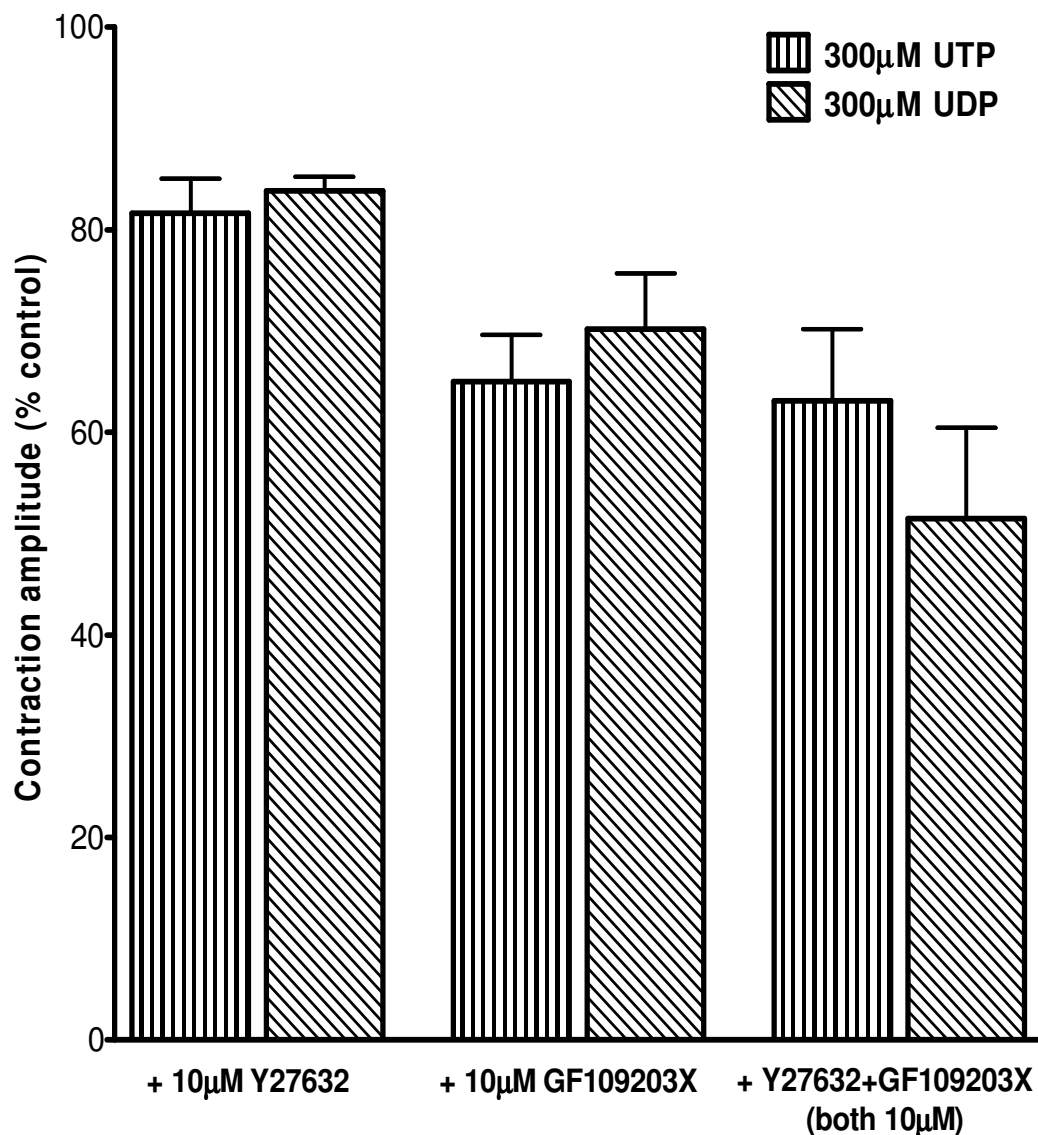


Figure 4.19. Effects of Y27632 and GF109203X on sustained contractions evoked by UTP and UDP in endothelium-denuded rat SPA. The mean resultant sustained contraction amplitude to UTP and UDP (both 300µM) following addition of the inhibitors (10µM), individually or both together, once the contractions had reached the plateau phase, i.e. 20 min after adding agonist. n=6, 8 and 7 for Y27632, GF109203X and GF109203X + Y27632, respectively, against UTP, and n=5 and 6 GF109203X and Y27632 and GF109203X + Y27632, respectively, against UDP. Contractions are expressed as % of the control amplitude obtained before the inhibitors were added. Data are shown as mean ± S.E.M.

3. DISCUSSION

The results of this study show that the peak responses evoked by UTP and UDP were significantly reduced after preincubation with the selective PI-PLC inhibitor U73122 at a concentration (10 μ M) that had no effect on KCl-induced contractions, but unaffected by its inactive analogue U73343 at the same concentration. In addition, both preincubation and post-addition of the Rho kinase inhibitor Y27632 and the PKC inhibitor GF109203X also resulted in a significant reduction of the nucleotide-evoked contractions. While no effect was observed with Y27632 intervention, GF109203X abolished the PMA-evoked contractions. Thus, these data indicate that UTP and UDP evoked contractions of rat SPA that are dependent upon PI-PLC, Rho kinase and PKC, and that Rho kinase and PKC are involved in both the peak contraction and the plateau phase.

3.1. Role of PI-PLC in Contractions Evoked by UTP and UDP

At 10 μ M U73122, but not its inactive analogue U73343, inhibited contractile responses evoked by UTP, UDP and PGF_{2 α} by over 50%, but had no effect on the response to KCl. Increasing the concentration of U73122 to 30 μ M produced further inhibition of the contractions, however, non-selective activity might be suspected, as a significant attenuation of the KCl response was now seen. KCl induces contraction of smooth muscle independently of PI-PLC by inducing membrane depolarisation and subsequent Ca²⁺ entry via voltage-gated Ca²⁺ channels (Nelson *et al.*, 1988). Moreover, 30 μ M U73343 also suppressed the action of all 4 agonists. Thus, at 10 μ M, but not 30 μ M, U73122 appears to selectively inhibit PI-PLC. These findings indicate for the first time a major role for PI-PLC in the development of P2Y receptor-mediated contractions in rat SPA. This is consistent with the UTP- and UDP-sensitive P2Y₂, P2Y₄ and P2Y₆ receptors coupling to G_{q11} (Abbracchio *et al.*, 2006; see also Table 1.3 in Chapter 1). Inhibition of P2Y receptor-mediated effects by U73122 has previously been reported in various tissues and cell types, including human coronary artery smooth muscle (Strøbaek *et al.*, 1996), mouse ventricular myocytes (Yamamoto *et al.*, 2007) and astrocytes (Weng *et al.*, 2008).

PGF_{2 α} was also used to evoke contractions in this part of the study as it is known to act via PI-PLC (Abramovitz *et al.*, 1994) and U73122 depressed the response to

PGF_{2α} to a similar extent as UTP and UDP. Indeed, this inhibitor has also been used to establish the possible involvement of PI-PLC in the activities of rat SPA induced by other agonists, including sphingosylphosphorylcholine (SPC)-induced potentiation of KCl-evoked contractions (Snetkov *et al.*, 2008) and inhibition of voltage-gated K⁺ currents by ET-1 (Shimoda *et al.*, 1998) and 5-HT (Cogolludo *et al.*, 2006).

3.2. Involvement of PKC and Rho Kinase in UTP- and UDP-Evoked Contractions

3.2.1. Effective Concentration of GF10923X and Effect of 10μM Y27632 on PKC

In this study, preliminary experiments to determine an effective concentration of the PKC inhibitor GF109203X found that contractions evoked by the PKC activator PMA were abolished by GF109203X at 10μM, but not 3μM. 3μM was initially used based on a previous study (Toullec *et al.*, 1991), where at this concentration GF109203X abolished the PKC-mediated phosphorylation of the protein P47 (plekstrin), evoked by the membrane permeant diacylglycerol analog diC₈ in human platelets. However, 3μM GF109203X was clearly not quite effective in the present study and so 10μM GF109203X was instead used to elucidate the extent of PKC contribution to the P2Y receptor-mediated contractions.

The current study also found that 10μM Y27632 did not alter contractile responses evoked by PMA. This is consistent with a previous report that 10μM Y27632 did not affect the cumulative concentration response curve to PMA generated in the permeabilised rat SPA (Jernigan *et al.*, 2004). Moreover, a study using purified PKC also showed that 10μM Y27632 did not inhibit activated PKC (Davies *et al.*, 2000). Thus, Y27632 at 10μM is highly selective for Rho kinase over PKC and hence, Y27632 at this concentration was used to establish any involvement of Rho kinase in the P2Y receptor-mediated contraction.

3.2.2. Role of Rho Kinase and PKC in P2Y Receptor-Mediated Contractions

A reduction of the peak contractions to UTP and UDP by about 20% and 30%, respectively, and of the plateau phase by about 20% by Y27632 observed in the current findings indicates a role for Rho kinase in both the peak and plateau phase of

P2Y receptor-mediated vasoconstriction of rat pulmonary artery. The present observation is consistent with a previous report (Jernigan *et al.*, 2004) in membrane-permeabilised preparations of rat pulmonary artery, showing virtual abolition of UTP-evoked vasoconstriction by Y27632.

Stimulation of receptor coupling to $G\alpha_{12/13}$ induces the formation of RhoA/GTP complex (Buhl *et al.*, 1995; Somlyo & Somlyo, 2000; Suzuki *et al.*, 2003, 2009), which then translocates to the plasma membrane before activating Rho kinase (Somlyo & Somlyo, 2000, 2003). Activation of Rho kinase subsequently phosphorylates MYPT1, the regulatory subunit of MLCP, and inhibits this phosphatase dephosphorylating MLC, leading to increased contraction without a rise in $[Ca^{2+}]_i$ (Somlyo & Somlyo, 2000). P2Y receptors are generally known to couple to $G\alpha_{q/11}$ (Filtz *et al.*, 1994; Abbracchio *et al.*, 2006), but coupling to other G protein subtypes, particularly $G\alpha_{12/13}$, had also been shown (Abbracchio *et al.*, 2006; Nishida *et al.*, 2008). Moreover, although RhoA activation following stimulation of a receptor is mainly mediated by $G\alpha_{12/13}$, as mentioned above, the involvement of $G\alpha_{q/11}$ in this process had also been demonstrated (Booden *et al.*, 2002; Vogt *et al.*, 2003). Sauzeau *et al.*, (2000) showed that stimulation of P2Y receptors in rat aortic smooth muscle increased the amount of membrane-bound RhoA and induced actin stress fiber formation that was sensitive to RhoA and Rho kinase inhibitors, such as C3 exoenzyme and Y27632, respectively. The above mechanism is also compatible with the observation whereby the activation of Rho kinase induced by ET-1 in normal and chronic hypoxic rat SPA was correlated with the MYPT-1 phosphorylation and vasoconstriction independent of change in $[Ca^{2+}]_i$ (Jernigan *et al.*, 2008). Furthermore, Tsai & Jiang, (2006) also demonstrated that the phenylephrine- and U46619-evoked contractions of rat tail artery were associated with MYPT1 and MLC phosphorylation. The contractile responses together with phosphorylation of the proteins were inhibited by Y27632. Rho kinase also appears to be involved in vasoconstriction of rat SPA by other agonists, including phenylephrine (Damron *et al.*, 2002) and SPC (Thomas *et al.*, 2005).

The current study showed that GF109203X also induced inhibition of contractions evoked by UTP and UDP by about 20% and 50%, respectively for the peak contraction and by about 30% for the plateau phase contractions to both

nucleotides, which indicates a role for PKC in P2Y receptor-mediated vasoconstriction. Stimulation of P2Y receptors can be assumed to activate PKC as the present results have indicated a clear association of the receptors with PI-PLC, the enzyme that hydrolyses PIP₂ to generate DAG, which then activates PKC. Several possible mechanisms could involve linking the activation of PKC with vasoconstriction of SPA. PKC could regulate the activity of Ca_v1.2 channel. Savineau *et al.*, (1991) demonstrated that vasoconstriction of rat pulmonary artery induced by the PKC activator PDB was enhanced and inhibited by the Ca_v1.2 channel agonist (Bay K 8644) and antagonist (verapamil), respectively. PKC also potentiated the activity of Ca_v1.2 channels during the active tone development of endothelium-denuded rabbit coronary artery (Cobine *et al.*, 2007). Furthermore, the constitutively active Ca_v1.2 channel in rat cerebral artery cells, which leads to sustained high Ca²⁺ influx (Ca²⁺ sparklets) was highly dependent on the activity of PKC (Navedo *et al.*, 2005). Interestingly, PKC may also affect this ion channel indirectly by depolarising the membrane via inhibition of voltage-gated K⁺ channels (Cogolludo *et al.*, 2003). In addition, PKC could act independently of changes in [Ca²⁺]_i by inducing CPI-17-associated Ca²⁺ sensitisation. At a constantly low [Ca²⁺]_i, phosphorylated, but not non-phosphorylated CPI-17 induced contraction of the β-escin-permeabilised rabbit femoral artery by more than 70% (Li *et al.*, 1998). An increase of phosphorylated CPI-17 was detected in rabbit femoral artery exposed to phenylephrine and histamine, but not to high K⁺ concentration, although all the interventions induced a comparable contractile response (Kitazawa *et al.*, 2000). To study direct and indirect increases in Ca²⁺ influx via Ca_v1.2 channels electrophysiological and Ca²⁺ imaging techniques could be used, but they were outwith the scope of this thesis. However, the potential involvement of Ca²⁺-sensitisation via PKC will be reported in a later chapter using membrane-permeabilised preparations.

The effect of adding Y27632 and GF109203X together was also investigated to determine whether these compounds act through similar or separate signalling mechanisms, and this treatment produced an additive inhibitory effect in the development of the peak of both UTP- and UDP-evoked contractions, while an additive effect was only observed in the sustained phase of the UDP-evoked

contractions. This indicates that Rho kinase and PKC contribute via separate signalling pathways to the peak contractile responses evoked by the nucleotides and the UDP-evoked sustained phase of contractions. In contrast, in the sustained contractions evoked by UTP, the Rho kinase-mediated pathway appears to converge with part of the downstream mechanism of PKC. The converging mechanism between Rho kinase and PKC could possibly be via inhibition of MLCP (Li *et al.*, 1998; Somlyo & Somlyo, 2003), however, the results in the subsequent permeabilised tissue experiment (Chapter 6) do not support such possibility. Alternatively, it cannot be ruled out that the inhibitors, especially GF109203X may have nonspecific activity at the concentration used in the current study (Davis *et al.*, 2000) and could inhibit other kinases which are responsible for the generation of contractions. This can be investigated by employing a biochemical technique, such as Western blotting, to monitor the association between inhibition of PKC activity at various concentrations of GF109203X and the effect to the contractile response. Interestingly, Y27632 and GF109203X added alone or together had nearly a two-fold greater effect against the peak contractions evoked by UDP compared to UTP, indicating a more prominent role of both Rho kinase and PKC in the development of peak contraction evoked by UDP. Since UDP is a potent agonist at P2Y₆ receptors (Chang *et al.*, 1995; Chen *et al.*, 1996; Nicholas *et al.*, 1996), this implies that the P2Y₆ receptor-mediated signalling mechanism is more dependent on Rho kinase and PKC compared to the signalling mechanisms mediated by other UTP-sensitive P2Y receptors known to exist in pulmonary artery smooth muscle.

3.2.3. Role of Rho Kinase and PKC in KCl-Induced Contractions

The present study also found that both Y27632 and GF109203X, when added alone or together diminished the contractions induced by KCl. As KCl acts via receptor-independent mechanisms to evoke vasoconstriction, this might seem to imply non-selective effects of these inhibitors. However, a recent review (Ratz *et al.*, 2005) highlights the association of KCl contractions and Ca²⁺ sensitisation. In several tissues Y27632 substantially inhibited contractions induced by KCl, but without altering the rise in cytoplasmic [Ca²⁺] (Mita *et al.*, 2002; Urban *et al.*, 2003). Urban *et al.*, (2003) further revealed that the KCl-induced response was associated

with the induction of Rho kinase translocation from the cytosol to the cell periphery, i.e. caveolae, and was dependent on Ca^{2+} . Ca^{2+} -dependent activation of Rho kinase was also implicated in KCl-induced contraction of rabbit thoracic aorta with the upstream mechanism involving the activation of calmodulin and Ca^{2+} /calmodulin-dependent protein kinase-II to induce the formation of the Rho-GTP complex (Sakurada *et al.*, 2003). Furthermore, Ca^{2+} -independent phospholipase A_2 can also mediate Rho kinase activation and contribute to KCl-induced contractions of rabbit femoral and renal arteries (Ratz *et al.*, 2009).

In contrast, Ratz *et al.*, (2005) reported that the involvement of PKC is minimal, if not absent, in the responses induced by KCl. However, their more recent papers did show a role for an atypical PKC isoform, PKC ζ , in the KCl-induced vasoconstriction of rabbit femoral and renal arteries (Ratz & Miner, 2009; Ratz *et al.*, 2009). The contractions of aorta and mesenteric arteries induced by KCl were also inhibited by PKC inhibitor Ro 31-8220 (Budzyn *et al.*, 2006). Thus, PKC does appear to play a role in KCl-induced vasoconstriction in some arteries at least. Possible mechanisms include potentiation of $\text{Ca}_v1.2$ currents, such that in the presence of GF109203X, the opening of $\text{Ca}_v1.2$ channels by KCl might have been less due to the lack of potentiation by PKC, as a consequence of inhibition of constitutively active PKC. Under these conditions, Ca^{2+} influx would be less. Patch clamp electrophysiology and Ca^{2+} imaging would be appropriate techniques with which to investigate these possibilities.

In summary, the findings in this chapter show for the first time that the activation of P2Y receptors leads to activation of PI-PLC, Rho Kinase and PKC, all of which play an important role in the pulmonary artery vasoconstriction. The response to KCl also involved Rho kinase and PKC. Both Rho kinase and PKC could potentially be acting to induce Ca^{2+} -sensitisation, but the techniques used thus far cannot conclusively establish such an association. Therefore, to address this issue, a membrane permeabilisation technique was used next that enabled to study Ca^{2+} sensitisation directly.

Chapter 5:

Establishing the optimum conditions for the permeabilisation protocol

1. INTRODUCTION

The role of Ca^{2+} in vasoconstriction can be investigated by employing two main techniques; a) fluorescent imaging with Ca^{2+} -sensitive dyes, e.g. fura 2, that enables quantification of $[\text{Ca}^{2+}]_i$ in an intact tissue, and b) permeabilising the smooth muscle cell membrane to allow tight control of $[\text{Ca}^{2+}]_i$. One advantage of the first technique is that it can achieve a high accuracy of $[\text{Ca}^{2+}]_i$ measurement, while causing minimal disruption to the structure and function of smooth muscle cells (Sato *et al.*, 1988; Somlyo & Himpens, 1989). However, it cannot be used to control $[\text{Ca}^{2+}]_i$. In order to do so, the permeabilisation technique must be used. In the early stage of its development, this technique used quite aggressive permeabilising compounds, such as saponin, to extensively disrupt the cell membrane, leaving the intracellular compartment readily accessible for clamping the global $[\text{Ca}^{2+}]_i$ at a desired level (Horiuti, 1986). Although the regulatory/contractile machinery was still functional there was considerable disruption of receptor/G-protein coupling (Itoh *et al.*, 1983; Kitazawa *et al.*, 1991). However, the subsequent introduction of a saponin derivative, β -escin, and ionophore compounds, such as ionomycin and α -toxin (Iizuka *et al.*, 1994; Evans *et al.*, 1999; Jernigan *et al.*, 2004), significantly improved the technique. Not only do these compounds create relatively small pores that allow access to low molecular weight solutes, such as ATP, they have much less effect on receptor/G-protein coupling.

Permeabilisation of the pulmonary artery preparation has routinely been studied at 26°C (Thomas *et al.*, 2005; Snetkov *et al.*, 2006), but successful experiments at room temperature (Crichton *et al.*, 1997), 24°C (Evans *et al.*, 1999), 25°C (Himpens *et al.*, 1990) and 37°C (Jernigan *et al.*, 2004, 2008) have also been reported. Most of these studies had used α -toxin as the permeabilising agent, at concentrations ranging from 60 $\mu\text{g}/\text{mL}$ to 2 mg/mL . Interestingly, Evans *et al.*, (1999) attempted to permeabilise the rat pulmonary artery using β -escin, but found that the preparation suffered a severe rundown of agonist response after 30 min. This was not improved even after preincubating the tissue with added calmodulin and GTP. This study also recorded a maximum response of about 0.28mN (~30mg) to Ca^{2+} at pCa 4.5 when the tissue was permeabilised with 120 $\mu\text{g}/\text{mL}$ α -toxin. This response was surprisingly much smaller than would be expected in this tissue. For example, as already indicated in this thesis

in a similar tissue preparation, 40mM KCl typically evokes a contraction of about 4 – 5mN. Furthermore, pulmonary artery from a different rat strain produced about 13.6mN tension (~33% of 80mM KCl-evoked response) when challenged with pCa 4.5 following α -toxin permeabilisation at 60 μ g/mL (Thomas *et al.*, 2005). Thus, these findings show the considerable impact that the type and concentration of permeabilising compound used can have on the outcome of the permeabilisation procedure.

As mentioned above, the pores created to allow Ca^{2+} movement across the membrane following permeabilisation are also large enough to permit other small compounds, notably ATP, to pass through them. As a common compensatory measure, ATP is added to the permeabilising buffer at millimolar concentrations, to ensure an adequate supply of this high energy molecule to the smooth muscle throughout the experiment. However, addition of millimolar ATP is problematic as it can activate P2X and P2Y receptors present in many preparations, including rat pulmonary artery (Chootip *et al.*, 2002).

Evidently, the permeabilisation technique can be quite challenging to execute successfully because it involves an assault on the cell membrane, and yet the normal cellular functions need to be preserved. However, with a carefully planned protocol, the interference to normal cellular functions can be kept to a minimum. The aim of this part of my studies was, therefore, to establish the optimum conditions for the permeabilisation of rat SPA in order to subsequently study the role of Ca^{2+} sensitisation in P2Y receptor-mediated contractions of rat SPA. The following key issues were explored; 1) effect of temperature on the contractile activity of the intact rat SPA, 2) preparation of permeabilising solution at various free $[\text{Ca}^{2+}]$, 3) effectiveness of the permeabilising agents, β -escin and α -toxin, and reproducibility of contractions of the permeabilised tissue and 4) the requirement for ATP in the permeabilisation solution.

2. RESULTS

2.1. Effect of Temperature on the Contractile Activity of Intact Rat SPA

In order to determine if changing the temperature alters the responsiveness of rat SPA, contractions were evoked at tissue bath temperatures of 37°C, 30°C and 26°C. It was immediately noticeable that the nucleotide-evoked contractions developed more slowly as the temperature decreased, particularly at 100µM and above (Figure 5.1). The average time from adding 100µM UTP and UDP to the development of peak contractions to 1mM was about 13, 18 and 30 min at 37°C, 30°C and 26°C, respectively (n=12 for UTP at 37°C, n=11 for UDP at 37°C, n=10 for both UTP and UDP at 30°C and 26°C).

UTP and UDP evoked concentration-dependent vasoconstriction at 37°C, but the cumulative concentration-response curves did not reach a maximum (Figure 5.1, 5.2a), and so EC₅₀ values could not be determined. Therefore, the concentration of nucleotides that induced a contraction that was 50% of the maximum response evoked by 1mM agonist (EC_{50max}) was used to compare the potency of the nucleotides. The cumulative concentration-response curves were then repeated two more times, at 30 min intervals.

For UTP-evoked contractile responses, the EC_{50max} of the first cumulative concentration-response curve was comparable with that for the second curve, but was significantly smaller than the third curve value (P<0.01) (Table 5.1). Lowering the temperature to 30°C did not change the potency pattern of repeated administration, as once again UTP was significantly less potent on the third addition compared with the first (P<0.01). When the temperature was further decreased to 26°C there was no significant difference in the EC_{50max} values for all the three UTP concentration-response curves. When comparing the responses between the above temperatures, UTP was slightly, but significantly less potent on first addition at 26°C compared with 37°C and 30°C (P<0.05 for both). However, UTP showed no difference in potency on second addition at each temperature, nor on third addition.

For UDP-evoked contractile responses, the EC_{50max} of the first cumulative concentration-response curve was comparable with that for the second curve, but was significantly smaller than the third curve value (P<0.05) (Table 5.1). When the temperature was decreased to 30°C there was no change of the potency pattern of

repeated administration as once again UDP was significantly less potent on the third addition compared with the first ($P < 0.01$). Lowering the temperature further to 26°C did not induce any significant difference in the $\text{EC}_{50\text{max}}$ values for all the three UDP concentration-response curves. When comparing the responses between the temperatures, UDP was slightly, but significantly less potent on first addition at 26°C compared with 37°C ($P < 0.05$) and 30°C ($P < 0.01$), whereas it was more potent on the third addition at 26°C compared with 37°C ($P < 0.05$). However, UDP showed no difference in potency on second addition at each temperature.

In order to determine if lowering the temperature affected response size, the amplitude of contraction produced by $300\mu\text{M}$ of UTP and UDP in each concentration response curve was compared (Figure 5.3a, b). For either nucleotide there were no significant differences in response amplitude at each temperature.

The contraction evoked by 40mM KCl, obtained 30 min after completing the third nucleotide cumulative-concentration response curve, and was found to be significantly larger at 5, 6, 7 and 8 min at 37°C ($n=23$) than at 26°C ($P < 0.001$ for 5 and 6 min, $P < 0.01$ for 7 and 8 min, $n=20$) and 30°C ($P < 0.01$ for 5 and 6 min, and $P < 0.05$ for 7 and 8 min, $n=20$) (Figure 5.3c). Additionally, the contractions at 26°C and 30°C at 8 min were similar compared to the contractions at 37°C at 5 min. Thus, it showed that the response of KCl was affected by lowering the temperature.

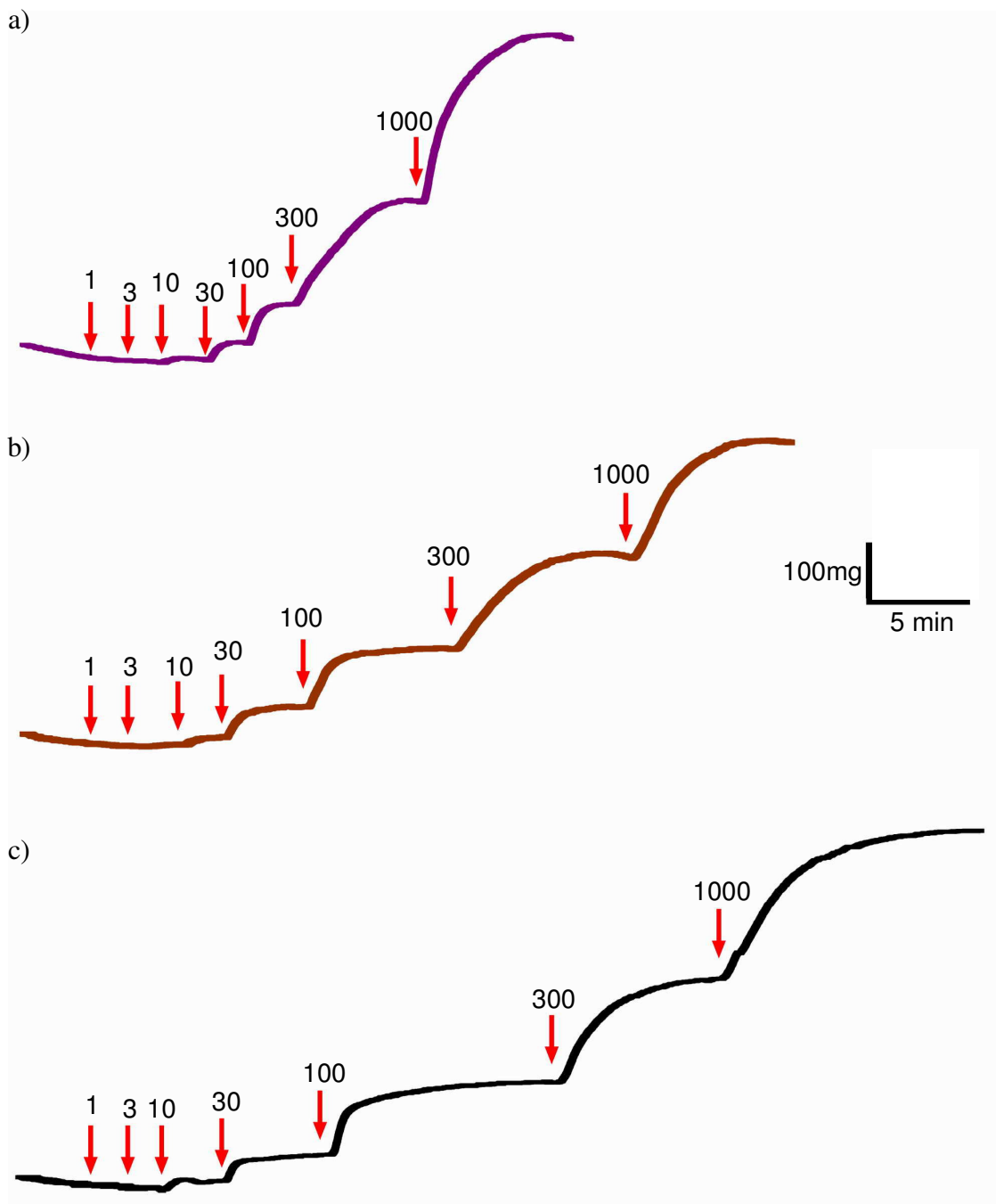


Figure 5.1. Vasoconstriction of endothelium-denuded rat SPA to UTP. The traces of the 2nd concentration-response curve at a) 37°C, b) 30°C and c) 26°C, obtained from different tissues, are shown. The arrow (red) and the number next to it indicate the time-point and concentrations in μM of UTP additions, respectively.

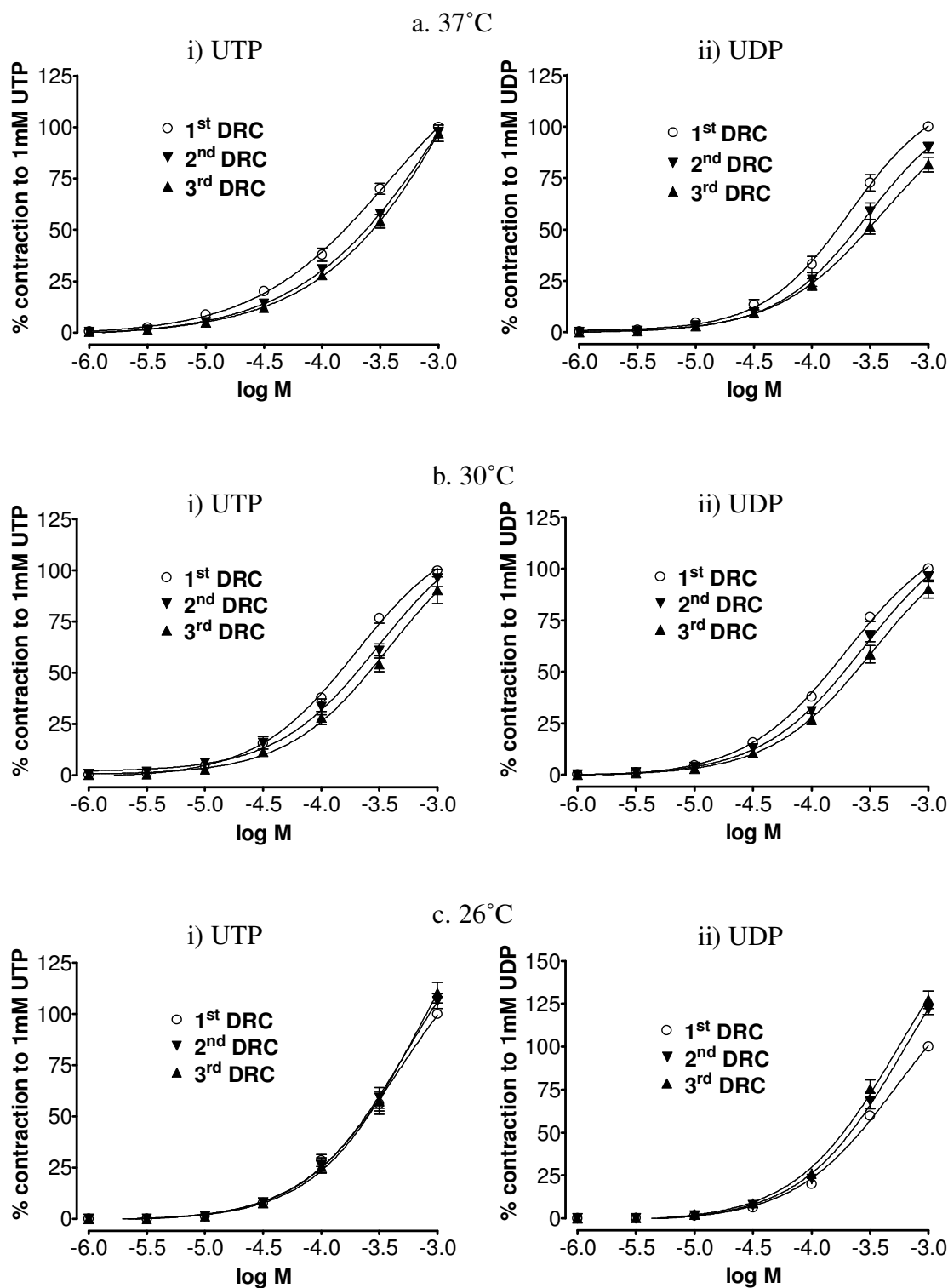


Figure 5.2. Contractile responses of endothelium-denuded rat SPA to nucleotides. Cumulative concentration-response curves at a) 37°C, b) 30°C and c) 26°C, evoked by i) UTP and ii) UDP (1 μ M – 1mM for both), expressed as % of the response to 1mM of the respective nucleotide of the first curve. Three curves were produced in every case, as shown by (\circ), (\blacktriangledown) and (\blacktriangle) for 1st, 2nd and 3rd response, respectively. n=12 for UTP at 37°C, n=11 UDP at 37°C and n=10 for the rest of the data groups. Each point indicates mean \pm S.E.M.

Table 5.1. The potency of nucleotides in inducing contractions of endothelium-denuded rat SPA.

Temp /°C	<u>UTP response</u>				<u>UDP response</u>			
	1	2	3	n	1	2	3	n
37	160 (120 – 199)	232 (187 – 277)	274** (218 – 330)	12	178 (122 – 234)	256 (178 – 333)	320 ^a (221 – 419)	11
30	153 (108 – 198)	207 (142 – 272)	298** (205 – 392)	10	147 (127 – 166)	191 (158 – 225)	259 ^{aa} (189 – 329)	10
26	255 ^{ϕκ} (176 – 334)	257 (189 – 326)	273 (207 – 340)	10	255 ^{ρΨΨ} (216 – 294)	223 (178 – 269)	201 [#] (158 – 243)	10

Values shown are EC_{50max} with 95% confidence limits (μM) for contractions evoked by UTP and UDP in the endothelium-denuded rat pulmonary artery. n values for each temperature are shown in the individual n column of each nucleotide.

**P<0.01 for UTP EC_{50max} of 3rd response versus 1st response at both 30°C and 37°C; ^ϕP<0.05 and ^κP<0.05 for UTP EC_{50max} of 1st response at 26°C versus 30°C and 37°C, respectively;

^aP<0.05 and ^{aa}P<0.01 for UDP EC_{50max} of 3rd response versus 1st response at 37°C and 30°C, respectively;

^ρP<0.05 and ^{ΨΨ}P<0.01 for UDP EC_{50max} of 1st response at 26°C versus 37°C and 30°C, respectively;

[#]P<0.05 for UDP EC_{50max} of 3rd response at 26°C versus 37°C.

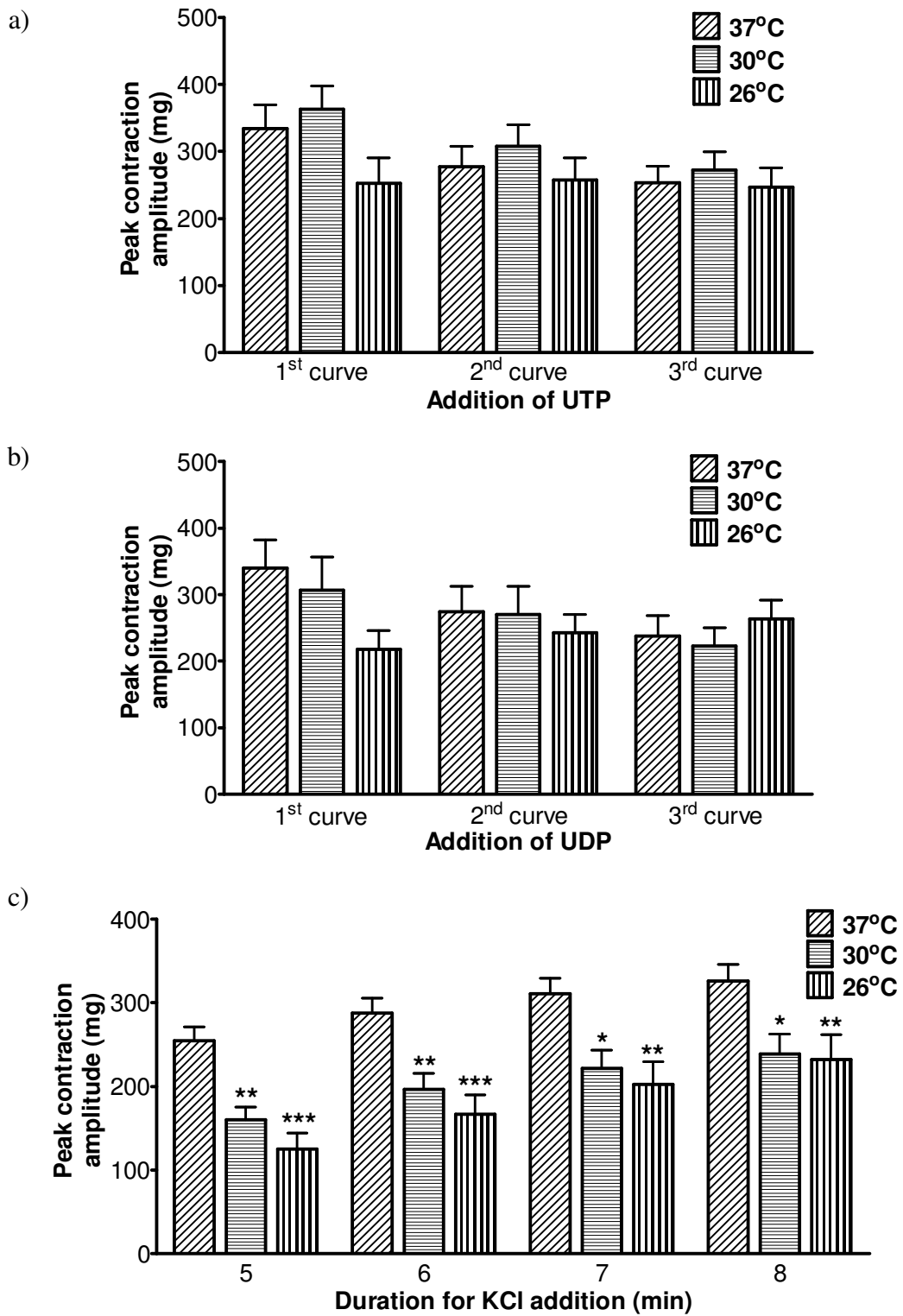


Figure 5.3. Vasoconstriction of endothelium-denuded rat SPA evoked by UTP, UDP and KCl. Mean peak contractile responses evoked by a) 300 μ M UTP and b) 300 μ M UDP, extracted from the cumulative concentration-response curves of the nucleotides, and c) 40mM KCl at 37°C, 30°C and 26°C. n=12 for UTP at 37°C, n=11 UDP at 37°C, n=23 for KCl at 37°C, n=20 for KCl at 26°C and 30°C, and n=10 for the rest of the data groups. Data are expressed as mean \pm S.E.M. *P<0.05, **P<0.01, ***P<0.001 for contractions at 30°C or 26°C versus at 37°C.

2.2. Effectiveness of Permeabilising Agents

2.2.1. β -Escin

Initially, permeabilisation experiments were carried out at 37°C. The effectiveness of β -escin to permeabilise the rat SPA was investigated by varying its concentration as it has been shown to have a concentration-dependent effect (Iizuka *et al.*, 1994). In two initial experiments 50 μ M β -escin was used, a concentration that has previously been reported to be effective in rat SPA (Evans *et al.*, 1999). As shown in Figure 5.5, the intact tissue was first challenged with 40mM KCl (response = 455mg) and cumulative addition of UTP (or UDP in the other case) before permeabilisation was carried out. The three concentrations of UTP (0.1, 0.3 and 1.0mM) evoked contractions of 136mg, 243mg and 547mg peak amplitude, respectively. During the permeabilising phase at pCa 4.5, a slowly developing contraction was seen that reached a peak of 107% of the KCl response after ~30 min, followed by a further 12% increase after adding 1mM ATP. From this point on, ATP was present in the buffer throughout the experiment. Upon several washes with buffer at pCa 9.0, the tissue underwent a slow relaxation and the tone returned to approximately the basal level prior to permeabilisation. Increasing the free $[Ca^{2+}]$ to pCa 6.5 and then pCa 4.5 induced peak contractions of 6% and 10% of the KCl response, respectively. After the tissue was washed with free $[Ca^{2+}]$ at pCa 9.0, the free $[Ca^{2+}]$ was raised again to pCa 6.5, which induced a contraction of 5% of the KCl response. 300 μ M UTP was then added and evoked a peak contraction that was about 10% of its response prior to permeabilisation. A similar pattern of responses was seen in the other tissue and UDP evoked vasoconstriction of ~10% of its response before permeabilisation. Thus, the tissue showed low sensitivity to Ca^{2+} and the nucleotides after permeabilisation with 50 μ M β -escin.

Next, the concentration of β -escin was reduced to 20 μ M and when applied to a tissue it evoked a contraction that was 60% of the KCl response, and which was augmented by a further 39% after 1mM ATP application (Figure 5.5b). After several washes with free $[Ca^{2+}]$ at pCa 9.0, a subsequent challenge with pCa 6.5 and pCa 4.5 evoked peak contractions of 15% and an additional 5% of the KCl response, respectively. At pCa 6.5, the tissue induced a contraction of 7% of the KCl response and addition of UDP evoked a further contraction that was equivalent to

approximately 10% of the response to 300 μ M UDP before permeabilisation. Thus, once again the permeabilised tissues showed low sensitivity to Ca²⁺ and the nucleotides, even though a lower concentration of β -escin was used.

Finally, the concentration of β -escin was lowered to 5 μ M. In addition, ATP was not applied to the permeabilised tissue in order to investigate whether coapplication of this P2Y receptor agonist contributed to the weak responses to UTP and UDP. Application of 5 μ M β -escin evoked a contraction of about 20% of the KCl response (100% = 230mg), which slowly returned to basal level after several washes with buffer at pCa 9.0 (Figure 5.5c). Increasing [Ca²⁺] from pCa 7.5 to pCa 2.0 failed to induce any response, however, addition of 300 μ M UDP buffered at pCa 4.5 evoked a contraction of about 60% of the response to the same concentration applied before β -escin treatment. Thus, overall, β -escin at 50 and 20 μ M fully permeabilised the rat SPA, whereas incomplete permeabilisation was suspected when the β -escin concentration was reduced to 5 μ M. However, it was apparent that the vessels permeabilised by both 50 and 20 μ M β -escin generated only weak responses to elevated free [Ca²⁺] and P2Y agonists.

Some of the previous permeabilisation studies were carried out at 30°C (Masuo *et al.*, 1994; Li *et al.*, 1998; Kitazawa *et al.*, 1999), therefore, the β -escin experiments were further carried out at this temperature. However, in 5 tissues the overall pattern of response was the same as that reported above at 37°C. Following permeabilisation with 50 or 20 μ M β -escin, increasing from pCa 9.0 to pCa 4.5 induced a contraction that was only 23% of the response to KCl before permeabilisation (n=2). Likewise, responses to UTP and UDP were 4% (n=1) and 8% (n=2), respectively, of their corresponding responses before permeabilisation. Given the total lack of improvement in the responsiveness of the permeabilised tissues at 30°C compared to 37°C, the studies with β -escin were terminated without further lowering the temperature to 26°C and instead the effects of α -toxin were investigated.

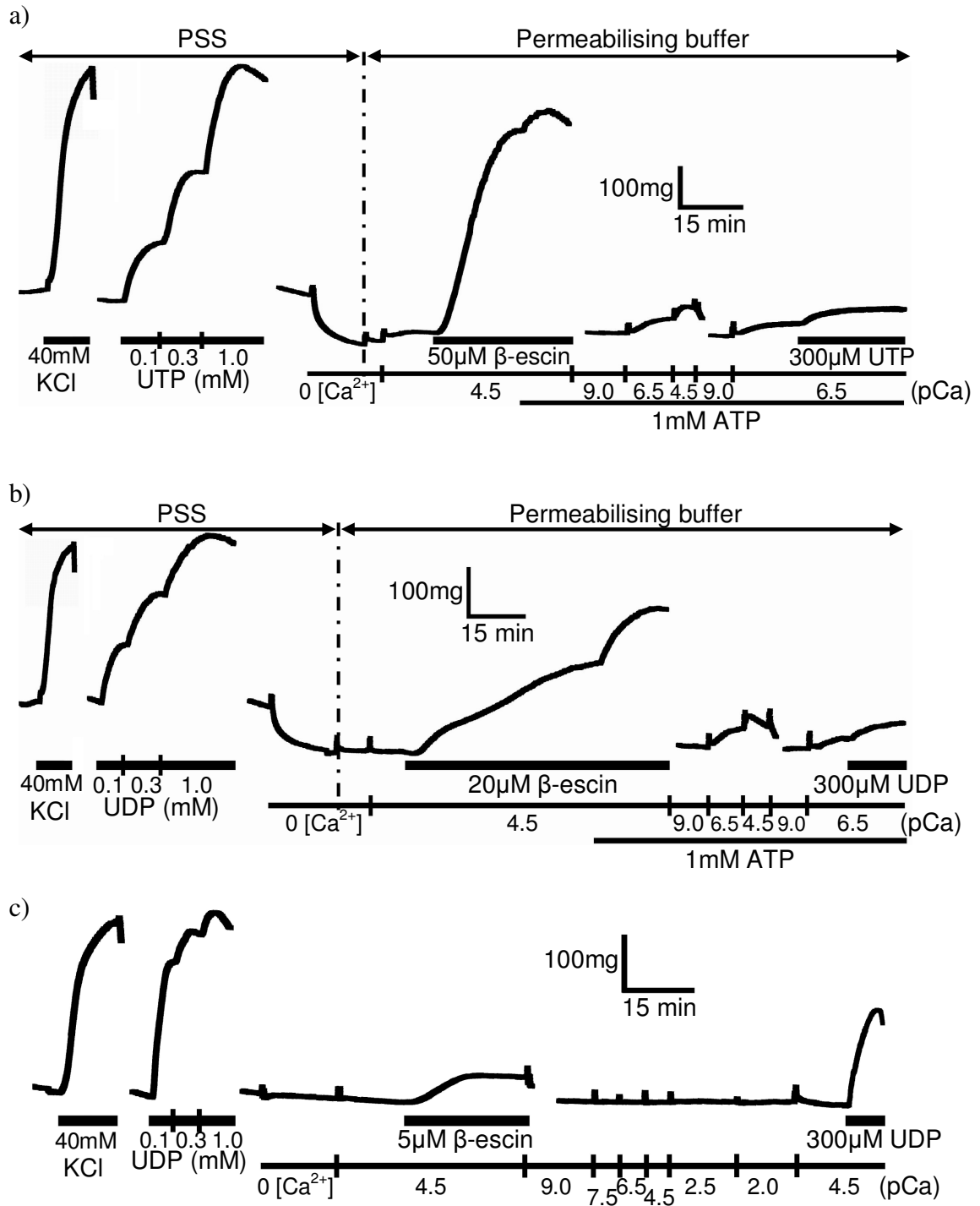


Figure 5.4. Effect of varying [β-escin] on the contractions evoked by cumulative free [Ca²⁺] additions and nucleotides in endothelium-denuded rat SPA following permeabilisation. The original traces show the initial vasoconstriction of rat SPA to 40mM KCl and UTP or UDP (0.1 – 1.0mM for both) in its intact tissue, and the subsequent responses to cumulative additions of free [Ca²⁺] and UTP or UDP (300μM for both) following permeabilisation with β-escin at a) 50μM, b) 20μM and c) 5μM. PSS was replaced by permeabilising buffer before adding β-escin, as shown by the black arrow. Only the tissue permeabilised by 5μM β-escin was bathed in PSS throughout the experiment. Addition of agonists and β-escin, and free [Ca²⁺] and ATP, are indicated by the thick and thin black solid bars, respectively.

2.2.2. α -Toxin

Permeabilisation of the rat SPA with α -toxin was studied in two preparations initially using 50 μ g/mL, similar to that used previously to permeabilise rat pulmonary arteries (Thomas *et al.*, 2005; Snetkov *et al.*, 2008). Adding 50 μ g/mL α -toxin to the tissue shown in Figure 5.6a induced a contraction that reached a peak of 176% of the KCl response after about 10 min. Subsequent washing with buffer at pCa 9.0 containing 1mM ATP, which was present for the rest of the experiment, induced relaxation of the tissue and the tone returned to the basal level after about an hour. When the tissue was then exposed to pCa 6.5, followed by pCa 4.5, it developed contractile responses that reached peak values of 33 and 61% of KCl response, respectively. A similar pattern of responses was seen in the other tissue and the peak contractions induced by pCa 6.5 and pCa 4.5 were equivalent to 55 and 83% of the KCl response, respectively.

A reduced amount of α -toxin was also tested and in this experiment, 1mM ATP was added before the application of α -toxin and then included in the buffer from thereon. 10 μ g/mL α -toxin evoked a contraction that reached a peak of $203 \pm 11\%$ of the KCl response ($100\% = 284 \pm 17\text{mg}$, $n=4$) in about 20 min (Figure 5.6b). The contraction reversed to near basal level in about an hour following several washes with buffer at pCa 9.0. Increasing free $[\text{Ca}^{2+}]$ to pCa 6.5 induced a contraction of $51 \pm 14\%$ of the KCl response. UTP and UDP (300 μ M for both) were subsequently added to two preparations each, and evoked additional contractions equivalent to 48 and 59%, respectively, of their response prior to permeabilisation.

To determine if the responses evoked in the permeabilised preparations were reproducible, pCa was raised to pCa 6.5 twice in the same two tissues. Figure 5.7 shows one example, where, following permeabilisation with 50 μ g/mL α -toxin pCa 6.5 initially induced a contraction of 238mg peak amplitude. This response was diminished by 70% on the second challenge. A similar pattern of response was also seen in the other tissue. Thus, overall, 50 and 10 μ g/mL α -toxin appeared to be equally effective at permeabilising the rat SPA and the permeabilised tissues were able to produce a substantial level of response to increased free $[\text{Ca}^{2+}]$ and P2Y agonists. However, contractions to Ca^{2+} showed rundown on repeated administration

and so in subsequent experiments Ca^{2+} and nucleotides were added once only to permeabilised preparations.

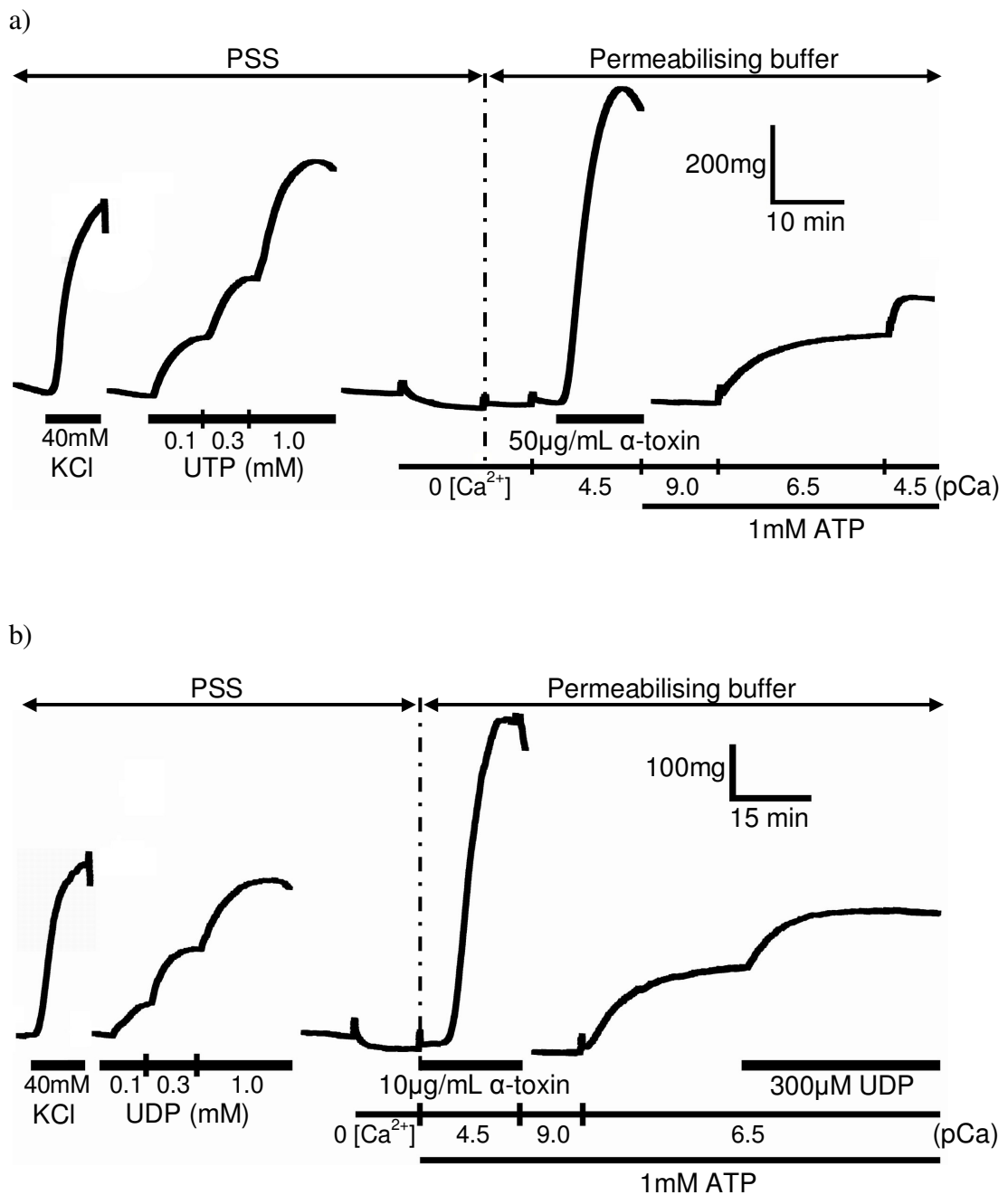


Figure 5.5. Effect of varying $[\alpha\text{-toxin}]$ on the contractile responses evoked by cumulative free $[\text{Ca}^{2+}]$ additions and UDP in endothelium-denuded rat SPA following permeabilisation. The traces show the initial vasoconstriction of rat SPA to 40mM KCl and; a) UTP (0.1 – 1.0mM) in its intact tissue, and the subsequent response to cumulative additions of free $[\text{Ca}^{2+}]$ after permeabilising with 50 $\mu\text{g/mL}$ α -toxin, or b) UDP (0.1 – 1.0mM) in the intact tissue, and the subsequent contraction to 300 μM UDP at pCa 6.5 following application of 10 $\mu\text{g/mL}$ α -toxin. PSS was replaced by permeabilising buffer prior to α -toxin addition, as shown by the black arrow. Addition of agonists and α -toxin, and free $[\text{Ca}^{2+}]$ and ATP, are indicated by the thick and thin black solid bars, respectively.

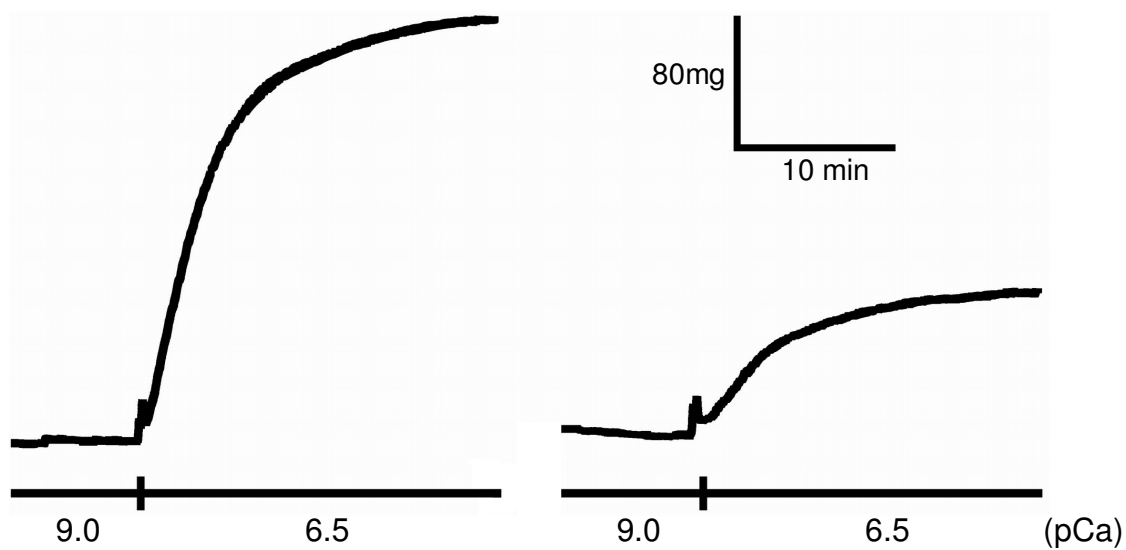


Figure 5.6. Vasoconstriction of α -toxin-permeabilised endothelium-denuded rat SPA in response to increasing free $[Ca^{2+}]$ at pCa 6.5. The original traces show the contractions of 50 μ g/mL α -toxin-permeabilised rat SPA in response to free $[Ca^{2+}]$ at pCa 6.5 applied twice. Level of free $[Ca^{2+}]$ is indicated by the black solid bar.

2.3. The Requirement for ATP in Permeabilisation Buffer

In previous studies (Himpens *et al.*, 1990; Kitazawa *et al.*, 1991; Crichton *et al.*, 1997) ATP was commonly present in the permeabilisation buffer at 5mM, however, as mentioned earlier, adding millimolar ATP can be problematic due to its ability to activate P2X and P2Y receptors and so, the influence of and requirement for ATP in the permeabilisation buffer was investigated.

2.3.1. The Response to P2Y Agonists and Free $[Ca^{2+}]$ after Permeabilisation

In order to evaluate the effect of co-stimulation of ATP-sensitisation and UTP- or UDP-sensitisation via P2 receptors, a preliminary study was carried by bathing the intact rat SPA with permeabilising buffer containing 5mM ATP and with zero $[Ca^{2+}]$, followed by application of either UTP or UDP. As shown in Figure 5.8a, exposing the tissue to the permeabilising buffer (without ATP) did not induce any response, however, when 5mM ATP was added, a substantial contraction was induced, even in the absence of Ca^{2+} . The peak contraction declined slightly, but was then maintained for more than 30 min. Additionally, a second ATP application still evoked a contraction, with a peak amplitude of more than half of that of the first addition. Once this contraction reached a plateau, 300 μ M UTP was added, but this only evoked a modest response. This experiment was also repeated by replacing UTP added in the final stage with 300 μ M UDP. The mean contraction amplitude for UTP and UDP was 47 ± 12 mg (n=4) and 66 ± 11 mg (n=4), respectively. Consequently, the concentration of ATP in the permeabilising buffer was reduced to 1mM. When using this reduced concentration of ATP in the permeabilising buffer, α -toxin (10 μ g/mL) permeabilised vessels contracted to UTP and UDP at pCa 6.5. The response was, however, abolished when ATP was excluded (Figure 5.8b.i). Equally, additions of free $[Ca^{2+}]$ at pCa 6.5 and pCa 4.5 failed to evoke a response if ATP was omitted from the buffer (Figure 5.8b.ii). Thus, ATP is an absolute requirement to enable contractions to Ca^{2+} and nucleotides in the permeabilised tissues.

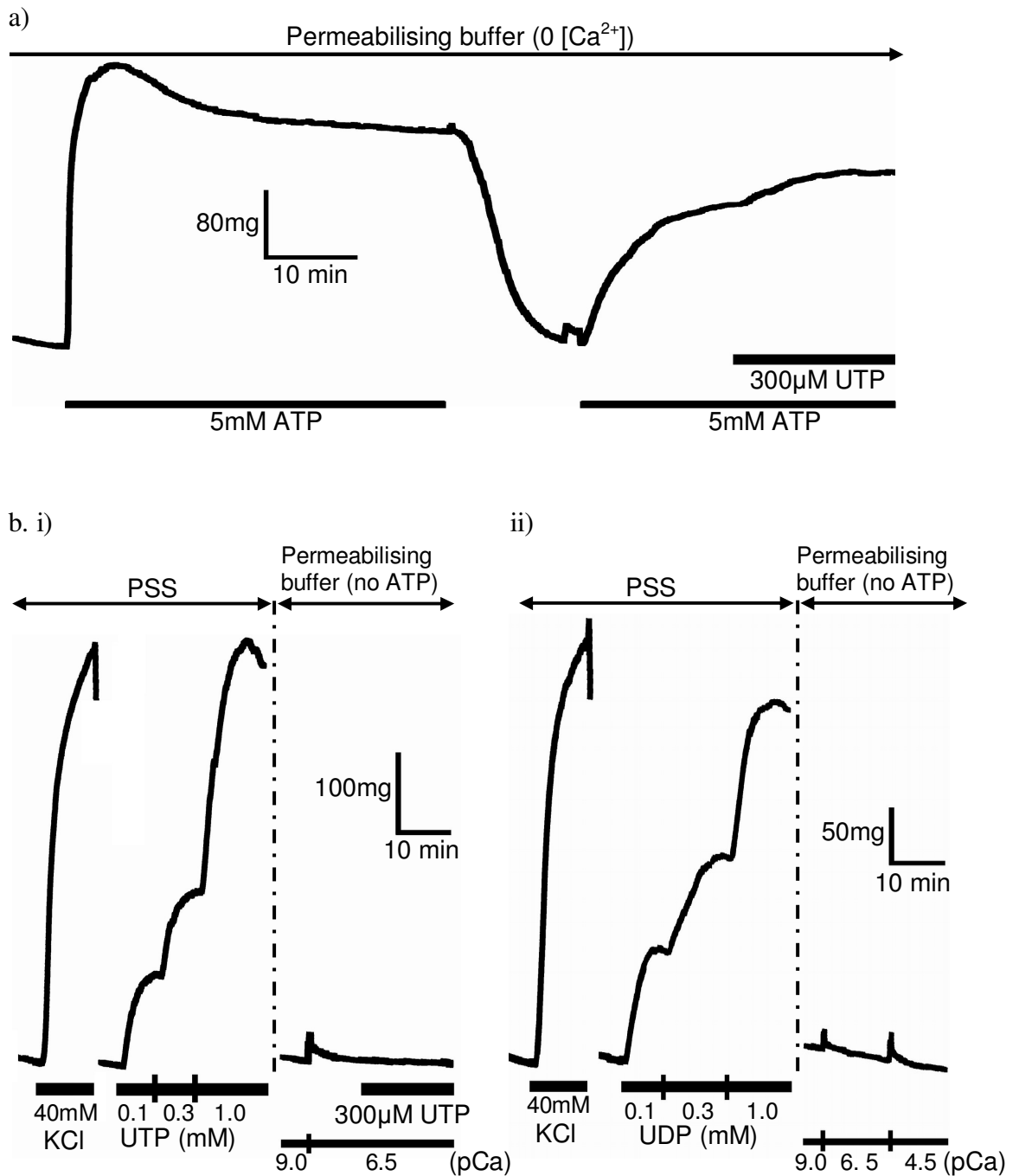


Figure 5.7. Effect of ATP on the responses to UTP and cumulative free [Ca²⁺] additions in intact and α -toxin-permeabilised endothelium-denuded rat SPA. a) The traces of vasoconstriction of the intact rat SPA evoked by 5mM ATP and 300μM UTP in the presence of 5mM ATP, bathed in the Ca²⁺-free permeabilising buffer, are shown. b) shows the traces of the initial responses of rat SPA to 40mM KCl and UTP or UDP (0.1 – 1.0mM for both) in its intact tissue, and the subsequent contractions to i) 300μM UTP at pCa 6.5, and ii) cumulative additions of free [Ca²⁺], following permeabilisation with 10μg/mL α -toxin. ATP was excluded in the permeabilising buffer for (b). PSS was replaced by permeabilising buffer prior to permeabilisation, as shown by the black arrow. Addition of agonists and free [Ca²⁺] and ATP are indicated by the thick and thin black solid bars, respectively.

2.3.2. ATP-Induced Contraction

As reported in the previous section ATP induced a large, prolonged contraction of rat SPA. In this section an attempt was made to minimise these contractions in order to reduce the length of the experiment and to allow the effects of α -toxin to be seen more clearly. Bathing the intact rat SPA with Ca^{2+} -free buffer for more than 10 min did not prevent a contraction evoked by 1mM ATP (n=3) (Figure 5.9a). The peak of this response was reached in about 5 min and decayed slowly, but tone did not return to the basal level even after 30 min. Adding Ca^{2+} to give pCa 4.5 induced a small, maintained contractions on top of the ATP response. The $\text{Ca}_v1.2$ Ca^{2+} channel blocker nifedipine (1 μM) and SERCA inhibitor thapsigargin (1 μM) were added to inhibit Ca^{2+} influx and deplete intracellular Ca^{2+} stores, respectively. When applied together for at least 15 min before Ca^{2+} -free PSS was introduced, these agents virtually abolished the contraction evoked by 1mM ATP and pCa 4.5 (Figure 5.9b). Therefore, nifedipine and thapsigargin were added to the permeabilising buffer in all subsequent experiments.

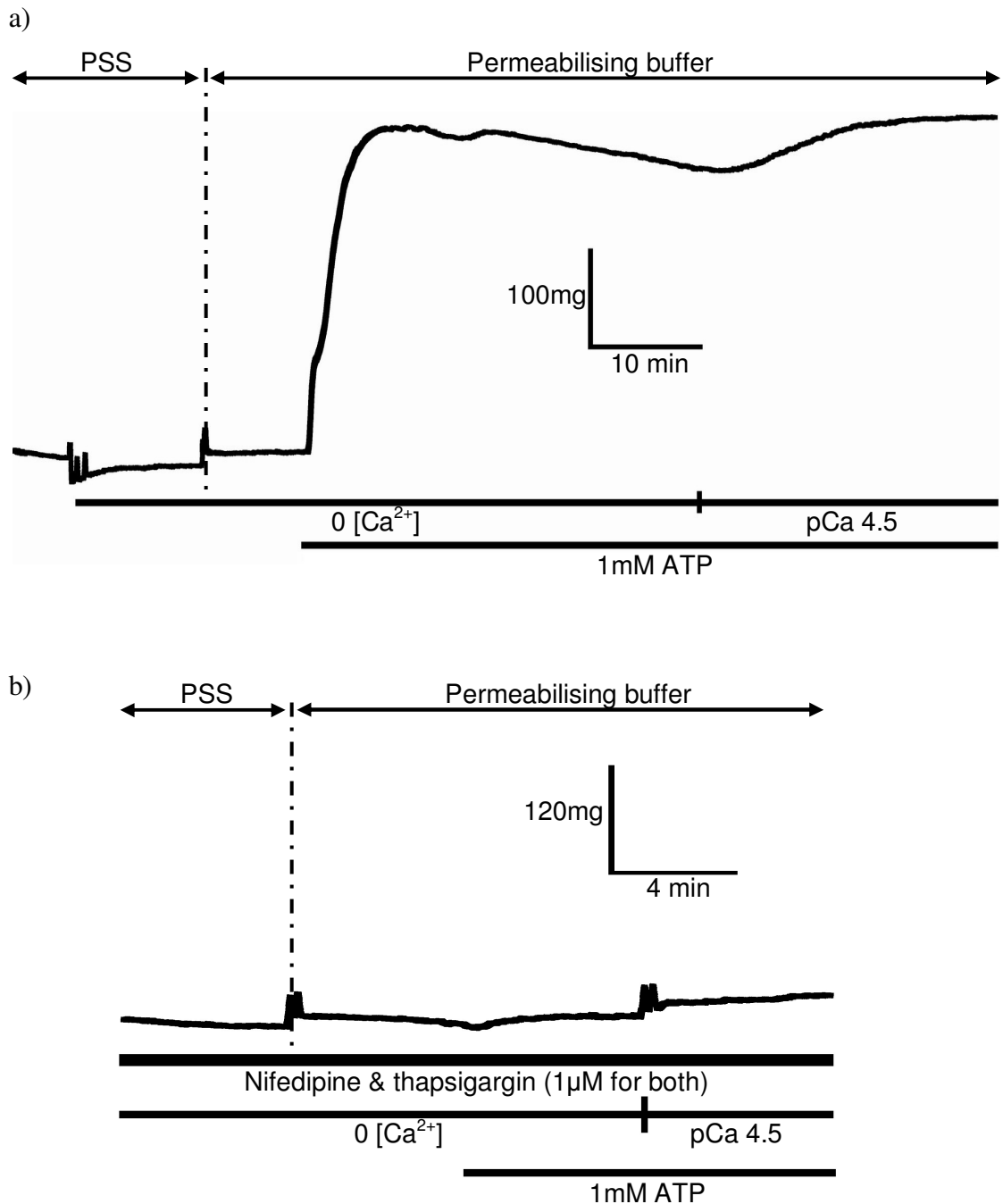


Figure 5.8. Effects of nifedipine and thapsigargin on the elevation of basal tension induced by application of the permeabilising buffer's active contractile components ATP and pCa 4.5. The traces show the basal tension of intact endothelium-denuded rat SPA after replacing the PSS with the permeabilising buffer in the a) presence or b) absence of both nifedipine and thapsigargin (1μM for both), applied at least 15 min before Ca²⁺-free PSS was introduced. The switching of bath solution between PSS and permeabilising buffer is shown by the black arrows. Addition of inhibitors and free [Ca²⁺] and ATP are indicated by the thick and thin black solid bars, respectively.

3. DISCUSSION

In this study, the amplitude of contractile responses evoked by the nucleotides UTP and UDP in the intact, unpermeabilised rat SPA were largely comparable at three different temperatures, i.e. 37°C, 30°C and 26°C, although the contractions developed more slowly at lower temperatures. Both β -escin and α -toxin permeabilised the tissue, but only the latter was effective at preserving the contractile activity of the vessel, together with the receptor-G protein coupling response. This response, however, was subjected to a substantial rundown when Ca^{2+} administration was repeated. In addition, ATP was an essential component of the permeabilising buffer and is needed to ensure that the permeabilised tissue retained its contractile activity.

3.1. Effect of Temperature on the Contractile Activity of Intact Rat SPA

The contractile activity of intact rat SPA in response to UTP and UDP was studied at 37°C, 30°C and 26°C in order to establish if lowering the temperature significantly modified the responses. This was important as permeabilisation experiments have been routinely performed at lower temperatures (Thomas *et al.*, 2005; Snetkov *et al.*, 2006). The results showed that the three concentration-response curves to UTP within and between each temperature were generally comparable, although UTP was slightly, but significantly less potent on the 3rd compared to the 1st addition at both 37°C and 30°C, and on 1st addition at 26°C UTP was also slightly less potent compared to the 1st addition at both 37°C and 30°C. Furthermore, the amplitude of responses to 300 μM UTP was highly reproducible within and across the three temperatures. Likewise, the UDP-evoked response was also largely stable within and between temperatures, apart from being significantly less potent for; the 3rd than the 1st curve at 37°C and 30°C, the 1st curve at 26°C compared to the corresponding curves at 37°C and 30°C, and the 3rd curve at 37°C than the 3rd curve at 26°C. Additionally, the amplitude of responses to 300 μM UDP was stable within and between temperatures. The most marked difference for both UTP- and UDP-evoked responses was the slower development of contractions at lower temperatures. This finding is consistent with the slowing of the kinetics of phasic contractions for both guinea pig and rat ureteric smooth muscles after being subjected to cooling (Burdyga & Wray, 2002).

The present study also showed that the cumulative concentration-response curves to both UTP and UDP did not reach a maximum. This result was comparable with previous studies using similar tissue preparations (Rubino & Burnstock, 1996; Chootip *et al.*, 2002). However, a more recent study (Kauffenstein *et al.*, 2010) using aorta and mesenteric artery from the transgenic mice lacking NTPDase1 found that the concentration-response curves to UTP and UDP did reach a maximum response and the curves were shifted substantially to the left compared with the wild-type animals. This indicates that NTPDase1 greatly modulates the contractions to UTP and UDP by actively hydrolysing these nucleotides and consequently depressing their apparent potency.

Temperature-dependent changes in the time-course of KCl-evoked contractions were also observed, as the contractions developed more slowly at the lower temperatures. A decrease of KCl response amplitude and a prolongation of its time-course were also observed in rat intestinal smooth muscle at low temperature (Sabeur, 1996). However, in the present study, the KCl response measured from 5 to 8 min for all studied temperatures did not reach a plateau and hence, the difference of amplitude at the respective time intervals might just be largely due to the slow kinetics of contraction at low temperature. Therefore, the tissues incubated at low temperature, e.g. 26°C, might reach the equivalent KCl-induced contraction amplitude at 37°C, provided it was measured at a later time-point than that of at 37°C.

3.2. EGTA and Free [Ca²⁺]

Addition of concentrated CaCl₂ stock solution directly to the EGTA-containing buffer substantially lowered its pH. This acidification was due to the ability of one Ca²⁺ to displace two H⁺ bound to EGTA (Tsien & Pozzan, 1989). An additional problem with adding a concentrated CaCl₂ stock solution (1M) to the EGTA-containing buffer is that a small error in volume measurement will lead to significant inaccuracy in the final free [Ca²⁺] (Tsien & Pozzan, 1989). However, adopting a procedure of mixing together two EGTA-containing buffers can prevent a substantial disturbance to the [H⁺] balance of the final mixture as effectively we are only varying the free [Ca²⁺] at micromolar concentrations (as opposed to millimolar

concentrations when adding a concentrated CaCl_2 stock solution directly), and hence liberates H^+ at a range that requires a negligible pH adjustment. Moreover, by adding Ca^{2+} in conjunction with EGTA, the variation of free [EGTA] can be kept at minimum level, and this can avoid upsetting the Mg^{2+} equilibria. Equally, not only does this technique provide a straightforward method of preparing a desired free [Ca^{2+}] by calculating the appropriate mixing ratio (v/v) of both solutions, but more importantly it enhanced the accuracy of the [Ca^{2+}] applied to the tissues.

3.3. Effectiveness of Permeabilising Agents - β -Escin and α -Toxin, and Reproducibility of Contractions of the Membrane-Permeabilised Tissue

The results showed that permeabilisation of the rat SPA by β -escin was successfully achieved at 20 and 50 μM , but not at 5 μM . 20 or 50 μM β -escin induced a more than five-fold increase of contraction amplitude compared to 5 μM β -escin during the permeabilising phase. Additionally, tissues permeabilised with 20 or 50 μM β -escin responded to increasing free [Ca^{2+}], whereas those treated with 5 μM β -escin were virtually quiescent even when exposed to a [Ca^{2+}] as high as pCa 2.0. Interestingly, the latter tissue contracted in response to agonist administration at pCa 4.5. This response was similar to the contraction of an intact tissue, thus further indicating the lack of tissue permeabilisation with this low concentration of β -escin.

The effectiveness of tissue permeabilisation by 20 or 50 μM β -escin, however, was severely compromised by the inability of the permeabilised tissue to retain its contractile viability, as clearly demonstrated by its weak response to both increasing free [Ca^{2+}] and P2Y agonists. This finding was consistent with a previous study (Evans *et al.*, 1999) in which severe rundown of agonist responses was observed after permeabilising the rat SPA with 50 μM β -escin. β -escin has been shown to create transmembrane pores, which are sufficient to allow access to the molecules as large as immunoglobulin G and lactate dehydrogenase, with the molecular weight of 135 – 150kD for both (Iizuka *et al.*, 1994). Therefore, the deterioration of contraction of the β -escin-permeabilised tissue observed here perhaps could be due to the substantial leakage of essential contractile proteins, particularly calmodulin and MLCK, which have a molecular weight of about 17 and 140kD, respectively.

In the permeabilisation experiments with α -toxin, 10 μ g/mL of this compound was as effective as 50 μ g/mL at permeabilising the rat SPA. During the permeabilising phase, both amounts of α -toxin produced an almost two-fold increase in contraction amplitude compared to the β -escin counterpart. Moreover, the resultant permeabilised tissues preserved contractile activity, as demonstrated by their ability to produce an average of more than 40% and nearly 80% of KCl-induced response following pCa 6.5 and pCa 4.5 challenges, respectively. α -toxin transmembrane pores are very small (~2nm) and rarely permit the passage of molecules with a molecular weight more than 17kD (Füssle *et al.*, 1981).

The reproducibility of contractile responses was also evaluated in α -toxin permeabilised tissues. The results clearly indicate that the peak amplitude of the second pCa 6.5-induced contraction was smaller than the first by as much as 70%. Diffusion or leakage of cellular substances cannot be rule out in contributing to this rundown effect, which is enhanced by the mechanical squeezing during the contractile activity. In this respect, Iizuka *et al.*, (1994) observed that about 8% of cellular lactate dehydrogenase leaked during contraction in α -toxin-treated tissues.

3.4. The Requirement for ATP in the Permeabilisation Buffer

The present results demonstrated that the contractile activity of the permeabilised rat SPA was highly dependent on the presence of added ATP, as the response of this tissue to an increase of free $[Ca^{2+}]_i$ and P2Y agonists was virtually abolished when ATP was excluded from the permeabilising buffer. However, the presence of ATP is also an issue since the application of both UTP and UDP only evoked modest contractions in the intact vessel when bathed in the permeabilising buffer containing 5mM ATP. Clearly, this high energy molecule can compete with UTP and UDP for binding to P2Y receptors (Chootip *et al.*, 2002). Thus, it was critical that the [ATP] in the buffer was adjusted to such a level where its essential role as an energy provider for the contractile activity of permeabilised tissue was optimally preserved, while keeping the unwanted effect of activating P2Y receptors as low as possible. This was achieved here by lowering the concentration of ATP to 1mM. This subtle balance can be accomplished considering ATP has relatively lower potency and efficacy towards P2Y receptors of the rat SPA than either UTP or UDP (Chootip *et*

al., 2002). Since P2Y receptors are widely distributed throughout smooth muscle tissues, these data have important implications for permeabilisation studies. ATP in the permeabilisation buffer, besides acting biochemically to provide energy, may also act pharmacologically to stimulate P2Y receptors and induce Ca^{2+} sensitisation, which in turn will influence the Ca^{2+} sensitisation induced by other agents. This does not appear to have been taken into account in previous permeabilisation studies.

Addition of ATP (1mM) in the buffer elevated tension in unpermeabilised preparations, even in the absence of Ca^{2+} . However, it was abolished by coapplying nifedipine and thapsigargin, which block voltage-gated Ca^{2+} channel and the SERCA Ca^{2+} pump, respectively. ATP stimulates both P2X and P2Y receptors to induce Ca^{2+} influx and intracellular Ca^{2+} release (Guibert *et al.*, 1996; Zheng *et al.*, 2005), which in turn induce membrane depolarisation and activation of $\text{Ca}_v1.2$ channels. As mentioned above, nifedipine can be used to block this channel. Additionally, inhibition of the SERCA Ca^{2+} pump by thapsigargin prevents the uptake of Ca^{2+} into the SR, which causes emptying of this Ca^{2+} . In addition, disabling the SR function was desirable as it could prevent the P2Y receptor-mediated SR Ca^{2+} release and hence, ensured the clamping of $[\text{Ca}^{2+}]_i$ was tightly maintained during application of P2Y agonists. Interestingly, the above ATP-evoked contraction was maintained for more than 30 min in the absence of Ca^{2+} . This suggests that that ATP induced Ca^{2+} sensitisation. In addition, initiation of this effect was prevented by inhibitors Ca^{2+} influx with nifedipine and depleting Ca^{2+} stores with thapsigargin. This is consistent with the results in the Chapter 6 which show that a minimum level of intracellular Ca^{2+} is required for Ca^{2+} sensitisation to be initiated.

3.5. Application to the Permeabilisation Protocol

The findings in this chapter enabled the optimum conditions for the permeabilisation protocol to be established, as summarised below;

- 1) Temperature was set at 37°C to mimic the physiological temperature.
- 2) Permeabilising solution was prepared by mixing Ca^{2+} -free and high Ca^{2+} EGTA-containing solutions in a v/v ratio to yield a more accurate free $[\text{Ca}^{2+}]$, with stable pH.

- 3) α -toxin was favoured over β -escin because of its superiority in preserving the contractile activity of the permeabilised tissue. 10 μ g/mL α -toxin was used since a comparable permeabilisation outcome was observed with 50 μ g/mL.
- 4) 1mM ATP was included in the permeabilising buffer to enable contractions to occur.
- 5) Nifedipine and thapsigargin (1 μ M for both) were applied before permeabilising the tissue, and during the rest of the experiment, to eliminate the influence of ATP-evoked cellular Ca²⁺ mobilisation and Ca²⁺ influx.
- 6) Contractile activity of permeabilised tissue was studied by a single cycle response per preparation due to the substantial rundown of the subsequent contraction.

Based on the above conditions, the adopted permeabilisation protocol was generally performed by first, obtaining appropriate control responses to KCl and UTP or UDP (details in the Methods) in the intact rat SPA. After washout, nifedipine and thapsigargin were added and kept throughout the experiment. Subsequently, the Ca²⁺-free PSS was introduced at least 15 min after addition of these blocking agents, and then replaced by the permeabilising buffer, which lack ATP or Ca²⁺. ATP, Ca²⁺ (pCa 4.5) and α -toxin were then each added in this respective order at 5 min intervals. It was noted that addition of both ATP and Ca²⁺ had virtually had no effect on the basal tension of the tissue. During this permeabilising phase, α -toxin was maintained in the solution until the contraction reached a peak, an indication that complete permeabilisation had taken place. The α -toxin-containing solution was extracted and stored at 4°C before re-using it in one more subsequent experiment. The permeabilised tissue was then washed several times with the permeabilising buffer at pCa 9.0 until a stable basal tension was reached. At this point, the appropriate interventions were ready to be carried out. These are reported in the next chapter.

Chapter 6:

Characterisation of Contraction in Membrane-Permeabilised Preparations

1. INTRODUCTION

Rho kinase and PKC have been proposed to play an important role in the vasoconstriction evoked by UTP and UDP and so far the results of the experiments that I have performed in the intact preparations presented in chapter 4 clearly indicate a positive involvement of these kinases in the nucleotide-evoked contractions. Several possible mechanisms through which these enzymes mediate their effects have been discussed in Chapter 4, and one of the downstream mechanisms could involve Ca^{2+} sensitisation, however, the findings so far still cannot conclusively establish such an association. Therefore, to address this issue, a membrane permeabilisation technique was used to enable the involvement of Ca^{2+} sensitisation to be investigated directly.

The present results also indicate that PI-PLC contributed in both UTP- and UDP-evoked contractions in the intact preparations. This could involve Ca^{2+} sensitisation, particularly via activation of PKC (details in Chapter 4). Thus, further investigation on the PI-PLC involvement performed in the permeabilised preparation is crucial to clarify this matter. Finally, characterisation of the P2Y receptor subtypes mediating the effects of UTP and UDP would also be useful, however, the current limited availability of the reliable selective P2Y receptor antagonists may limit the scope of this investigation.

As the optimum conditions for the permeabilisation protocol for studying the P2Y receptor-mediated vasoconstriction were established in Chapter 5, these studies were continued here by first exploring the contribution of Rho kinase and PKC to the cumulative Ca^{2+} concentration-response curve, by preincubating the tissues with the inhibitors Y27632 or GF109203X, prior to the generation of the curve. These inhibitors were used again to determine the role of Rho kinase and PKC in the UTP- and UDP-evoked contractions via Ca^{2+} sensitisation by applying them after the responses reached a peak. The inhibitors were also applied after the peak contraction was reached in response to pCa 6.5 alone and subsequent addition of PMA. The role of PI-PLC and the effect of the P2 receptor antagonist suramin on the Ca^{2+} sensitisation aspect of contractions evoked by both nucleotides were investigated by adding U73122 and suramin, respectively, before the agonists.

2. RESULTS

2.1. Effects of Preincubation with Y27632 and GF109203X on Cumulative Ca^{2+} Concentration-Response Curves

In these experiments the intact rat SPA was initially challenged with KCl and then UTP or UDP, each of which produced consistent responses and the tissues were then permeabilised with 10 $\mu\text{g}/\text{mL}$ α -toxin (Figure 6.1). After a steady basal tension was re-established following permeabilisation, the tissue was subsequently exposed to increasing concentrations of Ca^{2+} , in a cumulative manner. The tissue first started to contract at pCa 7.0 (Figure 6.1a, 6.3a), larger contractions were observed at pCa 6.5 and pCa 6.0, and the maximum response was reached at pCa 5.0, as no further augmentation of the contractile response was seen at pCa 4.5. The mean contraction amplitude evoked by pCa 4.5 was $355 \pm 79\text{mg}$ ($n=5$), which was $94.0 \pm 23.8\%$ of the contraction elicited by KCl (40mM) prior to permeabilisation. The EC_{50} and Hill slope of this control $[\text{Ca}^{2+}]$ -response curve were 336nM (95% Confidence limits = 238 – 474nM, $n=5$) and 2.67 ± 0.56 , respectively. Unpermeabilised preparations did not contract when exposed to the same range of free $[\text{Ca}^{2+}]$ ($n=3$) in the permeabilising buffer, although they did contract in response to KCl and nucleotides before changing to the permeabilising buffer (Figure 6.1b).

Preincubation of 10 μM Y27632 for 15 min caused a rightwards shift of the Ca^{2+} concentration-response curve, whereby the tissue only started to respond at pCa 6.5 (Figure 6.2a, 6.3a). The EC_{50} of the resultant curve was 820nM (95% Confidence limits = 541 – 1245nM, $n=5$), which was significantly higher than the EC_{50} of the control curve ($P<0.01$). The Hill slope of this curve was 1.72 ± 0.30 . In contrast, the Ca^{2+} concentration-response curve was not affected by 15 min preincubation with 10 μM GF109203X (Figure 6.2b, 6.3a). The EC_{50} obtained under these conditions (342nM (95% Confidence limits = 224 – 521nM, $n=5$)) was comparable to that of the control curve, but significantly lower than that when tissues were preincubated with Y27632 ($P<0.01$). Moreover, the Hill slope of this curve (2.79 ± 0.56) was similar to that of control curve. The peak contractile responses to pCa 4.5 in the presence of Y27632 and GF109203X were not significantly different from control (Figure 6.3b). Overall, these results show that Rho kinase, but not PKC, are active at basal tone, and in the absence of receptor agonists, to induce Ca^{2+} sensitisation.

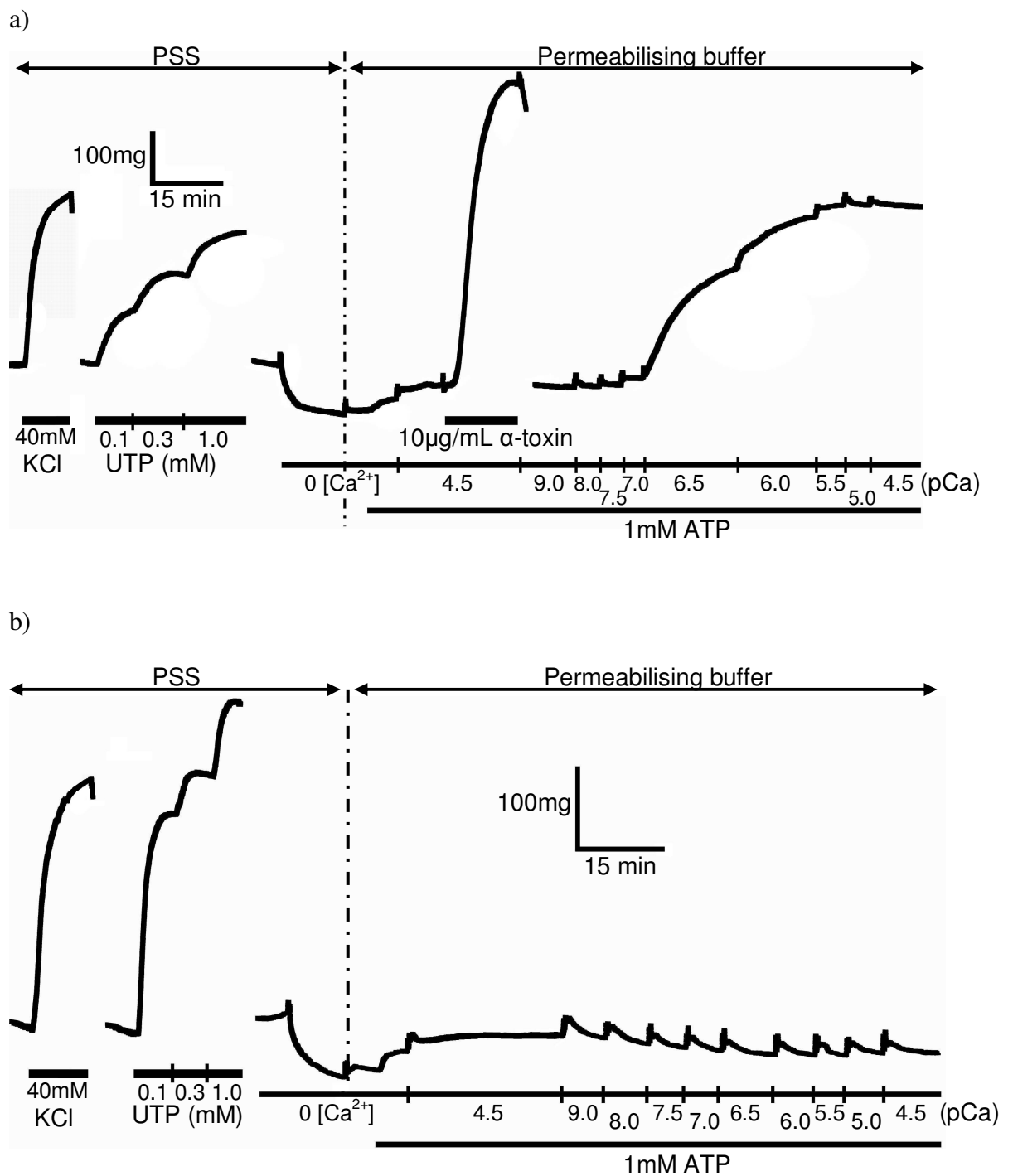


Figure 6.1. Contractile responses induced by cumulative free $[Ca^{2+}]$ addition in endothelium-denuded rat SPA treated with α -toxin. The traces show the initial vasoconstriction of rat SPA to 40mM KCl and UTP (0.1 – 1.0mM) in its unpermeabilised state, and the subsequent response to cumulative additions of free $[Ca^{2+}]$ (10nM – 31.6µM) a) following permeabilisation with 10µg/mL α -toxin, or b) in an unpermeabilised tissue. PSS was replaced by permeabilising solution as shown by the black arrows. Addition of agonists and α -toxin, and level of free $[Ca^{2+}]$ and ATP addition are indicated by the thick and thin black solid bars, respectively.

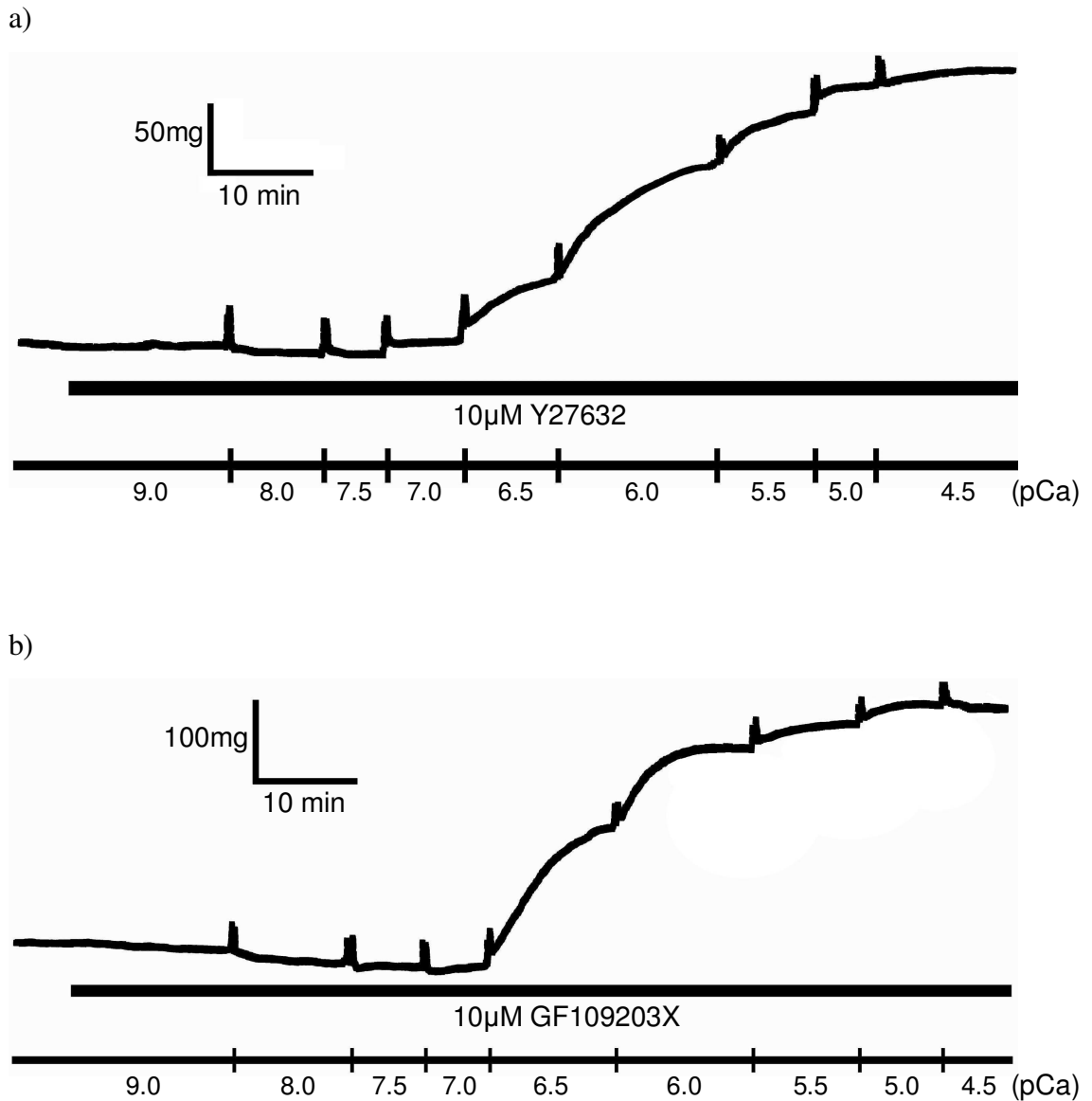


Figure 6.2. Effects of Y27632 and GF109203X on cumulative addition of free $[Ca^{2+}]$ in α -toxin-permeabilised endothelium-denuded rat SPA. Typical traces from different α -toxin-permeabilised tissues showing the contractions induced by cumulative free $[Ca^{2+}]$ additions (10nM – 31.6 μ M) after 15 min preincubation of a) 10 μ M Y27632 and b) 10 μ M GF109203X. Addition of inhibitors and level of free $[Ca^{2+}]$ are indicated by the thick and thin black solid bars, respectively.

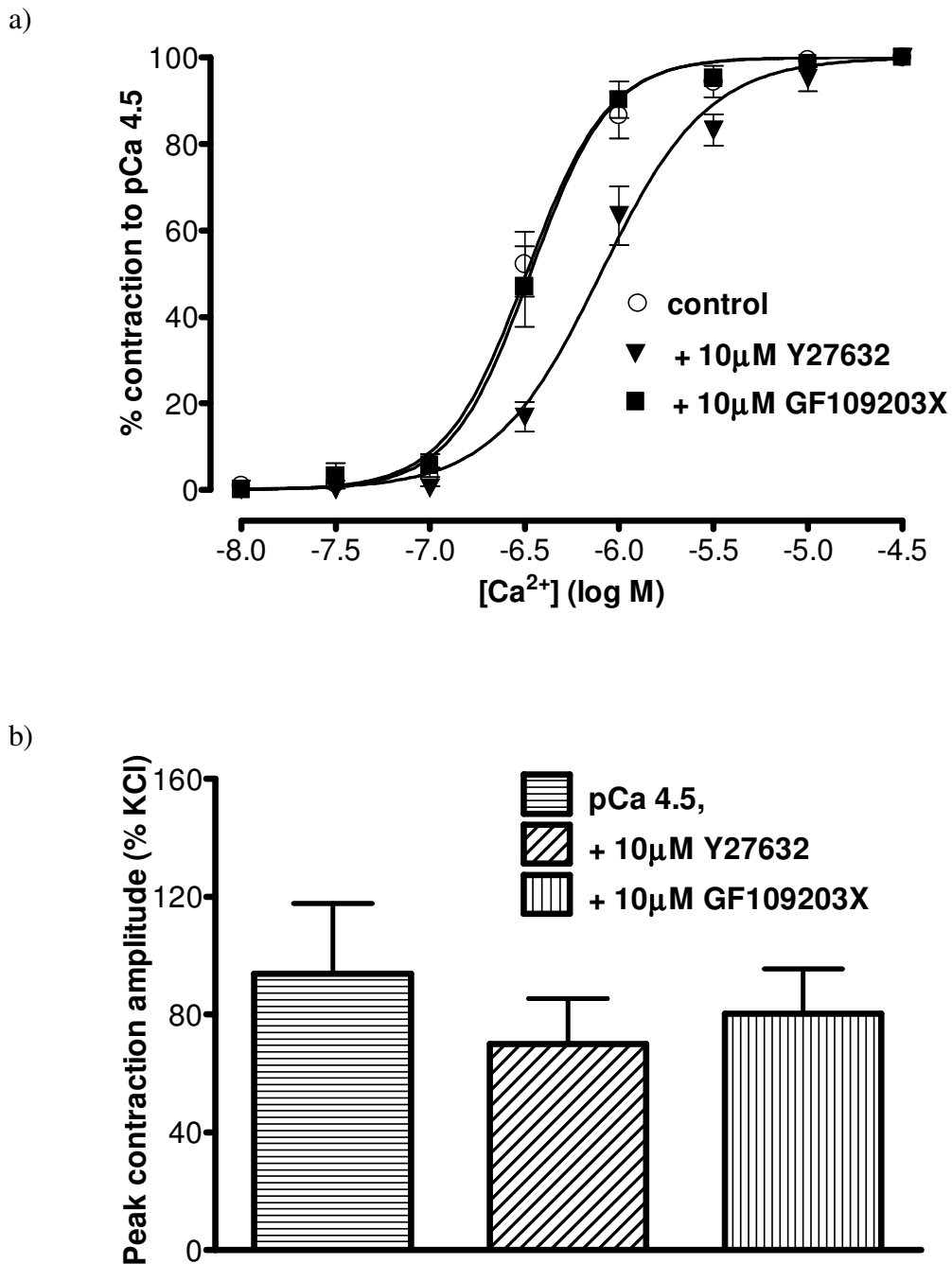


Figure 6.3. Effects of Y27632 and GF109203X on contractile responses to free $[Ca^{2+}]$ additions in α -toxin-permeabilised endothelium-denuded rat SPA. a) Cumulative Ca^{2+} concentration-response curves are shown in the absence (\circ) and presence of $10\mu M$ Y27632 (\blacktriangledown) or $10\mu M$ GF109203X (\blacksquare), added 15 min prior to increasing free $[Ca^{2+}]$. Contraction are expressed as a % of maximum contraction (pCa 4.5). b) shows the mean peak amplitude contractions to pCa 4.5 derived from the above cumulative $[Ca^{2+}]$ response curves in the absence and presence of the inhibitors, expressed as a % of the response to KCl (40mM) obtained prior to permeabilisation. $n=5$ for all. Data are shown as mean \pm S.E.M.

2.2. Characterisation of Contractions Evoked by pCa 6.5, UTP, UDP and PMA in α -Toxin-Permeabilised Rat SPA

The experiments reported in Chapter 5 showed that agonist-induced contractions of permeabilised tissues were not reproducible and showed substantial rundown. Therefore, it was important to characterise here the responses evoked by the agonists in the α -toxin-permeabilised rat SPA before any attempt was made to investigate the effect of the inhibitors against them. As usual, the rat SPA was first challenged with KCl and the respective agonist, and these additions evoked consistent responses (Figure 6.4 – 6.8). Subsequent exposure of the permeabilised tissue to pCa 6.5 evoked a contraction that reached a peak of 155.5 ± 7.5 mg (n=100) in about 20 min (Figure 6.4). In four of the tissues, the time-course of the contractions were further studied. The contraction decayed slowly and was $94.5 \pm 2.5\%$ and $81.1 \pm 9.8\%$ of peak at 20 and 40 min after peak, respectively, but these changes were not statistically significant.

Addition of either UTP or UDP at pCa 9.0 did not evoke any response, although a subsequent change to pCa 6.5 induced a contraction (Figure 6.5), showing that the contractile viability of the vessels was not compromised, and consistent with previous studies showing that GPCR agonists need a raised basal $[Ca^{2+}]$ (Evans *et al.*, 1999; Jernigan *et al.*, 2004; Wilson *et al.*, 2005; Knock *et al.*, 2008) in order to elicit contraction of permeabilised tissues. When the nucleotides were added once the contraction to pCa 6.5 had reached its peak, 300 μ M UTP evoked an additional contraction of 85.7 ± 7.6 mg (n=20), which reached a peak in about 20 min, and which was $31.9 \pm 3.8\%$ of the peak contraction evoked by the same concentration of UTP before permeabilising the tissue (P<0.001) (Figure 6.6a, b). The time-course of contractions was studied further in four tissues (Figure 6.6c). The contractions were not maintained and decayed slowly, and were $66.0 \pm 13.1\%$ and $6.0 \pm 28.8\%$ of peak at 20 and 40 min after peak, respectively. The contraction at 40 min was significantly smaller than at peak (P<0.05). Likewise, 300 μ M UDP evoked a contraction of 81.2 ± 8.4 mg (n=20) that reached a peak in about 20 min and which corresponds to $30.7 \pm 4.1\%$ of the peak response evoked before permeabilising the tissue (P<0.001) (Figure 6.7a, b). In four of the vessels, the time-course of contractions was further investigated (Figure 6.7c). This contraction decreased to $77.1 \pm 6.8\%$ and $27.6 \pm$

21.2% after 20 and 40 min, respectively, of reaching its peak, but only the latter reduction was statistically significant ($P < 0.01$).

In contrast, adding 10 μ M PMA at the peak of the contraction to pCa 6.5 did not evoke a further increase in tone, even after 60 min exposure (Figure 6.8a), the time in which PMA-induced contraction of unpermeabilised tissue usually reached a peak (Chapter 4). Instead, tone decreased slowly (Figure 6.8a, b) and there was no significant difference in the amplitude of contractions evoked by pCa 6.5 alone and pCa 6.5 plus PMA, 20 and 40 min after the peak (Figure 6.8c).

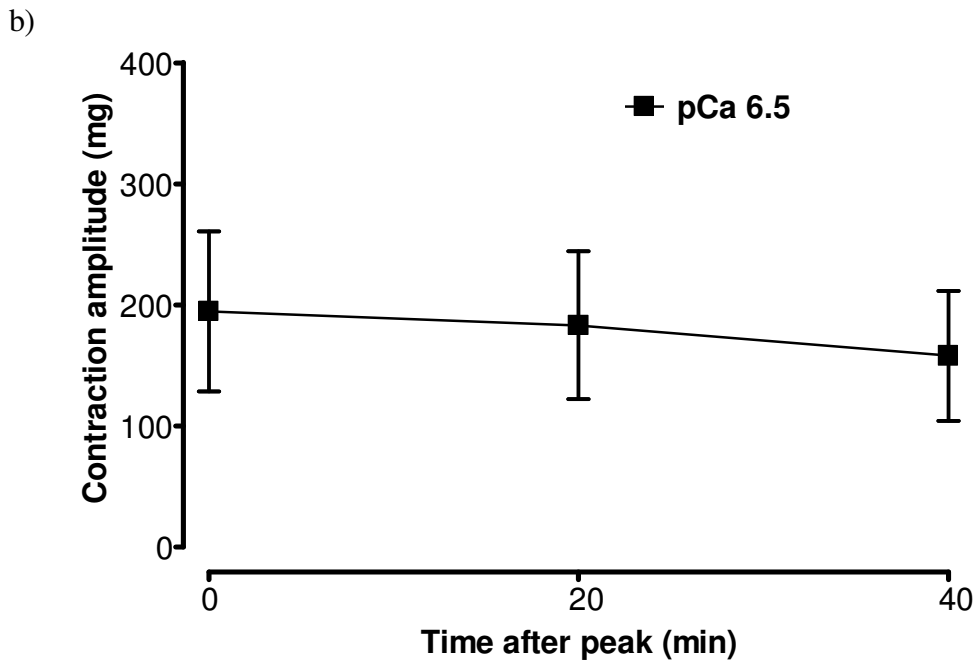
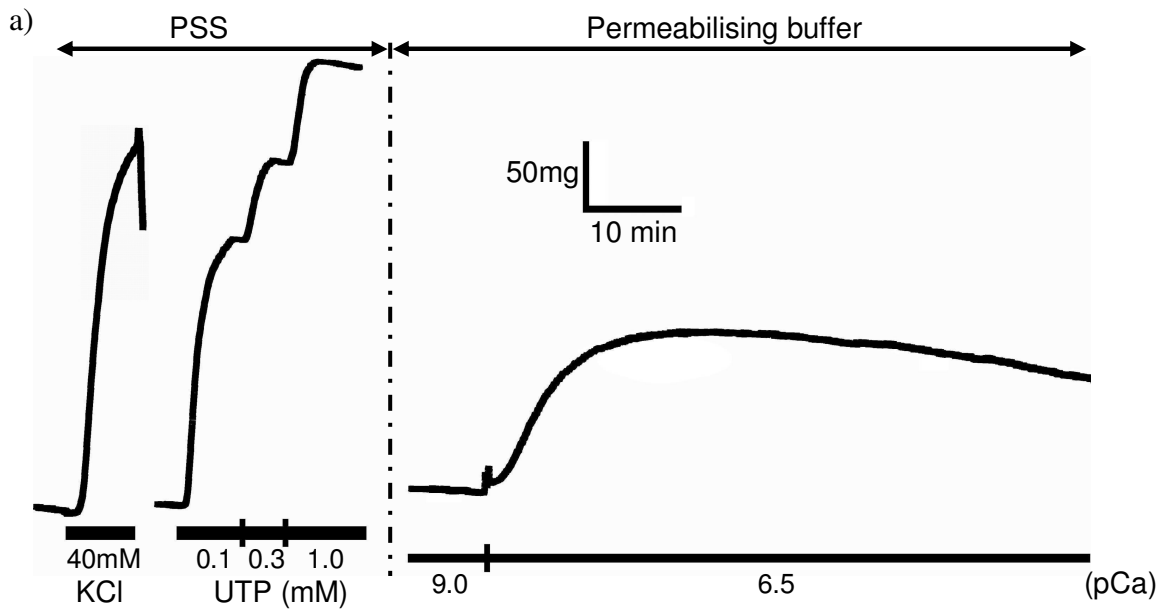


Figure 6.4. Contractile response of α -toxin-permeabilised endothelium-denuded rat SPA induced by pCa 6.5. a) The traces show the typical contractile responses of rat SPA induced by 40mM KCl and UTP (0.1 – 1.0mM) in its intact tissue, and subsequently by free $[Ca^{2+}]$ at pCa 6.5 after permeabilising the tissue with 10 μ g/mL α -toxin. PSS was replaced by permeabilising buffer, as shown by the black arrow. Addition of agonists and free $[Ca^{2+}]$ are indicated by the thick and thin black solid bars, respectively. b) The mean amplitude of contractions evoked by pCa 6.5 measured at peak and 20 and 40 min after that are shown. n=4. Data are expressed as mean \pm S.E.M.

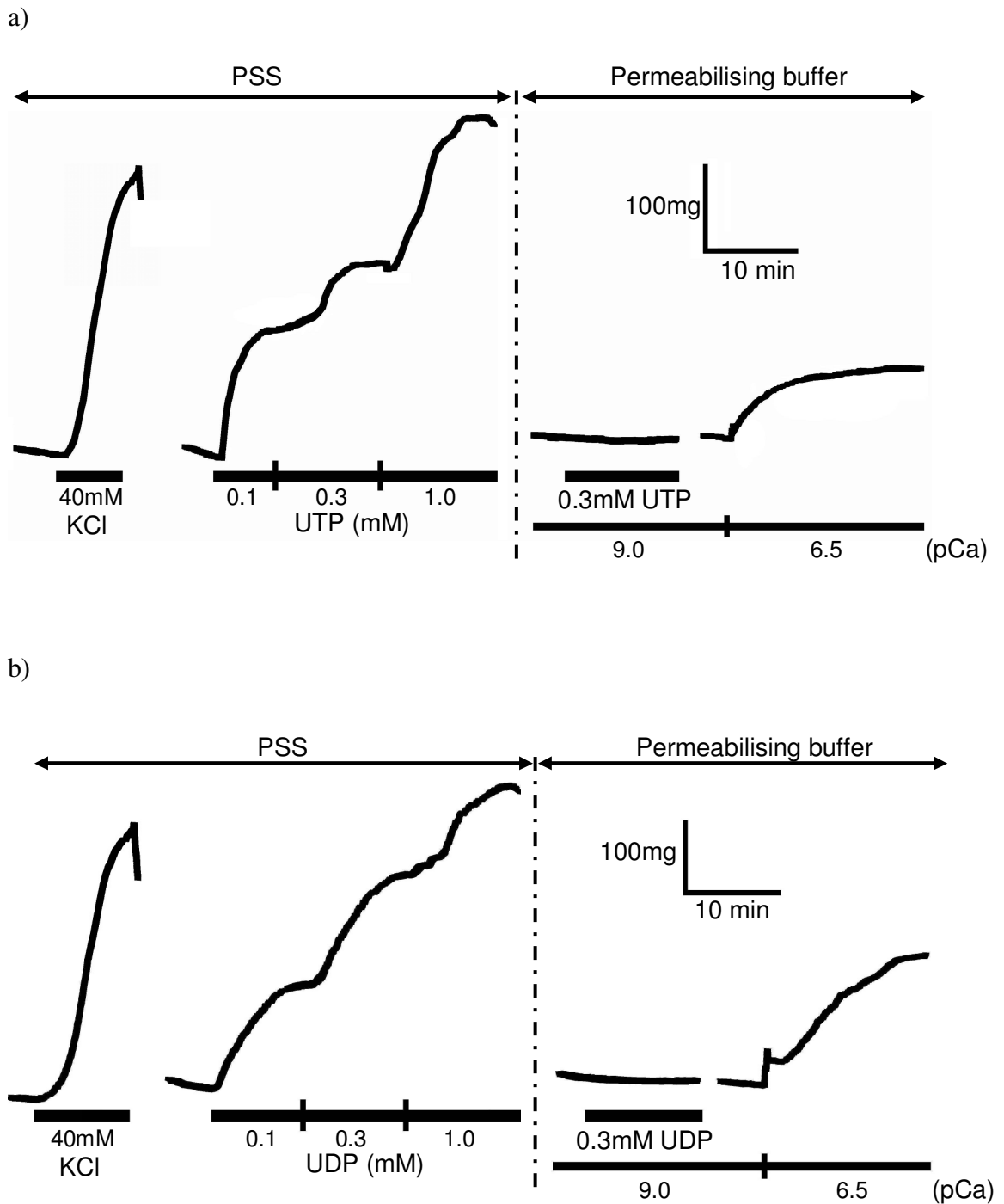


Figure 6.5. Addition of UTP and UDP at pCa 9.0 $[Ca^{2+}]$ in endothelium-denuded rat SPA permeabilised with α -toxin. The traces show the contractions of rat SPA induced by 40mM KCl and a) UTP and b) UDP (0.1 – 1.0mM for both) in the intact tissue, and subsequently by the respective nucleotides at 300 μ M at pCa 9.0 after permeabilisation with 10 μ g/mL α -toxin. Both tissues were then exposed to pCa 6.5. PSS was replaced by permeabilising buffer, as shown by the black arrow. Addition of agonists and free $[Ca^{2+}]$ are indicated by the thick and thin black solid bars, respectively.

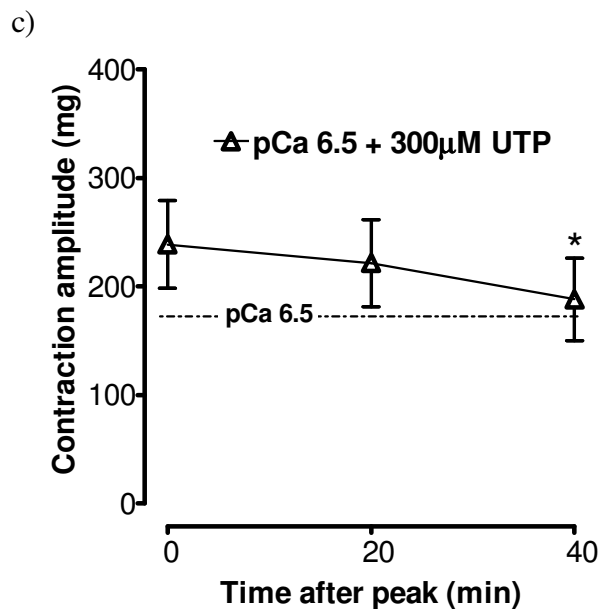
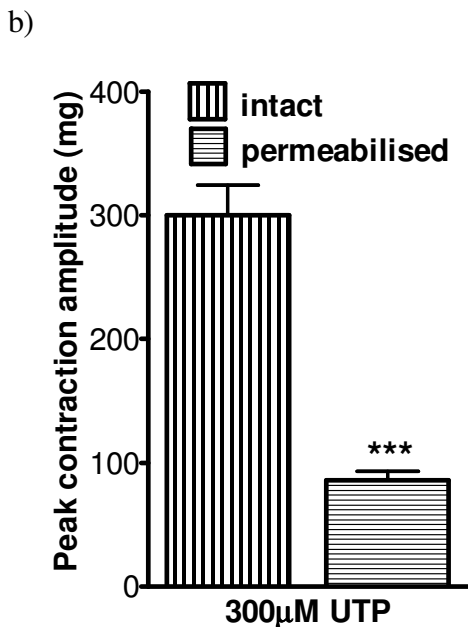
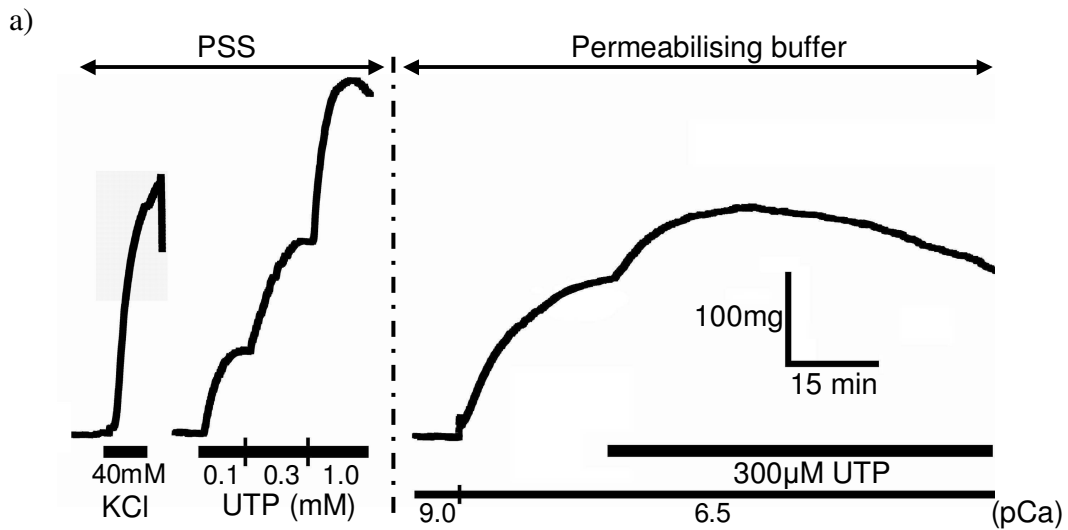


Figure 6.6. Vasoconstriction evoked by UTP in endothelium-denuded rat SPA treated with α -toxin. a) The traces show typical contractions of rat SPA induced by 40mM KCl and UTP (0.1 – 1.0mM) in the intact tissue, and subsequently by 300 μ M UTP in the presence of free $[Ca^{2+}]$ at pCa 6.5 after permeabilising the tissue with 10 μ g/mL α -toxin. PSS was replaced by permeabilising buffer, as shown by the black arrow. Agonist addition and free $[Ca^{2+}]$ are indicated by the thick and thin black solid bars, respectively. b) shows the mean peak amplitude of contractions to UTP in both intact and permeabilised state of rat SPA. The UTP response amplitude in the latter is measured by excluding the contraction amplitude of pCa 6.5. c) The mean amplitude of contractions to UTP at pCa 6.5 in the permeabilised tissue measured at peak and 20 and 40 min after that are shown. n=20 and 4 for data in (b) and (c), respectively. Data are expressed as mean \pm S.E.M. ***P<0.001 in (b) for the peak responses in permeabilised versus intact tissues and *P<0.05 in (c) for the responses at 40 min after peak versus at peak.

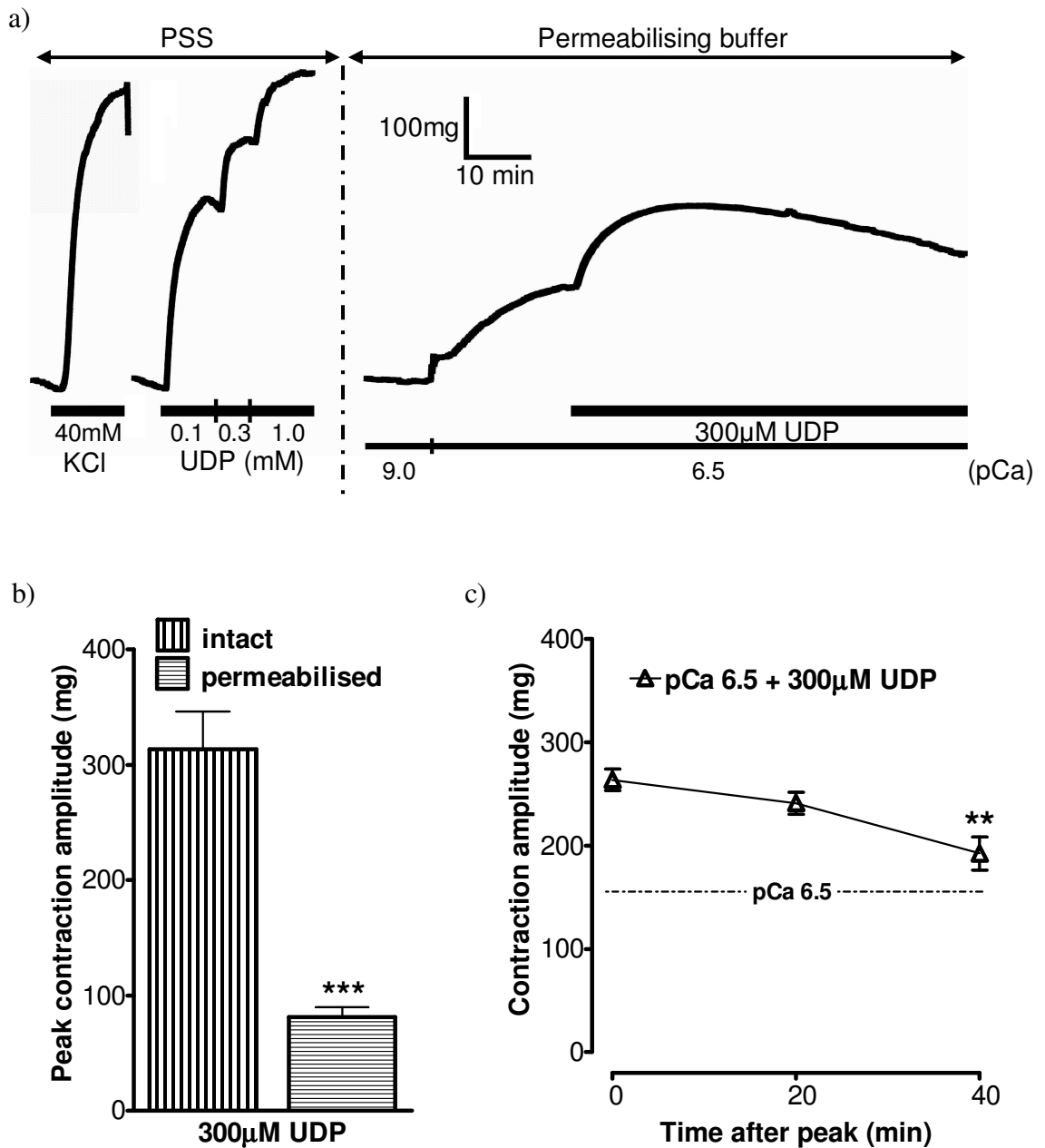


Figure 6.7. Contractile response of UDP in α -toxin-permeabilised endothelium-denuded rat SPA. a) The traces show the contractions of rat SPA evoked by 40mM KCl and UDP (0.1 – 1.0mM), and 300µM UDP (at pCa 6.5), before and after permeabilisation with 10µg/mL α -toxin, respectively. PSS was replaced by permeabilising buffer, as shown by the black arrow. Agonist addition and [Ca²⁺] are indicated by the thick and thin black solid bars, respectively. b) shows the mean peak amplitude of contractions of UDP in both intact and permeabilised state of rat SPA. The UDP response amplitude in the latter is measured by excluding the contraction amplitude of pCa 6.5. c) The mean amplitude of contractions of UDP at pCa 6.5 in the permeabilised vessel measured at peak and 20 and 40 min later are shown. n=20 and 4 for data in (b) and (c), respectively. Data are expressed as mean \pm S.E.M. ***P<0.001 in (b) for the peak responses in permeabilised versus intact tissues and **P<0.01 in (c) for the responses at 40 min after peak versus at peak.

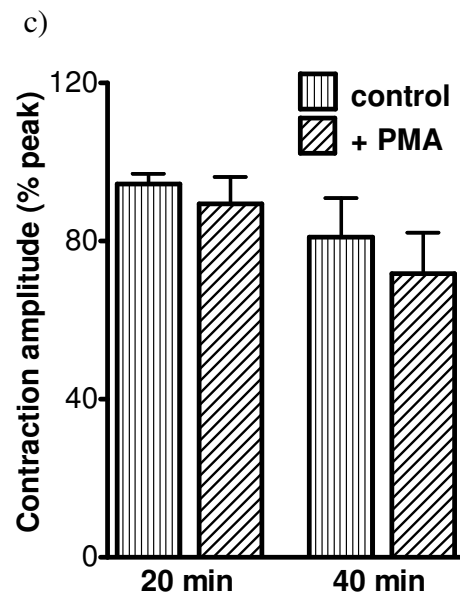
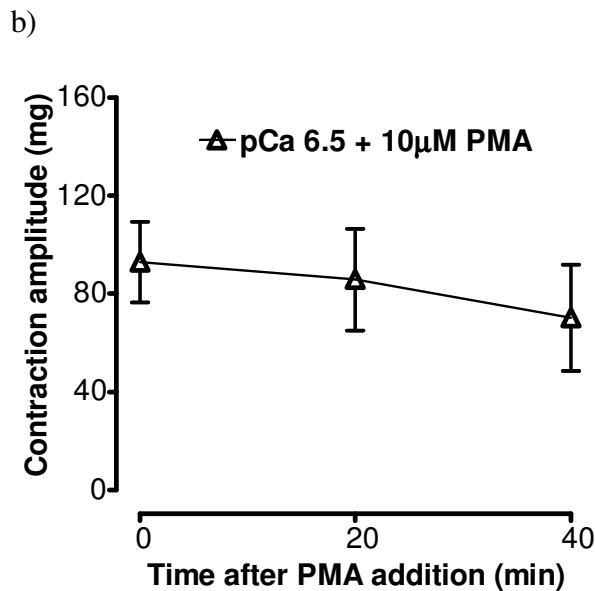
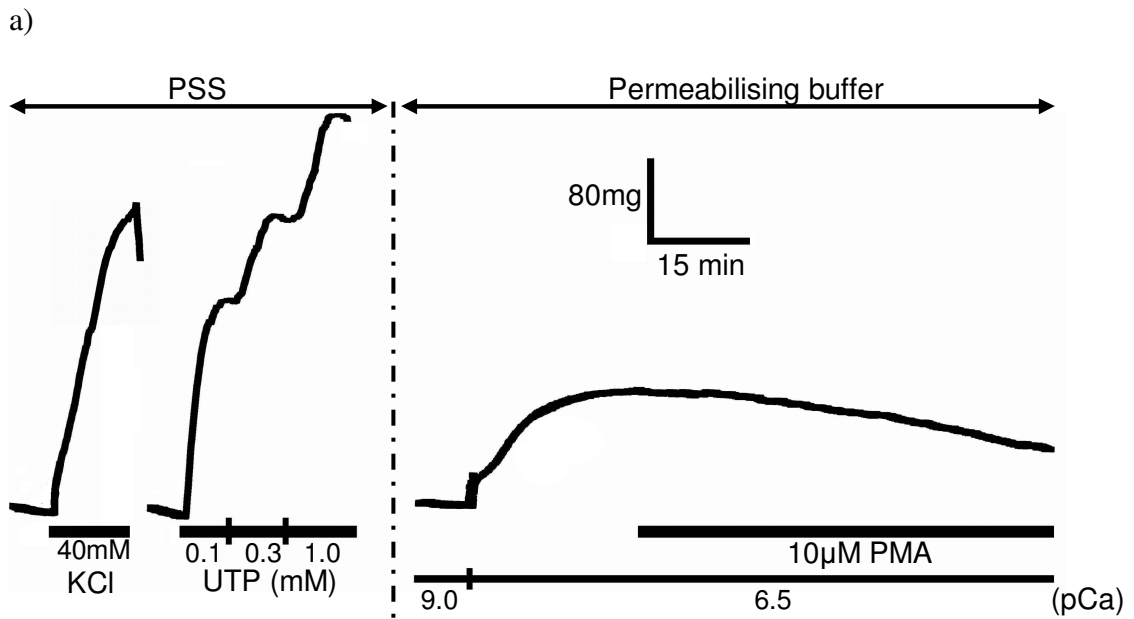


Figure 6.8. Effect of PMA addition in α -toxin-permeabilised endothelium-denuded rat SPA. a) The traces show typical contractions of rat SPA induced by 40mM KCl and UTP (0.1 – 1.0mM) in the intact tissue, and subsequently by free $[Ca^{2+}]$ at pCa 6.5 plus 10 μ M PMA, following permeabilisation with 10 μ g/mL α -toxin. PSS was replaced by permeabilising buffer, as shown by the black arrow. Addition of agonists and free $[Ca^{2+}]$ are indicated by the thick and thin black solid bars, respectively. The lower panels show the mean amplitude of contractions of the permeabilised vessel b) measured after adding PMA for 40 min and from the pCa 9.0 baseline, and then c) compared with the control (pCa 6.5) at the same time-point, are shown. $n=4$ both PMA and pCa 6.5. Data in (c) are expressed as % of the peak response. Data are shown as mean \pm S.E.M.

2.3. Effects of Post-Addition of Y27632 and GF109203X on Contractions Evoked by pCa 6.5, UTP, UDP and PMA

In the next series of experiments the effects of Y27632 and GF109203X on the contractions evoked by pCa 6.5, UTP and UDP were determined. To take into account the tendency for the contractions elicited by these agents to decay with time, Y27632 and GF109203X were added just after the contraction peak and the contraction amplitude was measured 20 min later. Under these conditions, 10 μ M Y27632 caused a rapid relaxation that did not reach a plateau and significantly diminished the pCa 6.5-induced contractions by $50.4 \pm 5.9\%$ (n=4) compared to a decay of $5.5 \pm 2.5\%$ (n=4) of the control response ($P < 0.001$) (Figure 6.9a). 10 μ M Y27632 not only rapidly and totally reversed responses to UTP (Figure 6.9b) and UDP (Figure 6.9c), but also depressed the contractions below the level established by pCa 6.5 by $32.8 \pm 6.5\%$ (n=4, $P < 0.01$) and $41.8 \pm 11.4\%$ (n=4, $P < 0.01$), respectively. Thus, it is apparent that Ca²⁺ sensitisation-mediated contractions by both nucleotides were fully dependent on Rho kinase.

To determine if the contribution of Ca²⁺ sensitisation was the same in permeabilised and intact tissues the amplitude of the agonist-induced responses in permeabilised preparations, expressed as a percentage of the earlier response in same tissue before permeabilisation, was compared with the percentage inhibition of the control response of unpermeabilised tissues induced by Y27632, as shown in Chapter 4 (Figure 4.15). The calculation of the percentage of Ca²⁺ sensitisation components in both intact and permeabilised preparations is illustrated in Figure 6.10a. Figure 6.10b shows that the reduction of UTP by Y27632 in intact tissues (~20%) was slightly, but not significantly smaller than the response to UTP seen in permeabilised tissues (~30%). For UDP, these measurements were comparable and Ca²⁺ sensitisation contributed approximately 30% of its peak response.

In contrast, 10 μ M GF109203X did not appear to induce a relaxation when added at the peak of the response to pCa 6.5, UTP or UDP (both 300 μ M) (Figure 6.11) and there was no significant difference in the extent of contraction decay after 20 min compared with the time-matched controls (Figure 6.11). PMA did not appear to evoke a contraction in the previous section, but in unpermeabilised tissue its contractile action developed very slowly, usually taking about an hour to reach peak.

Thus, in theory, a slow contractile effect in permeabilised preparations could be masked by the slow decay of the contraction to pCa 6.5. To test this possibility 10 μ M GF109203X was added 60 min after 10 μ M PMA had been added at the peak of the response to pCa 6.5. Under these conditions GF109203X evoked a clear, rapid relaxation and 20 min later the tone had returned to the basal level seen at pCa 9.0 (Figure 6.12).

Overall, these results show that the Ca²⁺ sensitisation aspect of contractions to UTP and UDP appears to be exclusively dependent on Rho kinase, without any apparent involvement of PKC. Additionally, Rho kinase is also likely to contribute via Ca²⁺ sensitisation to the contraction induced by the elevation of [Ca²⁺]_i. In contrast, although PKC can appear to be activated by PMA it does not contribute to contractions evoked by UTP, UDP and elevated [Ca²⁺]_i.

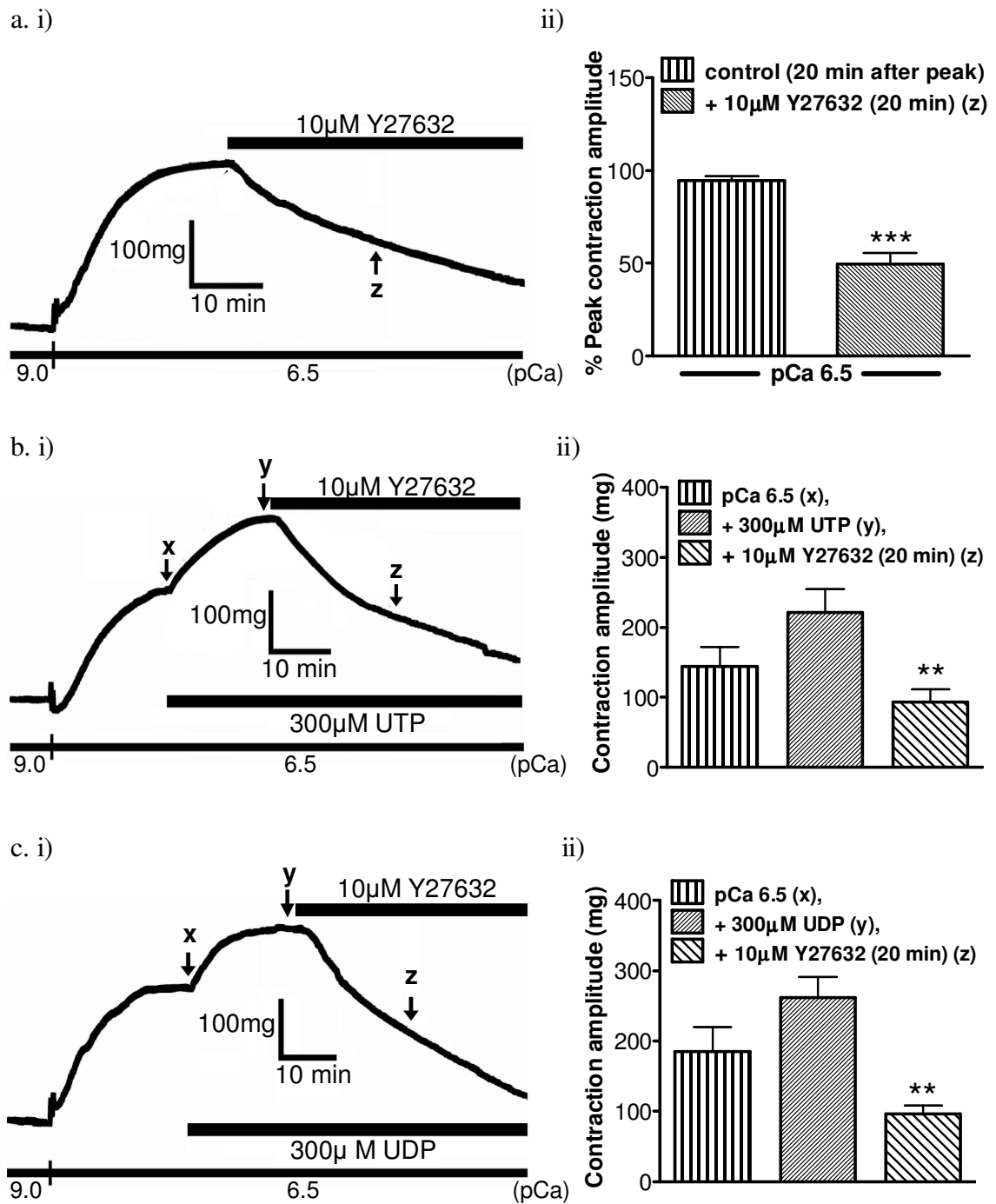


Figure 6.9. Effect of Y27632 on contractions evoked by pCa 6.5, UTP and UDP in α -toxin-permeabilised endothelium-denuded rat SPA. The effects of 10µM Y27632 on contractions evoked by a) pCa 6.5, b) 300µM UTP and c) 300µM UDP, in α -toxin-permeabilised rat SPA, are shown. The nucleotides were added once the contraction induced by pCa 6.5 had reached its peak. The left hand panels show typical traces for each, where Y27632 was added once the agonist-induced contraction had reached its peak and x, y and z indicates the peak contraction of pCa 6.5, pCa 6.5 plus agonist and 20 min after adding Y27632, respectively. Addition of

agonists and Y27632, and free $[Ca^{2+}]$ are shown by the thick and thin black solid bars, respectively.

The right hand panels; a. ii) shows the mean contraction amplitude 20 min after peak in the absence and presence of Y27632, b. ii) and c. ii) show the mean amplitude of; contractions to pCa 6.5 (x), the total peak response after subsequent addition of agonist (y), and the contractions remaining following treatment with Y27632 (z). Note that the data in a. ii) were obtained from different preparations. n=4 each and are expressed as a % of peak contraction amplitude. The data shown in b. ii) and c. ii) are expressed as mg tension, measured from the basal tone at pCa 9.0 and in either case the two sets of data were obtained in the same preparations. n=4 for both UTP and UDP. Data are shown as mean \pm S.E.M. ***P<0.001 in a. ii) for the response to pCa 6.5 in the presence of Y26732 compared with the control and **P<0.01 in b. ii) and c. ii) for the difference between the peak response to pCa 6.5 plus agonist (y) and the remaining contractions after 20 min application of Y27632 (z).

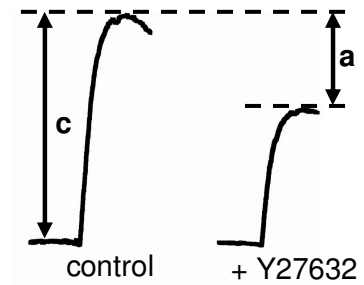
a)

% of Ca²⁺ sensitisation components in:-

Intact preparation (Ca_I) =

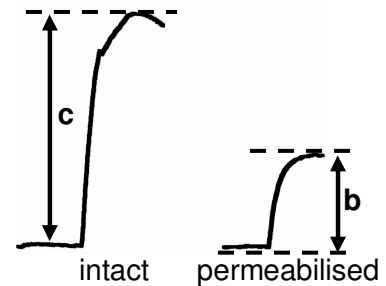
% peak response inhibited by Y27632

$$\left[\frac{\text{reduction of peak response by Y27632 (a)}}{\text{peak response intact preparation (c)}} \times 100 \right]$$



Permeabilised preparation (Ca_P) =

$$\frac{\text{peak response permeabilised preparation (b)}}{\text{peak response intact preparation (c)}} \times 100$$



c)

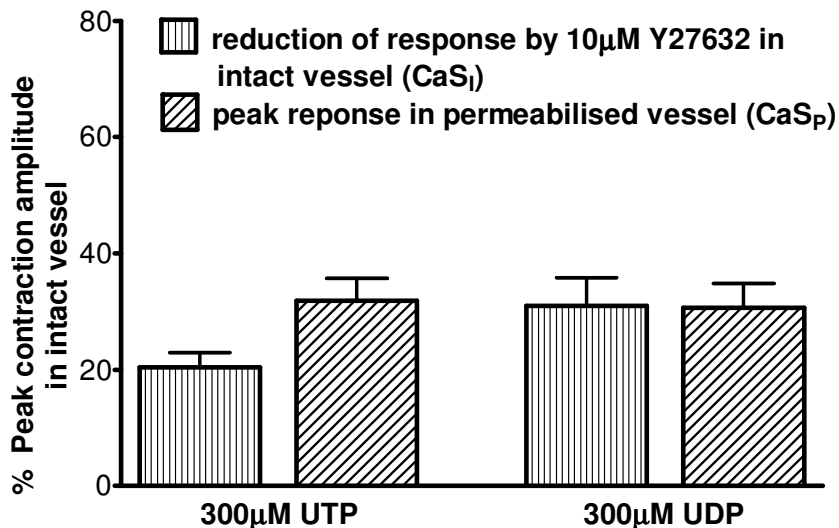


Figure 6.10. Comparison of the amplitude of the Ca²⁺ sensitisation components of contractions evoked by UTP and UDP in intact and permeabilised endothelium-denuded rat SPA. a) shows the calculation for the % of Ca²⁺ sensitisation components of an agonist in intact (Ca_I) and permeabilised (Ca_P) rat SPA. b) The mean reduction of peak contraction amplitude of UTP and UDP (both 300µM) in intact rat SPA after 15 min preincubation with 10µM Y27632, and the mean amplitude of peak response of the nucleotides at the same concentrations obtained in vessel permeabilised with 10µg/mL α-toxin. Both data sets are normalised as % of control peak contraction to agonist in intact preparation, as indicated in (a). n=5 and 6 for UTP and UDP in intact vessels, respectively and n=20 for both nucleotides in permeabilised vessels. Data are shown as mean ± S.E.M.

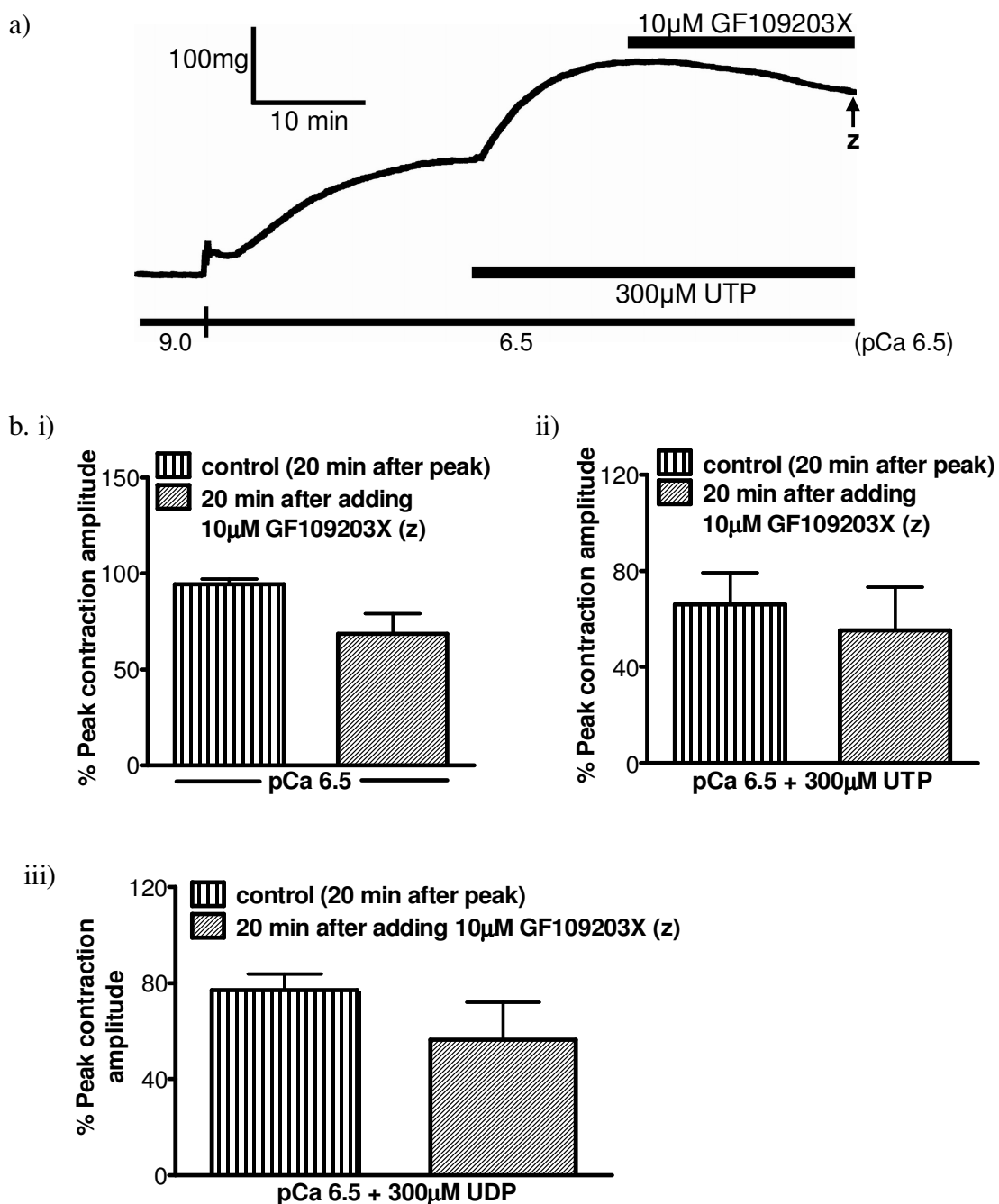


Figure 6.11. Effect of GF109203X on contractions evoked by pCa 6.5, UTP and UDP in α -toxin-permeabilised endothelium-denuded rat SPA. a) The trace shows the effect of adding 10μM GF109203X for 20 min once the contraction of α -toxin-permeabilised rat SPA evoked by 300μM UTP had reached a peak. UTP was applied after the contraction induced by pCa 6.5 had reached its peak. z indicates where contraction amplitude was measured, 20 min after adding GF109203X. Agonist and GF109203X addition, and free $[Ca^{2+}]$ are indicated by the thick and thin black solid bars, respectively. b) shows the mean contractions to i) pCa 6.5, ii) UTP and iii) UDP (both 300μM) in the absence and presence of GF109203X for 20 min application following the peak responses. The control and treated groups were obtained from separate preparations. n=4 for all. Contractions are expressed as % of the peak response. Data are shown as mean \pm S.E.M.

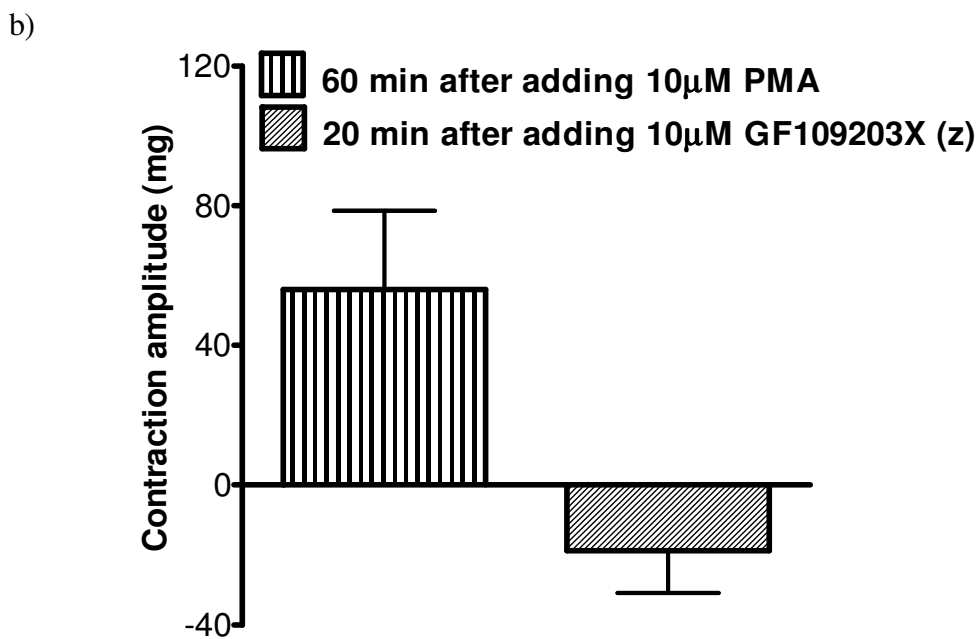
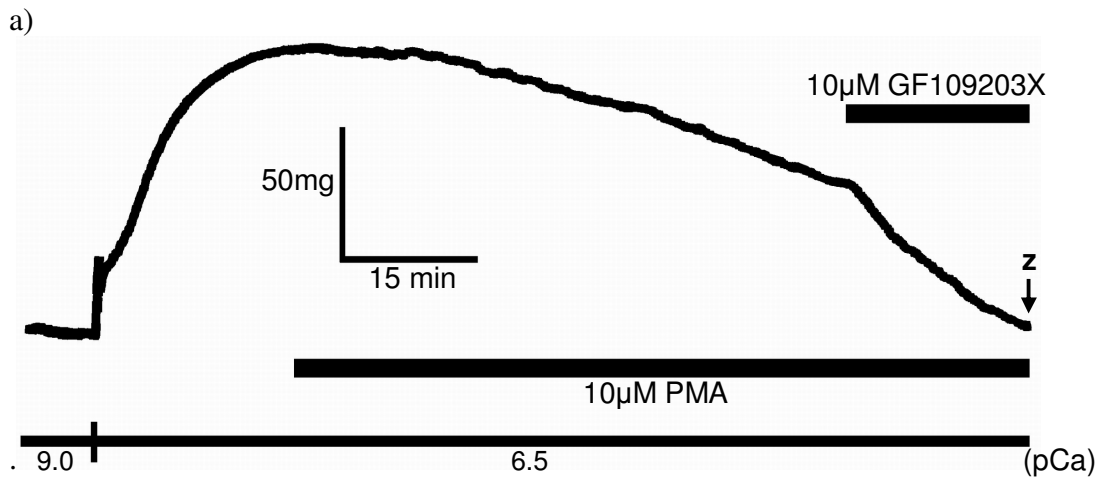


Figure 6.12. Effect of GF109203X on contractions evoked by PMA in α -toxin-permeabilised endothelium-denuded rat SPA. a) The trace shows the effect of adding 10µM GF109203X for 20 min once 10µM PMA had been added for 60 min in the α -toxin-permeabilised rat SPA. PMA was applied after the contraction induced by pCa 6.5 had reached its peak. z indicates where contraction amplitude was measured 20 min after adding GF109203X. PMA and GF109203X addition, and free $[Ca^{2+}]$ are shown by the thick and thin black solid bars, respectively. b) shows the mean contractions to PMA in the absence and presence of GF109203X for 20 min application after 60 min addition of PMA, obtained from similar tissue. n=4. Data are shown as mean \pm S.E.M.

2.4. Effects of Post-Addition of U73122 and Suramin on Contractions Evoked by pCa 6.5, UTP and UDP

The involvement of PI-PLC in the Ca^{2+} sensitisation-dependent contractions of UTP and UDP was investigated by applying U73122 after the contractile response reached a maximum level (as described in the above Section 2.2). 10 μM U73122 had no significant effect on the UTP-evoked contraction (Figure 6.13). U73122 did not appear to induce a clear relaxation of the UDP-induced tone in any of four tissues (Figure 6.13), but nonetheless it significantly reduced the contractions evoked by UDP by about 20% compared to the time-matched control response (n=4, P<0.05).

Finally, the effects of the P2 receptor antagonist suramin were investigated, as it was shown to inhibit part of the response to UTP and UDP in intact rat SPA, with a maximal effect at 100 μM (Chootip *et al.*, 2002). Therefore, it was investigated if the Ca^{2+} sensitisation component in permeabilised preparations was suramin-sensitive or -insensitive. 100 μM suramin significantly diminished contractions evoked by pCa 6.5 and UTP by about 50% (n=4, P<0.05) and 30% (n=4, P<0.05), respectively, compared to the time-matched control response (Figure 6.14b). In addition, 100 μM suramin abolished the UDP-evoked contractions in three out of four tissues (Figure 6.14) although the remaining preparation appeared to be unaffected. Moreover, the resultant tone of the three affected tissues was dropped below the tension induced by pCa 6.5 by $81 \pm 30\%$ of the peak contraction to pCa 6.5.

Thus, PI-PLC appears to contribute modestly to the Ca^{2+} sensitisation evoked by UDP, but such contribution was absent in the UTP response. In addition, the contractions induced by pCa 6.5 and UTP and UDP were inhibited by suramin and this antagonistic effect appears to be greater against UDP.

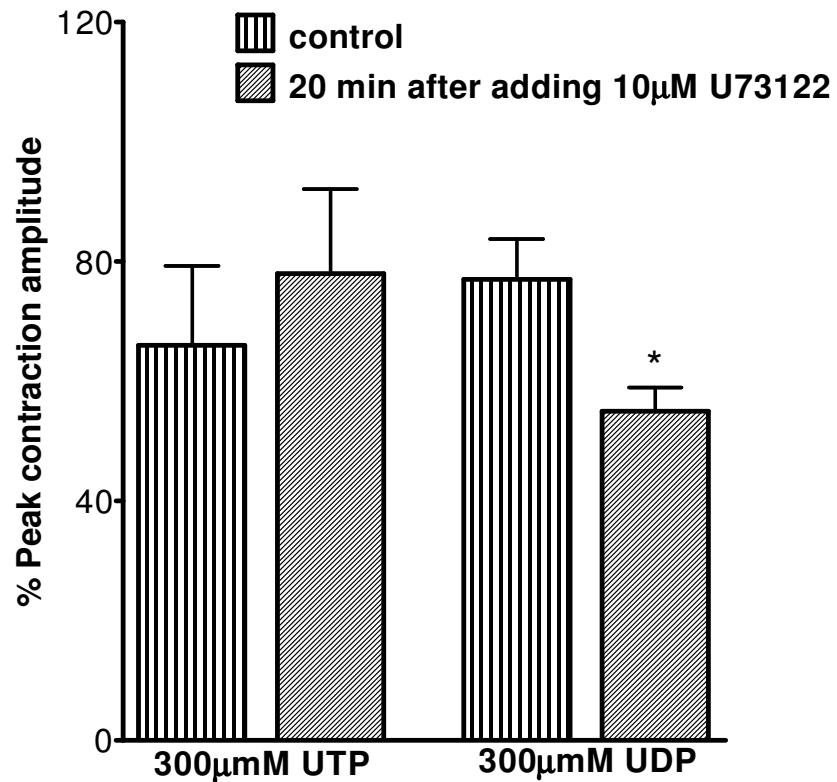


Figure 6.13. Effect of U73122 on contractions evoked by UTP and UDP in α -toxin-permeabilised endothelium-denuded rat SPA. The mean peak amplitude of contractions to UTP and UDP in the absence and presence of 10µM U73122 for 20 min application following the peak responses. The control and treated groups were obtained from different preparations. n=4 for all data groups. The data represent the actual contraction amplitudes of both nucleotides, i.e. without the initial response to pCa 6.5, and are expressed as a % of the peak response as mean \pm S.E.M. *P<0.05 for the treated group versus control.

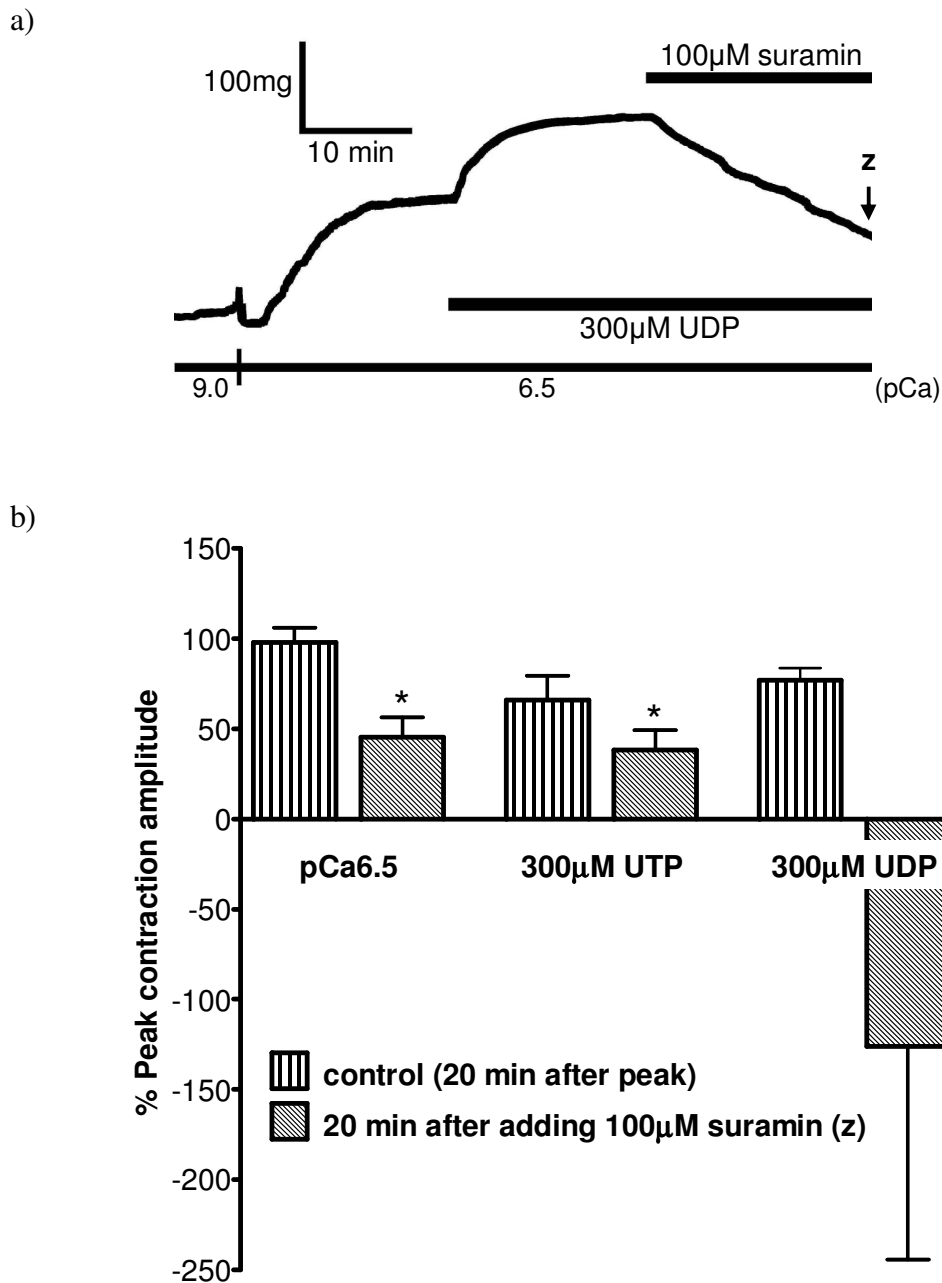


Figure 6.14. Effect of suramin on contractions evoked by pCa 6.5, UTP and UDP in α -toxin-permeabilised endothelium-denuded rat SPA. a) The trace shows the effect of adding 100µM suramin for 20 min once the contractions evoked by 300µM UDP in α -toxin-permeabilised rat SPA had reached a peak. UDP was applied after the contractions induced by pCa 6.5 had reached its peak. UDP and suramin addition, and free $[Ca^{2+}]$ are indicated by the thick and thin black solid bars, respectively. b) The mean peak amplitude of contractions of pCa 6.5, UTP and UDP in the absence and presence of 100µM suramin 20 min after their peak responses are shown. The control and treated groups for pCa 6.5, UTP and UDP were obtained from different preparations. $n=4$ for all. The data represent the actual contraction amplitudes of UTP and UDP, i.e. without the initial response to pCa 6.5, and are expressed as a % of the peak response. Data are shown as mean \pm S.E.M. * $P<0.05$ for treated groups versus control.

3. DISCUSSION

In this chapter Ca^{2+} concentration-response curves were generated in the α -toxin-permeabilised rat SPA with a maximum response at pCa 4.5. At pCa 6.5, UTP and UDP evoked contractions in permeabilised tissues, which decayed slowly. Y27632 abolished the contractions evoked by UTP and UDP, and substantially inhibited the response to pCa 6.5. Moreover, it also caused a right shift of the $[\text{Ca}^{2+}]$ -force relationship curve. In contrast, the responses to both nucleotides, pCa 6.5, and the Ca^{2+} concentration-response curves were unaffected by GF109203X. U73122 modestly inhibited the response to UDP, but had no effect on UTP-evoked contractions. Suramin reduced the contractions induced by pCa 6.5, UTP and UDP, although the reduction was more prominent against the UDP-evoked response.

3.1. Characterisation of Ca^{2+} -Force Relationship and Agonist Responses in α -Toxin-Permeabilised Rat SPA

Initially, cumulative Ca^{2+} concentration-response curves were generated in the α -toxin-permeabilised SPA to examine the relationship between $[\text{Ca}^{2+}]$ and force production. The tissue started to contract at pCa 7.0, and continued to contract following each further increase of $[\text{Ca}^{2+}]$, until a peak was reached at pCa 4.5. The EC_{50} and Hill slope of the curve were 336nM and 2.67, respectively. This pattern of results was comparable with a previous permeabilisation study in the same vessel (Thomas *et al.*, 2005) where the EC_{50} of the $[\text{Ca}^{2+}]$ -force curve was 240nM. In permeabilisation studies in other tissues, such as rabbit pulmonary artery (Crichton *et al.*, 1997) and pig portal vein (Kitazawa *et al.*, 1989) the EC_{50} values for $[\text{Ca}^{2+}]$ -force curve were 719nM and ~1000nM, respectively. In addition, the peak response in the present study was induced at a $[\text{Ca}^{2+}]$ that typically produces a maximum response in permeabilised preparations (Horiuti, 1986; Iizuka *et al.*, 1994). Since increasing the $[\text{Ca}^{2+}]$ of the buffer in a similar fashion did not produce any response in unpermeabilised tissues these data clearly indicate that membrane permeabilisation by α -toxin had been achieved.

Next, the contractions induced by pCa 6.5, UTP, UDP and PMA in permeabilised preparations were characterised. First, UTP and UDP were added at pCa 9.0, but no response was observed. This is consistent with previous reports that raised $[\text{Ca}^{2+}]$ is

needed for GPCR agonists to induce contraction (Evans, *et al.*, 1999; Jernigan *et al.*, 2004; Wilson *et al.*, 2005; Knock *et al.*, 2008), therefore, $[Ca^{2+}]$ was raised to pCa 6.5. This in itself induced a peak contraction of about half of the maximum (pCa 4.5) response. Likewise, addition of UTP and UDP at pCa 6.5 also evoked a peak contraction of about 30 and 40%, respectively, of the response produced before permeabilising the tissue. These findings are the first to report that UDP evoked contractions in the permeabilised smooth muscle. Moreover, the Ca^{2+} sensitisation-mediated contractions to UTP seen here are consistent with a previous study in rat pulmonary artery (Jernigan *et al.*, 2004). All of the above contractions decayed slowly and it was apparent in the UTP- and UDP-evoked contractions that a significant reduction of about 70% was noted 40 min after peak. In contrast, addition of PMA at pCa 6.5 did not evoke any additional response, even after 60 min exposure. This result conflicts with a previous report (Jernigan *et al.*, 2004) that showed a contraction to PMA (maximum concentration at 1 μ M) addition in the permeabilised rat pulmonary artery. Thus, the present results appear to suggest that PKC cannot be activated in the permeabilised rat SPA. However, as will be discussed below, this is not necessarily the case. Overall, all the above responses decayed slowly, therefore, to minimise the influence of decay the effect of an inhibitor was measured 20 min after its addition. Additionally, these responses were then compared statistically against time-matched control responses.

3.2. Involvement of Rho kinase and PKC in Contractions Evoked by Elevation of $[Ca^{2+}]$, UTP and UDP in α -Toxin-Permeabilised Rat SPA

Y27632 shifted the $[Ca^{2+}]$ concentration-response curve to the right and inhibited the response to pCa 6.5 by about 45%. These results indicate a clear involvement of Rho kinase in sensitising the Ca^{2+} -force relationship in rat SPA. Additionally, it implies the presence of constitutively active Rho kinase, which mediates this effect. Similar effects of Y27632 have been reported previously in permeabilised rat pulmonary artery (Knock *et al.*, 2008) and mouse femoral artery (Bonnevier & Arner, 2004). Furthermore, Tsai & Jiang, (2006) and Dimopoulos *et al.*, (2007) demonstrated that the basal level of phosphorylated MYPT-1 was substantially reduced by Y27632, which further supports the existence of constitutively active Rho

kinase in the unstimulated unpermeabilised tissue. However, it should be noted that Rho kinase in the present study could also have been activated by the stimulation of P2Y receptors, as the tissues was exposed to the ATP-containing permeabilising buffer. Indeed, Wilson *et al.*, (2005) examined the levels of RhoA in the unstimulated intact and α -toxin-permeabilised rat tail artery, and found a low level of activated RhoA (RhoA/GTP complex) in the permeabilised preparation, which was absent in the intact tissue. The use of P2Y receptor antagonists to block the pharmacological action of ATP might be able to address this issue, but at present there is a lack of selective P2Y antagonists.

The current study also found that Y27632 abolished the contractions to both UTP and UDP in the permeabilised tissues. Furthermore, in both cases the tone dropped below that established by pCa 6.5. This indicates that Rho kinase fully mediates the Ca^{2+} sensitisation component of P2Y receptor-mediated vasoconstriction of rat SPA, consistent with the data presented in Chapter 4 that showed a role of Rho kinase in P2Y receptor-mediated contractions of intact tissues. Indeed, the inhibitory effect of Y27632 against the response to UTP and UDP in the intact vessel was comparable with the peak response to these agonists in the permeabilised preparation, further supporting the contribution of Rho kinase in mediating the Ca^{2+} sensitisation components of P2Y receptor-evoked contractions. Additionally, the drop of basal tension below the level induced by pCa 6.5 again provides further evidence of the existence of constitutively active Rho kinase in the rat SPA. The present observation is in good agreement with a previous report (Jernigan *et al.*, 2004) showing virtual abolition of UTP-evoked vasoconstriction by Y27632 in membrane-permeabilised preparations of rat pulmonary artery. Rho kinase-mediated Ca^{2+} sensitisation was also observed in contractions of rat pulmonary artery evoked by SPC (Thomas *et al.*, 2005) and $\text{PGF}_{2\alpha}$ (Knock *et al.*, 2008), and of rat tail artery evoked by the thromboxane A_2 analogue U-46619 (Wilson *et al.*, 2005).

The present study, however, did not observe any effect of GF109203X on the $[\text{Ca}^{2+}]$ -force relationship or the contractions in response to either nucleotides. This clearly indicates a lack of PKC involvement in Ca^{2+} sensitisation, consistent with Jernigan *et al.*, (2004), who failed to establish any PKC influence in UTP-evoked vasoconstriction of membrane-permeabilised rat pulmonary artery. PMA did not

induce vasoconstriction, but addition of GF109203X induced a clear relaxation in the presence of PMA, therefore PMA may well evoke vasoconstriction, but it is masked by slow decline of contraction. Thus, the PKC influence in both UTP- and UDP-evoked responses observed earlier (Chapter 4) appears to involve pathways other than those associated with Ca^{2+} sensitisation.

3.3. Effects of U73122 and Suramin on Contractions Evoked by pCa 6.5, UTP and UDP in α -Toxin-Permeabilised Rat SPA

U73122 had no effect of the UTP-evoked contraction, but reduced the contractions evoked by UDP by about 20%. This suggests that a role of PI-PLC in Ca^{2+} sensitisation of P2Y receptor-mediated contractions is restricted to the UDP-sensitive P2Y receptors. This finding was rather unexpected considering the results discussed above in which Ca^{2+} sensitisation induced by P2Y receptors was mediated solely by Rho kinase, and not PKC, a downstream effector of PI-PLC. Moreover, as outlined in Chapter 4, the signalling pathway that lead to the activation of Rho kinase usually involve stimulation of receptor coupling to $\text{G}\alpha_{12/13}$ (Buhl *et al.*, 1995; Somlyo & Somlyo, 2000; Suzuki *et al.*, 2003, 2009), rather than $\text{G}\alpha_{q/11}$, which stimulates PI-PLC. Interestingly, Vogt *et al.*, (2003) did find a role for $\text{G}\alpha_{q/11}$ in the activation of RhoA, but it was unaffected by U73122. Rather this RhoA activation was associated with a family of RhoGEF protein leukemia-associated Rho guanine nucleotide exchange factors. How PI-PLC contributed to the UDP-evoked response in the present study is unclear and warrants further study.

The present study showed that suramin reduced contractions evoked by pCa 6.5 and UTP by about 40% and 30%, respectively and abolished the UDP-evoked contractions in three out of four tissues, such that the tone fell below the tension induced by pCa 6.5 prior to UDP addition. These results indicate that suramin might influence the Ca^{2+} -force relationship. Additionally, these findings also imply that the Ca^{2+} sensitisation-dependent contractions to UDP in particular, and UTP to a lesser extent, can be mediated via suramin P2Y-sensitive receptors. Suramin was found to have no effect on UTP-and UDP-evoked contractions of rat pulmonary artery, but abolished the contractions to ATP (Rubino *et al.*, 1999). However, Chootip *et al.*, (2002) showed the response to both UTP and UDP in rat SPA was partially inhibited

by suramin, thus indicating that UTP and UDP act at at least two types of receptor, i.e. suramin-sensitive and suramin-resistant receptors. Consistent with these findings, the current results indicate that the Ca^{2+} sensitisation-dependent contractions can be evoked at least via a suramin-sensitive UDP receptor and suramin-resistant UTP receptor. Since the P2Y₆ receptor is highly selective for UDP (Nicholas *et al.*, 1996), it is probable that the suramin-sensitive UDP receptor is in fact the P2Y₆ receptor. Compatible with this view, Nishida *et al.*, (2008) found that RhoA activation in mouse heart was mediated by stimulation of the P2Y₆ receptor. However, caution needs to be exercised when interpreting the effect of suramin in the membrane-permeabilised preparation. Suramin is a large molecule with multi-charged groups and has been shown to interact with various intracellular proteins, such as G proteins to inhibit their activity (Lambrecht *et al.*, 2002). Thus, it cannot be ruled out that the effect of suramin in the present study might have been masked by its non-specific activities, since it can readily gain access into the intracellular compartment via α -toxin pores. The inhibitory effect of suramin on the contractions induced by pCa 6.5 alone is consistent with this. In summary, UTP and UDP act mainly at its suramin-resistant and suramin-sensitive P2Y receptors, respectively, to induce Ca^{2+} sensitisation-dependent contractions via Rho kinase activation.

Chapter 7:

Profile of INS45973-, INS48823- and 3-phenacyl UDP-evoked responses in intact and membrane-permeabilised preparations

1. INTRODUCTION

The contractile studies of P2Y receptor-mediated vasoconstriction of pulmonary artery are largely dependent on the use of endogenous agonists, and so far three distinct receptors, the P2Y₂, P2Y₄ and P2Y₆ receptors, have been identified on the basis of their sensitivity towards UTP and UDP. However, these agonists are relatively unselective, as they can activate more than one of these three P2Y subtypes. Additionally, RT-PCR revealed the presence of P2Y₂, P2Y₄ and P2Y₆ mRNA in this tissue (Konduri *et al.*, 2004; Gui *et al.*, 2008). Thus, it still remains unclear which of the P2Y subtypes are actually involved in mediating contractions evoked by these endogenous agonists.

The progress of designing selective P2Y agonist has led to the development of several compounds, including INS45973, INS48823 and 3-phenacyl UDP, which show improved selectivity for P2Y receptors subtypes. INS45973 is an analogue of the naturally occurring dinucleotide P2Y agonist Up₄A (Jacobson *et al.*, 2009; Jankowski *et al.*, 2009). While inactive at the human P2Y₁ receptor, this agonist is highly potent at the recombinant human P2Y₂ and P2Y₄ receptors, but not P2Y₆ receptors in elevating [Ca²⁺]_i (EC₅₀ of 0.52, 0.28 and >10μM for P2Y₂, P2Y₄ and P2Y₆ receptors, respectively) (Shaver *et al.*, 2005). Moreover, it was found to be effective in stimulating vaginal moisture in the ovariectomised rabbit via P2Y₂ receptor activation (Min *et al.*, 2003), and has been shown to activate presynaptic inhibition of glutamate release from the nerve terminal in rat hippocampus via P2Y₂ and/or P2Y₄ receptors (Rodrigues *et al.*, 2005).

Another dinucleotide P2Y agonist INS48823 has a high potency at the recombinant human P2Y₆ receptor (EC₅₀ of 0.125μM) with no appreciable activity at P2Y₁, P2Y₂ or P2Y₄ receptors, in inducing the elevation of [Ca²⁺]_i (Korcok *et al.*, 2005). In human dendritic cells, INS48823 was shown to induce the release of chemokine CCL20 with an EC₅₀ of 12.7 ± 4.4μM (Marcet *et al.*, 2007). The same study also found that at 100μM, INS48823 was more effective than UDP in stimulating CCL20 release in the human airway epithelial cells. Likewise, INS48823 induced higher rabbit oestoclast survival than UDP at 10μM for both agonists (Korcok *et al.*, 2005). However, INS48823 and UDP were equi-effective in inducing Cl⁻ secretion in the mouse trachea (Schreiber & Kunzelmann, 2005).

3-phenacyl UDP is also a much more potent agonist at the recombinant human P2Y₆ receptor than at P2Y₂ and P2Y₄ receptors for inducing an increase in [³H]inositol phosphates (EC₅₀ = 40, >100 and 0.07μM at P2Y₂, P2Y₄ and P2Y₆ receptors, respectively) (El-Tayeb *et al.*, 2006). Moreover, it failed to induce a rise of intracellular Ca²⁺ at concentrations of up to 10μM in rat basophilic leukemia-2H3 cells, which express an abundant level of native P2Y₁₄ receptor compared to P2Y₂, P2Y₄ and P2Y₆ receptors (Gao *et al.*, 2010). Kauffenstein *et al.*, (2010) have recently shown that 3-phenacyl UDP evoked vasoconstriction of thoracic aorta from the transgenic mice lacking NTPDase1 with the potency of about 20-fold lower than UTP and UDP (EC₅₀ = 22.8 ± 12.4μM, 1.06 ± 0.64μM, 1.76 ± 0.94μM for 3-phenacyl UDP, UTP and UDP, respectively).

It is clear that the development and use of selective P2Y agonists is essential to improve our understanding of which particular P2Y subtypes are involved in mediating vasoconstriction of rat SPA. Therefore, the aim of this chapter was to further characterise the P2Y receptor-mediated vasoconstriction of rat SPA by using the above three compounds, i.e. INS45973, INS48823 and 3-phenacyl UDP. In the first part of the study the profile of the contractile responses evoked by these compounds in the intact preparation was established, and in the second part, the characterisation of these responses was further performed in the permeabilised vessels. In both parts, the effects of Y27632 and suramin on the agonist-induced contractions were also investigated.

2. RESULTS

2.1 Intact Rat SPA

2.1.1 Contractile Responses of INS45973, INS48823 and 3-Phenacyl UDP

Cumulative concentration-response curves for INS45973, INS48823 and 3-phenacyl UDP (1 – 300 μ M) were generated to determine the potency of these compounds and then compared with the endogenous agonists UTP and UDP. INS45973, INS48823 and 3-phenacyl UDP each evoked contractions that rapidly reached a maintained peak within several minutes (Figure 7.1). INS45973 and INS48823 generated similar concentration-response curves, which appeared to nearly reach a plateau (Figure 7.1, 7.2). In contrast, the curve to 3-phenacyl UDP was shallower and clearly still rising at the highest concentration applied. As observed with UTP and UDP in Chapter 5, the concentration-response curves did not reach a maximum (Figure 7.1, 7.2), and so EC₅₀ values could not be determined. Therefore, the concentration of agonists that induced 40% of 40mM KCl response (EC_{40K}) was used to compare the potency of the agonists (Chootip *et al.*, 2002). Additionally, it was noted that the EC_{40K} of the above agonists evoked contractions below 50% of their responses at 300 μ M, thus the concentration of agonists that induced 80% of 40mM KCl response (EC_{80K}) was also used to further compare the potency of the agonists. EC_{40K} and EC_{80K} values for both UTP and UDP were also determined before comparing them with the synthetic agonists.

The potencies of all three synthetic agonists were comparable, as the EC_{40K} and EC_{80K} values of both INS45973 and INS48823 were not significantly different from 3-phenacyl UDP (Table 7.1). In contrast, INS45973 was significantly more potent than both UTP (P<0.05 for EC_{80K}) and UDP (P<0.01 and P<0.05 for EC_{40K} and EC_{80K}, respectively). In addition, INS48823 was also significantly more potent than both UTP and UDP at the EC_{80K} level (P<0.05 for both). However, the potency of 3-phenacyl UDP was not significantly different from that of UTP and UDP.

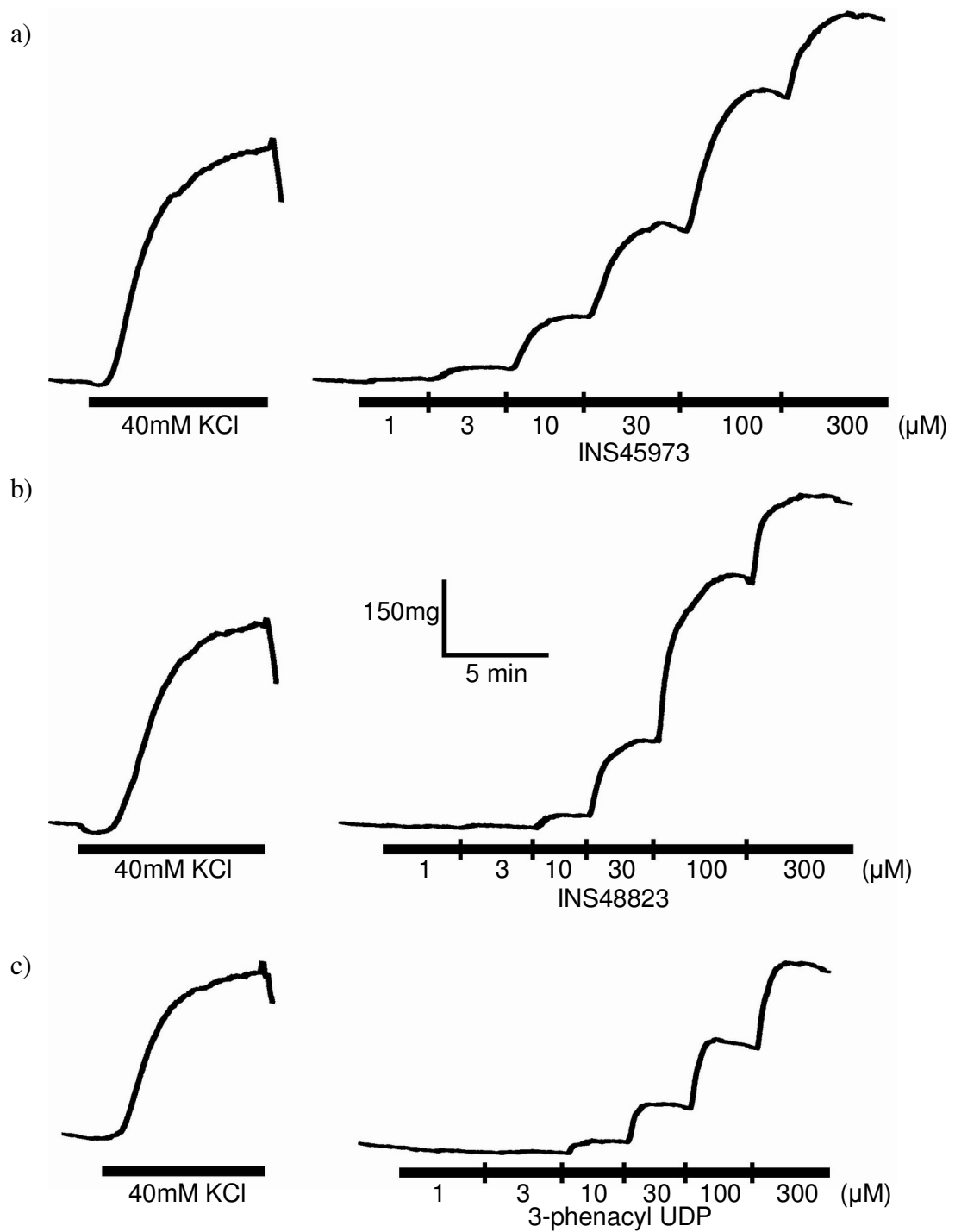


Figure 7.1. Vasoconstriction of intact, endothelium-denuded rat SPA to INS45973, INS48823 and 3-phenacyl UDP. Original traces of the contractions of rat SPA to 40mM KCl and subsequently to cumulative addition of a) INS45973, b) INS48823 and c) 3-phenacyl UDP, obtained in different tissues, are shown. Addition of KCl and agonists, is indicated by the horizontal bars.

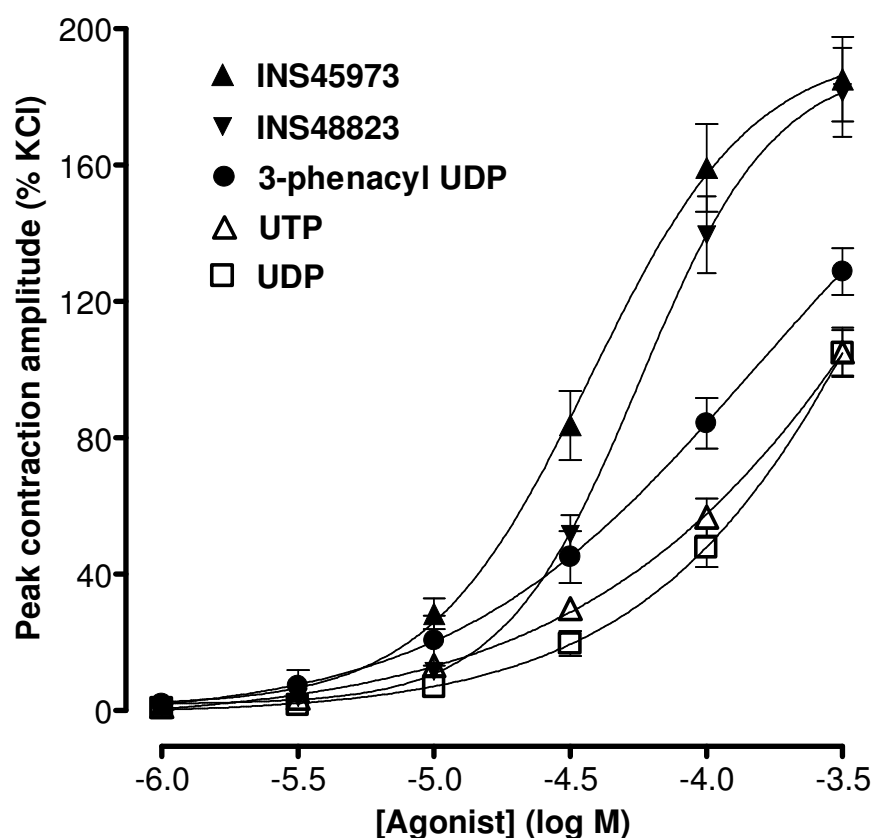


Figure 7.2. Contractile responses of intact, endothelium-denuded rat SPA to P2Y agonists. Cumulative concentration-response curves to INS45973 (▲), INS48823 (▼), 3-phenacyl UDP (●), UTP (△) and UDP (□) (1µM – 300µM for all), expressed as % of response to 40mM KCl, are shown. n=5 for INS45973, n=4 for INS48823 and 3-phenacyl UDP, n=12 for UTP and n=11 for UDP. Each point indicates mean ± S.E.M.

Table 7.1. The potency of P2Y agonists in evoking contractions of intact, endothelium-denuded rat SPA.

Agonist	EC _{40K}	EC _{80K}	N
INS45973	13 (9 – 18) ^{pp}	32 (18 – 46)*φ	5
INS48823	24 (15 – 37)	47 (32 – 62)*φ	4
3-phenacyl UDP	27 (7 – 48)	92 (41 – 144)	4
UTP	65 (34 – 97)	211 (124 – 299)	12
UDP	85 (59 – 112)	208 (154 – 263)	11

Values of EC_{40K} and EC_{80K} are expressed as mean (95% confidence limits) (µM) for contractions evoked by INS45973, INS48823, 3-phenacyl UDP, UTP and UDP in the rat SPA. n values for each agonist are shown in the individual n column. ^{pp}P<0.01 for EC_{40K} values of INS45973 versus UDP. *P<0.05 and φP<0.05 for EC_{80K} values of synthetic agonists versus UTP and UDP, respectively.

2.1.2. Effects of Y27632 and Suramin on Peak Contractions Evoked by INS45973, INS48823 and 3-Phenacyl UDP

The involvement of Rho kinase in, and the effect of suramin on the contractions evoked by INS45973, INS48823 and 3-phenacyl UDP were investigated using a single concentration of each agonist. 30 μ M INS45973, 50 μ M INS48823 and 50 μ M 3-phenacyl UDP evoked peak contractions of similar amplitudes (Figure 7.3), which were not different from the mean responses evoked by 300 μ M UTP and 300 μ M UDP. Preincubation of tissues with 10 μ M Y27632 for 15 min beforehand significantly reduced the peak amplitude of contractions evoked by INS45973, INS48823 and 3-phenacyl UDP by $64.9 \pm 4.0\%$ (n=4), $33.4 \pm 12.2\%$ (n=4) and $44.1 \pm 4.6\%$ (n=4) (P<0.05 for all), respectively (Figure 7.4a). Interestingly, the inhibitory effect of Y27632 was significantly larger against contractions evoked by INS45973 compared with INS48823 (P<0.05) (Figure 7.4b).

Application of 100 μ M suramin substantially inhibited the peak amplitude of contractions evoked by INS45973, INS48823 and 3-phenacyl UDP by $76.3 \pm 13.3\%$ (n=4, P<0.05), $82.9 \pm 4.0\%$ (n=4, P<0.01) and $80.5 \pm 9.4\%$ (n=4, P<0.05), respectively (Figure 7.5). There was no significant difference between these values.

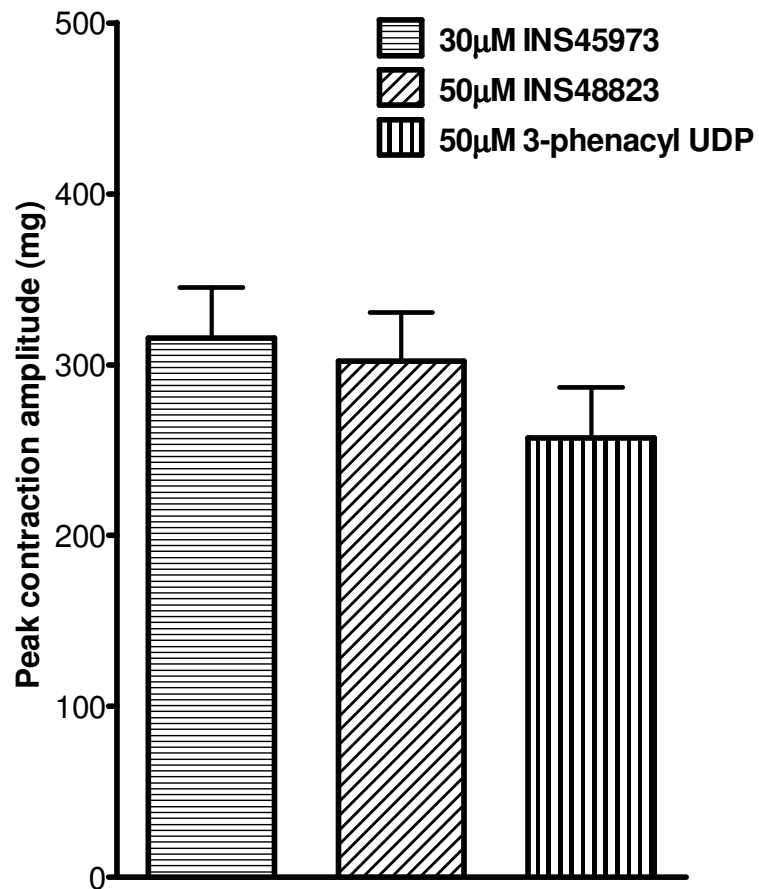


Figure 7.3. Vasoconstriction of intact, endothelium-denuded rat SPA evoked by INS45973, INS48823 and 3-phenacyl UDP. Mean peak contractile responses of rat SPA evoked by 30µM INS45973, 50µM INS48823 and 50µM 3-phenacyl UDP, are shown. n=20 and 21 for INS45973 and 3-phenacyl UDP, and INS48823, respectively. Data are expressed as mean \pm S.E.M.

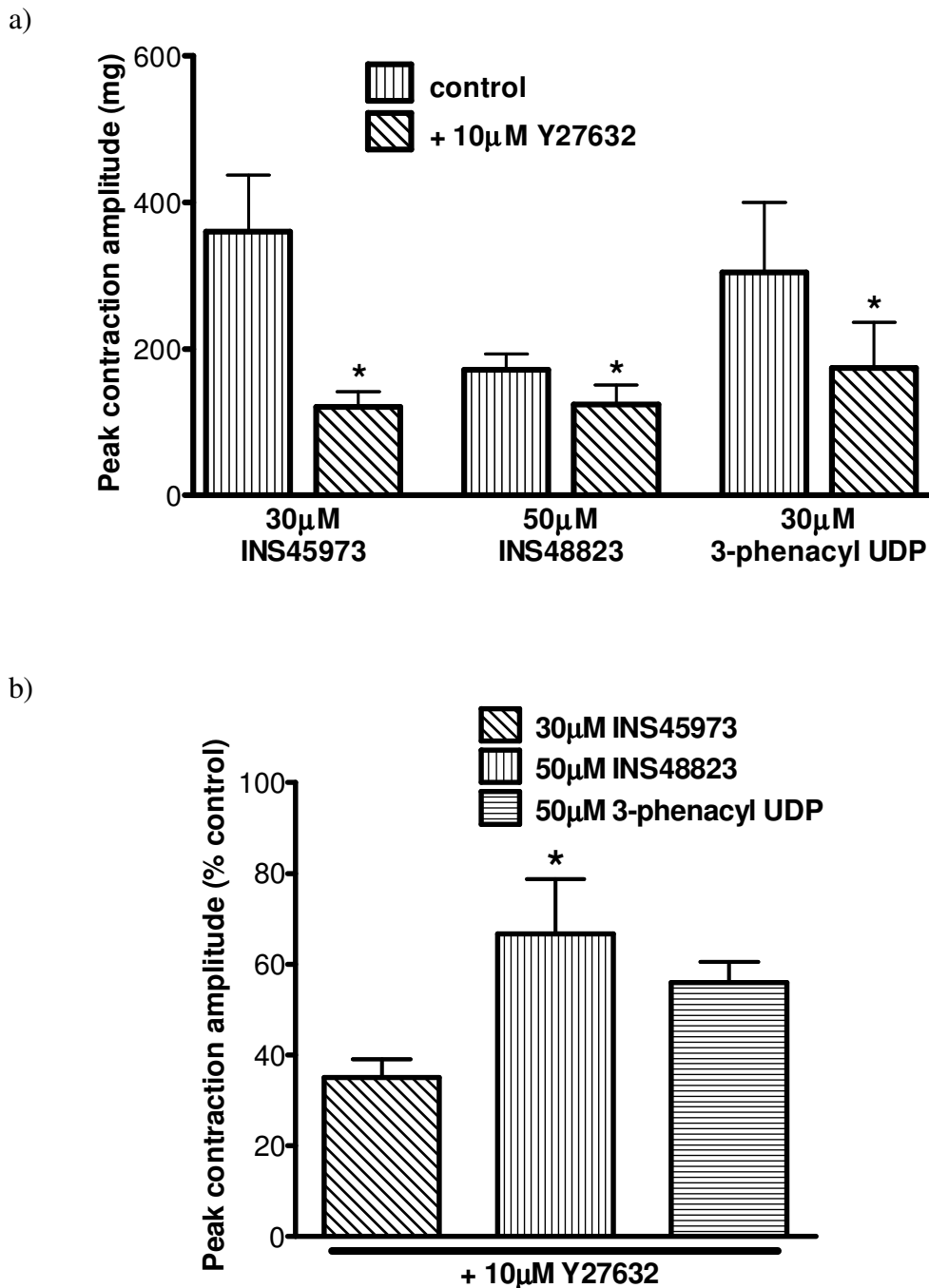


Figure 7.4. Effect of Y27632 on peak contractions evoked by INS45973, INS48823 and 3-phenacyl UDP in intact, endothelium-denuded rat SPA. a) The mean peak contraction amplitude of 30µM INS45973, 50µM INS48823 and 50µM 3-phenacyl UDP before and after 15 min preincubation with 10µM Y27632, are shown. b) shows the effect of Y27632, expressed as a % of the control contractions obtained before the inhibitor was added. n=4 for all. Contractions are shown as mean \pm S.E.M. *P<0.05 in (a) for the response in the presence of Y27632 compared with the control, and *P<0.05 in (b) for the effect of Y27632 against INS45973 versus against INS48823.

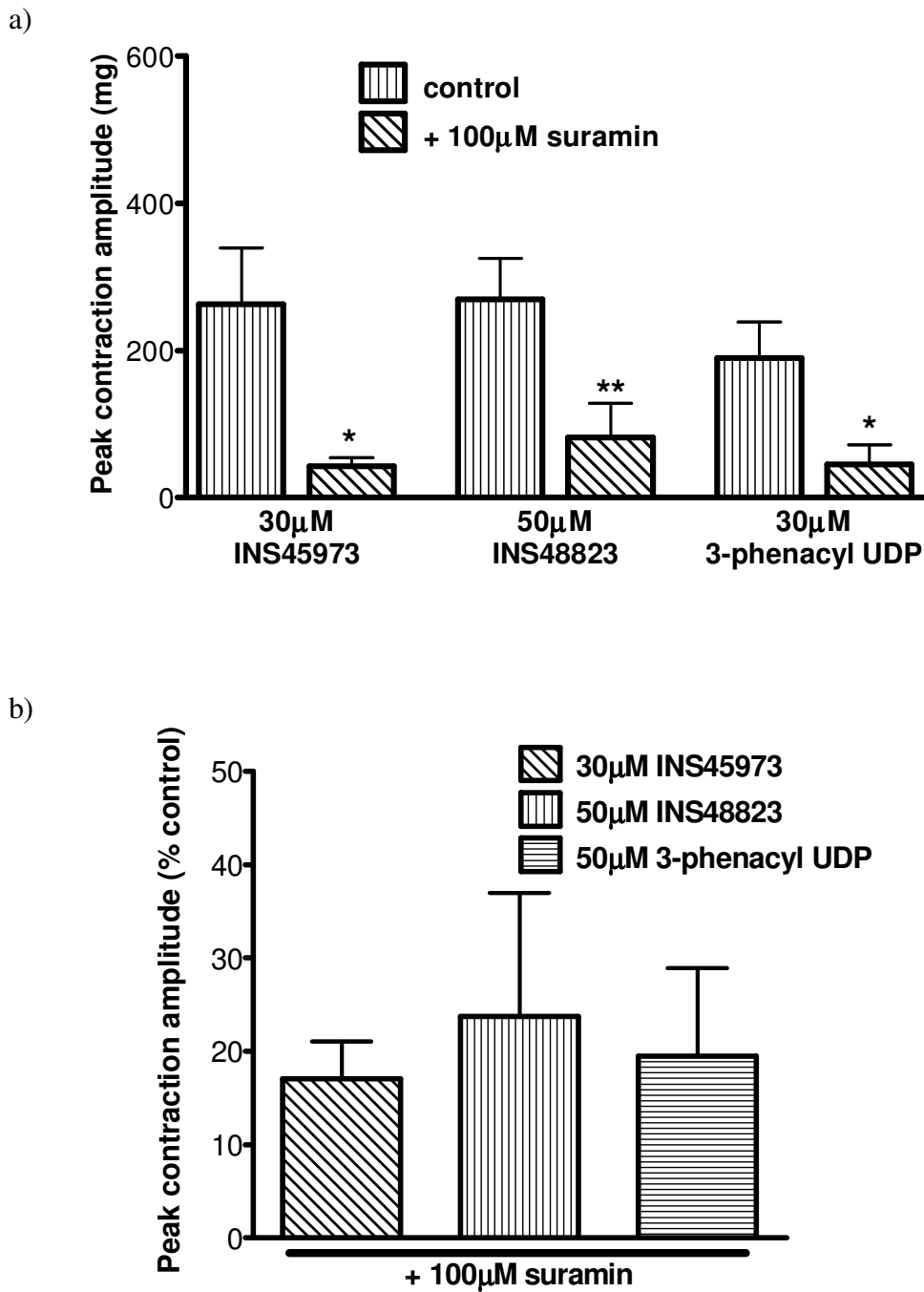


Figure 7.5. Effect of suramin on peak contractions evoked by INS45973, INS48823 and 3-phenacyl UDP in intact, endothelium-denuded rat SPA. a) The mean peak contraction amplitudes of 30µM INS45973, 50µM INS48823 and 50µM 3-phenacyl UDP before and after 15 min preincubation with 100µM suramin, are shown. b) shows the effect of suramin, expressed as a % of the control contractions obtained before the inhibitor was added. n=4 for INS45973 and 3-phenacyl UDP and n=5 for INS48823. Contractions are shown as mean \pm S.E.M. *P<0.05 and **P<0.01 for the response in the presence of suramin compared with the control.

2.2. Membrane-Permeabilised Rat SPA

2.2.1. Characterisation of Contractions Evoked by INS45973, INS48823 and 3-Phenacyl UDP

The same experimental protocol used in Chapter 6 was applied here to study the response to INS45973, INS48823 and 3-phenacyl UDP in permeabilised preparations and the effect of Y27632 and suramin on these responses. As shown in Figure 7.6 to 7.8, intact tissues were first challenged with 40mM KCl and then twice with one of the agonists, and in each case these additions evoked consistent responses. Following permeabilisation, 30 μ M INS45973 evoked a contraction, which reached a peak in about 10 min, with an amplitude of 44 ± 7 mg (n=12) and that was $15.4 \pm 2.7\%$ of the response before permeabilisation ($P < 0.001$) (Figure 7.6a, b). The time-course of contraction was studied further in four tissues (Figure 7.6c). The contraction was not maintained and the tone decayed steadily such that at 20 min it was similar to that immediately prior to addition of INS45973 ($-11.4 \pm 30.2\%$ of peak) and 40 min it was substantially below that level ($-221.1 \pm 90.9\%$ of peak).

Adding 50 μ M INS48823 evoked a peak contraction in about 20 min with an amplitude of 75 ± 10 mg (n=12), which was $21.1 \pm 2.6\%$ of the response before permeabilising the tissue ($P < 0.001$) (Figure 7.7a, b). In four tissues, the time-course of contraction was studied further (Figure 7.7c). The contraction showed some decay over 40 min, but was more maintained than the response to INS45973. It decreased to $78.0 \pm 10.1\%$ and $35.1 \pm 12.5\%$ after 20 and 40 min, respectively, of reaching its peak, though these reductions were not statistically significant.

A contraction was also produced in response to 50 μ M 3-phenacyl UDP that reached a peak in about 10 min with an amplitude of 94 ± 11 mg (n=12), which was equivalent to $42.1 \pm 6.7\%$ of the response before permeabilisation ($P < 0.001$) (Figure 7.8a, b). The time-course of contraction was also further studied in four of the tissues (Figure 7.8c). The contraction decayed slowly and at 20 min it was $56.6 \pm 9.1\%$ of the peak response ($P < 0.05$) and at 40 min the tone was similar to that immediately prior to addition of 3-phenacyl UDP ($-16.9 \pm 21.2\%$ of peak).

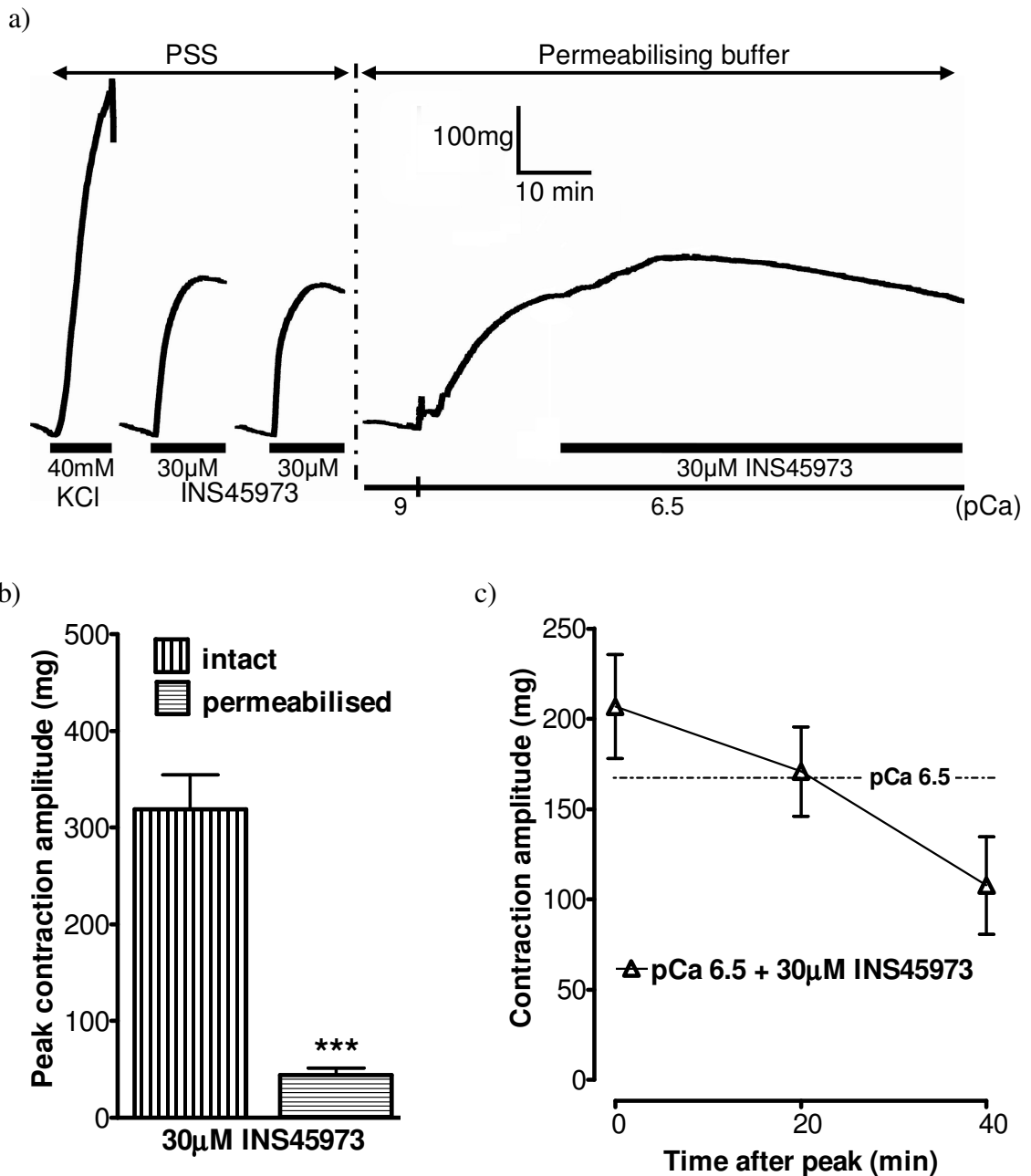


Figure 7.6. Vasoconstriction evoked by INS45973 in endothelium-denuded rat SPA treated with α -toxin. a) The traces show the typical contractions of rat SPA induced by 40mM KCl and 30μM INS45973 (twice) in the intact tissue, and subsequently by 30μM INS45973 at pCa 6.5 after permeabilising the tissue with 10μg/mL α -toxin. PSS was replaced by permeabilising buffer, as shown by the black arrows. Agonist additions and free [Ca²⁺] are indicated by the thick and thin black solid bars, respectively. b) shows the mean amplitude of the peak of contractions to INS45973 in intact and permeabilised rat SPA. The INS45973 response in the latter condition was measured by subtracting the contraction amplitude of pCa 6.5. c) The mean contractions to INS45973 at pCa 6.5 in the permeabilised vessels measured at peak and 20 and 40 min after that, are shown. n=12 and 4 for data in (b) and (c), respectively. Data are expressed as mean \pm S.E.M. ***P<0.001 for the peak responses in permeabilised versus intact tissues.

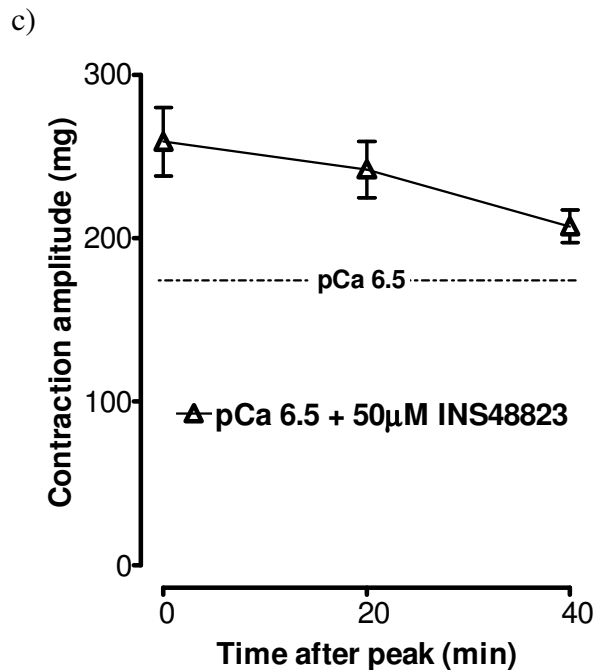
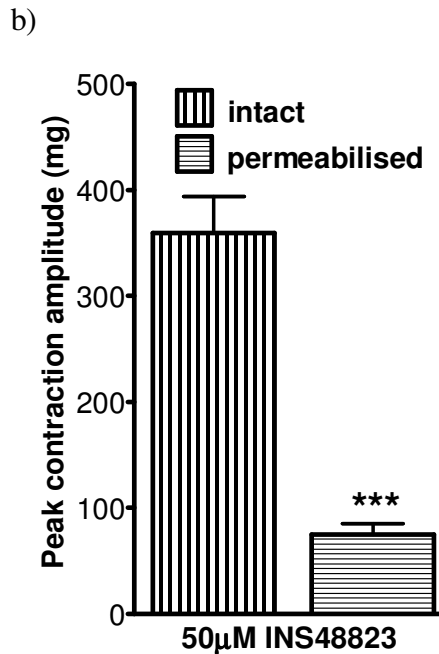
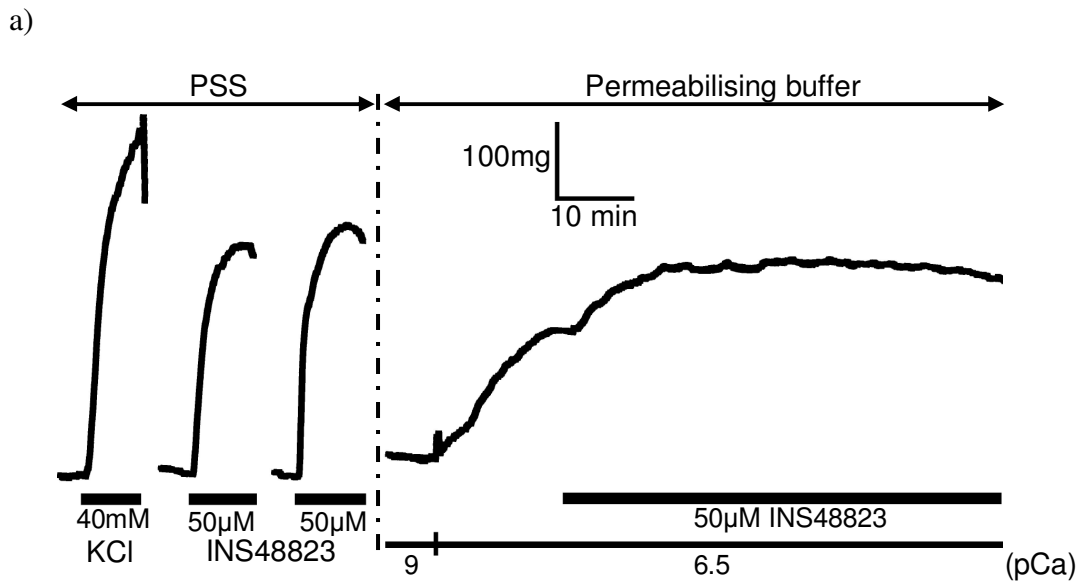


Figure 7.7. Contractile response of INS48823 in α -toxin-permeabilised endothelium-denuded rat SPA. a) The traces show the contractions of rat SPA evoked by 40mM KCl and 50 μ M INS48823 (twice), and 50 μ M INS48823 (at pCa 6.5), before and after permeabilisation with 10 μ g/mL α -toxin, respectively. PSS was replaced by permeabilising buffer, as shown by the black arrows. Agonist additions and free $[Ca^{2+}]$ are indicated by the thick and thin black solid bars, respectively. b) shows the mean amplitude of the peak of contractions to INS48823 in intact and permeabilised rat SPA. The INS48823 response in the latter condition was obtained by subtracting the response to pCa 6.5. c) The mean contractions of INS48823 at pCa 6.5 in the permeabilised vessels measured at peak and 20 and 40 min later, are shown. $n=12$ and 4 for data in (b) and (c), respectively. Data are expressed as mean \pm S.E.M. *** $P<0.001$ for the peak responses in permeabilised versus intact tissues.

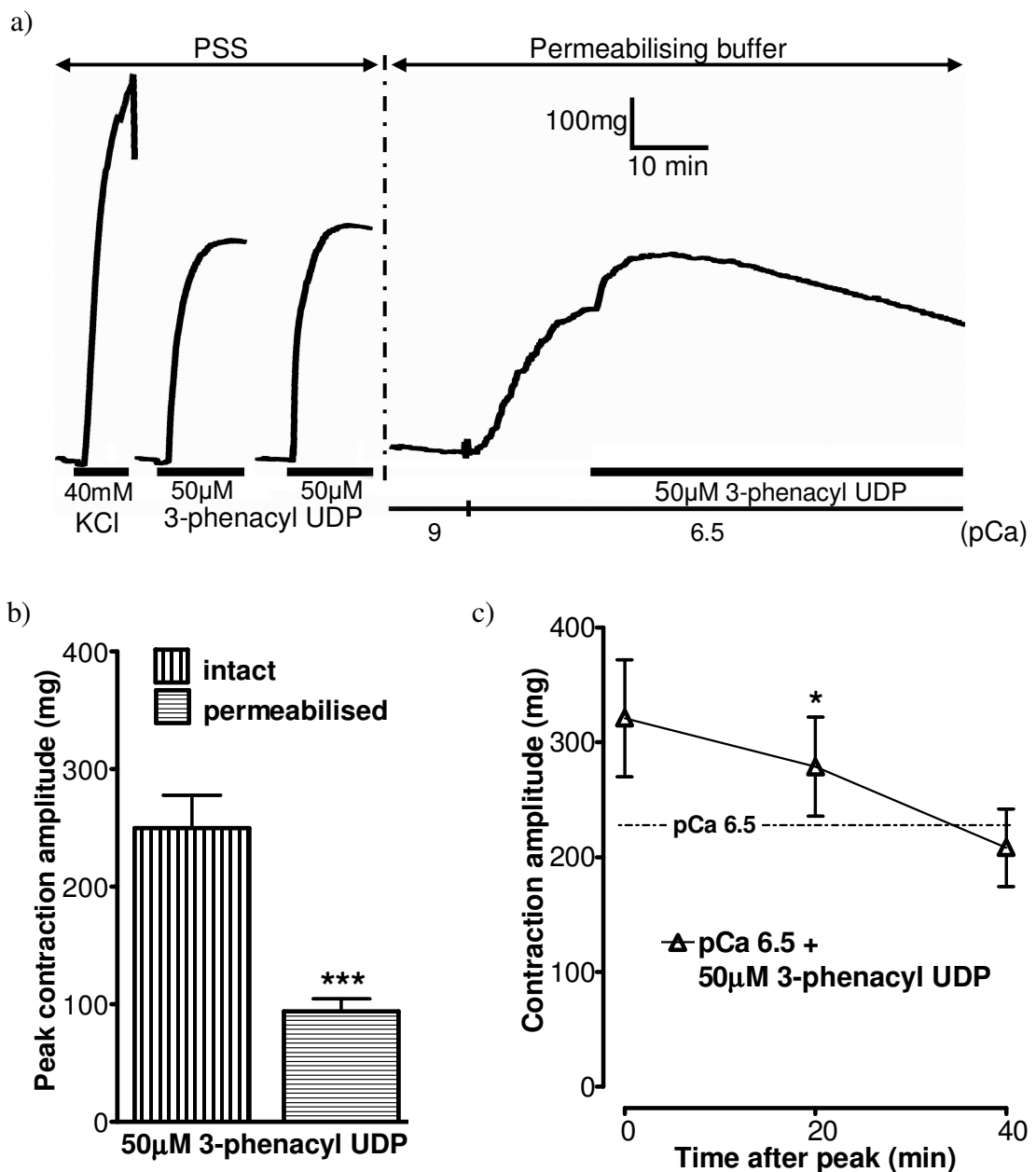


Figure 7.8. Contractions to 3-phenacyl UDP in α -toxin-permeabilised endothelium-denuded rat SPA. a) The traces show the contractions of rat SPA evoked by 40mM KCl and 50μM 3-phenacyl UDP (twice), and 50μM 3-phenacyl UDP (at pCa 6.5), before and after permeabilisation with 10μg/mL α -toxin, respectively. PSS was replaced by permeabilising buffer, as shown by the black arrow. Agonist additions and free [Ca²⁺] are indicated by the thick and thin black solid bars, respectively. b) shows the mean amplitude of the peak of contractions to 3-phenacyl UDP in both intact and permeabilised of rat SPA. The 3-phenacyl UDP response in the latter condition is obtained by subtracting the response to pCa 6.5. c) The mean contractions of 3-phenacyl UDP at pCa 6.5 in the permeabilised vessel measured at peak and 20 and 40 min later, are shown. n=12 and 4 for data in (a) and (b), respectively. Data are expressed as mean \pm S.E.M. ***P<0.001 in (a) for the peak responses in permeabilised versus intact tissues, and *P<0.05 in (b) for the responses at 20 min after peak versus at peak.

2.2.2. Effects of Y27632 and Suramin on Contractions Evoked by INS45973, INS48823 and 3-Phenacyl UDP

The data in the previous section show that the responses to INS45973, INS48823 and 3-phenacyl UDP undergo time-dependent decay. Therefore, similar measures as in Chapter 6 were applied when investigating the effect of an inhibitor on these responses. Y27632 and suramin were applied once the agonist-induced contractions reached a peak. The degree of inhibition induced by the inhibitors was then measured 20 min later, and compared with the control responses measured 20 min after the peak response.

Application of 10 μ M Y27632 for 20 min caused a clear rapid relaxation from the peak contractions evoked by 30 μ M INS45973, 50 μ M INS48823 and 50 μ M 3-phenacyl UDP (n=4 for all) (Figure 7.9) and in all cases vessel tone dropped significantly and substantially below the level established by pCa 6.5 (P<0.01 for all). Thus, it is apparent that Ca²⁺ sensitisation-mediated contractions of all three agonists were fully dependent on Rho kinase.

To determine if the contribution of Ca²⁺ sensitisation was the same in permeabilised and intact tissues the amplitude of the agonist-induced responses in permeabilised preparations, expressed as a percentage of the earlier response in same tissue before permeabilisation, was compared with the percentage inhibition of the control response of unpermeabilised tissues induced by Y27632, as shown in Figure 7.4b. The calculation of the percentage of Ca²⁺ sensitisation components in both intact and permeabilised preparations is demonstrated in Figure 7.10a. Figure 7.10b shows that for INS48823 and 3-phenacyl UDP there was no significant difference between these measurements and Ca²⁺ sensitisation contributed approximately 30% and 40% of their peak responses, respectively. However, the reduction of INS45973 by Y27632 in intact tissues was substantially and significantly greater (P<0.001) than the response seen in permeabilised tissues.

When the contraction amplitude 20 min after addition of 100 μ M suramin was compared with control responses at the same time-point, no significant difference was seen for the contractions evoked by 30 μ M INS45973, 50 μ M INS48823 and 50 μ M 3-phenacyl UDP 20 min after addition (Figure 7.11). Thus, suramin appeared to be ineffective against the responses to these agonists.

Because control responses to INS45973 almost fully decayed by 20 min after peak the effects of suramin were also measured 10 min after peak and compared with the control responses at the same time point. Under control conditions the contraction to 30 μ M INS45973 decayed by $31.3 \pm 7.6\%$ (n=4) and this was not significantly affected by 100 μ M suramin, where the corresponding value was $30.5 \pm 7.7\%$ (n=4).

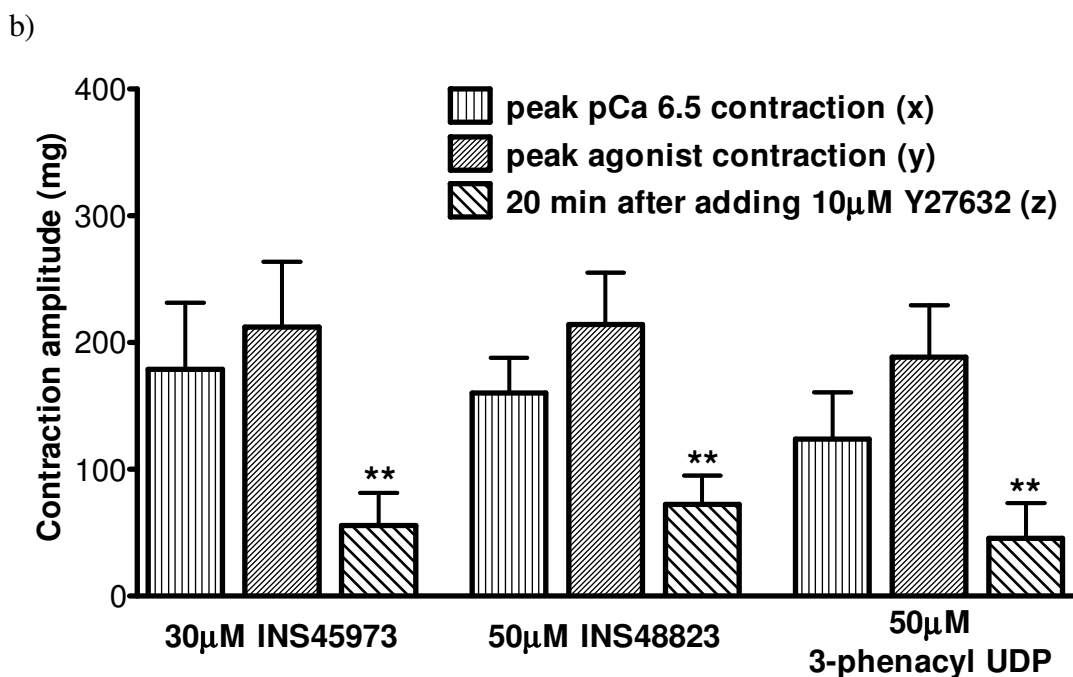
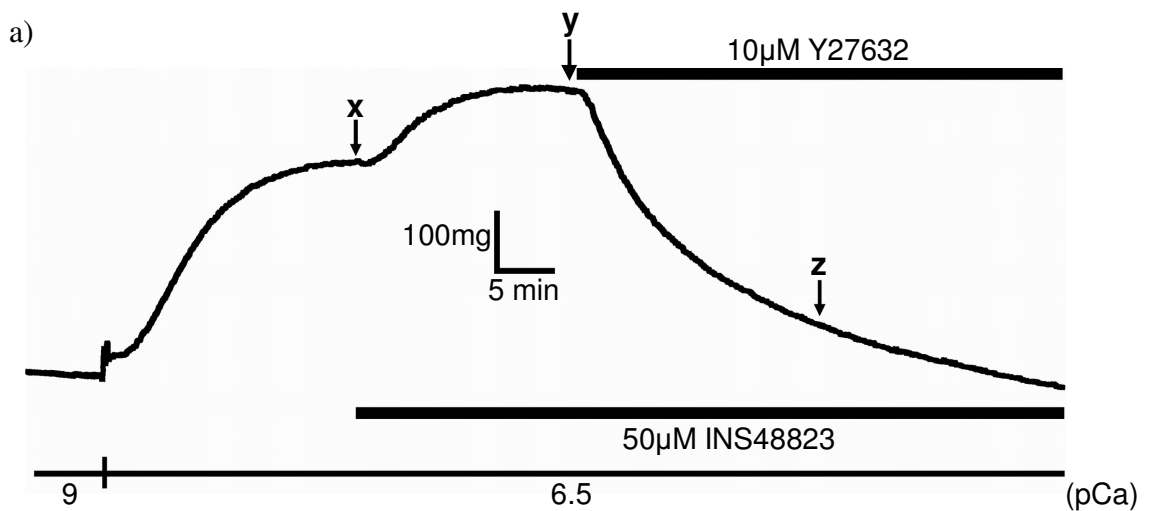


Figure 7.9. Effect of Y27632 on contractions evoked by INS45973, INS48823 and 3-phenacyl UDP in α -toxin-permeabilised endothelium-denuded rat SPA. a) Typical trace of vasoconstriction to 50µM INS48823 in α -toxin-permeabilised rat SPA after treatment with 10µM Y27632, applied once the response reached a peak, is shown. Points x, y and z indicate the peak contraction to pCa 6.5, INS48823 and 20 min after adding Y27632, respectively. Additions of agonists and Y27632, and free $[Ca^{2+}]$ are shown by the thick and thin black solid bars, respectively. b) shows the mean amplitude of; contractions to pCa 6.5 (x), the total peak response after subsequent addition of 30µM INS45973, 50µM INS48823 and 50µM 3-phenacyl UDP (y), and the contractions remaining following treatment with Y27632 (z). n=4 for all. Data are shown as mean \pm S.E.M. **P<0.01 for the difference between the peak response to pCa 6.5 plus agonist (y) and the remaining contractions after 20 min application of Y27632 (z).

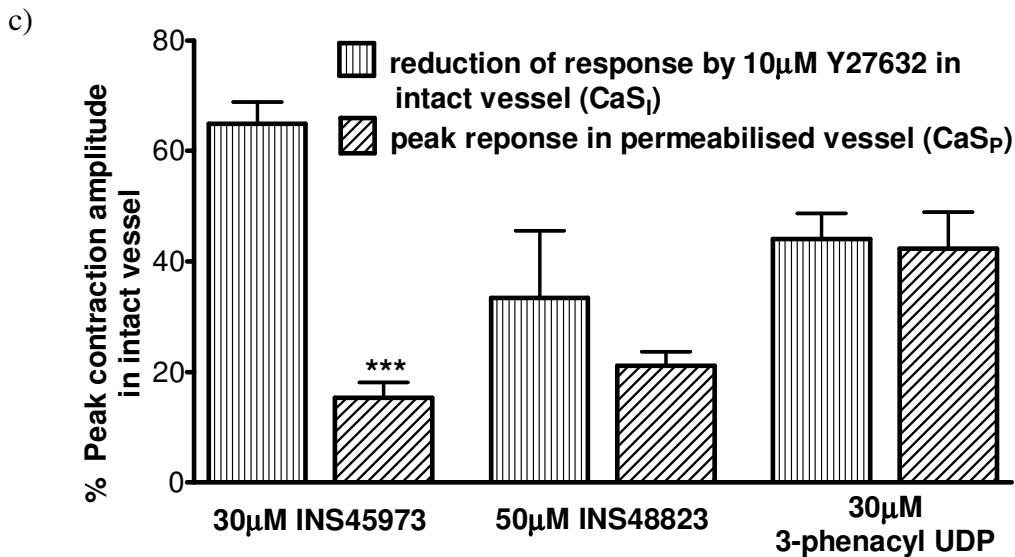
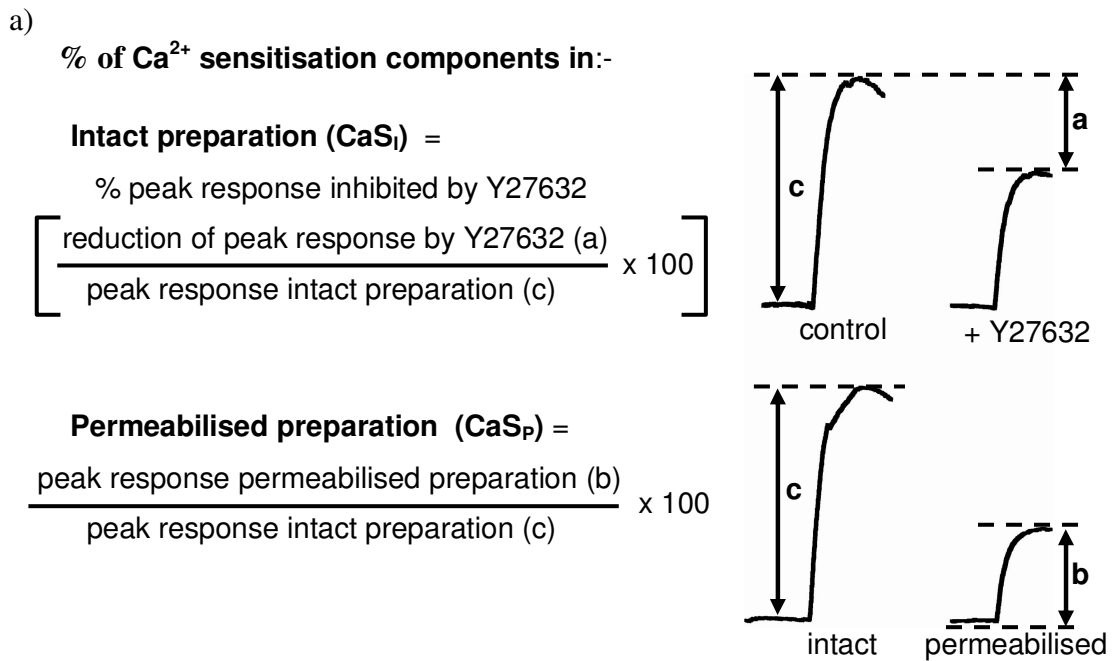


Figure 7.10. Comparison of the amplitude of the Ca²⁺ sensitisation components of contractions evoked by INS45973, INS48823 and 3-phenacyl UDP in intact and permeabilised endothelium-denuded rat SPA. a) shows the calculation for the % of Ca²⁺ sensitisation components of an agonist in intact (CaS_I) and permeabilised (CaS_P) rat SPA. b) The mean reduction of peak contraction amplitude of 30µM INS45973, 50µM INS48823 and 50µM 3-phenacyl UDP in intact rat SPA after 15 min preincubation with 10µM Y27632, and the mean amplitude of peak response of the agonists at the same concentrations obtained in vessel permeabilised with 10µg/mL α -toxin. Both data sets are normalised as % of control peak contraction to agonist in intact preparation, as indicated in (a). n=4 and 12 for intact and permeabilised vessels, respectively. Data are shown as mean \pm S.E.M. *** P<0.001 for the effect of Y27632 against INS45973 in intact tissues versus peak response to INS45973 in permeabilised vessel.

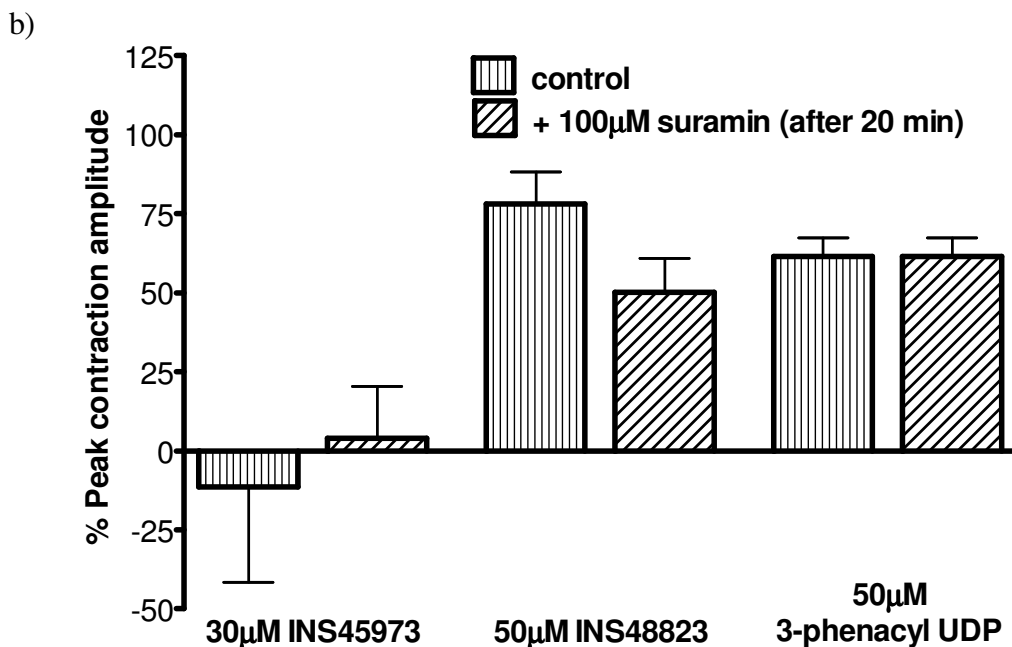
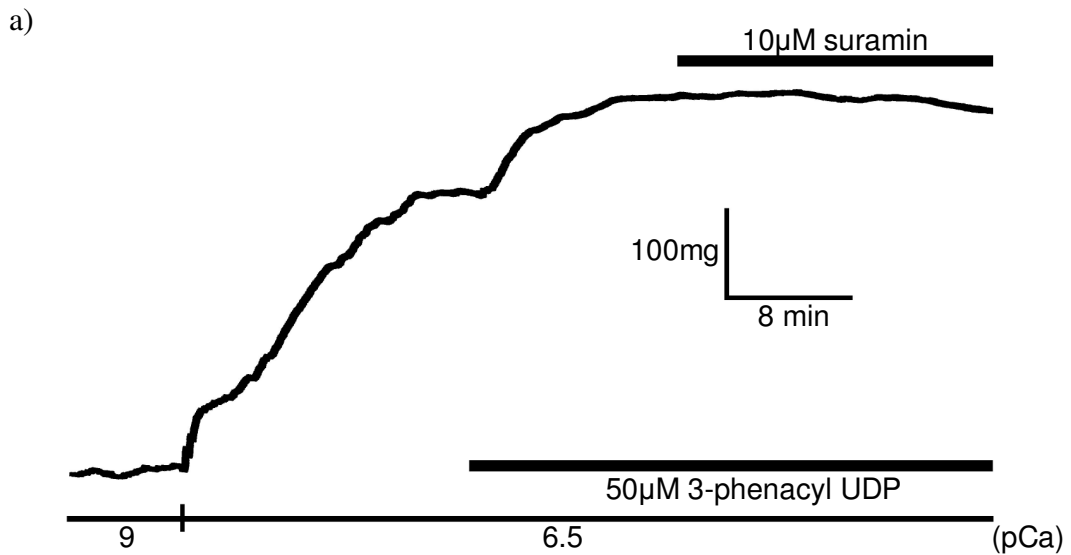


Figure 7.11. Effect of suramin on contractions evoked by INS45973, INS48823 and 3-phenacyl UDP in α -toxin-permeabilised endothelium-denuded rat SPA. a) The trace shows a contraction to 50µM 3-phenacyl UDP in α -toxin-permeabilised rat SPA, and the effect of 100µM suramin, added once the response reached a peak. Addition of agonists and suramin, and the level of free $[Ca^{2+}]$ are shown by the thick and thin black solid bars, respectively. b) shows the mean peak amplitude of contractions to 30µM INS45973, 50µM INS48823 and 50µM 3-phenacyl UDP in the absence and presence of 100µM suramin, 20 min after peak response, obtained from different preparations. $n=4$ for all. The data represent the actual contraction amplitudes of agonists, i.e. without the initial response to pCa 6.5, and are expressed as a % of the peak response. Data are shown as mean \pm S.E.M.

3. DISCUSSION

INS45973, INS48823 and 3-phenacyl UDP evoked vasoconstriction of the intact rat SPA, but only the first two compounds had greater potencies than the endogenous P2Y agonists UTP and UDP. Preincubation with Y27632 and suramin reduced the contractions evoked by all three agonists. In the α -toxin-permeabilised vessels, INS45973, INS48823 and 3-phenacyl UDP evoked peak contractions that decayed steadily over 40 min and the extent of decay was greater for INS45973. The responses to all three agonists were abolished by Y27632, but unaffected by suramin.

3.1. Potency of INS45973, INS48823 and 3-Phenacyl UDP in Evoking Contractions of Intact Rat SPA and Characterisation of the Responses in α -Toxin-Permeabilised Rat SPA

The cumulative concentration-response curves for INS45973, INS48823 and 3-phenacyl UDP showed that their potencies were comparable as the EC_{40K} and EC_{80K} values of both INS45973 and INS48823 were not significantly different from 3-phenacyl UDP. In contrast, INS45973 was significantly more potent than UTP at the level of EC_{80K} and UDP at the level of EC_{40K} and EC_{80K} values. In addition, INS48823 was also significantly more potent than both UTP and UDP at the level of EC_{80K} value. However, the potency of 3-phenacyl UDP was not significantly different from that of UTP and UDP. The potencies of these three agonists and/or their closely related analogues had been mostly studied in the cell lines expressing recombinant P2Y receptors, and the results showed that INS45973 was selective for the P2Y₂ and P2Y₄ receptors over the P2Y₁ and P2Y₆ receptors, whereas INS48823 and 3-phenacyl UDP were selective for P2Y₆ receptor over the P2Y₂ and P2Y₄ receptors (Pendergast *et al.*, 2001; Yerxa *et al.*, 2002; El-Tayeb *et al.*, 2006; Ko *et al.*, 2008). Additionally, in these studies the potencies of the compounds were generally equivalent, if not lower than UTP and UDP. Furthermore, INS48823 and UDP induced a comparable level of NF- κ B translocation and survival in oestoclasts (Korcok *et al.*, 2006). Thus, conflicting with the previous findings, the current study is the first to find that these synthetic P2Y agonists are more potent than their endogenous counterparts, at least in evoking vasoconstriction of rat SPA.

Consistent with the procedure followed in Chapter 6, the contractions to INS45973, INS48823 and 3-phenacyl UDP were first characterised before investigating the effect of an inhibitor against the responses to these agonists, in the membrane-permeabilised rat SPA. Addition of INS45973, INS48823 and 3-phenacyl UDP at pCa 6.5 evoked peak contractions, which were equivalent to about 15%, 25% and 40% of the responses produced before permeabilising the tissue, respectively. The contractions decayed steadily after reaching peak and 40 min after peak the responses to INS45973 and 3-phenacyl UDP, except INS48823 were abolished. Overall, it is clear that none of these responses was maintained even for a 20 min period. Therefore, to take into account the tendency of the responses to decay, the effect of an inhibitor was measured 20 min after its addition, and compared statistically with the control contractions of the corresponding agonists at the same time-point.

3.2. Involvement of Rho Kinase and Effect of Suramin in Contractions Evoked by INS45973, INS48823 and 3-Phenacyl UDP in the Intact and α -Toxin-Permeabilised Rat SPA

The results showed that the peak contractions to INS45973, INS48823 and 3-phenacyl UDP in the intact rat SPA were reduced by Y27632 by about 65%, 35% and 45%, respectively. Additionally, in the α -toxin-permeabilised preparation the contractions were abolished. Thus, these findings further reaffirm the exclusive role of Rho kinase in the Ca^{2+} sensitisation-dependent contractions of rat SPA mediated via at least two P2Y receptors, i.e. the P2Y₂ and/or P2Y₄, and P2Y₆ receptors. The inhibitory effect of Y27632 against the responses to INS48823 and 3-phenacyl UDP in the intact vessel was comparable with the peak response to these agonists in the permeabilised preparation, i.e. their Ca^{2+} sensitisation components were very similar. Indeed, this pattern of results was similarly observed for the UDP-evoked response in Chapter 6. However, the inhibitory effect of Y27632 against the response to INS45973 in the intact vessel was found to be larger than the peak response to INS45973 in the permeabilised preparation. This was unexpected since these values should, in theory, be the same. Furthermore, the data for UTP reported in Chapter 4 and Chapter 6 showed good agreement between the extent of inhibition by Y27632

of the contraction to UTP in the intact preparation and the peak amplitude of contraction to UTP in permeabilised tissues. The reason for the difference in the apparent contribution of Rho kinase to the INS45973-evoked contractions in intact and permeabilised tissues is unclear. The smaller than expected INS45973-evoked peak response in the permeabilised tissue could possibly be due to faster and greater desensitisation of P2Y receptors upon their activation by this agonist, though why this should be the case is unclear. Consistent with this possibility is the rapid and substantial rundown of the response to INS45973 seen in the permeabilised preparation. In this respect, Hoffmann *et al.*, (2008) found that six recombinant P2Y receptors, including the P2Y₂ and P2Y₄ receptors, expressed in human embryonic kidney-293 cells underwent internalisation upon stimulation. Interestingly, ATP and UTP induced different degrees of translocation of β -arrestin-1 and -2, the proteins that play an important role in the internalisation process, in cells expressing the recombinant P2Y₂ receptor. They suggested that each of the full agonists at a particular receptor can induce a unique 'active' conformation of the receptor, which activates different signalling pathways or similar signalling pathways but to a different extent, and these consequently mediate rather distinct cellular effects. The reason for this inconsistency is, at present, unclear.

The current study also showed that suramin induced a substantial inhibition of more than 75% of the contractions evoked by INS45973, INS48823 and 3-phenacyl UDP in the intact rat SPA. However, it was ineffective in the α -toxin-permeabilised vessels. Thus, this suggests that in the intact rat SPA the agonists evoked vasoconstriction via both suramin-sensitive and suramin-resistant P2Y receptors, but only the latter were stimulated in the permeabilised tissue. This in turn implies that each agonist acted at more than one P2Y subtype to evoke vasoconstriction, which is inconsistent with the data obtained using recombinant receptors.

In the present studies the concentrations at which INS45973, INS48823 and 3-phenacyl UDP were effective (3 - 300 μ M) were higher than those needed to activate recombinant receptors expressed in a cell line; INS45973 has EC₅₀ values of 0.52, 0.28 and >10 μ M at recombinant P2Y₂, P2Y₄ and P2Y₆ receptors, respectively (Shaver *et al.*, 2005); INS48823 has an EC₅₀ of 0.125 μ M at recombinant P2Y₆ receptors and no appreciable activity at P2Y₂ and P2Y₄ receptors (Karcok *et al.*,

2005); 3-phenacyl UDP has EC₅₀ values of 40, >100 and 0.07μM at recombinant P2Y₂, P2Y₄ and P2Y₆ receptors, respectively (El-Tayeb *et al.*, 2005). The most likely explanation for these differences is that native receptors tend to be expressed at much lower levels than recombinant receptors and because of the amplification inherent in GPCR systems, i.e. increased GPCR expression leads to increased downstream signalling, agonists are more potent in recombinant GPCR expression systems. However, the possibility must be considered that the low potency of the agonists was due to them acting at the P2Y receptors subtypes at which they have lower potency, i.e. INS45973, the selective P2Y_{2/4} agonist, evoked contraction via P2Y₆ receptors, whilst 3-phenacyl UDP, the selective P2Y₆ agonist, acted via P2Y_{2/4} receptors. It is difficult to envisage how both of these statements could be true. The simplest way to confirm the site of action of each agonist would be to determine the effects of the selective P2Y₆ antagonist, MRS2578 (Mamedova *et al.*, 2004), against each, but there was insufficient time to carry out these experiments. MRS2578 has previously been shown to inhibit contractions of rat SPA by 300μM UTP and UDP by about 40% (Mitchell, 2008), confirming the existence of contractile P2Y₆ receptors in this tissue.

In summary, INS45973, INS48823 and 3-phenacyl UDP evoked vasoconstriction of rat SPA, and the former two compounds were more potent than UTP and UDP. All of these synthetic agonists mediated the contractile responses predominantly via suramin-sensitive P2Y receptors, however, suramin-resistant P2Y receptors were involved in mediating the Rho kinase-dependent Ca²⁺ sensitisation-mediated component of contractions to these compounds.

Chapter 8:

General Discussion

The results of this project have enhanced our knowledge of which P2Y subtypes are expressed in the rat pulmonary artery smooth muscle and the mechanisms through which they induce contractile response. The presence of P2Y receptors in rat SPA was initially demonstrated by contractions in response to the endogenous P2Y agonists UTP and UDP. Further use of selective P2Y agonists clearly indicated that at least two P2Y receptor subtypes are expressed in rat SPA. The initial investigation of the signalling mechanisms in the intact preparation revealed significant contributions of PI-PLC, PKC and Rho kinase to P2Y receptor-induced vasoconstriction. Subsequent experiments in membrane-permeabilised vessels showed that Rho kinase appears to exclusively mediate the Ca^{2+} sensitisation-dependent components of P2Y receptor-induced contractions. In contrast, PKC is not involved in Ca^{2+} sensitisation and how it contributes to UTP- and UDP-induced contractions remains to be determined.

1. CHARACTERISATION OF P2Y RECEPTOR-INDUCED CONTRACTIONS IN RAT SPA AND P2Y SUBTYPES

Both P2Y agonists UTP and UDP evoked a typical pattern of slowly developing contractions in rat SPA that was largely comparable to previous studies in this vessel (Hartley *et al.*, 1998; Chootip *et al.*, 2002). On prolonged exposure to these agonists the contractions decayed slightly after their peak until a maintained plateau phase was reached. Disruption of the endothelium led to an augmentation of the peak contractions evoked by both UTP and UDP, a clear indication of the presence of an opposing, endothelium-dependent vasodilator action generated by activation of endothelial P2Y receptors. Gui *et al.*, (2008) showed that UTP and UDP both induced a vasodilator response of precontracted endothelium-intact left and right rat pulmonary arteries, whilst the vasodilator response induced by UTP in the precontracted endothelium-intact rabbit pulmonary artery was subsequently abolished by denudation of the endothelium (Konduri *et al.*, 2004).

The present study also showed that the cumulative concentration-response curves to both UTP and UDP did not reach a maximum. This result was comparable with previous studies using similar tissue preparations (Rubino & Burnstock, 1996; Chootip *et al.*, 2002). However, the nucleotides are subject to rapid

degradation/conversion of the nucleotides into mono-, di- and triphosphate equivalents by extracellular enzymes. For example, UDP can be converted to UTP by ectonucleoside diphosphokinase and UTP broken down to UDP by ectonucleotidases. As a result, full concentration-response curves for the nucleotides could not be constructed and this effectively underestimates the potency of the nucleotides. The above effect has been highlighted recently by Kauffenstein *et al.*, (2010) using aorta and mesenteric artery from wild-type and transgenic mice lacking NTPDase1 and found that the concentration-response curves to UTP and UDP did reach a maximum response in the knockout, but not the wild-type animals. Moreover, the curves obtained in knockout preparations were shifted substantially to the left compared with the wild-type animals. This clearly indicates that NTPDase1 greatly modulates the contractions to UTP and UDP by actively hydrolysing these nucleotides and consequently depressing their apparent potency.

Identification of the P2Y receptor subtypes through which nucleotides mediate their effects has proven to be a very challenging task, primarily due to the current lack of commercially-available stable, potent subtype-selective P2Y agonists and antagonists. The need of such compounds is even more obvious considering UTP and UDP are readily susceptible to the enzyme degradation and this can cause confusion as to which receptors UTP and UDP actually act at in tissues, as has been highlighted previously (Chootip *et al.*, 2002). However, this study has utilised several novel compounds that have been developed recently. INS45973, an agonist that is selective for P2Y₂ and P2Y₄ receptors over other P2Y subtypes, evoked vasoconstriction of rat SPA with a higher potency than both UTP and UDP. Likewise, INS48823, which has high selectivity at the P2Y₆ receptor, also induced contractile response and was more potent than both nucleotides. In contrast, another P2Y₆ selective agonist 3-phenacyl UDP only displayed similar potency to UTP and UDP. This study is the first to characterise the actions of these newly developed compounds in the vascular smooth muscle. The findings are vital in evaluating the selectivity of these compounds at the designated P2Y subtypes and their actions, which are valuable for their development as a potential therapeutic drug.

Overall, this pharmacological data implicates that at least two P2Y receptors, i.e. P2Y₂ and/or P2Y₄, and P2Y₆ receptors, were involved in mediating vasoconstriction

in rat SPA. Additionally, several studies also suggested P2Y₂ and P2Y₆ are the predominant P2Y receptors to mediate contractile responses in rat intrapulmonary artery (Hartley *et al.*, 1998; Chootip *et al.*, 2002).

The use of the newly developed compounds to identify P2Y receptor subtypes nevertheless, has been hindered by several factors. Both INS45973 and INS48823 were supplied to Dr. Charles Kennedy personally by Inspire Pharmaceuticals (Durham, USA) and in small amounts, so there was a considerable restriction on the number of experiments that could be carried out. Equally, 3-phenacyl UDP has only recently become commercially available and there is very little published literature on its action. Furthermore, it is also very expensive.

Pharmacological characterisation of the P2Y subtypes using the above selective agonists may have a limitation in the lack of contractile response of the SPA at the concentrations of their EC₅₀ values obtained from the cell lines preparation. Thus, it is not absolutely certain that the response to these agonists is entirely due to the activation of the designated P2Y receptors and a contribution from other P2Y receptor subtypes could in theory, be possible. However, as discussed in section 3.2 (Chapter 7) the reference EC₅₀ values for these agonists were obtained using recombinant human P2Y receptors expressed in cell lines, which are likely to be overexpressed relative to native P2Y receptors. Therefore, it may not necessarily reflect similar results when studying the P2Y receptors from a different species (rat) in the isolated tissue preparations. Supporting this view, Marcet *et al.*, (2007) reported that the EC₅₀ value of INS48823 for inducing the release of CCL20 from human dendritic cells was about 10-fold higher compared to the reference EC₅₀ value for the recombinant P2Y₆ receptor. In order to clarify this issue, the pharmacological characterisation of P2Y subtypes can be continued with the use of potent, subtype selective P2Y antagonists, e.g. MRS2578 at P2Y₆ receptor (Mamedova *et al.*, 2004), which became available during the course of these studies. These compounds can provide the definitive answer as to which P2Y subtypes are expressed in rat SPA.

In the absence of antagonists, P2Y₂, P2Y₄ and P2Y₆ knock-out mice (Bar *et al.*, 2008; Kauffenstein *et al.*, 2010) could be used to further characterise the P2Y receptor-mediated contractions of pulmonary artery and provide a better understanding of which of P2Y subtypes are actually expressed and mediate the

response. The expression and distribution of the P2Y receptors present in the pulmonary artery could also be identified by using immunohistochemical and Western blotting techniques, and these would complement the pharmacological data. However, a lack of specificity of the current commercial antibodies to P2Y receptor proteins may limit the application of these techniques.

2. SIGNALLING MECHANISMS UNDERLYING P2Y RECEPTOR-INDUCED CONTRACTILE RESPONSES

The signalling mechanisms mediating P2Y receptor-induced contractions in pulmonary artery smooth muscle remain largely unclear. Three main signalling pathways involving PI-PLC, PKC and Rho kinase were investigated in this project. It has been shown that stimulation of P2Y receptors by both UTP and UDP led to the activation of PI-PLC, which is consistent with the current understanding that the UTP- and UDP-sensitive P2Y₂, P2Y₄ and P2Y₆ receptors couple to G_{q/11} (Abbracchio *et al.*, 2006; see also Table 1.3 in Chapter 1). Moreover, the contribution of PI-PLC in the development of P2Y receptor-mediated peak contractions in rat SPA is substantial, as reflected by more than 50% inhibition of these responses by U73122. The involvement of PI-PLC in P2Y receptor-mediated effects has previously been reported in various tissues and cell types, including human coronary artery smooth muscle (Strøbaek *et al.*, 1996), mouse ventricular myocytes (Yamamoto *et al.*, 2007) and astrocytes (Weng *et al.*, 2008).

This study also showed that PKC plays a role in mediating the peak and plateau phase of contractions to UTP and UDP. PKC contributes about 25% and 50%, respectively of the development of peak contraction evoked by UTP and UDP, and about 30% of the plateau phase. This finding is not unexpected considering that PKC is one of the downstream effectors of PI-PLC, which plays a substantial role in the P2Y receptor-mediated responses. Interestingly, PKC appeared to play a greater role in the response to UDP (>70%) than UTP (~45%).

Several possible mechanisms could underlie the contribution of PKC to the vasoconstriction of SPA. For example, PKC has been shown to regulate directly the activity of the voltage-dependent Ca_v1.2 channels that mediate Ca²⁺ influx in vascular smooth muscle (Savineau *et al.*, 1991; Navedo *et al.*, 2005; Cobine *et al.*,

2007). Interestingly, PKC may also affect this ion channel indirectly by depolarising the membrane via inhibition of voltage-gated K^+ channels (Cogolludo *et al.*, 2003). Ca^{2+} imaging, using Ca^{2+} -sensitive dyes such as fura 2, could be employed in order to determine if the rise in $[Ca^{2+}]_i$ induced by UTP and UDP is inhibited by GF109203X. Moreover, since one of the possible mechanisms for the contribution of PKC to the vasoconstriction of SPA is associated with the regulation of ion channels, the patch clamp technique could be used to address this issue. Ca^{2+} and K^+ currents in dissociated rat SPA smooth muscle cells would be recorded and it then determined if these currents are modified by GF109203X, UTP and UDP.

PKC could act independently of changes in $[Ca^{2+}]_i$ by inducing CPI-17-associated Ca^{2+} sensitisation (Li *et al.*, 1998; Kitazawa *et al.*, 2000; Ward *et al.*, 2004). This might be possible at least in the case of the sustained phase of UDP-evoked contraction whereby adding Y27632 and GF109203X together did not produce an additive inhibitory effect, indicating that part of the PKC-mediated mechanisms might perhaps converge with the downstream mechanism of Rho kinase-mediated Ca^{2+} sensitisation, as discussed below. However, the results in the subsequent permeabilised experiment do not support such possibility as PKC is not involved in either UTP- or UDP-evoked vasoconstriction in the α -toxin-permeabilised rat SPA. The absence of a contribution by PKC to Ca^{2+} sensitisation of P2Y receptor-mediated contractions is consistent with the observations of Jernigan *et al.*, (2004), who failed to establish any PKC influence in UTP-evoked vasoconstriction of membrane-permeabilised rat pulmonary artery, although they did see a contractile response to PMA. Alternatively, it cannot be rule out that GF109203X may have nonspecific activity at the concentration used in the current study (Davis *et al.*, 2000) and could inhibit other kinases which are responsible for the generation of contractions. To investigate this possibility, a biochemical study, such as Western blotting technique could be used to monitor the PKC activity and phosphorylation of MYPT-1 and MLCK following treatment of GF109203X at various concentrations against the nucleotide-evoked contractions.

Interestingly, the present study in the α -toxin-permeabilised rat SPA demonstrated a modest role of PI-PLC in Ca^{2+} sensitisation-dependent, UDP-evoked contractions. This finding was rather unexpected considering that Ca^{2+} sensitisation

induced by P2Y receptors is not mediated by PKC (a downstream effector of PI-PLC), but was exclusively mediated by Rho kinase (discussed below). Moreover, activation of Rho kinase usually involves receptor coupling to $G\alpha_{12/13}$ (Buhl *et al.*, 1995; Somlyo & Somlyo, 2000; Suzuki *et al.*, 2003, 2009), rather than $G\alpha_{q/11}$, which stimulates PI-PLC. Vogt *et al.*, (2003) did find a role for $G\alpha_{q/11}$ in the activation of RhoA, but it was unaffected by U73122. Rather, it was associated with a family of RhoGEF protein leukemia-associated Rho guanine nucleotide exchange factors.

This study also demonstrates a role for Rho kinase in both the peak and plateau phase of P2Y receptor-mediated vasoconstriction of rat SPA. In intact arteries, Rho kinase contributes about; 20-40% of the peak contraction evoked by UTP, UDP, INS48823 and 3-phenacyl UDP, 65% of the peak contraction to INS45973, and 30% of the plateau phase contractions to both UTP and UDP. Moreover, in the membrane-permeabilised vessel, UTP, UDP, INS48823 and 3-phenacyl UDP evoked around 20-40%, while INS4973 only evoked about 15% of the peak contraction before permeabilising the tissue. These responses were abolished by Y27632, confirming an exclusive role of Rho kinase in the Ca^{2+} sensitisation component of P2Y receptor-mediated vasoconstriction of rat SPA. This observation is consistent with a previous report (Jernigan *et al.*, 2004) in membrane-permeabilised preparations of rat pulmonary artery, showing virtual abolition of UTP-evoked vasoconstriction by Y27632.

Stimulation of receptor coupling to $G\alpha_{12/13}$ induces the formation of RhoA/GTP complex (Buhl *et al.*, 1995; Somlyo & Somlyo, 2000; Suzuki *et al.*, 2003, 2009), which then translocates to the plasma membrane before activating Rho kinase (Somlyo & Somylo, 2000, 2003). Rho kinase subsequently phosphorylates MYPT1, the regulatory subunit of MLCP, and prevents this phosphatase dephosphorylating MLC, leading to increased contraction without a rise in $[Ca^{2+}]_i$ (Somlyo & Somlyo, 2000). P2Y receptors are generally known to couple to $G\alpha_{q/11}$ (Filtz *et al.*, 1994; Abbracchio *et al.*, 2006), but coupling to other G protein subtypes, particularly $G\alpha_{12/13}$, has also been shown (Abbracchio *et al.*, 2006; Nishida *et al.*, 2008). Moreover, although RhoA activation following stimulation of a GPCR is mediated mainly by $G\alpha_{12/13}$, an involvement of $G\alpha_{q/11}$ in this process has also been demonstrated (Booden *et al.*, 2002; Vogt *et al.*, 2003). In rat aortic smooth muscle,

stimulation of P2Y receptors activated RhoA and Rho kinase (Sauzeau *et al.*, 2000). Rho kinase also appears to be involved in vasoconstriction of rat SPA induced by other agonists, including phenylephrine (Damron *et al.*, 2002), SPC (Thomas *et al.*, 2005) and ET-1 (Jernigan *et al.*, 2008). Additionally, Rho kinase is also involved in the contractions of rat tail artery to phenylephrine and U46619 (Tsai & Jiang, 2006).

This study also examined the correlation of the Ca²⁺ sensitisation component of P2Y receptor-mediated contractions in intact and membrane-permeabilised tissues. The inhibitory effect of Y27632 against UTP, UDP, INS48823 and 3-phenacyl UDP contractions in the intact vessel was comparable with the peak response to these agonists in membrane-permeabilised vessels. However, the inhibitory effect of Y27632 against the response to INS45973 in the intact vessel was found to be larger than the peak response to INS45973 in the permeabilised preparation. This was unexpected since the remaining P2Y agonists used here showed a good agreement between these two mechanisms. This smaller than expected INS45973-evoked peak response in the permeabilised tissue could perhaps be due to the desensitisation of P2Y receptors by this agonist. Consistent with this possibility, the response to INS45973 showed substantial rundown in the permeabilised preparation. In this respect, Hoffmann *et al.*, (2008) found that six recombinant P2Y receptors, including P2Y₂ and P2Y₄ receptors, expressed in human embryonic kidney-293 cell lines underwent internalisation upon stimulation. Interestingly, they also noted that ATP and UTP induced different degree of translocation of β -arrestin-1 and -2, the proteins that play an important role in the internalisation process, in the cells expressing the recombinant P2Y₂ receptor. They suggested that each of the full agonists at a particular receptor can induce a unique 'active' conformation of the receptor, which activates different signalling pathways or similar signalling pathways, but to a different extent, and these consequently mediate rather distinct cellular effects.

The pharmacological approach used in the present study to investigate the role of Rho kinase in P2Y receptor-mediated contractions is limited by its inability to monitor intracellular Ca²⁺ levels and to correlate Rho kinase activity and phosphorylation of MYPT-1. However, both of these limitations could be overcome by employing Ca²⁺ imaging and Western blotting techniques, respectively.

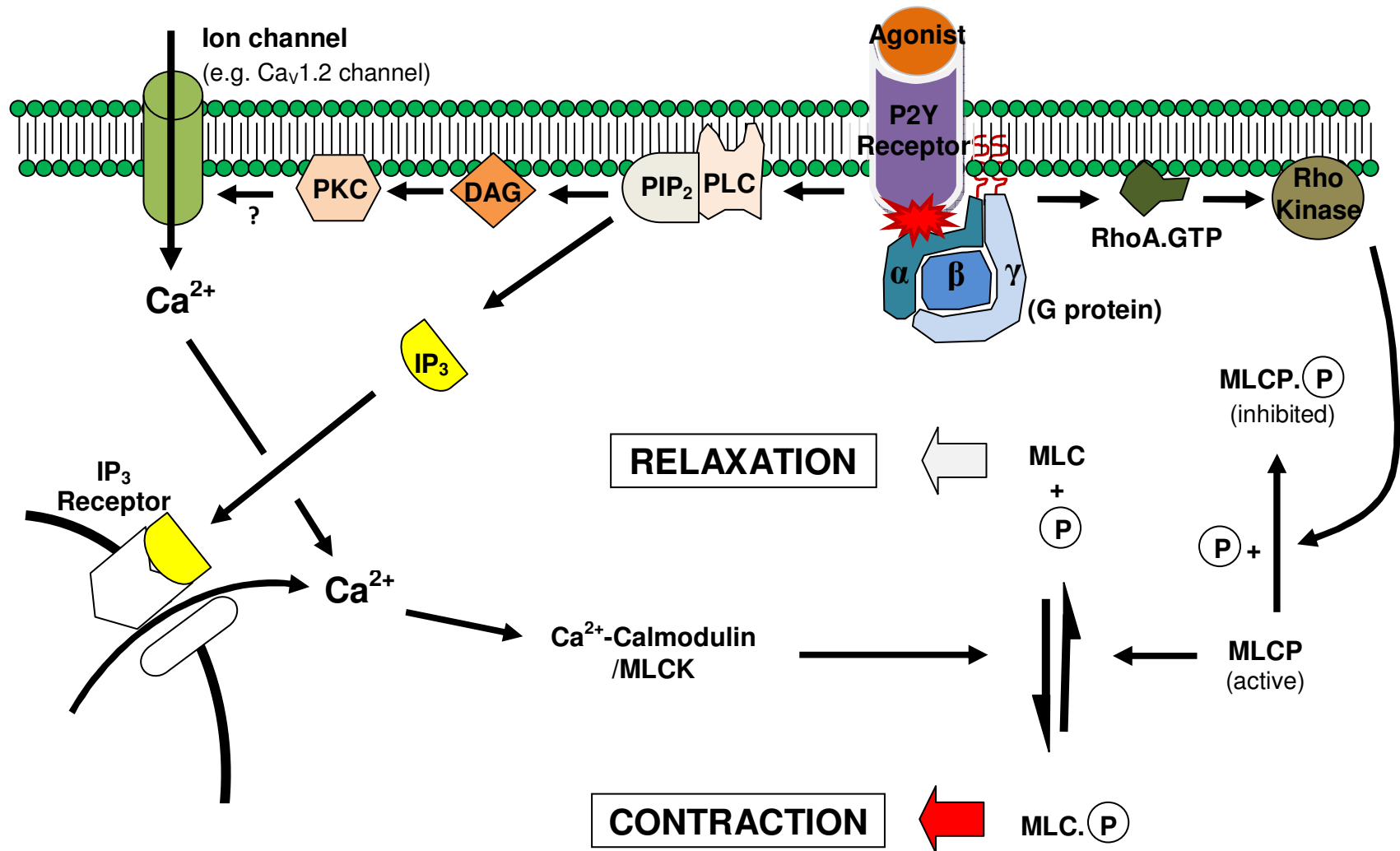
Taken together, the results in this study suggest that stimulation of P2Y receptors by nucleotides evoked vasoconstriction of pulmonary artery via PLC, PKC and Rho kinase-associated Ca^{2+} sensitisation. The use of newly developed compounds INS45973 and INS48823 has revealed that at least two P2Y receptors mediate this contractile effect. Nucleotides are relevant chemical mediators in the cardiovascular system both in physiological and pathological conditions, so characterising their underlying signalling mechanisms is of importance. Additionally, nucleotides, such as ATP can be released by red blood cells in response to mechanical deformation during passage through the lungs (Sprague *et al.*, 1996, 2003). Of some interest is the novel finding in this study that stimulation of P2Y receptors, particularly the P2Y₆ subtype, induced a Rho kinase-associated Ca^{2+} sensitisation component of vasoconstriction in pulmonary artery. This signalling pathway is implicated in the physiological response of pulmonary arteries to hypoxia as hypoxia-induced vasoconstriction is associated with the activation of Rho kinase (Robertson *et al.*, 2000). A role for nucleotides in this response is also indicated by Baek *et al.*, (2008) who showed that the apparent role of the smooth muscle P2Y receptors in hypoxic pulmonary vasoconstriction observed in perfused rabbit lungs.

The Rho kinase-associated Ca^{2+} sensitisation induced by P2Y receptors activation is likely to be augmented in the pathological conditions, especially when endothelial-relaxant function is compromised, such as in hypoxia- or monocrotaline-induced pulmonary hypertension (Adnot *et al.*, 1991; Mam *et al.*, 2010) and chronic obstructive pulmonary disease (Dinh-Xuan *et al.*, 1991). Indeed, extracellular ATP is elevated in the latter disease, which would increase the contribution of P2Y receptors to artery regulation. Furthermore, the contribution of Rho kinase in mediating vasoconstriction of pulmonary artery is enhanced in chronic hypoxia (Adnot *et al.*, 1991; Nagaoka *et al.*, 2004; Broughton *et al.*, 2008). Therefore, a complete understanding of the signalling mechanisms of pulmonary artery smooth muscle contractions is certainly essential, as this could provide a basis for the effective development of novel therapeutic strategies. In conclusion, the data presented in this study should provide to a comprehensive model of P2Y receptor-mediated pulmonary vasoconstriction being outline in the near future. Stimulation of P2Y

receptors by nucleotides substantially contributes in the regulation of pulmonary vasculature both in physiological and pathological conditions.

2.1. A Model for P2Y Receptor-induced Vasoconstriction of Rat SPA

The data in this project provide valuable information on how P2Y receptors induce vasoconstriction of rat SPA. Figure 8.1 represents a model of signalling mechanisms of this response. Stimulation of P2Y receptors, such as P2Y₂ and/or P2Y₄, and P2Y₆ receptors, activates PI-PLC via G $\alpha_{q/11}$ to hydrolyse PIP₂ to IP₃ and DAG. IP₃ triggers Ca²⁺ release from IP₃-sensitive intracellular Ca²⁺ stores, while DAG activates PKC. The former causes an increase in [Ca²⁺]_i, which commonly activates the Ca²⁺-calmodulin/MLCK pathway, which subsequently phosphorylates MLC to generate the contraction of smooth muscle. Activated PKC mediates the contractile response, not through Ca²⁺ sensitisation mechanism, but more likely via increasing the [Ca²⁺]_i, presumably by influencing ion channels. On the other hand, Rho kinase is also activated upon stimulation of P2Y receptors via G $\alpha_{12/13}$ (or possibly G $\alpha_{q/11}$) and RhoA. Activated Rho kinase then phosphorylates MYPT-1, which inactivates MLCP from dephosphorylating MLC, and effectively potentiates the contractions independent of [Ca²⁺]_i rise, i.e. Ca²⁺ sensitisation.



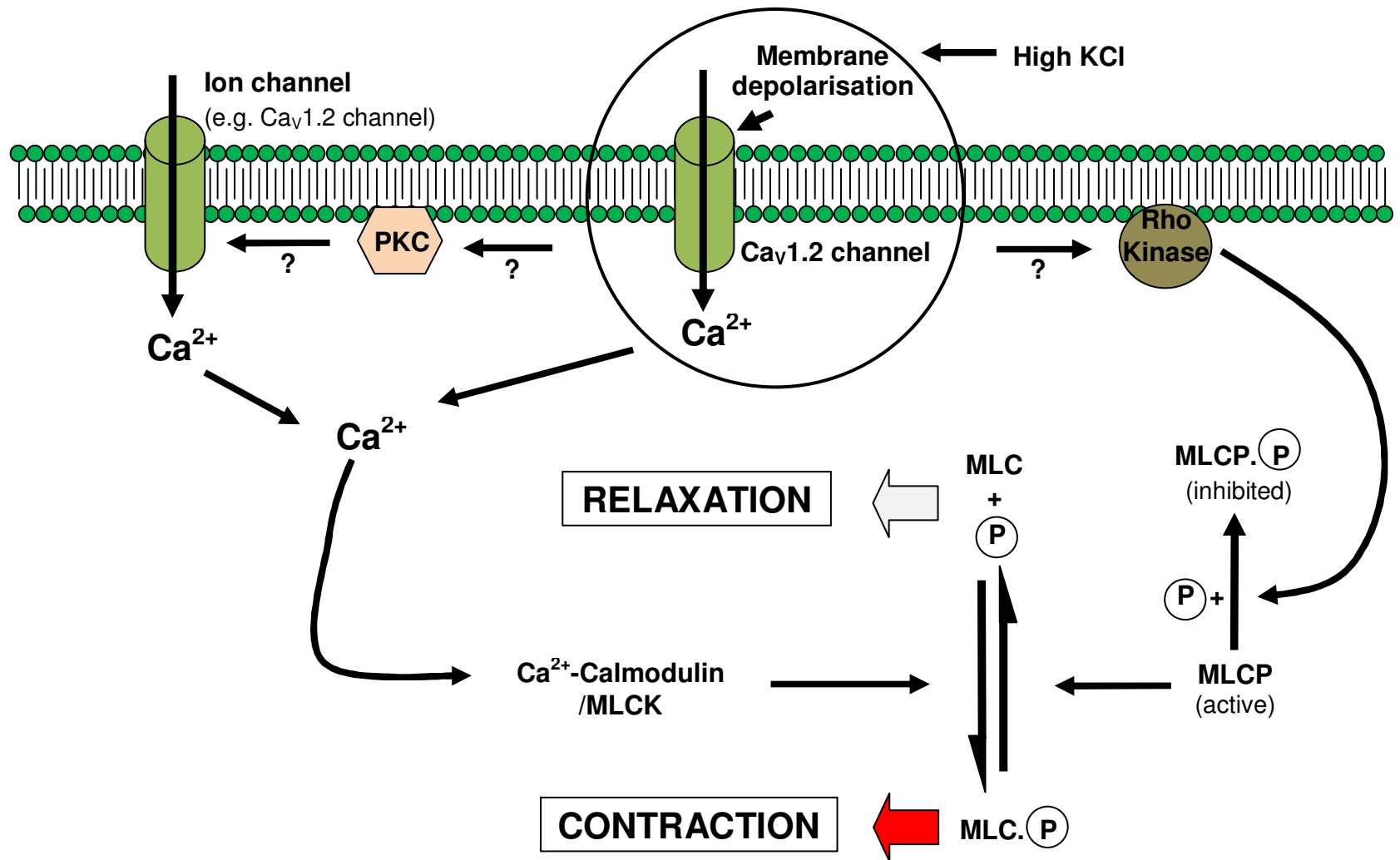
8.1. A model of signalling mechanisms underlying activation of P2Y receptor.

3. SIGNALLING MECHANISMS INVOLVED IN KCl-INDUCED CONTRACTILE RESPONSES

In this study, both Rho kinase and PKC were shown to play an important role in the contractions induced by KCl. Although KCl-induced contractions are widely regarded as merely being due to membrane depolarisation and Ca^{2+} influx, a recent review (Ratz *et al.*, 2005) has highlighted the association of KCl-induced contractions and Ca^{2+} sensitisation. An involvement of Rho kinase in the contractile response induced by KCl has been demonstrated in several tissues, for example rat caudal artery (Mita *et al.*, 2002), mouse anococcygeus smooth muscle (Ayman *et al.*, 2003), rabbit renal and femoral arteries (Urban *et al.*, 2003; Ratz *et al.*, 2009), rabbit thoracic aorta (Sakurada *et al.*, 2003) and bovine trachea (Liu *et al.*, 2005). In contrast, Ratz *et al.*, (2005) reported that the involvement of PKC is minimal, if not absent, in the responses induced by KCl. However, their more recent papers did show a role for an atypical PKC isoform, PKC ζ , in the KCl-induced vasoconstriction of rabbit femoral and renal arteries (Ratz & Miner, 2009; Ratz *et al.*, 2009). Additionally, PKC has also been implicated in the contractions induced by KCl in aorta and mesenteric arteries (Budzyn *et al.*, 2006). Thus, it is clear that besides the key membrane depolarisation/ Ca^{2+} influx pathway, other mechanisms, such as PKC and Ca^{2+} sensitisation via Rho kinase, also contribute to KCl-induced vasoconstriction in rat SPA.

3.1. A Model for KCl-Induced Vasoconstriction of Rat SPA

The present study also improves our knowledge on how KCl induces vasoconstriction in rat SPA (Figure 8.2). According to the Nerst equation, application of 40mM KCl depolarises the smooth muscle cell membrane, and this activates and opens voltage-dependent $\text{Ca}_V1.2$ channels to allow influx of Ca^{2+} . A rise of $[\text{Ca}^{2+}]_i$ follows, which then activates the Ca^{2+} -calmodulin/MLCK pathway to generate contractions of smooth muscle. Additionally, KCl-induced membrane depolarisation and $[\text{Ca}^{2+}]_i$ rise, via as yet unknown mechanisms, also activates Rho kinase-dependent Ca^{2+} sensitisation and PKC pathways, and collectively these mediate the contractile response.



8.2. Overview of possible signalling mechanisms involved in KCl-induced contractions in rat SPA.

References

Abbracchio, M.P., Boeynaems, J.M., Barnard, E.A., Boyer, J.L., Kennedy, C., Miras-Portugal, M.T., King, B.F., Gachet, C., Jacobson, K.A., Weisman, G.A. & Burnstock, G. (2003). Characterization of the UDP-glucose receptor (re-named here the P2Y₁₄ receptor) adds diversity to the P2Y receptor family. *Trends Pharmacol. Sci.*, **24**: 52-55.

Abbracchio, M.P. & Burnstock, G. (1994). Purinoceptors: are there families of P2X and P2Y purinoceptors? *Pharmacol. Ther.*, **64**: 445-475.

Abbracchio, M.P., Burnstock, G., Boeynaems, J.M., Barnard, E.A., Boyer, J.L., Kennedy, C., Knight, G.E., Fumagalli, M., Gachet, C., Jacobson, K.A. & Weisman, G.A. (2006). International Union of Pharmacology LVIII: update on the P2Y G protein-coupled nucleotide receptors: from molecular mechanisms and pathophysiology to therapy. *Pharmacol. Rev.*, **58**: 281-341.

Abramovitz, M., Boie, Y., Nguyen, T., Rushmore, T.H., Bayne, M.A., Metters, K.M., Slipetz, D.M. & Grygorczyk, R. (1994). Cloning and expression of a cDNA for the human prostanoid FP receptor. *J. Biol. Chem.*, **269**: 2632-2636.

Adnot, S., Raffestin, B., Eddahibi, S., Braquet, P. & Chabrier, P.E. (1991). Loss of endothelium-dependent relaxant activity in the pulmonary circulation of rats exposed to chronic hypoxia. *J. Clin. Invest.*, **87**: 155-162.

Altieri, R.J., Travis, D.C., Roberts, J. & Thompson, D.C. (1994). Pharmacological characterization of muscarinic receptors mediating acetylcholine-induced contraction and relaxation in rabbit intrapulmonary arteries. *J. Pharmacol. Exp. Ther.*, **270**: 269-276.

Alvarenga, É.C., Rodrigues, R., Caricati-Neto, A., Silva-Filho, F.C., Paredes-Gamero, E.J. & Ferreira, A.T. (2010). Low-intensity pulsed ultrasound-dependent osteoblast proliferation occurs by via activation of the P2Y receptor: role of the P2Y₁ receptor. *Bone*, **46**: 355-362.

Amadio, S., Montilli, C., Magliozzi, R., Bernardi, G., Reynolds, R. & Volonte, C. (2009). P2Y₁₂ Receptor Protein in Cortical Gray Matter Lesions in Multiple Sclerosis. *Cereb Cortex*, doi 10.1093/cercor/bhp193 (Epub ahead of print).

Andrassy, M., Belov, D., Harja, E., Zou, Y.S., Leitges, M., Katus, H.A., Nawroth, P.P., Yan, S.D., Schmidt, A.M. & Yan, S.F. (2005). Central role of PKC β in neointimal expansion triggered by acute arterial injury. *Circ. Res.*, **96**: 476-483.

Ayman, S., Wallace, P., Wayman, C.P., Gibson, A. & McFadzean, I. (2003). Receptor-independent activation of Rho-kinase-mediated calcium sensitisation in smooth muscle. *Br. J. Pharmacol.*, **139**: 1532-1538.

Baek, E.B., Yoo, H.Y., Park, S.J., Kim, H.S., Kim, S.D., Earm, Y.E. & Kim, S.J. (2008). Luminal ATP-induced contraction of rabbit pulmonary arteries and role of purinoceptors in the regulation of pulmonary arterial pressure. *Pflugers Arch.*, **457**: 281-291.

Bailey, M.A., Turner, C.M., Hus-Citharel, A., Marchetti, J., Imbert-Teboul, M., Milner, P., Burnstock, G. & Unwin, R.J. (2004). P2Y receptors present in the native and isolated rat glomerulus. *Nephron Physiol.*, **96**: p79-90.

Balasubramanian, R., de Azua, I.R., Wess, J. & Jacobson, K.A. (2010). Activation of distinct P2Y receptor subtypes stimulates insulin secretion in MIN6 mouse pancreatic β cells. *Biochem. Pharmacol.*, **79**: 1317-1326.

Bar, I., Guns, P.J., Metallo, J., Cammarata, D., Wilkin, F., Boeynants, J.M., Bult, H. & Robaye, B. (2008). Knockout mice reveal a role for P2Y₆ receptor in macrophages, endothelial cells, and vascular smooth muscle cells. *Mol. Pharmacol.*, **74**: 777-784.

Barnes, P.J., Baraniuk, J.N. & Belvisi, M.G. (1991). Neuropeptides in the respiratory tract. Part I. *Am. Rev. Respir. Dis.*, **144**: 1187-1198.

Barnes, P.J. & Liu, S.F. (1995). Regulation of pulmonary vascular tone. *Pharmacol. Rev.*, **47**: 87-131.

Bassil, A.K., Bourdu, S., Townson, K.A., Wheeldon, A., Jarvie, E.M., Zebda, N., Abuin, A., Grau, E., Livi, G.P., Punter, L., Latcham, J., Grimes, A.M., Hurp, D.P., Downham, K.M., Sanger, G.J., Winchester, W.J., Morrison, A.D. & Moore, G.B. (2009). UDP-glucose modulates gastric function through P2Y₁₄ receptor-dependent and -independent mechanisms. *Am. J. Physiol. Gastrointest. Liver Physiol.*, **296**: G923-930.

Berchtold, S., Ogilvie, A.L., Bogdan, C., Mühl-Zürbes, P., Ogilvie, A., Schuler, G. & Steinkasserer, A. (1999). Human monocyte derived dendritic cells express functional P2X and P2Y receptors as well as ecto-nucleotidases. *FEBS Lett.*, **458**: 424-428.

Berman, D.M., Sugiyama, T. & Goldman, W.F. (1994). Ca²⁺ stores in smooth muscle cells: Ca²⁺ buffering and coupling to AVP-evoked inositol phosphate synthesis. *Am. J. Physiol.*, **266**: C276-283.

Berridge, M.J. (2008). Smooth muscle cell calcium activation mechanisms. *J. Physiol.*, **586**: 5047-5061.

Bleasdale, J.E., Thakur, N.R., Gremban, R.S., Bundy, G.L., Fitzpatrick, F.A., Smith, R.J. & Bunting, S. (1990). Selective inhibition of receptor-coupled phospholipase C-dependent processes in human platelets and polymorphonuclear neutrophils. *J. Pharmacol. Exp. Ther.*, **255**: 756-768.

Bogdanov, Y.D., Dale, L., King, B.F., Whittock, N. & Burnstock, G. (1997). Early expression of a novel nucleotide receptor in the neural plate of *xenopus* embryos. *J. Biol. Chem.*, **272**: 12583-12590.

Bogdanov, Y.D., Wildman, S.S., Clements, M.P., King, B.F. & Burnstock, G. (1998). Molecular cloning and characterization of rat P2Y₄ nucleotide receptor. *Br. J. Pharmacol.*, **124**: 428-430.

Bonnevier, J. & Arner, A. (2004). Actions downstream of cyclic GMP/protein kinase G can reverse protein kinase C-mediated phosphorylation of CPI-17 and Ca²⁺ sensitization in smooth muscle. *J. Biol. Chem.*, **279**: 28998-29003.

Booden, M.A., Siderovski, D.P. & Der, C.J. (2002). Leukemia-associated Rho guanine nucleotide exchange factor promotes Gαq-coupled activation of RhoA. *Mol. Cell. Biol.*, **22**: 4053-4061.

Boyer, J.L., Adams, M., Ravi, R.G., Jacobson, K.A. & Harden, T.K. (2002). 2-Chloro N⁶-methyl-(N)-methanocarpa-2'-deoxyadenosine-3',5'-bisphosphate is a selective high affinity P2Y₁ receptor antagonist. *Br. J. Pharmacol.*, **135**: 2004-2010.

Boyer, J.L., Delaney, S.M., Villanueva, D. & Harden, T.K. (2000). A molecularly identified P2Y receptor simultaneously activates phospholipase C and inhibits adenylyl cyclase and is nonselectively activated by all nucleoside triphosphates. *Mol. Pharmacol.*, **57**: 805-810.

Boyer, J.L., Mohanram, A., Camaioni, E., Jacobson, K.A. & Harden, T.K. (1998). Competitive and selective antagonism of P2Y₁ receptors by N⁶-methyl 2'-deoxyadenosine 3',5'-bisphosphate. *Br. J. Pharmacol.*, **124**: 1-3.

Brinson, A.E. & Harden, T.K. (2001). Differential regulation of the uridine nucleotide-activated P2Y₄ and P2Y₆ receptors. SER-333 and SER-334 in the carboxyl terminus are involved in agonist-dependent phosphorylation desensitization and internalization of the P2Y₄ receptor. *J. Biol. Chem.*, **276**: 11939-11948.

Broughton, B.R., Walker, B.R. & Resta, T.C. (2008). Chronic hypoxia induces Rho kinase-dependent myogenic tone in small pulmonary arteries. *Am. J. Physiol. Lung Cell. Mol. Physiol.*, **294**: L797-806.

Budzyn, K., Paull, M., Marley, P.D. & Sobey, C.G. (2006). Segmental differences in the roles of rho-kinase and protein kinase C in mediating vasoconstriction. *J. Pharmacol. Exp. Ther.*, **317**: 791-796.

Buhl, A.M., Johnson, N.L., Dhanasekaran, N. & Johnson, G.L. (1995). $G\alpha_{12}$ and $G\alpha_{13}$ stimulate Rho-dependent stress fiber formation and focal adhesion assembly. *J. Biol. Chem.*, **270**: 24631-24634.

Burdyga, T.V. & Wray, S. (2002). On the mechanisms whereby temperature affects excitation-contraction coupling in smooth muscle. *J. Gen. Physiol.*, **119**: 93-104.

Burnstock, G. (1978). A basis for distinguishing two types of purinergic receptor. In: *Cell Membrane Receptors for Drugs and Hormones: A Multidisciplinary Approach*. Ed. Straub, R.W. & Bolis, L., pp. 107-118. New York: Raven Press.

Burnstock, G. (1972). Purinergic nerves. *Pharmacol. Rev.*, **24**: 509-581.

Burnstock, G. (2006). Purinergic signalling. *Br. J. Pharmacol.*, **147 Suppl 1**: S172-181.

Burnstock, G. & Kennedy, C. (1986). A dual function for adenosine 5'-triphosphate in the regulation of vascular tone. Excitatory cotransmitter with noradrenaline from perivascular nerves and locally released inhibitory intravascular agent. *Circ. Res.*, **58**: 319-330.

Buvinic, S., Briones, R. & Huidobro-Toro, J.P. (2002). P2Y₁ and P2Y₂ receptors are coupled to the NO/cGMP pathway to vasodilate the rat arterial mesenteric bed. *Br. J. Pharmacol.*, **136**: 847-856.

Buvinic, S., Poblete, M.I., Donoso, M.V., Delpiano, A.M., Briones, R., Miranda, R. & Huidobro-Toro, J.P. (2006). P2Y₁ and P2Y₂ receptor distribution varies along the human placental vascular tree: role of nucleotides in vascular tone regulation. *J. Physiol.*, **573**: 427-443.

Carter, R.L., Fricks, I.P., Barrett, M.O., Burianek, L.E., Zhou, Y., Ko, H., Das, A., Jacobson, K.A., Lazarowski, E.R. & Harden, T.K. (2009). Quantification of G_i-mediated inhibition of adenylyl cyclase activity reveals that UDP is a potent agonist of the human P2Y₁₄ receptor. *Mol. Pharmacol.*, **76**: 1341-1348.

Cattaneo, M., Zighetti, M.L., Lombardi, R., Martinez, C., Lecchi, A., Conley, P.B., Ware, J. & Ruggeri, Z.M. (2003). Molecular bases of defective signal transduction in the platelet P2Y₁₂ receptor of a patient with congenital bleeding. *Proc. Natl. Acad. Sci. U. S. A.*, **100**: 1978-1983.

Chambers, J.K., Macdonald, L.E., Sarau, H.M., Ames, R.S., Freeman, K., Foley, J.J., Zhu, Y., McLaughlin, M.M., Murdock, P., McMillan, L., Trill, J., Swift, A., Aiyar, N., Taylor, P., Vawter, L., Naheed, S., Szekeres, P., Hervieu, G., Scott, C., Watson, J.M., Murphy, A.J., Duzic, E., Klein, C., Bergsma, D.J., Wilson, S. & Livi, G.P. (2000). A G protein-coupled receptor for UDP-glucose. *J. Biol. Chem.*, **275**: 10767-10771.

Chang, K., Hanaoka, K., Kumada, M. & Takuwa, Y. (1995). Molecular cloning and functional analysis of a novel P₂ nucleotide receptor. *J. Biol. Chem.*, **270**: 26152-26158.

Charlton, M.E., Williams, A.S., Fogliano, M., Sweetnam, P.M. & Duman, R.S. (1997). The isolation and characterization of a novel G protein-coupled receptor regulated by immunologic challenge. *Brain Res.*, **764**: 141-148.

Chen, W.C. & Chen, C.C. (1998). ATP-induced arachidonic acid release in cultured astrocytes is mediated by Gi protein coupled P2Y₁ and P2Y₂ receptors. *Glia*, **22**: 360-370.

Chen, Z.P., Krull, N., Xu, S., Levy, A. & Lightman, S.L. (1996). Molecular cloning and functional characterization of a rat pituitary G protein-coupled adenosine triphosphate (ATP) receptor. *Endocrinology*, **137**: 1833-1840.

Cheng, A.W., Kong, L.W., Tung, E.K., Siow, N.L., Choi, R.C., Zhu, S.Q., Peng, B.H. & Tsim, K.W. (2003). cDNA encodes *Xenopus* P2Y₁ nucleotide receptor: expression at the neuromuscular junctions. *Neuroreport*, **14**: 351-357.

Chhatriwala, M., Ravi, R.G., Patel, R.I., Boyer, J.L., Jacobson, K.A. & Harden, T.K. (2004). Induction of novel agonist selectivity for the ADP-activated P2Y₁ receptor versus the ADP-activated P2Y₁₂ and P2Y₁₃ receptors by conformational constraint of an ADP analog. *J. Pharmacol. Exp. Ther.*, **311**: 1038-1043.

Chootip, K., Ness, K.F., Wang, Y., Gurney, A.M. & Kennedy, C. (2002). Regional variation in P2 receptor expression in the rat pulmonary arterial circulation. *Br. J. Pharmacol.*, **137**: 637-646.

Chopra, B., Gever, J., Barrick, S.R., Hanna-Mitchell, A.T., Beckel, J.M., Ford, A.P. & Birder, L.A. (2008). Expression and function of rat urothelial P2Y receptors. *Am. J. Physiol. Renal Physiol.*, **294**: F821-829.

Clarke, C.J., Forman, S., Pritchett, J., Ohanian, V. & Ohanian, J. (2008). Phospholipase C- δ_1 modulates sustained contraction of rat mesenteric small arteries in response to noradrenaline, but not endothelin-1. *Am. J. Physiol. Heart Circ. Physiol.*, **295**: H826-834.

Cobine, C.A., Callaghan, B.P. & Keef, K.D. (2007). Role of L-type calcium channels and PKC in active tone development in rabbit coronary artery. *Am. J. Physiol. Heart Circ. Physiol.*, **292**: H3079-3088.

Cogolludo, A., Moreno, L., Bosca, L., Tamargo, J. & Perez-Vizcaino, F. (2003). Thromboxane A₂-induced inhibition of voltage-gated K⁺ channels and pulmonary vasoconstriction: role of protein kinase C ζ . *Circ. Res.*, **93**: 656-663.

Cogolludo, A., Moreno, L., Lodi, F., Frazziano, G., Cobeño, L., Tamargo, J. & Perez-Vizcaino, F. (2006). Serotonin inhibits voltage-gated K⁺ currents in pulmonary artery smooth muscle cells: role of 5-HT_{2A} receptors, caveolin-1, and K_v1.5 channel internalization. *Circ. Res.*, **98**: 931-938.

Communi, D., Gonzalez, N.S., Detheux, M., Brézillon, S., Lannoy, V., Parmentier, M. & Boeynaems, J.M. (2001). Identification of a novel human ADP receptor coupled to G_i. *J. Biol. Chem.*, **276**: 41479-41485.

Communi, D., Govaerts, C., Parmentier, M. & Boeynaems, J.M. (1997). Cloning of a human purinergic P_{2Y} receptor coupled to phospholipase C and adenylyl cyclase. *J. Biol. Chem.*, **272**: 31969-31973.

Communi, D., Motte, S., Boeynaems, J.M. & Piroton, S. (1996a). Pharmacological characterization of the human P_{2Y4} receptor. *Eur. J. Pharmacol.*, **317**: 383-389.

Communi, D., Parmentier, M. & Boeynaems, J.M. (1996b). Cloning, functional expression and tissue distribution of the human P_{2Y6} receptor. *Biochem. Biophys. Res. Commun.*, **222**: 303-308.

Communi, D., Piroton, S., Parmentier, M. & Boeynaems, J.M. (1995). Cloning and functional expression of a human uridine nucleotide receptor. *J. Biol. Chem.*, **270**: 30849-30852.

Communi, D., Robaye, B. & Boeynaems, J.M. (1999). Pharmacological characterization of the human P2Y₁₁ receptor. *Br. J. Pharmacol.*, **128**: 1199-1206.

Cressman, V.L., Lazarowski, E., Homolya, L., Boucher, R.C., Koller, B.H. & Grubb, B.R. (1999). Effect of loss of P2Y₂ receptor gene expression on nucleotide regulation of murine epithelial Cl⁻ transport. *J. Biol. Chem.*, **274**: 26461-26468.

Crichton, C.A., Smith, G.C. & Smith, G.L. (1997). α -Toxin-permeabilised rabbit fetal ductus arteriosus is more sensitive to Ca²⁺ than aorta or main pulmonary artery. *Cardiovasc. Res.*, **33**: 223-229.

Dallas, A. & Khalil, R.A. (2003). Ca²⁺ antagonist-insensitive coronary smooth muscle contraction involves activation of ϵ -protein kinase C-dependent pathway. *Am. J. Physiol. Cell Physiol.*, **285**: C1454-1463.

Daly, I.D.B., Hebb, C. (1966). Innervation of the lungs. In: *Pulmonary and Bronchial Vascular systems*. Ed. Daly, I.D.B. & Hebb, C., pp 89-117. Baltimore: William & Wilkins.

Damron, D.S., Kanaya, N., Homma, Y., Kim, S.O. & Murray, P.A. (2002). Role of PKC, tyrosine kinases, and Rho kinase in α -adrenoreceptor-mediated PASM contraction. *Am. J. Physiol. Lung Cell. Mol. Physiol.*, **283**: L1051-1064.

Davies, S.P., Reddy, H., Caivano, M. & Cohen, P. (2000). Specificity and mechanism of action of some commonly used protein kinase inhibitors. *Biochem. J.*, **351**: 95-105.

De Mey, J.G. & Vanhoutte, P.M. (1982). Heterogeneous behavior of the canine arterial and venous wall. Importance of the endothelium. *Circ. Res.*, **51**: 439-447.

DiCarlo, V.S., Chen, S.J., Meng, Q.C., Durand, J., Yano, M., Chen, Y.F. & Oparil, S. (1995). ET_A-receptor antagonist prevents and reverses chronic hypoxia-induced pulmonary hypertension in rat. *Am. J. Physiol.*, **269**: L690-697.

Dimopoulos, G.J., Semba, S., Kitazawa, K., Eto, M. & Kitazawa, T. (2007). Ca²⁺-dependent rapid Ca²⁺ sensitization of contraction in arterial smooth muscle. *Circ. Res.*, **100**: 121-129.

Dinh-Xuan, A.T., Higenbottam, T.W., Clelland, C.A., Pepke-Zaba, J., Cremona, G., Butt, A.Y., Large, S.R., Wells, F.C. & Wallwork, J. (1991). Wallwork J. Impairment of endothelium-dependent pulmonary-artery relaxation in chronic obstructive lung disease. *N. Engl. J. Med.*, **324**: 1539-1547.

Dixon, C.J., Bowler, W.B., Littlewood-Evans, A., Dillon, J.P., Bilbe, G., Sharpe, G.R. & Gallagher, J.A. (1999). Regulation of epidermal homeostasis through P2Y₂ receptors. *Br. J. Pharmacol.*, **127**: 1680-1686.

Dolphin, A.C. (2003). G protein modulation of voltage-gated calcium channels. *Pharmacol. Rev.*, **55**: 607-627.

Drury, A.N. & Szent-Györgyi, A. (1929). The physiological activity of adenine compounds with especial reference to their action upon the mammalian heart. *J. Physiol.*, **68**: 213-237.

Eddinger, T.J. & Meer, D.P. (2007). Myosin II isoforms in smooth muscle: heterogeneity and function. *Am. J. Physiol. Cell Physiol.*, **293**: C493-508.

Egan, T.M., Samways, D.S. & Li, Z. (2006). Biophysics of P2X receptors. *Pflugers Arch.*, **452**: 501-512.

Ehre, C., Zhu, Y., Abdullah, L.H., Olsen, J., Nakayama, K.I., Nakayama, K., Messing, R.O. & Davis, C.W. (2007). nPKC ϵ , a P2Y₂-R downstream effector in regulated mucin secretion from airway goblet cells. *Am. J. Physiol. Cell Physiol.*, **293**: C1445-1454.

El-Bermani, A.W., Bloomquist, E.I. & Montvilo, J.A. (1982). Distribution of pulmonary cholinergic nerves in the rabbit. *Thorax.*, **37**: 703-710.

El-Bermani, A.W., McNary, W.F., & Bradley, D.E. (1970). The distribution of acetylcholinesterase and catecholamine containing nerves in the rat lung. *Anat. Rec.*, **167**: 205-212.

El-Tayeb, A., Qi, A. & Müller, C.E. (2006). Synthesis and structure-activity relationships of uracil nucleotide derivatives and analogues as agonists at human P2Y₂, P2Y₄, and P2Y₆ receptors. *J. Med. Chem.*, **49**: 7076-7087.

Elliott, M.R., Chekeni, F.B., Trampont, P.C., Lazarowski, E.R., Kadl, A., Walk, S.F., Park, D., Woodson, R.I., Ostankovich, M., Sharma, P., Lysiak, J.J., Harden, T.K., Leitinger, N. & Ravichandran, K.S. (2009). Nucleotides released by apoptotic cells act as a find-me signal to promote phagocytic clearance. *Nature*, **461**: 282-286.

Ennion, S.J., Powell, A.D. & Seward, E.P. (2004). Identification of the P2Y₁₂ receptor in nucleotide inhibition of exocytosis from bovine chromaffin cells. *Mol. Pharmacol.*, **66**: 601-611.

Erb, L., Garrad, R., Wang, Y., Quinn, T., Turner, J.T. & Weisman, G.A. (1995). Site-directed mutagenesis of P_{2U} purinoceptors. Positively charged amino acids in transmembrane helices 6 and 7 affect agonist potency and specificity. *J. Biol. Chem.*, **270**: 4185-4188.

Erb, L., Liu, J., Ockerhausen, J., Kong, Q., Garrad, R.C., Griffin, K., Neal, C., Krugh, B., Santiago-Pérez, L.I., González, F.A., Gresham, H.D., Turner, J.T. & Weisman, G.A. (2001). An RGD sequence in the P2Y₂ receptor interacts with $\alpha_v\beta_3$ integrins and is required for G_o-mediated signal transduction. *J. Cell Biol.*, **153**: 491-501.

Erlinge, D. & Burnstock, G. (2008). P2 receptors in cardiovascular regulation and disease. *PUSI*, **4**: 1-20.

Erlinge, D., Hou, M., Webb, T.E., Barnard, E.A. & Möller, S. (1998). Phenotype changes of the vascular smooth muscle cell regulate P2 receptor expression as measured by quantitative RT-PCR. *Biochem. Biophys. Res. Commun.*, **248**: 864-870.

Eto, M., Kitazawa, T., Yazawa, M., Mukai, H., Ono, Y. & Brautigan, D.L. (2001). Histamine-induced vasoconstriction involves phosphorylation of a specific inhibitor protein for myosin phosphatase by protein kinase C α and δ isoforms. *J. Biol. Chem.*, **276**: 29072 - 29078.

Evans, A.M., Cobban, H.J. & Nixon, G.F. (1999). ET_A receptors are the primary mediators of myofilament calcium sensitization induced by ET-1 in rat pulmonary artery smooth muscle: a tyrosine kinase independent pathway. *Br. J. Pharmacol.*, **127**: 153-160.

Fabiato, A. & Fabiato, F. (1979). Calculator programs for computing the composition of the solutions containing multiple metals and ligands used for experiments in skinned muscle cells. *J. Physiol., Paris*, **75**: 463-505.

Feng, C., Mery, A.G., Beller, E.M., Favot, C. & Boyce, J.A. (2004). Adenine nucleotides inhibit cytokine generation by human mast cells through a G_s-coupled receptor. *J. Immunol.*, **173**: 7539-7547.

Filtz, T.M., Li, Q., Boyer, J.L., Nicholas, R.A. & Harden, T.K. (1994). Expression of a cloned P_{2Y} purinergic receptor that couples to phospholipase C. *Mol. Pharmacol.*, **46**: 8-14.

Fishman, A.P. (1961). Respiratory gases in the regulation of the pulmonary circulation. *Physiol. Rev.*, **41**: 214-280.

Foster, C.J., Prosser, D.M., Agans, J.M., Zhai, Y., Smith, M.D., Lachowicz, J.E., Zhang, F.L., Gustafson, E., Monsma, F.J., Jr., Wiekowski, M.T., Abbondanzo, S.J., Cook, D.N., Bayne, M.L., Lira, S.A. & Chintala, M.S. (2001). Molecular identification and characterization of the platelet ADP receptor targeted by thienopyridine antithrombotic drugs. *J. Clin. Invest.*, **107**: 1591-1598.

Freeman, K., Tsui, P., Moore, D., Emson, P.C., Vawter, L., Naheed, S., Lane, P., Bawagan, H., Herrity, N., Murphy, K., Sarau, H.M., Ames, R.S., Wilson, S., Livi, G.P. & Chambers, J.K. (2001). Cloning, pharmacology, and tissue distribution of G-protein-coupled receptor GPR105 (KIAA0001) rodent orthologs. *Genomics*, **78**: 124-128.

Fricks, I.P., Maddileti, S., Carter, R.L., Lazarowski, E.R., Nicholas, R.A., Jacobson, K.A. & Harden, T.K. (2008). UDP is a competitive antagonist at the human P_{2Y}₁₄ receptor. *J. Pharmacol. Exp. Ther.*, **325**: 588-594.

Füssle, R., Bhakdi, S., Sziegoleit, A., Tranum-Jensen, J., Kranz, T. & Wellensiek, H.J. (1981). On the mechanism of membrane damage by *Staphylococcus aureus* α -toxin. *J. Cell Biol.*, **91**: 83-94.

Fumagalli, M., Brambilla, R., D'Ambrosi, N., Volonte, C., Matteoli, M., Verderio, C. & Abbracchio, M.P. (2003). Nucleotide-mediated calcium signaling in rat cortical astrocytes: Role of P_{2X} and P_{2Y} receptors. *Glia*, **43**: 218-230.

Fumagalli, M., Trincavelli, L., Lecca, D., Martini, C., Ciana, P. & Abbracchio, M.P. (2004). Cloning, pharmacological characterisation and distribution of the rat G-protein-coupled P2Y₁₃ receptor. *Biochem. Pharmacol.*, **68**: 113-124.

Gachet, C., Léon, C. & Hechler, B. (2006). The platelet P2 receptors in arterial thrombosis. *Blood Cells Mol. Dis.*, **36**: 223-227.

Ganong, W.F. (1995). *Review of Medical Physiology*. 17th edn, Appleton & Lange: Norwalk, Connecticut.

Gao, Y., Tolsa, J.F., Shen, H. & Raj, J.U. (1998). Effect of selective phosphodiesterase inhibitors on response of ovine pulmonary arteries to prostaglandin E₂. *J. Appl. Physiol.*, **84**: 13-18.

Gao, Z.G., Ding, Y. & Jacobson, K.A. (2010). UDP-glucose acting at P2Y₁₄ receptors is a mediator of mast cell degranulation. *Biochem. Pharmacol.*, **79**: 873-879.

Garrad, R.C., Otero, M.A., Erb, L., Theiss, P.M., Clarke, L.L., Gonzalez, F.A., Turner, J.T. & Weisman, G.A. (1998). Structural basis of agonist-induced desensitization and sequestration of the P2Y₂ nucleotide receptor: Consequences of truncation of the C terminus. *J. Biol. Chem.*, **273**: 29437-29444.

Ghanem, E., Robaye, B., Leal, T., Leipziger, J., Van Driessche, W., Beauwens, R. & Boeynaems, J.M. (2005). The role of epithelial P2Y₂ and P2Y₄ receptors in the regulation of intestinal chloride secretion. *Br. J. Pharmacol.*, **146**: 364-369.

Gonzales, E.B., Kawate, T. & Gouaux, E. (2009). Pore architecture and ion sites in acid-sensing ion channels and P2X receptors. *Nature*, **460**: 599-604.

Govindaraju, V., Martin, J.G., Maghni, K., Ferraro, P. & Michoud, M.C. (2005). The effects of extracellular purines and pyrimidines on human airway smooth muscle cells. *J. Pharmacol. Exp. Ther.*, **315**: 941-948.

Graciano, M.L., Nishiyama, A., Jackson, K., Seth, D.M., Ortiz, R.M., Prieto-Carrasquero, M.C., Kobori, H. & Navar, L.G. (2008). Purinergic receptors contribute to early mesangial cell transformation and renal vessel hypertrophy during angiotensin II-induced hypertension. *Am. J. Physiol. Renal Physiol.*, **294**: F161-169.

Greig, A.V., James, S.E., McGrouther, D.A., Terenghi, G. & Burnstock, G. (2003). Purinergic receptor expression in the regeneration epidermis in a rat model of normal and delayed wound healing. *Exp. Dermatol.*, **12**: 860-871.

Gschwendt, M., Dieterich, S., Rennecke, J., Kittstein, W., Mueller, H.J. & Johannes, F.J. (1996). Inhibition of protein kinase C μ by various inhibitors. Differentiation from protein kinase C isoenzymes. *FEBS Lett.*, **392**: 77-80.

Gui, Y., Walsh, M.P., Jankowski, V., Jankowski, J. & Zheng, X.L. (2008). Up $_4$ A stimulates endothelium-independent contraction of isolated rat pulmonary artery. *Am. J. Physiol. Lung Cell. Mol. Physiol.*, **294**: L733-738.

Guibert, C., Pacaud, P., Loirand, G., Marthan, R. & Savineau, J.P. (1996). Effect of extracellular ATP on cytosolic Ca $^{2+}$ concentration in rat pulmonary artery myocytes. *Am. J. Physiol.*, **271**: L450-458.

Guns, P.J., Korda, A., Crauwels, H.M., Van Assche, T., Robaye, B., Boeynaems, J.M. & Bult, H. (2005). Pharmacological characterization of nucleotide P $_2$ Y receptors on endothelial cells of the mouse aorta. *Br. J. Pharmacol.*, **146**: 288-295.

Guzmán-Aránguez, A., Irazu, M., Yayon, A. & Pintor, J. (2008). P $_2$ Y receptors activated by diadenosine polyphosphates reestablish Ca $^{2+}$ transients in achondroplastic chondrocytes. *Bone*, **42**: 516-523.

Harden, T.K., Boyer, J.L. & Nicholas, R.A. (1995). P2-purinergic receptors: subtype-associated signaling responses and structure. *Annu. Rev. Pharmacol. Toxicol.*, **35**: 541-579.

Harper, S., Webb, T.E., Charlton, S.J., Ng, L.L. & Boarder, M.R. (1998). Evidence that P2Y₄ nucleotide receptors are involved in the regulation of rat aortic smooth muscle cells by UTP and ATP. *Br. J. Pharmacol.*, **124**: 703-710.

Hartley, S.A., Kato, K., Salter, K.J. & Kozlowski, R.Z. (1998). Functional evidence for a novel suramin-insensitive pyrimidine receptor in rat small pulmonary arteries. *Circ. Res.*, **83**: 940-946.

Hayashi, T., Kawakami, M., Sasaki, S., Katsumata, T., Mori, H., Yoshida, H. & Nakahari, T. (2005). ATP regulation of ciliary beat frequency in rat tracheal and distal airway epithelium. *Exp. Physiol.*, **90**: 535-544.

Heinrich, A., Kittel, Á., Csölle, C., Sylvester Vizi, E. & Sperlág, B. (2008). Modulation of neurotransmitter release by P2X and P2Y receptors in the rat spinal cord. *Neuropharmacology*, **54**: 375-386.

Henderson, D.J., Elliot, D.G., Smith, G.M., Webb, T.E. & Dainty, I.A. (1995). Cloning and characterisation of a bovine P_{2Y} receptor. *Biochem. Biophys. Res. Commun.*, **212**: 648-656.

Herold, C.L., Qi, A.D., Harden, T.K. & Nicholas, R.A. (2004). Agonist versus antagonist action of ATP at the P2Y₄ receptor is determined by the second extracellular loop. *J. Biol. Chem.*, **279**: 11456-11464.

Himpens, B., Kitazawa, T. & Somlyo, A.P. (1990). Agonist-dependent modulation of Ca²⁺ sensitivity in rabbit pulmonary artery smooth muscle. *Pflugers Arch.*, **417**: 21-28.

- Hoffmann, C., Moro, S., Nicholas, R.A., Harden, T.K. & Jacobson, K.A. (1999). The role of amino acids in extracellular loops of the human P₂Y₁ receptor in surface expression and activation processes. *J. Biol. Chem.*, **274**: 14639-14647.
- Hoffmann, C., Ziegler, N., Reiner, S., Krasel, C. & Lohse, M.J. (2008). Agonist-selective, receptor-specific interaction of human P₂Y receptors with β -arrestin-1 and -2. *J. Biol. Chem.*, **283**: 30933-30941.
- Hollopeter, G., Jantzen, H.M., Vincent, D., Li, G., England, L., Ramakrishnan, V., Yang, R.B., Nurden, P., Nurden, A., Julius, D. & Conley, P.B. (2001). Identification of the platelet ADP receptor targeted by antithrombotic drugs. *Nature*, **409**: 202-207.
- Hong, Z., Weir, E.K., Nelson, D.P. & Olschewski, A. (2004). Subacute hypoxia decreases voltage-activated potassium channel expression and function in pulmonary artery myocytes. *Am. J. Respir. Cell. Mol. Biol.*, **31**: 337-343.
- Horiuti, K. (1986). Some properties of the contractile system and sarcoplasmic reticulum of skinned slow fibres from *Xenopus* muscle. *J. Physiol.*, **373**: 1-23.
- Hughes, J.M.B. & Morrell, N.W. (2001). *Pulmonary Circulation, from Basic Mechanisms to Clinical Practice*. Imperial College Press: London.
- Hyman, A.L. & Kadowitz, P.J. (1989). Influence of tone on responses to acetylcholine in the rabbit pulmonary vascular bed. *J. Appl. Physiol.*, **67**: 1388-1394.
- Hyman, A.L. & Kadowitz, P.J. (1988). Tone-dependent responses to acetylcholine in the feline pulmonary vascular bed. *J. Appl. Physiol.*, **64**: 2002-2009.
- Hyman, A.L., Lipton, H.L. & Kadowitz, P.J. (1990). Analysis of pulmonary vascular responses in cats to sympathetic nerve stimulation under elevated tone conditions. Evidence that neuronally released norepinephrine acts on α_1 -, α_2 -, and β_2 -adrenoceptors. *Circ. Res.*, **67**: 862-870.

Iizuka, K., Ikebe, M., Somlyo, A.V. & Somlyo, A.P. (1994). Introduction of high molecular weight (IgG) proteins into receptor coupled, permeabilized smooth muscle. *Cell Calcium*, **16**: 431-445.

Ingall, A.H., Dixon, J., Bailey, A., Coombs, M.E., Cox, D., McNally, J.I., Hunt, S. F., Kindon, N.D., Teobald, B.J., Willis, P.A., Humphries, R.G., Leff, P., Clegg, J.A., Smith, J.A. & Tomlinson, W. (1999). Antagonists of the platelet P_{2T} receptor: a novel approach to antithrombotic therapy. *J. Med. Chem.*, **42**: 213-220.

Inoue, K., Hosoi, J. & Denda, M. (2007). Extracellular ATP has stimulatory effects on the expression and release of IL-6 via purinergic receptors in normal human epidermal keratinocytes. *J. Invest. Dermatol.*, **127**: 362-371.

Inoue, T. & Kannan, M.S. (1988). Nonadrenergic and noncholinergic excitatory neurotransmission in rat intrapulmonary artery. *Am. J. Physiol.*, **254**: H1142-1148.

Insel, P.A., Ostrom, R.S., Zambon, A.C., Hughes, R.J., Balboa, M.A., Shehnaz, D., Gregorian, C., Torres, B., Firestein, B.L., Xing, M. & Post, S.R. (2001). P_{2Y} receptors of MDCK cells: epithelial cell regulation by extracellular nucleotides. *Clin. Exp. Pharmacol. Physiol.*, **28**: 351-354.

Itoh, T., Kuriyama, H. & Suzuki, H. (1983). Differences and similarities in the noradrenaline- and caffeine-induced mechanical responses in the rabbit mesenteric artery. *J. Physiol.*, **337**: 609-629.

Jackson, V.M., Trout, S.J. & Cunnane, T.C. (2002). Regional variation in electrically-evoked contractions of rabbit isolated pulmonary artery. *Br. J. Pharmacol.*, **137**: 488-496.

Jacobson, K.A., Ivanov, A.A., de Castro, S., Harden, T.K. & Ko, H. (2009). Development of selective agonists and antagonists of P_{2Y} receptors. *Purinergic Signal.*, **5**: 75-89.

Jacquet, S., Malaval, C., Martinez, L.O., Sak, K., Rolland, C., Perez, C., Nauze, M., Champagne, E., Tercé, F., Gachet, C., Perret, B., Collet, X., Boeynaems, J.M. & Barbaras, R. (2005). The nucleotide receptor P2Y₁₃ is a key regulator of hepatic high-density lipoprotein (HDL) endocytosis. *Cell. Mol. Life Sci.*, **62**: 2508-2515.

Jähnichen, S., Glusa, E. & Pertz, H.H. (2005). Evidence for 5-HT_{2B} and 5-HT₇ receptor-mediated relaxation in pulmonary arteries of weaned pigs. *Naunyn-Schmiedeberg's Arch. Pharmacol.*, **371**: 89-98.

Jankowski, M., Szczepańska-Konkel, K., Kalinowski, L. & Angielski, S. (2003). Involvement of Rho-kinase in P2Y-receptor-mediated contraction of renal glomeruli. *Biochem. Biophys. Res. Commun.*, **302**: 855-859.

Jankowski, V., van der Giet, M., Mischak, H., Morgan, M., Zidek, W. & Jankowski, J. (2009). Dinucleoside polyphosphates: strong endogenous agonists of the purinergic system. *Br. J. Pharmacol.*, **157**: 1142-1153.

Janssens, R., Paindavoine, P., Parmentier, M. & Boeynaems, J.M. (1999). Human P2Y₂ receptor polymorphism: identification and pharmacological characterization of two allelic variants. *Br. J. Pharmacol.*, **127**: 709-716.

Jarvis, M.F. & Khakh, B.S. (2009). ATP-gated P2X cation-channels. *Neuropharmacology*, **56**: 208-215.

Jernigan, N.L., Walker, B.R. & Resta, T.C. (2004). Chronic hypoxia augments protein kinase G-mediated Ca²⁺ desensitization in pulmonary vascular smooth muscle through inhibition of RhoA/Rho kinase signaling. *Am. J. Physiol. Lung Cell. Mol. Physiol.*, **287**: L1220-1229.

Jernigan, N.L., Walker, B.R. & Resta, T.C. (2008). Reactive oxygen species mediate RhoA/Rho kinase-induced Ca²⁺ sensitization in pulmonary vascular smooth muscle following chronic hypoxia. *Am. J. Physiol. Lung Cell. Mol. Physiol.*, **295**: L515-529.

Jiang, H. & Stephens, N.L. (1994). Calcium and smooth muscle contraction. *Mol. Cell. Biochem.*, **135**: 1-9.

Jiang, Q., Guo, D., Lee, B.X., Van Rhee, A.M., Kim, Y.C., Nicholas, R.A., Schachter, J.B., Harden, T.K. & Jacobson, K.A. (1997). A mutational analysis of residues essential for ligand recognition at the human P2Y₁ receptor. *Mol. Pharmacol.*, **52**: 499-507.

Kapilevich, L.V., Anfinogenova, Y.D., Nosarev, A.V., Baskakov, M.B., Kovalev, I.V., D'yakova, E. Y. & Medvedev, M.A. (2001). Histaminergic regulation of smooth muscles in rabbit pulmonary arteries. *Bull. Exp. Biol. Med.*, **132**: 731-733.

Kauffenstein, G., Drouin, A., Thorin-Trescases, N., Bachelard, H., Robaye, B., D'Orléans-Juste, P., Marceau, F., Thorin, É. & Sévigny, J. (2010). NTPDase1 (CD39) controls nucleotide-dependent vasoconstriction in mouse. *Cardiovasc. Res.*, **85**: 204-213.

Kauffenstein, G., Hechler, B., Cazenave, J.P. & Gachet, C. (2004). Adenine triphosphate nucleotides are antagonists at the P2Y₁₂ receptor. *J. Thromb. Haemost.*, **2**: 1980-1988.

Kawanabe, Y., Masaki, T. & Hashimoto, N. (2006). Involvement of phospholipase C in endothelin 1-induced stimulation of Ca²⁺ channels and basilar artery contraction in rabbits. *J. Neurosurg.*, **105**: 288-293.

Kawate, T., Michel, J.C., Birdsong, W.T. & Gouaux, E. (2009). Crystal structure of the ATP-gated P2X₄ ion channel in the closed state. *Nature*, **460**: 592-598.

Kellerman, D., Evans, R., Mathews, D. & Shaffer, C. (2002). Inhaled P2Y₂ receptor agonists as a treatment for patients with Cystic Fibrosis lung disease. *Adv. Drug Deliv. Rev.*, **54**: 1463-1474.

Kellerman, D., Rossi Mospan, A., Engels, J., Schaberg, A., Gorden, J. & Smiley, L. (2008). Denufosol: a review of studies with inhaled P2Y₂ agonists that led to Phase 3. *Pulm. Pharmacol. Ther.*, **21**: 600-607.

Kennedy, C. (2000). The discovery and development of P2 receptor subtypes. *J. Auton. Nerv. Syst.*, **81**: 158-163.

Kennedy, C. & Burnstock, G. (1985). Evidence for two types of P₂-purinoceptor in longitudinal muscle of the rabbit portal vein. *Eur. J. Pharmacol.*, **111**: 49-56.

Kennedy, C., Delbro, D. & Burnstock, G. (1985). P₂-purinoceptors mediate both vasodilation (via the endothelium) and vasoconstriction of the isolated rat femoral artery. *Eur. J. Pharmacol.*, **107**: 161-168.

Kennedy, C., Qi, A.D., Herold, C.L., Harden, T.K. & Nicholas, R.A. (2000). ATP, an agonist at the rat P2Y₄ receptor, is an antagonist at the human P2Y₄ receptor. *Mol. Pharmacol.*, **57**: 926-931.

Keys, J.R., Greene, E.A., Koch, W.J. & Eckhart, A.D. (2002). Gq-coupled receptor agonists mediate cardiac hypertrophy via the vasculature. *Hypertension*, **40**: 660-666.

Khakh, B.S., Burnstock, G., Kennedy, C., King, B.F., North, R.A., Séguéla, P., Voigt, M. & Humphrey, P.P. (2001). International union of pharmacology. XXIV. Current status of the nomenclature and properties of P2X receptors and their subunits. *Pharmacol. Rev.*, **53**: 107-118.

Kim, S.G., Soltysiak, K.A., Gao, Z.G., Chang, T.S., Chung, E. & Jacobson, K.A. (2003). Tumor necrosis factor α -induced apoptosis in astrocytes is prevented by the activation of P2Y₆, but not P2Y₄ nucleotide receptors. *Biochem. Pharmacol.*, **65**: 923-931.

Kim, U.H., Kim, J.W. & Rhee, S.G. (1989). Phosphorylation of phospholipase C- γ by cAMP-dependent protein kinase. *J. Biol. Chem.*, **264**: 20167-20170.

King, B.F. & Townsend-Nicholson, A. (2008). Involvement of P2Y₁ and P2Y₁₁ purinoceptors in parasympathetic inhibition of colonic smooth muscle. *J. Pharmacol. Exp. Ther.*, **324**: 1055-1063.

Kitazawa, T., Eto, M., Woodsome, T.P. & Brautigan, D.L. (2000). Agonists trigger G protein-mediated activation of the CPI-17 inhibitor phosphoprotein of myosin light chain phosphatase to enhance vascular smooth muscle contractility. *J. Biol. Chem.*, **275**: 9897-9900.

Kitazawa, T., Kobayashi, S., Horiuti, K., Somlyo, A.V. & Somlyo, A.P. (1989). Receptor-coupled, permeabilized smooth muscle. Role of the phosphatidylinositol cascade, G-proteins, and modulation of the contractile response to Ca²⁺. *J. Biol. Chem.*, **264**: 5339-5342.

Kitazawa, T., Masuo, M. & Somlyo, A.P. (1991). G protein-mediated inhibition of myosin light-chain phosphatase in vascular smooth muscle. *Proc. Natl. Acad. Sci. U. S. A.*, **88**: 9307-9310.

Kitazawa, T., Takizawa, N., Ikebe, M. & Eto, M. (1999). Reconstitution of protein kinase C-induced contractile Ca²⁺ sensitization in Triton X-100-demembrated rabbit arterial smooth muscle. *J. Physiol.*, **520.1**: 139-152.

Knight, D.S., Ellison, J.P., Hibbs, R.G., Hyman, A.L. & Kadowitz, P.J. (1981). A light and electron microscopic study of the innervation of pulmonary arteries in the cat. *Anat. Rec.*, **201**: 513-521.

Knock, G.A., Shaifita, Y., Snetkov, V.A., Vowles, B., Drndarski, S., Ward, J.P. & Aaronson, P.I. (2008). Interaction between *src* family kinases and rho-kinase in agonist-induced Ca²⁺-sensitization of rat pulmonary artery. *Cardiovasc. Res.*, **77**: 570-579.

Ko, H., Carter, R.L., Cosyn, L., Petrelli, R., de Castro, S., Besada, P., Zhou, Y., Cappellacci, L., Franchetti, P., Grifantini, M., Van Calenbergh, S., Harden, T.K. & Jacobson, K.A. (2008). Synthesis and potency of novel uracil nucleotides and derivatives as P2Y₂ and P2Y₆ receptor agonists. *Bioorg. Med. Chem.*, **16**: 6319-6332.

Koltsova, S.V., Maximov, G.V., Kotelevtsev, S.V., Lavoie, J.L., Tremblay, J., Grygorczyk, R., Hamet, P. & Orlov, S.N. (2009). Myogenic tone in mouse mesenteric arteries: evidence for P2Y receptor-mediated, Na⁺, K⁺, 2Cl⁻ cotransport-dependent signaling. *Purinergic Signal.*, **5**: 343-349.

Konduri, G.G., Bakhutashvili, I., Frenn, R., Chandrasekhar, I., Jacobs, E.R. & Khanna, A.K. (2004). P2Y purine receptor responses and expression in the pulmonary circulation of juvenile rabbits. *Am. J. Physiol. Heart Circ. Physiol.*, **287**: H157-164.

Korcok, J., Raimundo, L.N., Du, X., Sims, S.M. & Dixon, S.J. (2005). P2Y₆ nucleotide receptors activate NF-κB and increase survival of osteoclasts. *J. Biol. Chem.*, **280**: 16909-16915.

Köttgen, M., Löffler, T., Jacobi, C., Nitschke, R., Pavenstädt, H., Schreiber, R., Frische, S., Nielsen, S. & Leipziger, J. (2003). P2Y₆ receptor mediates colonic NaCl secretion via differential activation of cAMP-mediated transport. *J. Clin. Invest.*, **111**: 371-379.

Lakshminrusimha, S., Porta, N.F., Farrow, K.N., Chen, B., Gugino, S.F., Kumar, V.H., Russell, J.A. & Steinhorn, R.H. (2009). Milrinone enhances relaxation to prostacyclin and iloprost in pulmonary arteries isolated from lambs with persistent pulmonary hypertension of the newborn. *Pediatr. Crit. Care Med.*, **10**: 106-112.

Lambrecht, G., Braun, K., Damer, M., Ganso, M., Hildebrandt, C., Ullmann, H., Kassack, M.U. & Nickel, P. (2002). Structure-activity relationships of suramin and pyridoxal-5'-phosphate derivatives as P2 receptor antagonists. *Curr. Pharm. Des.*, **8**: 2371-2399.

Lau, W.H., Kwan, Y.W., Au, A.L. & Cheung, W.H. (2003). An in vitro study of histamine on the pulmonary artery of the Wistar-Kyoto and spontaneously hypertensive rats. *Eur. J. Pharmacol.*, **470**: 45-55.

Lazarowski, E.R., Rochelle, L.G., O'Neal, W.K., Ribeiro, C.M., Grubb, B.R., Zhang, V., Harden, T.K. & Boucher, R.C. (2001). Cloning and functional characterization of two murine uridine nucleotide receptors reveal a potential target for correcting ion transport deficiency in cystic fibrosis gallbladder. *J. Pharmacol. Exp. Ther.*, **297**: 43-49.

Lazarowski, E.R., Watt, W.C., Stutts, M.J., Brown, H.A., Boucher, R.C. & Harden, T.K. (1996). Enzymatic synthesis of UTP γ S, a potent hydrolysis resistant agonist of P_{2U}-purinoceptors. *Br. J. Pharmacol.*, **117**: 203-209.

Léon, C., Hechler, B., Vial, C., Leray, C., Cazenave, J.P. & Gachet, C. (1997). The P2Y₁ receptor is an ADP receptor antagonized by ATP and expressed in platelets and megakaryoblastic cells. *FEBS Lett.*, **403**: 26-30.

Lewis, C.J. & Evans, R.J. (2001). P2X receptor immunoreactivity in different arteries from the femoral, pulmonary, cerebral, coronary and renal circulations. *J. Vasc. Res.*, **38**: 332-340.

- Li, L., Eto, M., Lee, M.R., Morita, F., Yazawa, M. & Kitazawa, T. (1998). Possible involvement of the novel CPI-17 protein in protein kinase C signal transduction of rabbit arterial smooth muscle. *J. Physiol.*, **508.3**: 871-881.
- Liu, C., Zuo, J., Pertens, E., Helli, P.B. & Janssen, L.J. (2005). Regulation of Rho/ROCK signaling in airway smooth muscle by membrane potential and $[Ca^{2+}]_i$. *Am. J. Physiol. Lung Cell. Mol. Physiol.*, **289**: L574-582.
- Liu, S.F., Crawley, D.E., Evans, T.W. & Barnes, P.J. (1991). Endogenous nitric oxide modulates adrenergic neural vasoconstriction in guinea-pig pulmonary artery. *Br. J. Pharmacol.*, **104**: 565-569.
- Liu, S.F., Crawley, D.E., Evans, T.W. & Barnes, P.J. (1992a). Endothelium-dependent nonadrenergic, noncholinergic neural relaxation in guinea pig pulmonary artery. *J. Pharmacol. Exp. Ther.*, **260**: 541-548.
- Liu, S.F., Crawley, D.E., Rohde, J.A., Evans, T.W. & Barnes, P.J. (1992b). Role of nitric oxide and guanosine 3',5'-cyclic monophosphate in mediating nonadrenergic, noncholinergic relaxation in guinea-pig pulmonary arteries. *Br. J. Pharmacol.*, **107**: 861-866.
- Liu, S.F., McCormack, D.G., Evans, T.W. & Barnes, P.J. (1989). Characterization and distribution of P₂-purinoceptor subtypes in rat pulmonary vessels. *J. Pharmacol. Exp. Ther.*, **251**: 1204-1210.
- Logantha, S. (2009). Electrical properties and calcium signalling in cardiomyocytes of the pulmonary vein. University of Strathclyde, Glasgow, Scotland, PhD Thesis.
- Loirand, G., Guérin, P. & Pacaud, P. (2006). Rho kinases in cardiovascular physiology and pathophysiology. *Circ. Res.*, **98**: 322-334.

López, C., Sánchez, M., Hidalgo, A. & García de Boto, M.J. (2000). Mechanisms involved in UTP-induced contraction in isolated rat aorta. *Eur. J. Pharmacol.*, **391**: 299-303.

Lustig, K.D., Shiau, A.K., Brake, A.J. & Julius, D. (1993). Expression cloning of an ATP receptor from mouse neuroblastoma cells. *Proc. Natl. Acad. Sci. U. S. A.*, **90**: 5113-5117.

MacLean, M.R., Herve, P., Eddahibi, S. & Adnot, S. (2000). 5-hydroxytryptamine and the pulmonary circulation: receptors, transporters and relevance to pulmonary arterial hypertension. *Br. J. Pharmacol.*, **131**: 161-168.

Maggi, C.A., Patacchini, R., Perretti, F., Tramontana, M., Manzini, S., Geppetti, P. & Santicoli, P. (1990). Sensory nerves, vascular endothelium and neurogenic relaxation of the guinea-pig isolated pulmonary artery. *Naunyn-Schmiedeberg's Arch. Pharmacol.*, **342**: 78-84.

Malmsjö, M., Hou, M., Pendergast, W., Erlinge, D. & Edvinsson, L. (2003). Potent P2Y₆ receptor mediated contractions in human cerebral arteries. *BMC Pharmacol.*, **3**: 4.

Mam, V., Tanbe, A.F., Vitali, S.H., Arons, E., Christou, H.A. & Khalil, R.A. (2010). Impaired vasoconstriction and nitric oxide-mediated relaxation in pulmonary arteries of hypoxia- and monocrotaline-induced pulmonary hypertensive rats. *J. Pharmacol. Exp. Ther.*, **332**: 455-462.

Mamedova, L.K., Joshi, B.V., Gao, Z.G., von Kügelgen, I. & Jacobson, K.A. (2004). Diisothiocyanate derivatives as potent, insurmountable antagonists of P2Y₆ nucleotide receptors. *Biochem. Pharmacol.*, **67**: 1763-1770.

- Marcet, B., Horckmans, M., Libert, F., Hassid, S., Boeynaems, J.M. & Communi, D. (2007). Extracellular nucleotides regulate CCL20 release from human primary airway epithelial cells, monocytes and monocyte-derived dendritic cells. *J. Cell. Physiol.*, **211**: 716-727.
- Marteau, F., Le Poul, E., Communi, D., Labouret, C., Savi, P., Boeynaems, J.M. & Gonzalez, N.S. (2003). Pharmacological characterization of the human P2Y₁₃ receptor. *Mol. Pharmacol.*, **64**: 104-112.
- Martiny-Baron, G., Kazanietz, M.G., Mischak, H., Blumberg, P.M., Kochs, G., Hug, H., Marmé, D. & Schächtele, C. (1993). Selective inhibition of protein kinase C isozymes by the indolocarbazole Gö 6976. *J. Biol. Chem.*, **268**: 9194-9197.
- Masuo, M., Reardon, S., Ikebe, M. & Kitazawa, T. (1994). A novel mechanism for the Ca²⁺-sensitizing effect of protein kinase C on vascular smooth muscle: inhibition of myosin light chain phosphatase. *J. Gen. Physiol.*, **104**: 265-286.
- Matsumoto, T., Nakane, T. & Chiba, S. (1997). UTP induces vascular responses in the isolated and perfused canine epicardial coronary artery via UTP-preferring P2Y receptors. *Br. J. Pharmacol.*, **122**: 1625-1632.
- Matsushita, T., Hislop, A.A., Boels, P.J., Deutsch, J. & Haworth, S.G. (1999). Changes in ANP responsiveness of normal and hypertensive porcine intrapulmonary arteries during maturation. *Pediatr. Res.*, **46**: 411-418.
- McLaren, G.J., Burke, K.S., Buchanan, K.J., Sneddon, P. & Kennedy, C. (1998). Evidence that ATP acts at two sites to evoke contraction in the rat isolated tail artery. *Br. J. Pharmacol.*, **124**: 5-12.
- McLean, J.R., Twarog, B.M. & Bergofsky, E.H. (1985). The adrenergic innervation of pulmonary vasculature in the normal and pulmonary hypertensive rat. *J. Auton. Nerv. Syst.*, **14**: 111-123.

McMillan, M., Chernow, B. & Roth, B.L. (1986). Phorbol esters inhibit α_1 -adrenergic receptor-stimulated phosphoinositide hydrolysis and contraction in rat aorta: evidence for a link between vascular contraction and phosphoinositide turnover. *Biochem. Biophys. Res. Commun.*, **134**: 970-974.

Meng, F., To, W., Kirkman-Brown, J., Kumar, P. & Gu, Y. (2007). Calcium oscillations induced by ATP in human umbilical cord smooth muscle cells. *J. Cell. Physiol.*, **213**: 79-87.

Miike, T., Shirahase, H., Kanda, M., Kunishiro, K. & Kurahashi, K. (2009). NK₁ receptor-mediated endothelium-dependent relaxation and contraction with different sensitivity to post-receptor signaling in pulmonary arteries. *Vascul. Pharmacol.*, **51**: 147-153.

Min, K., Munarriz, R., Yerxa, B.R., Goldstein, I., Shaver, S.R., Cowlen, M.S. & Traish, A.M. (2003). Selective P2Y₂ receptor agonists stimulate vaginal moisture in ovariectomized rabbits. *Fertil. Steril.*, **79**: 393-398.

Mita, M., Yanagihara, H., Hishinuma, S., Saito, M. & Walsh, M.P. (2002). Membrane depolarization-induced contraction of rat caudal arterial smooth muscle involves Rho-associated kinase. *Biochem. J.*, **364**: 431-440.

Mitchell, C. (2008). Signalling mechanisms underlying P2Y receptor-mediated vasoconstriction in pulmonary arteries. University of Strathclyde, Glasgow, Scotland, PhD Thesis.

Miyagi, Y., Kobayashi, S., Nishimura, J., Fukui, M. & Kanaide, H. (1996). P_{2U} receptor is linked to cytosolic Ca²⁺ transient and release of vasorelaxing factor in bovine endothelial cells *in situ*. *J. Physiol.*, **492.3**: 751-761.

Moore, D.J., Murdock, P.R., Watson, J.M., Faull, R.L., Waldvogel, H.J., Szekeres, P.G., Wilson, S., Freeman, K.B. & Emson, P.C. (2003). GPR105, a novel G_{i/o}-

coupled UDP-glucose receptor expressed on brain glia and peripheral immune cells, is regulated by immunologic challenge: possible role in neuroimmune function. *Brain Res. Mol. Brain Res.*, **118**: 10-23.

Moro, S., Guo, D., Camaioni, E., Boyer, J.L., Harden, T.K. & Jacobson, K.A. (1998). Human P2Y₁ receptor: molecular modeling and site-directed mutagenesis as tools to identify agonist and antagonist recognition sites. *J. Med. Chem.*, **41**: 1456-1466.

Morrell, N.W., Adnot, S., Archer, S.L., Dupuis, J., Jones, P.L., MacLean, M.R., McMurtry, I.F., Stenmark, K.R., Thistlethwaite, P.A., Weissmann, N., Yuan, J.X. & Weir, E.K. (2009). Cellular and molecular basis of pulmonary arterial hypertension. *J. Am. Coll. Cardiol.*, **54**: S20-31.

Müller, T., Bayer, H., Myrtek, D., Ferrari, D., Sorichter, S., Ziegenhagen, M.W., Zissel, G., Virchow, J.C., Jr., Luttmann, W., Norgauer, J., Di Virgilio, F. & Idzko, M. (2005). The P2Y₁₄ receptor of airway epithelial cells: coupling to intracellular Ca²⁺ and IL-8 secretion. *Am. J. Respir. Cell. Mol. Biol.*, **33**: 601-609.

Mundasad, M.V., Novack, G.D., Allgood, V.E., Evans, R.M., Gorden, J.C. & Yerxa, B.R. (2001). Ocular safety of INS365 ophthalmic solution: a P2Y₂ agonist in healthy subjects. *J. Ocul. Pharmacol. Ther.*, **17**: 173-179.

Murphy, R.A. & Rembold, C.M. (2005). The latch-bridge hypothesis of smooth muscle contraction. *Can. J. Physiol. Pharmacol.*, **83**: 857-864.

Murray, P.A., Lodato, R.F. & Michael, J.R. (1986). Neural antagonists modulate pulmonary vascular pressure-flow plots in conscious dogs. *J. Appl. Physiol.*, **60**: 1900-1907.

Murray, T.R., Chen, L., Marshall, B.E. & Macarak, E.J. (1990). Hypoxic contraction of cultured pulmonary vascular smooth muscle cells. *Am. J. Respir. Cell. Mol. Biol.*, **3**: 457-465.

- Murthy, K.S. & Makhlof, G.M. (1998). Coexpression of ligand-gated P_{2X} and G protein-coupled P_{2Y} receptors in smooth muscle. Preferential activation of P_{2Y} receptors coupled to phospholipase C (PLC)- β 1 via G $\alpha_{q/11}$ and to PLC- β 3 via G $\beta\gamma_{13}$. *J Biol. Chem.*, **273**: 4695-4704.
- Nagaoka, T., Morio, Y., Casanova, N., Bauer, S.G., McMurtry, I. & Oka, M. (2004). Rho/Rho kinase signaling mediates increased basal pulmonary vascular tone in chronically hypoxic rats. *Am. J. Physiol. Lung Cell. Mol. Physiol.*, **287**: L665-672.
- Nagumo, H., Sasaki, Y., Ono, Y., Okamoto, H., Seto, M. & Takuwa, Y. (2000). Rho kinase inhibitor HA-1077 prevents Rho-mediated myosin phosphatase inhibition in smooth muscle cells. *Am. J. Physiol. Cell Physiol.*, **278**: C57-65.
- Navedo, M.F., Amberg, G.C., Votaw, V.S. & Santana, L.F. (2005). Constitutively active L-type Ca²⁺ channels. *Proc. Natl. Acad. Sci. U. S. A.*, **102**: 11112-11117.
- Neary, J.T., Kang, Y., Willoughby, K.A. & Ellis, E.F. (2003). Activation of extracellular signal-regulated kinase by stretch-induced injury in astrocytes involves extracellular ATP and P2 purinergic receptors. *J. Neurosci.*, **23**: 2348-2356.
- Neary, J.T., Whittemore, S.R., Zhu, Q. & Norenberg, M.D. (1994). Synergistic activation of DNA synthesis in astrocytes by fibroblast growth factors and extracellular ATP. *J. Neurochem.*, **63**: 490-494.
- Nelson, M.T., Standen, N.B., Brayden, J.E. & Worley, J.F., III (1988). Noradrenaline contracts arteries by activating voltage-dependent calcium channels. *Nature*, **336**: 382-385.
- Nguyen, T., Erb, L., Weisman, G.A., Marchese, A., Heng, H.H., Garrad, R.C., George, S.R., Turner, J.T. & O'Dowd, B.F. (1995). Cloning, expression, and chromosomal localization of the human uridine nucleotide receptor gene. *J. Biol. Chem.*, **270**: 30845-30848.

Nguyen, T.D., Meichle, S., Kim, U.S., Wong, T. & Moody, M.W. (2001). P2Y₁₁, a purinergic receptor acting via cAMP, mediates secretion by pancreatic duct epithelial cells. *Am. J. Physiol. Gastrointest. Liver Physiol.*, **280**: G795-804.

Nicholas, R.A., Watt, W.C., Lazarowski, E.R., Li, Q. & Harden, T.K. (1996). Uridine nucleotide selectivity of three phospholipase C-activating P₂ receptors: identification of a UDP-selective, a UTP-selective, and an ATP- and UTP-specific receptor. *Mol. Pharmacol.*, **50**: 224-229.

Nishida, M., Sato, Y., Uemura, A., Narita, Y., Tozaki-Saitoh, H., Nakaya, M., Ide, T., Suzuki, K., Inoue, K., Nagao, T. & Kurose, H. (2008). P2Y₆ receptor-Gα_{12/13} signalling in cardiomyocytes triggers pressure overload-induced cardiac fibrosis. *EMBO J.*, **27**: 3104-3115.

Norel, X., Walch, L., Costantino, M., Labat, C., Gorenne, I., Dulmet, E., Rossi, F. & Brink, C. (1996). M₁ and M₃ muscarinic receptors in human pulmonary arteries. *Br. J. Pharmacol.*, **119**: 149-157.

Nori, S., Fumagalli, L., Bo, X., Bogdanov, Y. & Burnstock, G. (1998). Coexpression of mRNAs for P2X₁, P2X₂ and P2X₄ receptors in rat vascular smooth muscle: an in situ hybridization and RT-PCR study. *J. Vasc. Res.*, **35**: 179-185.

Ohlmann, P., Laugwitz, K.L., Nürnberg, B., Spicher, K., Schultz, G., Cazenave, J.P. & Gachet, C. (1995). The human platelet ADP receptor activates G_{i2} proteins. *Biochem. J.*, **312.3**: 775-779.

Okada, M., Nakagawa, T., Minami, M. & Satoh, M. (2002). Analgesic effects of intrathecal administration of P2Y nucleotide receptor agonists UTP and UDP in normal and neuropathic pain model rats. *J. Pharmacol. Exp. Ther.*, **303**: 66-73.

Orriss, I.R., Utting, J.C., Brandao-Burch, A., Colston, K., Grubb, B.R., Burnstock, G. & Arnett, T.R. (2007). Extracellular nucleotides block bone mineralization *in vitro*: evidence for dual inhibitory mechanisms involving both P2Y₂ receptors and pyrophosphate. *Endocrinology*, **148**: 4208-4216.

Ortega, F., Pérez-Sen, R. & Miras-Portugal, M.T. (2008). Gi-coupled P2Y-ADP receptor mediates GSK-3 phosphorylation and β -catenin nuclear translocation in granule neurons. *J. Neurochem.*, **104**: 62-73.

Palmer, R.K., Boyer, J.L., Schachter, J.B., Nicholas, R.A. & Harden, T.K. (1998). Agonist action of adenosine triphosphates at the human P2Y₁ receptor. *Mol. Pharmacol.*, **54**: 1118-1123.

Pastore, S., Mascia, F., Gulinelli, S., Forchap, S., Dattilo, C., Adinolfi, E., Girolomoni, G., Di Virgilio, F. & Ferrari, D. (2007). Stimulation of purinergic receptors modulates chemokine expression in human keratinocytes. *J. Invest. Dermatol.*, **127**: 660-667.

Patel, K., Barnes, A., Camacho, J., Paterson, C., Boughtflower, R., Cousens, D. & Marshall, F. (2001). Activity of diadenosine polyphosphates at P2Y receptors stably expressed in 1321N1 cells. *Eur. J. Pharmacol.*, **430**: 203-210.

Pauvert, O., Marthan, R. & Savineau, J. (2000). NO-induced modulation of calcium-oscillations in pulmonary vascular smooth muscle. *Cell Calcium*, **27**: 329-338.

Pendergast, W., Yerxa, B.R., Douglass, J.G., III, Shaver, S.R., Dougherty, R.W., Redick, C.C., Sims, I.F. & Rideout, J.L. (2001). Synthesis and P2Y receptor activity of a series of uridine dinucleoside 5'-polyphosphates. *Bioorg. Med. Chem. Lett.*, **11**: 157-160.

Pfefferkorn, J.A., Choi, C., Winters, T., Kennedy, R., Chi, L., Perrin, L.A., Lu, G., Ping, Y.W., McClanahan, T., Schroeder, R., Leininger, M.T., Geyer, A., Schefzick, S. & Atherton, J. (2008). P2Y₁ receptor antagonists as novel antithrombotic agents. *Bioorg Med Chem Lett.*, **18**: 3338-3343.

Pocock, G. & Richards, C.D. (2004). *Human Physiology. The Basic of Medicine*. 2nd edn, Oxford University Press: Oxford.

Pochynyuk, O., Bugaj, V., Rieg, T., Insel, P.A., Mironova, E., Vallon, V. & Stockand, J.D. (2008). Paracrine regulation of the epithelial Na⁺ channel in the mammalian collecting duct by purinergic P2Y₂ receptor tone. *J. Biol. Chem.*, **283**: 36599-36607.

Qi, A.D., Zambon, A.C., Insel, P.A. & Nicholas, R.A. (2001). An arginine/glutamine difference at the juxtaposition of transmembrane domain 6 and the third extracellular loop contributes to the markedly different nucleotide selectivities of human and canine P2Y₁₁ receptors. *Mol. Pharmacol.*, **60**: 1375-1382.

Ralevic, V. & Burnstock, G. (1998). Receptors for purines and pyrimidines. *Pharmacol. Rev.*, **50**: 413-492.

Ralevic, V. & Burnstock, G. (1996). Relative contribution of P_{2U}- and P_{2Y}-purinoceptors to endothelium-dependent vasodilatation in the golden hamster isolated mesenteric arterial bed. *Br. J. Pharmacol.*, **117**: 1797-1802.

Ratz, P.H., Berg, K.M., Urban, N.H. & Miner, A.S. (2005). Regulation of smooth muscle calcium sensitivity: KCl as a calcium-sensitizing stimulus. *Am. J. Physiol. Cell Physiol.*, **288**: C769-783.

Ratz, P.H. & Miner, A.S. (2009). Role of protein kinase C ζ and calcium entry in KCl-induced vascular smooth muscle calcium sensitization and feedback control of cellular calcium levels. *J. Pharmacol. Exp. Ther.*, **328**: 399-408.

- Ratz, P.H., Miner, A.S. & Barbour, S.E. (2009). Calcium-independent phospholipase A₂ participates in KCl-induced calcium sensitization of vascular smooth muscle. *Cell Calcium*, **46**: 65-72.
- Reeves, J.T. & Rubin, L.J. (1998). The pulmonary circulation: snapshots of progress. *Am. J. Respir. Crit. Care Med.*, **157**: S101-108.
- Robaye, B., Boeynaems, J.M. & Communi, D. (1997). Slow desensitization of the human P2Y₆ receptor. *Eur. J. Pharmacol.*, **329**: 231-236.
- Robertson, T.P., Dipp, M., Ward, J.P.T., Aaronson, P.I. & Evans, A.M. (2000). Inhibition of sustained hypoxic vasoconstriction by Y-27632 in isolated intrapulmonary arteries and perfused lung of the rat. *Br. J. Pharmacol.*, **131**: 5-9.
- Rodat-Despoix, L., Aires, V., Ducret, T., Marthan, R., Savineau, J.P., Rousseau, E. & Guibert, C. (2009). Signalling pathways involved in the contractile response to 5-HT in the human pulmonary artery. *Eur. Respir. J.*, **34**: 1338-1347.
- Rodrigues, R.J., Almeida, T., Richardson, P.J., Oliveira, C.R. & Cunha, R.A. (2005). Dual presynaptic control by ATP of glutamate release via facilitatory P2X₁, P2X_{2/3}, and P2X₃ and inhibitory P2Y₁, P2Y₂, and/or P2Y₄ receptors in the rat hippocampus. *J. Neurosci.*, **25**: 6286-6295.
- Roman, R.M., Feranchak, A.P., Salter, K.D., Wang, Y. & Fitz, J.G. (1999). Endogenous ATP release regulates Cl⁻ secretion in cultured human and rat biliary epithelial cells. *Am. J. Physiol.*, **276**: G1391-1400.
- Rost, S., Daniel, C., Schulze-Lohoff, E., Bäumert, H.G., Lambrecht, G. & Hugo, C. (2002). P2 receptor antagonist PPADS inhibits mesangial cell proliferation in experimental mesangial proliferative glomerulonephritis. *Kidney Int.*, **62**: 1659-1671.

Rubino, A. & Burnstock, G. (1996). Evidence for a P₂-purinoceptor mediating vasoconstriction by UTP, ATP and related nucleotides in the isolated pulmonary vascular bed of the rat. *Br. J. Pharmacol.*, **118**: 1415-1420.

Rubino, A., Ziabary, L. & Burnstock, G. (1999). Regulation of vascular tone by UTP and UDP in isolated rat intrapulmonary arteries. *Eur. J. Pharmacol.*, **370**: 139-143.

Sabeur, G. (1996). Effect of temperature on the contractile response of isolated rat small intestine to acetylcholine and KCl: calcium dependence. *Arch. Physiol. Biochem.*, **104**: 220-228.

Sañag, B., Milon, D., Alláin, H., Rault, B. & Van den Driessche, J. (1990). Constriction of the smooth muscle of rat tail and femoral arteries and dog saphenous vein is induced by uridine triphosphate via 'pyrimidinoceptors', and by adenosine triphosphate via P_{2x} purinoceptors. *Blood Vessels*, **27**: 352-364.

Saino, T., Matsuura, M. & Satoh, Y.I. (2002). Comparison of the effect of ATP on intracellular calcium ion dynamics between rat testicular and cerebral arteriole smooth muscle cells. *Cell Calcium*, **32**: 153-163.

Sakurada, S., Takuwa, N., Sugimoto, N., Wang, Y., Seto, M., Sasaki, Y. & Takuwa, Y. (2003). Ca²⁺-dependent activation of Rho and Rho kinase in membrane depolarization-induced and receptor stimulation-induced vascular smooth muscle contraction. *Circ. Res.*, **93**: 548-556.

Sato, K., Ozaki, H. & Karaki, H. (1988). Changes in cytosolic calcium level in vascular smooth muscle strip measured simultaneously with contraction using fluorescent calcium indicator fura 2. *J. Pharmacol. Exp. Ther.*, **246**: 294-300.

Sauzeau, V., Le Jeune, H., Cario-Toumaniantz, C., Vaillant, N., Gadeau, A.P., Desgranges, C., Scalbert, E., Chardin, P., Pacaud, P. & Loirand, G. (2000). P2Y₁, P2Y₂, P2Y₄, and P2Y₆ receptors are coupled to Rho and Rho kinase activation in vascular myocytes. *Am. J. Physiol. Heart Circ. Physiol.*, **278**: H1751-1761.

Savineau, J.P., Marthan, R. & Crevel, H. (1991). Contraction of vascular smooth muscle induced by phorbol 12,13 dibutyrate in human and rat pulmonary arteries. *Br J. Pharmacol.*, **104**: 639-644.

Schachter, J.B., Li, Q., Boyer, J.L., Nicholas, R.A. & Harden, T.K. (1996). Second messenger cascade specificity and pharmacological selectivity of the human P₂Y₁-purinoceptor. *Br. J. Pharmacol.*, **118**: 167-173.

Schäfer, R., Sedehizade, F., Welte, T. & Reiser, G. (2003). ATP- and UTP-activated P2Y receptors differently regulate proliferation of human lung epithelial tumor cells. *Am. J. Physiol. Lung Cell. Mol. Physiol.*, **285**: L376-385.

Schindler, M.B., Hislop, A.A. & Haworth, S.G. (2004). Postnatal changes in response to norepinephrine in the normal and pulmonary hypertensive lung. *Am. J. Respir. Crit. Care Med.*, **170**: 641-646.

Schreiber, R. & Kunzelmann, K. (2005). Purinergic P2Y₆ receptors induce Ca²⁺ and CFTR dependent Cl⁻ secretion in mouse trachea. *Cell. Physiol. Biochem.*, **16**: 99-108.

Segarra, G., Medina, P., Revert, F., Masiá, S., Vila, J.M., Such, L. & Aldasoro, M. (1999). Modulation of adrenergic contraction of dog pulmonary arteries by nitric oxide and prostacyclin. *Gen. Pharmacol.*, **32**: 583-589.

Shahbazian, A., Petkov, V., Baykuscheva-Gentscheva, T., Hoeger, H., Painsipp, E., Holzer, P. & Mosgoeller, W. (2007). Involvement of endothelial NO in the dilator effect of VIP on rat isolated pulmonary artery. *Regul. Pept.*, **139**: 102-108.

- Shaver, S.R., Rideout, J.L., Pendergast, W., Douglass, J.G., Brown, E.G., Boyer, J.L., Patel, R.I., Redick, C.C., Jones, A.C., Picher, M. & Yerxa, B.R. (2005). Structure-activity relationships of dinucleotides: Potent and selective agonists of P2Y receptors. *Purinergic Signal.*, **1**: 183-191.
- Shen, J., Seye, C.I., Wang, M., Weisman, G.A., Wilden, P.A. & Sturek, M. (2004). Cloning, up-regulation, and mitogenic role of porcine P2Y₂ receptor in coronary artery smooth muscle cells. *Mol. Pharmacol.*, **66**: 1265-1274.
- Shimoda, L.A., Sylvester, J.T. & Sham, J.S. (1998). Inhibition of voltage-gated K⁺ current in rat intrapulmonary arterial myocytes by endothelin-1. *Am. J. Physiol.*, **274**: L842-853.
- Shmygol, A. & Wray, S. (2004). Functional architecture of the SR calcium store in uterine smooth muscle. *Cell Calcium*, **35**: 501-508.
- Snetkov, V.A., Knock, G.A., Baxter, L., Thomas, G.D., Ward, J.P. & Aaronson, P.I. (2006). Mechanisms of the prostaglandin F_{2α}-induced rise in [Ca²⁺]_i in rat intrapulmonary arteries. *J. Physiol.*, **571**: 147-163.
- Snetkov, V.A., Thomas, G.D., Teague, B., Leach, R.M., Shaifta, Y., Knock, G.A., Aaronson, P.I. & Ward, J.P. (2008). Low concentrations of sphingosylphosphorylcholine enhance pulmonary artery vasoreactivity: the role of protein kinase Cδ and Ca²⁺ entry. *Hypertension*, **51**: 239-245.
- Somlyo, A.P. & Himpens, B. (1989). Cell calcium and its regulation in smooth muscle. *FASEB J.*, **3**: 2266-2276.
- Somlyo, A.P. & Somlyo, A.V. (2003). Ca²⁺ sensitivity of smooth muscle and nonmuscle myosin II: modulated by G proteins, kinases, and myosin phosphatase. *Physiol. Rev.*, **83**: 1325-1358.

Somlyo, A.P. & Somlyo, A.V. (2000). Signal transduction by G-proteins, rho-kinase and protein phosphatase to smooth muscle and non-muscle myosin II. *J. Physiol.*, **522.2**: 177-185.

Sprague, R.S., Ellsworth, M.L., Stephenson, A.H. & Lonigro, A.J. (1996). ATP: the red blood cell link to NO and local control of the pulmonary circulation. *Am. J. Physiol.*, **271**: H2717-H2722.

Sprague, R.S., Olearczyk, J.J., Spence, D.M., Stephenson, A.H., Sprung, R.W. & Lonigro, A.J. (2003). Extracellular ATP signaling in the rabbit lung: erythrocytes as determinants of vascular resistance. *Am. J. Physiol.*, **285**: H693-H700.

Strøbaek, D., Olesen, S.P., Christophersen, P. & Dissing, S. (1996). P₂-purinoceptor-mediated formation of inositol phosphates and intracellular Ca²⁺ transients in human coronary artery smooth muscle cells. *Br. J. Pharmacol.*, **118**: 1645-1652.

Suarez-Huerta, N., Pouillon, V., Boeynaems, J.M. & Robaye, B. (2001). Molecular cloning and characterization of the mouse P2Y₄ nucleotide receptor. *Eur. J. Pharmacol.*, **416**: 197-202.

Suggett, A.J., Mohammed, F.H. & Barer, G.R. (1980). Angiotensin, hypoxia, verapamil and pulmonary vessels. *Clin. Exp. Pharmacol. Physiol.*, **7**: 263-274.

Sumpio, B.E., Riley, J.T. & Dardik, A. (2002). Cells in focus: endothelial cell. *Int. J. Biochem. Cell Biol.*, **34**: 1508-1512.

Suzuki, N., Hajicek, N. & Kozasa, T. (2009). Regulation and physiological functions of G12/13-mediated signaling pathways. *Neurosignals*, **17**: 55-70.

Suzuki, N., Nakamura, S., Mano, H. & Kozasa, T. (2003). Gα₁₂ activates Rho GTPase through tyrosine-phosphorylated leukemia-associated RhoGEF. *Proc. Natl. Acad. Sci. U. S. A.*, **100**: 733-738.

Swärd, K., Dreja, K., Susnjar, M., Hellstrand, P., Hartshorne, D.J. & Walsh, M.P. (2000). Inhibition of Rho-associated kinase blocks agonist-induced Ca²⁺ sensitization of myosin phosphorylation and force in guinea-pig ileum. *J. Physiol.*, **522.1**: 33-49.

Sylvester, J.T. (2004). The tone of pulmonary smooth muscle: ROK and Rho music? *Am. J. Physiol. Lung Cell. Mol. Physiol.*, **287**: L624-630.

Szarek, J.L., Bailly, D.A., Stewart, N.L. & Gruetter, C.A. (1992). Histamine H₁-receptors mediate endothelium-dependent relaxation of rat isolated pulmonary arteries. *Pulm. Pharmacol.*, **5**: 67-74.

Takasaki, J., Kamohara, M., Saito, T., Matsumoto, M., Matsumoto, S., Ohishi, T., Soga, T., Matsushime, H. & Furuichi, K. (2001). Molecular cloning of the platelet P2T_{AC} ADP receptor: pharmacological comparison with another ADP receptor, the P2Y₁ receptor. *Mol. Pharmacol.*, **60**: 432-439.

Tan, L.M. & Sim, M.K. (2000). Actions of angiotensin peptides on the rabbit pulmonary artery. *Life Sci.*, **66**: 1839-1847.

Tasatargil, A., Sadan, G. & Ozdem, S.S. (2003). The effects of selective phosphodiesterase III and V inhibitors on adrenergic and non-adrenergic, non-cholinergic relaxation responses of guinea-pig pulmonary arteries. *Auton. Autacoid Pharmacol.*, **23**: 117-124.

Tauber, J., Davitt, W.F., Bokosky, J.E., Nichols, K.K., Yerxa, B.R., Schaberg, A.E., LaVange, L.M., Mills-Wilson, M.C. & Kellerman, D.J. (2004). Double-masked, placebo-controlled safety and efficacy trial of diquafosol tetrasodium (INS365) ophthalmic solution for the treatment of dry eye. *Cornea*, **23**: 784-792.

Thomas, G.D., Snetkov, V.A., Patel, R., Leach, R.M., Aaronson, P.I. & Ward, J.P. (2005). Sphingosylphosphorylcholine-induced vasoconstriction of pulmonary artery: activation of non-store-operated Ca²⁺ entry. *Cardiovasc. Res.*, **68**: 56-64.

- Toba, M., Nagaoka, T., Morio, Y., Sato, K., Uchida, K., Homma, N. & Takahashi, K. (2010). Involvement of Rho kinase in the pathogenesis of acute pulmonary embolism-induced polystyrene microspheres in rats. *Am. J. Physiol. Lung Cell. Mol. Physiol.*, **298**: L297-303.
- Tokuyama, Y., Hara, M., Jones, E.M., Fan, Z. & Bell, G.I. (1995). Cloning of rat and mouse P_{2Y} purinoceptors. *Biochem. Biophys. Res. Commun.*, **211**: 211-218.
- Toullec, D., Pianetti, P., Coste, H., Bellevergue, P., Grand-Perret, T., Ajakane, M., Baudet, V., Boissin, P., Boursier, E., Loriolle, F., Duhame, L., Charon, D. & Kirilovsky, J. (1991). The bisindolylmaleimide GF 109203X is a potent and selective inhibitor of protein kinase C. *J. Biol. Chem.*, **266**: 15771-15781.
- Tracey, A., Bunton, D., Irvine, J., MacDonald, A. & Shaw, A.M. (2002). Relaxation to bradykinin in bovine pulmonary supernumerary arteries can be mediated by both a nitric oxide-dependent and -independent mechanism. *Br. J. Pharmacol.*, **137**: 538-544.
- Tsai, M.H. & Jiang, M.J. (2006). Rho-kinase-mediated regulation of receptor-agonist-stimulated smooth muscle contraction. *Pflugers Arch.*, **453**: 223-232.
- Tseng, C.M. & Mitzner, W. (1992). Antagonists of EDRF attenuate acetylcholine-induced vasodilation in isolated hamster lungs. *J. Appl. Physiol.*, **72**: 2162-2167.
- Tsien, R. & Pozzan, T. (1989). Measurement of cytosolic free Ca²⁺ with Quin2. *Methods Enzymol.*, **172**: 230-262.
- Uehata, M., Ishizaki, T., Satoh, H., Ono, T., Kawahara, T., Morishita, T., Tamakawa, H., Yamagami, K., Inui, J., Maekawa, M. & Narumiya, S. (1997). Calcium sensitization of smooth muscle mediated by a Rho-associated protein kinase in hypertension. *Nature*, **389**: 990-994.

Unterberger, U., Moskvina, E., Scholze, T., Freissmuth, M. & Boehm, S. (2002). Inhibition of adenylyl cyclase by neuronal P2Y receptors. *Br. J. Pharmacol.*, **135**: 673-684.

Urban, N.H., Berg, K.M. & Ratz, P.H. (2003). K⁺ depolarization induces RhoA kinase translocation to caveolae and Ca²⁺ sensitization of arterial muscle. *Am. J. Physiol. Cell Physiol.*, **285**: C1377-1385.

van der Weyden, L., Adams, D.J., Luttrell, B.M., Conigrave, A.D. & Morris, M.B. (2000). Pharmacological characterisation of the P2Y₁₁ receptor in stably transfected haematological cell lines. *Mol. Cell. Biochem.*, **213**: 75-81.

Veysier-Belot, C. & Cacoub, P. (1999). Role of endothelial and smooth muscle cells in the physiopathology and treatment management of pulmonary hypertension. *Cardiovasc. Res.*, **44**: 274-282.

Vogt, S., Grosse, R., Schultz, G. & Offermanns, S. (2003). Receptor-dependent RhoA activation in G₁₂/G₁₃-deficient cells: genetic evidence for an involvement of G_q/G₁₁. *J. Biol. Chem.*, **278**: 28743-28749.

von Kügelgen, I. (2006). Pharmacological profiles of cloned mammalian P2Y-receptor subtypes. *Pharmacol. Ther.*, **110**: 415-432.

von Kügelgen, I. & Wetter, A. (2000). Molecular pharmacology of P2Y-receptors. *Naunyn-Schmiedeberg's Arch. Pharmacol.*, **362**: 310-323.

Waldo, G.L., Corbitt, J., Boyer, J.L., Ravi, G., Kim, H.S., Ji, X.D., Lacy, J., Jacobson, K.A. & Harden, T.K. (2002). Quantitation of the P2Y₁ receptor with a high affinity radiolabeled antagonist. *Mol. Pharmacol.*, **62**: 1249-1257.

Waldo, G.L. & Harden, T.K. (2004). Agonist binding and Gq-stimulating activities of the purified human P2Y₁ receptor. *Mol. Pharmacol.*, **65**: 426-436.

Wallentin, L., Becker, R.C., Budaj, A., Cannon, C.P., Emanuelsson, H., Held, C., Horrow, J., Husted, S., James, S., Katus, H., Mahaffey, K.W., Scirica, B.M., Skene, A., Steg, P.G., Storey, R.F., Harrington, R.A., Freij, A. & Thorsen, M. (2009). Ticagrelor versus clopidogrel in patients with acute coronary syndromes. *N. Engl. J. Med.*, **361**: 1045-1057.

Wang, L., Karlsson, L., Moses, S., Hultgårdh-Nilsson, A., Andersson, M., Borna, C., Gudbjartsson, T., Jern, S. & Erlinge, D. (2002). P2 receptor expression profiles in human vascular smooth muscle and endothelial cells. *J. Cardiovasc. Pharmacol.*, **40**: 841-853.

Ward, J.P., Knock, G.A., Snetkov, V.A. & Aaronson, P.I. (2004). Protein kinases in vascular smooth muscle tone - role in the pulmonary vasculature and hypoxic pulmonary vasoconstriction. *Pharmacol. Ther.*, **104**: 207-231.

Warny, M., Aboudola, S., Robson, S.C., Sévigny, J., Communi, D., Soltoff, S.P. & Kelly, C.P. (2001). P2Y₆ nucleotide receptor mediates monocyte interleukin-8 production in response to UDP or lipopolysaccharide. *J. Biol. Chem.*, **276**: 26051-26056.

Webb, T.E., Simon, J., Krishek, B.J., Bateson, A.N., Smart, T.G., King, B.F., Burnstock, G. & Barnard, E.A. (1993). Cloning and functional expression of a brain G-protein-coupled ATP receptor. *FEBS Lett.*, **324**: 219-225.

Weigand, L., Sylvester, J.L. & Shimoda, L.A. (2006). Mechanisms of endothelin-1-induced contraction in pulmonary arteries from chronically hypoxic rats. *Am. J. Physiol. Lung Cell. Mol. Physiol.*, **290**: L284-290.

Welsh, D.G. & Brayden, J.E. (2001). Mechanisms of coronary artery depolarization by uridine triphosphate. *Am. J. Physiol. Heart Circ. Physiol.*, **280**: H2545-2553.

Weng, J.Y., Hsu, T.T. & Sun, S.H. (2008). Functional characterization of P2Y₁ versus P2X receptors in RBA-2 astrocytes: elucidate the roles of ATP release and protein kinase C. *J. Cell. Biochem.*, **104**: 554-567.

White, P.J., Webb, T.E. & Boarder, M.R. (2003). Characterization of a Ca²⁺ response to both UTP and ATP at human P2Y₁₁ receptors: evidence for agonist-specific signaling. *Mol. Pharmacol.*, **63**: 1356-1363.

Wihlborg, A.K., Wang, L., Braun, O.Ö., Eyjolfsson, A., Gustafsson, R., Gudbjartsson, T. & Erlinge, D. (2004). ADP receptor P2Y₁₂ is expressed in vascular smooth muscle cells and stimulates contraction in human blood vessels. *Arterioscler. Thromb. Vasc. Biol.*, **24**: 1810-1815.

Wilkin, F., Duhant, X., Bruyns, C., Suarez-Huerta, N., Boeynaems, J.M. & Robaye, B. (2001). The P2Y₁₁ receptor mediates the ATP-induced maturation of human monocyte-derived dendritic cells. *J. Immunol.*, **166**: 7172-7177.

Wilson, D.P., Susnjar, M., Kiss, E., Sutherland, C. & Walsh, M.P. (2005). Thromboxane A₂-induced contraction of rat caudal arterial smooth muscle involves activation of Ca²⁺ entry and Ca²⁺ sensitization: Rho-associated kinase-mediated phosphorylation of MYPT1 at Thr-855, but not Thr-697. *Biochem. J.*, **389**: 763-774.

Xu, M., Platoshyn, O., Makino, A., Dillmann, W.H., Akassoglou, K., Remillard, C. V. & Yuan, J.X. (2008). Characterization of agonist-induced vasoconstriction in mouse pulmonary artery. *Am. J. Physiol. Heart Circ. Physiol.*, **294**: H220-228.

Yamamoto, S., Ichishima, K. & Ehara, T. (2007). Regulation of extracellular UTP-activated Cl⁻ current by P2Y-PLC-PKC signaling and ATP hydrolysis in mouse ventricular myocytes. *J. Physiol. Sci.*, **57**: 85-94.

Yanagisawa, T. & Okada, Y. (1994). KCl depolarization increases Ca²⁺ sensitivity of contractile elements in coronary arterial smooth muscle. *Am. J. Physiol.*, **267**: H614-621.

Yerxa, B.R., Sabater, J.R., Davis, C.W., Stutts, M.J., Lang-Furr, M., Picher, M., Jones, A.C., Cowlen, M., Dougherty, R., Boyer, J., Abraham, W.M. & Boucher, R.C. (2002). Pharmacology of INS37217 [P¹-(uridine 5')-P⁴-(2'-deoxycytidine 5')tetrphosphate, tetrasodium salt], a next-generation P2Y₂ receptor agonist for the treatment of cystic fibrosis. *J. Pharmacol. Exp. Ther.*, **302**: 871-880.

Zambon, A.C., Brunton, L.L., Barrett, K.E., Hughes, R.J., Torres, B. & Insel, P.A. (2001). Cloning, expression, signaling mechanisms, and membrane targeting of P2Y₁₁ receptors in Madin Darby canine kidney cells. *Mol. Pharmacol.*, **60**: 26-35.

Zhang, F.L., Luo, L., Gustafson, E., Lachowicz, J., Smith, M., Qiao, X., Liu, Y.H., Chen, G., Pramanik, B., Laz, T.M., Palmer, K., Bayne, M. & Monsma, F.J., Jr. (2001). ADP is the cognate ligand for the orphan G protein-coupled receptor SP1999. *J. Biol. Chem.*, **276**: 8608-8615.

Zhang, F.L., Luo, L., Gustafson, E., Palmer, K., Qiao, X., Fan, X., Yang, S., Laz, T. M., Bayne, M. & Monsma, F., Jr. (2002). P2Y₁₃: identification and characterization of a novel G_{α_i}-coupled ADP receptor from human and mouse. *J. Pharmacol. Exp. Ther.*, **301**: 705-713.

Zheng, Y.M., Wang, Q.S., Rathore, R., Zhang, W.H., Mazurkiewicz, J.E., Sorrentino, V., Singer, H.A., Kotlikoff, M.I. & Wang, Y.X. (2005). Type-3 ryanodine receptors mediate hypoxia-, but not neurotransmitter-induced calcium release and contraction in pulmonary artery smooth muscle cells. *J. Gen. Physiol.*, **125**: 427-440.